# *Hydrometallurgical & Electrochemical Recycling of Mixed Li-ion Battery Waste*

**Johannes Josephus Michaël Maria van de Ven**

# Hydrometallurgical & Electrochemical Recycling of Mixed Li-ion Battery Waste

# Hydrometallurgical & Electrochemical Recycling of Mixed Li-ion Battery Waste

## Dissertation

For the purpose of obtaining the degree of doctor
at Delft University of Technology,
by the authority of the Rector Magnificus Prof. Dr. Ir. H. Bijl,
chair of the Board for Doctorates
to be defended publicly on
Thursday, June 11th 2026, at 17:30

by

**Johannes Josephus Michaël Maria VAN DE VEN**

This dissertation has been approved by the (co)promotors.

Composition of the doctoral committee:

| | |
|---|---|
| Rector Magnificus | Chairperson |
| Dr. Y. Yang | Delft University of Technology, promotor |
| Dr.ir. S.T. Abrahami | Delft University of Technology, copromotor |

Independent members:

| | |
|---|---|
| Dr. E.M. Kelder | Delft University of Technology |
| Prof.dr.ir. J.M.C. Mol | Delft University of Technology |
| Dr. S. Bandyopadhyay | Norwegian University of Science and Technology, Norway |
| Dr. M. Petranikova | Chalmers University of Technology, Sweden |
| Dr.ir. S.C. Lans | Back to Battery, the Netherlands |
| Prof.dr. J. Dik | Delft University of Technology, reserve member |

*Keywords*: Recycling, Critical Raw Materials, Lithium-ion Batteries, Hydrometallurgy, Electrochemistry, Inorganic Chemistry

*Cover design*: Cazaki
*Layout by*: Arul Raja | www.ridderprint.nl
*Printing by*: www.ridderprint.nl


ISBN: 978-94-6537-501-4

# TABLE OF CONTENTS

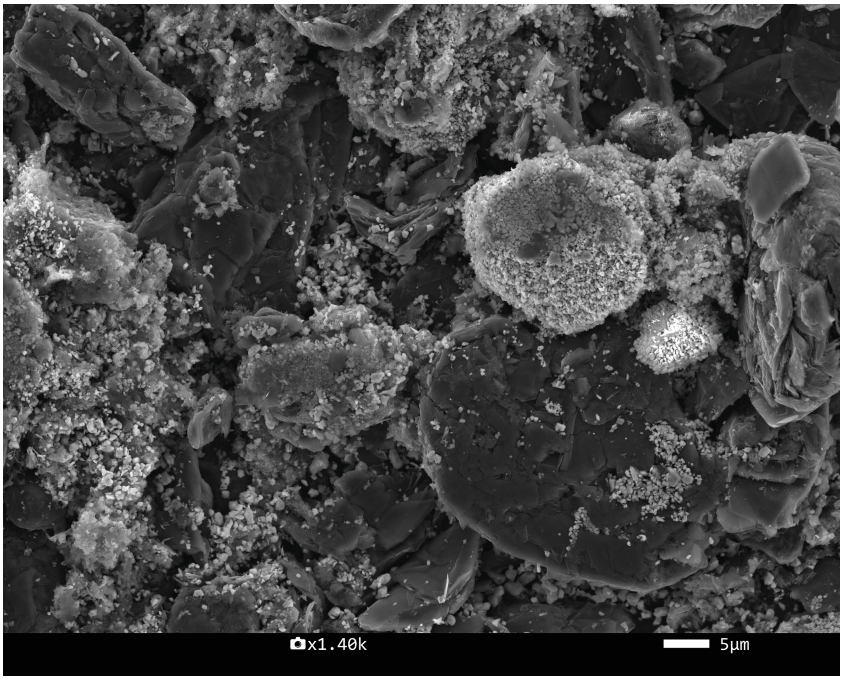


Above, you see the original image of the cover of this thesis, taken with a Scanning Electron Microscope (SEM) at 1400 times magnification. It represents a solid product that was taken during the leaching procedure as explained in Chapter 5 of this thesis. The two different cathode active material types, NMC (green on the cover) and LFP (red on the cover), are clearly distinguishable, alongside the graphite (grey on the cover), originally present in LiBs as anode active material.

*Als dit Ierland was,*
*zou ik beter kijken*

K. Schippers – *Bij Loosdrecht* – Een leeuwerik boven een weiland (1996)

# Summary

Lithium-ion batteries (LiBs) play a key role in the electrification of our society, and contain materials that are associated with supply risks, rendering them critical- or strategic raw materials (CRMs and SRMs, respectively). Examples of such materials are Li, Co, and Mn (CRMs), or Ni and Cu (SRMs). Recycling is a key contributor to relieve some of the pressure on the supply of these materials. This dissertation focuses on mixed battery waste streams of complex and varying chemistries, and on how this end-of-life product influences hydrometallurgical recycling, with the ultimate goal of designing a flexible, closed loop recycling process that combines high product quality with minimal environmental footprint.

**Chapter 1** gives a brief introduction of the importance of LiBs, their working principle and reliance on CRMs, and shows why extensive research on hydrometallurgical recycling of LiBs has not resulted in their large scale comprehensive recovery yet. To lay the fundamentals around the recycling of LiBs, **Chapter 2** explains the background on the preliminary treatment and hydrometallurgical recycling steps that are commonly applied in LiB recycling. This leads to a good understanding of the state-of-the-art of LiB recycling in industry and research, and further illustrates the research gap this thesis attempts to fill in.

**Chapter 3** is the first experimental chapter of this dissertation, and starts with a detailed characterization of the composition of LiB-containing e-waste from consumer electronics. The hereby isolated LiB-modules are then disassembled and the battery cells are opened, followed by the isolation of the CAMs. The morphology and chemical composition of these CAMs are compared with one pristine CAM, showing that while the general composition of the LiB-cells is very consistent, variations in CAM-type may occur and no definitive link with LiB application can be found. The research also shows that industrially pre-treated LiB-waste, also called black mass (BM), contains impurities such as Fe, Al, Cu, and graphite as result of the pre-treatment, which originate from other parts of the LiB-cells. Although the investigated LiB-waste types in this research exhibit similar dissolution trends during leaching, the different oxidation states of Ni, Co, and Mn, ranging from +II to +IV, result in a different need for reductive conditions, as these elements dissolve best in the +II-oxidation state. Hence, it is apparent that the reductive acid leaching step can be strongly influenced by the composition and pre-treatment of the LiB-waste.

The following **Chapter 4** focusses on lowering the environmental footprint of the reductive acid leaching procedure. Instead of $H_2O_2$, a commonly used reductant in LiB recycling, the reducing capability of another type of waste LiB-cathode active material, $LiFePO_4$ (LFP), is investigated. Comparing three leaching approaches

using spent LFP to reduce either pristine $LiNi_xCo_yMn_zO_2$ (NMC), manually liberated NMC, or industrial NMC BM, leads to understanding of the conjoint dissolution mechanism. The $Fe^{2+}$ resulting from LFP dissolution can reduce the Ni, Co, and Mn from NMC, enhancing their dissolution, while any metallic Cu and Al impurities can transform the generated $Fe^{3+}$ back to $Fe^{2+}$, further increasing the reducing capabilities of the leaching system. Hence, no additional $H_2O_2$ is necessary for complete leaching of NMC, and a low acid concentration of 0.63 mol/L $H_2SO_4$ could be applied. Subsequent selective precipitation through pH adjustment also shows that any $Fe^{3+}$ can be removed at pH 3, alongside minimal losses of Ni, Co, and Mn. However, any remaining $Fe^{2+}$, either not reacted with NMC or regenerated by metallic Al and Cu, is not easily removed through pH adjustment, emphasising that further optimization is necessary to avoid downstream contamination with Fe. Moreover, a stepwise increase in pH from 1.7 to 10.7 shows that a significant amount of Fe, Al, and Cu can coprecipitate with Ni, Co, and Mn when no prior purification is conducted.

To pursue a flexible and environmentally friendly LiB-recycling process, **Chapter 5** combines an optimized version of the leaching step presented in Chapter 4 with electrochemical purification and selective precipitation through pH adjustment, using solely industrially pre-treated LiB-waste. This process includes the electrochemical oxidation of $Fe^{2+}$ to $Fe^{3+}$ to decrease its solubility at higher pH values. This method is effective for leaching solutions containing only Fe as transition metal, but in a pregnant leach solution (PLS) of both LFP and NMC, Cu and Fe interfere with each other's effective electrochemical removal. Hence, an approach containing four purification steps was developed. The pH of the PLS is first increased to selectively precipitate Fe (if present as $Fe^{3+}$) , Al and Cu, after which electrodeposition of the remaining Cu is conducted, followed by electro-oxidation of $Fe^{2+}$, after which a second selective precipitation recovers Ni, Co, and Mn products, leaving Li in solution. Since the resulting Ni, Co, and Mn products merely contain 0.1% - 0.6% Cu, Al, and Fe in total, and the electrochemical treatment progression can be monitored in situ, this approach has great potential as a flexible recycling route for closed loop recycling of mixed LiB waste, resulting in high purity Ni, Co and Mn precursors.

To investigate the effect of the lixiviant on downstream purification, **Chapter 6** explores how three different acids, $H_2SO_4$, HCl, and $H_3PO_4$, impact the purification method described in Chapter 5. Only $H_2SO_4$ results in complete NMC dissolution due to its high acidic strength and diprotic nature, whereas HCl is limited by its monoprotic nature and $H_3PO_4$ by its lower acidic strength. Although electrochemical treatment significantly improves the purity of the precipitates in all three systems, the $H_2SO_4$- system performed best, combining complete leaching with effective

Cu and Fe removal during the electrochemical treatment. The HCl- system also results in good separation of Li, Ni, Co and Mn from the impurities, but suffers from lower initial leaching efficiency. The $H_3PO_4$-system shows the lowest leaching efficiency of all systems, and results in co-precipitation of all elements except Li, showing the lowest selectivity of all. Overall, while the developed process shows promising results for flexible, closed-loop LiB-recycling, more research is necessary for optimization of the electrochemical treatment and effective removal of Al.

Lastly, **Chapter 7** summarises the key conclusions of this PhD study, including the substitution of reductant through simultaneous LFP and NMC leaching, and the strong dependence of the electrochemical purification effectiveness on lixiviant choice. It also provides recommendations to address newly identified research gaps, including more in-depth research on electrochemical purification in complex systems, as well as testing the performance of the recovered products in new Li-ion batteries.

# Samenvatting

Lithium-ion batterijen (LiBs) spelen een sleutelrol in de elektrificatie van onze maatschappij en bevatten materialen met risico's omtrent toevoer, waardoor ze ook wel kritieke of strategische grondstoffen worden genoemd (CRMs en SRMs, respectievelijk). Voorbeelden van zulke grondstoffen in LiBs zijn Li, Co en Mn (CRMs) of Ni en Cu (SRMs). Recycling kan ervoor zorgen dat de druk op de toevoer van deze grondstoffen verkleint. Dit proefschrift richt zich op een gemengde batterijafvalstroom met een complexe en variabele samenstelling en hoe dit afgedankte product de hydrometallurgische recycling beïnvloedt, met het ontwerp van een flexibel en gesloten-lus recycleprogramma waarin hoge productkwaliteit en kleine ecologische voetafdruk gecombineerd worden als uiteindelijke doel.

**Hoofdstuk 1** geeft een beknopte inleiding over het belang van LiBs, hun werkingsprincipe en nood aan kritieke grondstoffen en laat zien waarom uitgebreid onderzoek tot nu toe nog niet tot grootschalige, allesomvattende herwinning heeft geleid. Vervolgens verdiept **Hoofdstuk 2** zich meer in de achtergrond omtrent de voorbehandeling en hydrometallurgische recyclestappen die gehanteerd worden in recycling. Dit zorgt voor een goed begrip van de fundamentele principes en de huidige stand van zaken in het kader van LiB recycling op industriële schaal en in het wetenschappelijk onderzoek en verduidelijkt de onderzoekskloof die dit proefschrift tracht te vullen.

**Hoofdstuk 3** is het eerste experimentele hoofdstuk van dit proefschrift en begint met een gedetailleerd onderzoek naar de samenstelling van LiB-bevattend elektronisch afval uit consumentenelektronica. De verkregen LiB-modules worden vervolgens ontmanteld, waarna de batterijcellen worden geopend en de actieve cathodematerialen (CAMs) worden afgezonderd. De morfologie en chemische samenstelling van deze CAMs worden onderling vergeleken, alsook met een zuiver CAM. Hieruit blijkt dat de algemene samenstelling van LiBs zeer consistent is, maar niet te koppelen valt aan de toepassing van de batterij. Het onderzoek wijst ook uit dat industrieel voorbehandeld LiB-afval, ook wel black mass (BM) genoemd, vele onzuiverheden afkomstig van andere batterijonderdelen bevat, zoals Cu, Al, Fe en grafiet, ten gevolge van dit soort voorbehandeling. Hoewel de hier onderzochte LiB-afvaltypes zich gelijkaardig gedragen tijdens het uitlogen, zorgen de verschillende oxidatietoestanden van Ni, Mn en Co die zich bevinden tussen II en IV ervoor dat de nood aan een reducerende omgeving verschilt, aangezien de meest oplosbare oxidatietoestand van deze elementen II is. Het is daardoor duidelijk dat de reductieve, zure uitlogingsstap sterk beïnvloed kan worden door de samenstelling en voorbehandeling van het LiB-afval.

Het daaropvolgende **Hoofdstuk 4** richt zich op de beperking van de ecologische voetafdruk van het reductieve, zure uitlogingsproces. In plaats van $H_2O_2$, een courant reducerend agens in LiB-recycling, worden de reducerende eigenschappen van een ander LiB-afvalproduct, zijnde $LiFePO_4$ (LFP), onderzocht. Het vergelijken van drie uitlogingsprocessen die gebruikmaken van afgedankt LFP ter reductie van oftewel zuiver $LiNi_xCo_yMn_zO_2$ (NMC), afgedankt NMC of industrieel NMC BM, leidt tot de fundamentele kennis van het gezamenlijke oplossingsmechanisme. Het $Fe^{2+}$ dat resulteert uit het oplossen van LFP kan Ni, Co en Mn uit NMC reduceren, waardoor hun oplosbaarheid verhoogt, terwijl metallisch Cu en Al het gevormde $Fe^{3+}$ weer kunnen herreduceren tot $Fe^{2+}$, met verdere verhoging van de reductiecapaciteit van het uilogingssysteem tot gevolg. Hierdoor is er geen $H_2O_2$ nodig voor het volledig uitlogen van NMC en kan een lage concentratie van 0.63 mol/L $H_2SO_4$ toegepast worden. Vervolgens selectief neerslaan door middel van het aanpassen van de pH wijst uit dat $Fe^{3+}$ verwijderd kan worden op pH 3, gepaard met miniem verlies van Ni, Co en Mn. Echter, overblijvend $Fe^{2+}$, zowel hetgeen niet gereageerd heeft met NMC alsook hetgeen geregenereerd is door reactie met Al en Cu, kan niet eenvoudig verwijderd worden door aanpassing van de pH. Dit benadrukt dat verdere ontwikkeling nodig is om stroomafwaartse vervuiling door Fe te voorkomen. Stapsgewijze verhoging van de pH van 1.7 naar 10.7 laat bovendien zien dat een beduidende hoeveelheid Fe, Al en Cu kan coprecipiteren met Ni, Co en Mn wanneer geen eerdere zuivering is uitgevoerd.

Ter nastreving van een flexibel en milieuvriendelijk LiB-recycleproces combineert **Hoofdstuk 5** een geoptimaliseerde versie van het uitlogingsproces dat gepresenteerd is in Hoofdstuk 4 met elektrochemische zuivering en selectief neerslaan door middel van pH-verhoging, uitsluitend gebruikmakend van industrieel voorbehandeld afval. Elektrochemische oxidatie van $Fe^{2+}$ naar $Fe^{3+}$ ter verlaging van de oplosbaarheid blijkt effectief te zijn voor oplossingen die slechts Fe als transitiemetaal bevatten, terwijl in een uitlogingsoplossing (PLS) van LFP en NMC Cu en Fe interfereren met elkaars effectieve, elektrochemische verwijdering. Om deze reden wordt er een zuiveringsproces in vier stappen gehanteerd. Eerst wordt de pH van de PLS verhoogd om Fe (aanwezig als $Fe^{3+}$), Al en Cu neer te slaan, gevolgd door elektrodepositie van het overblijvende Cu en elektro-oxidatie van $Fe^{2+}$, waarna een tweede selectieve neerslagstap resulteert in producten van Ni, Co en Mn terwijl Li achterblijft in oplossing. Deze benadering heeft veel potentie om als flexibele schakel te fungeren in een gesloten-lus LiB-recycleproces, aangezien de producten van Co, Ni en Mn slechts 0.1% - 0.6% Cu, Al en Fe bevatten en de elektrochemische behandeling in-situ gecontroleerd kan worden.

Om de invloed van het uitlogingsagens voor stroomafwaartse zuivering vast te stellen verkent **Hoofdstuk 6** het effect van drie zuren, $H_2SO_4$, HCl en $H_3PO_4$, op de zuiveringsstappen zoals beschreven in Hoofdstuk 5. Enkel $H_2SO_4$ resulteert in volledige oplossing van NMC wegens de hoge zuursterkte en biprotische eigenschap, waar HCl beperkt wordt door het enkele proton en $H_3PO_4$ door de lage zuursterkte. Hoewel in elk van de drie systemen de elektrochemische zuivering een substantiële verhoging in zuiverheid van de uiteindelijk gevormde producten teweeg brengt, is het $H_2SO_4$-systeem het effectiefst. Het combineert complete uitloging met effectieve Cu en Fe verwijdering gedurende de elektrochemische zuivering. Het HCl-systeem resulteert ook in goede scheiding van Li, Ni, Co en Mn van de onzuiverheden, maar is gepaard met een lagere uitlogingsefficiëntie. Het $H_3PO_4$-systeem heeft de laagste efficiëntie van de drie systemen, resulteert in het gezamenlijk neerslaan van alle elementen behalve Li en heeft dus de laagste selectiviteit. Hoewel de gepresenteerde recyclestrategie veelbelovend is voor flexibele gesloten-lus LiB-recycling, vergen de verwijdering van Al en elektrochemische zuivering verdere ontwikkeling.

Ten laatste vat **Hoofdstuk 7** alle belangrijke conclusies samen, zoals onder meer de mogelijkheid een reducerend agens te vervangen door het gezamenlijk uitlogen van LFP en NMC, alsook de sterke afhankelijkheid van elektrochemische zuivering van het gekozen uitlogingszuur. Er worden ook suggesties gedaan voor vervolgonderzoek, zoals onder meer een gedetailleerder onderzoek naar de elektrochemische zuivering alsook het testen van de herwonnen materialen in nieuwe Li-ion batterijen.

*Als je goed*
*om je heen kijkt*
*zie je dat alles*
*gekleurd is*

K. Schippers – *De ontdekking* – Een leeuwerik boven een weiland (1996)

# 1

# *Chapter 1*

## Introduction

## 1.1. LITHIUM-ION BATTERIES & THEIR CHEMISTRIES

Lithium-ion Batteries (LiBs) are key contributors to modern energy storage and the energy transition [1]. They are widely used in daily-life products, including mobile phones, headphones and laptops, providing electrical energy on the go [2]. Their use is also rapidly increasing in the electrification of transport and mobility, thereby reducing greenhouse gas emissions by allowing replacement of combustion engines with electric motors [3,4], as well as storing electricity from wind turbines and solar panels, making renewable energy available even when production fluctuates [5–7]. Consequently, the global LiBs market size has more than doubled from 2018 to 2021, with exponential growth also continuing in the following years [8].

LiBs require many different materials to function, as illustrated in Fig. 1.1 and Table 1.1. When fully charged, the electrons are stored in the active material of the anode, or negative electrode, alongside lithium ions ($Li^+$) to compensate for the negative charge [9,10]. The anode usually consists of graphite particles attached with a polymer such as Polyvinylidene Difluoride (PVDF) to a copper foil, which conducts the electrons from the anode to the electric circuit [10–12]. When the battery is in use, electrons flow through the connected device, to the cathode or positive electrode, as shown in Eqs. 1.1 and 1.2 [2,11]. The cathode consists of a cathode active material (CAM) made from a lithium-metal-oxide powder such as $LiCoO_2$, $LiNi_xMn_yCo_zO_2$ or $LiFePO_4$, which is attached to an aluminium foil with a binder, allowing the electrons to move from the electric circuit to the CAM [10–12]. During the discharging, a charge balance in the battery cell needs to be maintained. This is done by the $Li^+$-ions, which move from the anode to the electrolyte, which consists of a Li salt such as $LiBF_4$ or $LiPF_6$ dissolved in a carbonate solvent, and then to the cathode [10–12]. The plastic foil, often made of polypropylene, avoids direct contact and thereby short circuit of the anode and cathode. Therefore, it is referred to as the separator.

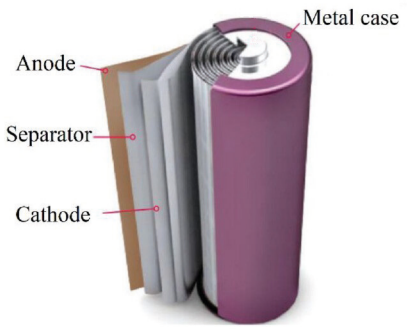


*Figure. 1.1*: *Schematic overview of a Li-ion battery cell*

*Table 1.1: Components of a LiB along with their relative weight and commonly used compounds [13].*

| Battery component | Component share (average wt.%) | Most Commonly Used Material |
|---|---|---|
| Case | 25% | Steel/plastics |
| Cathode | 27% | $LiCoO_2$, $LiNi_xMn_yCo_zO_2$, $LiFePO_4$, $LiMn_2O_4$, $LiNiO_2$ |
| Anode | 17% | Graphite or $Li_4Ti_5O_{12}$ |
| Current collectors | 13% | Cu/Al |
| Electrolyte | 10% | Solution of $LiPF_6$, $LiBF_4$, $LiClO_4$, and $LiSO_2$ dissolved in propylene carbonate, ethylene carbonate, or dimethyl sulfoxide |
| Separator | 4% | Microporous polypropylene |
| Binder | 4% | Polyvinylidene Difluoride (PVDF) |



Anode $$LiC_6 \rightleftharpoons C_6 + e^- + Li^+ \quad (1.1)$$

Cathode $$CoO_2 + e^- + Li^+ \rightleftharpoons LiCoO_2 \quad (1.2)$$

## 1.2. WHY LITHIUM-ION BATTERIES NEED TO BE RECYCLED

In 2008 the European commission noted that the European Union (EU) relies heavily on import of raw materials, making the EU member states very vulnerable to market instabilities. Hence, the EU presented quantitative ways to define the reliance on raw materials, resulting in the term “critical raw materials” or “CRMs” [14,15]. These materials are of great economic importance to the EU, while also being associated with major supply risks [15]. LiBs apply several of such CRMs for their functioning, including Li, Co, Mn, and Al, as well as the strategic raw materials (SRMs) Ni and Cu. Recycling these materials helps to reduce the reliance on primary resources, since it lowers our dependence on imports, and prevents CRMs from being lost after use. The importance of recycling becomes even more apparent considering the recent demand growth of LiBs, mainly driven by automotive applications and increase in use of portable electronic devices [8]. With this sustained increase in demand, recycling can relieve some pressure on raw material extraction.

Another important reason for recycling is the hazardous nature of the materials used in LiBs, as improper handling can release substances that are extremely

harmful to both human health and the environment. A prevalent example is the electrolyte, which contains fluorinated substances such as $LiPF_6$ [16]. When LiBs are not stored and recycled properly, these compounds can leak into the environment where, upon contact with water, compounds such as HF are formed. HF is known to penetrate the skin and react with tissue inside the human body leading to serious health risks [17]. Moreover, transition metals such as Co and Ni are strongly suspicious of being carcinogenic [18,19]. In addition, stockpiling of LiBs increases the risk of thermal runaway and fires [20]. Recycling provides an effective treatment route for these batteries, ensuring that their constituent elements are not lost after a single use, promoting circularity, reducing the criticality of the incorporated elements, and preventing danger to humans and the environment.

## 1.3. THE MISSING LINK BETWEEN STATE-OF-THE-ART & CLOSED LOOP RECYCLING OF LITHIUM-ION BATTERIES

Two overarching technologies are currently applied for the recovery of CRMs from LiBs: pyrometallurgy and hydrometallurgy [21,22]. In pyrometallurgy, high temperatures are applied to disintegrate the LiBs, remove organic impurities and liberate the valuable metals. It is a versatile process that can be applied to pre-treated batteries, as well as cells or modules in their entirety. Such a process is usually robust towards impurities and varying waste composition resulting in frequent application of pyrometallurgical unit operations in industry. However, these processes target certain high value material, such as Co, Ni, and Cu, while downgrading or even failing to recover other components, including graphite, lithium and plastics. They are energy intensive and rely on further hydrometallurgical treatment to produce final products with the desired composition and purity. Pyrometallurgical processes on industrial scale include the Umicore Valéas process, which makes use of a shaft furnace with temperatures ranging from 300 °C to 1450 °C to smelt the metals from LiBs, producing a Ni-Co-Cu metal alloy. This alloy is then further processed hydrometallurgically to separate and purify the Fe, Cu, Ni, and Co [13]. More recently, the Accurec process was established, starting with sorting and dismantling of spent LiBs, followed by milling, grinding and size classification, removing a portion of the Fe, Ni and Al [13]. The remainder is subjected to reduction smelting, resulting in a metal alloy of Co, Ni, Mn and Fe, and a slag containing the Li. The slag is leached, after which the Li is converted to usable end products.

Hydrometallurgical recycling of LiBs first requires an extensive pre-treatment to expose and separate their internal components. However, researchers often use pristine or manually liberated CAMs, of which the target elements Li, Ni, Co, and

Mn, are dissolved in an aqueous solution in a step called leaching [23,24]. Subsequent steps involve the purification and recovery of the target elements, eventually leading to products that are high grade and suitable for use in new batteries. One of the first studies dates to 1998 [22]. In this study, the cathode active material, $LiCoO_2$, was manually removed from waste LiBs, followed by leaching of Li and Co in solutions of $H_2SO_3$, $NH_2OH$*HCl and HCl. More research on leaching was conducted in the following decades using a wide variety of chemicals, including acids such as $H_2SO_4$, HCl, and $H_3PO_4$ [21,22,25–29], as well as other reagents to accelerate the dissolution process, such as $H_2O_2$ and ascorbic acid [30–39]. Overall, these studies found that an increasing acid concentration, temperature and leaching time are beneficial for the leaching process, whereas a higher solid-to-liquid-ratio results in a lower leaching efficiency [22]. These trends are, after decades of research, well-known and widely proven. However, the conditions under which the experiments were conducted vary significantly, demonstrating that there is no one-size-fits-all approach. Further purification of Li, Ni, Co, and Mn has been investigated as well, with the most important methods being solvent extraction, precipitation and electrochemical purification [22,30,31,36,39,40]. Under well-controlled conditions, these purification routes can result in high purity products, while high energy consuming pyrometallurgical steps can be avoided. Therefore, hydrometallurgy is becoming the recycling strategy of choice for Li-ion batteries.

On industrial scale, hydrometallurgical LiB recycling is often preceded by an array of size reduction steps, such as shredding and milling, followed by physical separation steps to increase the metallic content, eventually resulting in a black powder called “Black Mass” (BM) which mainly contains the CAMs [41]. This so-called pre-treatment is followed by a combination of hydrometallurgical unit operations to extract and purify CRMs from LiBs. Exclusive hydrometallurgical recycling of LiBs has also been conducted on industrial scale. The Recupyl Valibat process starts by shredding and milling the spent LiBs, after which a size classification step is done by sieving. This is followed by magnetic separation and density separation, which remove most Fe, Cu, Al, and plastics. The Li and Co are removed through leaching and electrolysis. Another example is the Akkuser process [13], which also starts by mechanical size reduction followed by leaching. Although not reported how, recovery of Fe, Cu, and Co are claimed.

On one hand, research on LiB-recycling has been conducted intensively over the last decades, but many studies have focused on optimizing process parameters under ideal circumstances. This involves using synthetic or manually liberated starting materials for leaching experiments, or solutions free of impurities for purification research. On the other hand, current state-of-the-art industrial recycling processes do not yet achieve complete regeneration of the elements from LiBs

since they are often directed solely towards recovery of the valuable elements, such as Co, Ni, and Cu. However, end-of-life (EoL) LiB waste composition is complex and prone to variations. The CAMs listed in Table 1.1 can all be present together in a single stream in varying ratios, while materials from other parts of the LiB cell, such as Fe from the casing, graphite and Cu from the anode or Al from the cathode, are not fully separated from the target elements, Li, Ni, Co and Mn, during industrial scale pre-treatment [13]. This complicates hydrometallurgical recycling and results in high reagent consumption and the need for an extensive and costly purification process, since high grade battery precursors of Li, Ni, Co and Mn need near-complete removal of impurities. Hence, not all of the elements are often recovered, with a significant number of elements being downcycled or lost, and processes are paired with large costs, $CO_2$-emissions and waste-water generation [13,22,39,40,42–46]. Therefore, research is a needed to understand how the complex LiB waste stream influences the hydrometallurgical recycling process, how the process can be made flexible to accommodate this complexity, and how this can be achieved with limited energy and reagent consumption.

## 1.4. RESEARCH OBJECTIVES & THESIS OUTLINE

The shortcomings presented in the previous sections lead to the following research question:

***How can hydrometallurgical recycling be applied to a mixture of industrially pre-treated lithium-ion-battery waste to achieve comprehensive recovery of high quality products while minimizing environmental impact?***



To answer this question, five sub questions are formulated and answered during the thesis:

1. What compositional variabilities can be expected in mixed end-of-life Li-ion battery waste streams? (Ch 2, 3)
2. What is the influence of black mass composition on leaching? (Ch 3, 4)
3. How can the chemical consumption during leaching of mixed Li-ion battery waste be decreased? (Ch 4, 5, 6)
4. What purification approach enables low chemical consumption alongside flexibility towards varying and heterogeneous waste streams? (Ch 5, 6)
5. How can the choice of lixiviant impact downstream recycling? (Ch 6)

These sub questions are answered through the course of 7 chapters. A visual overview of the chapters, their objectives and experimental approach is given in Fig. 1.2.

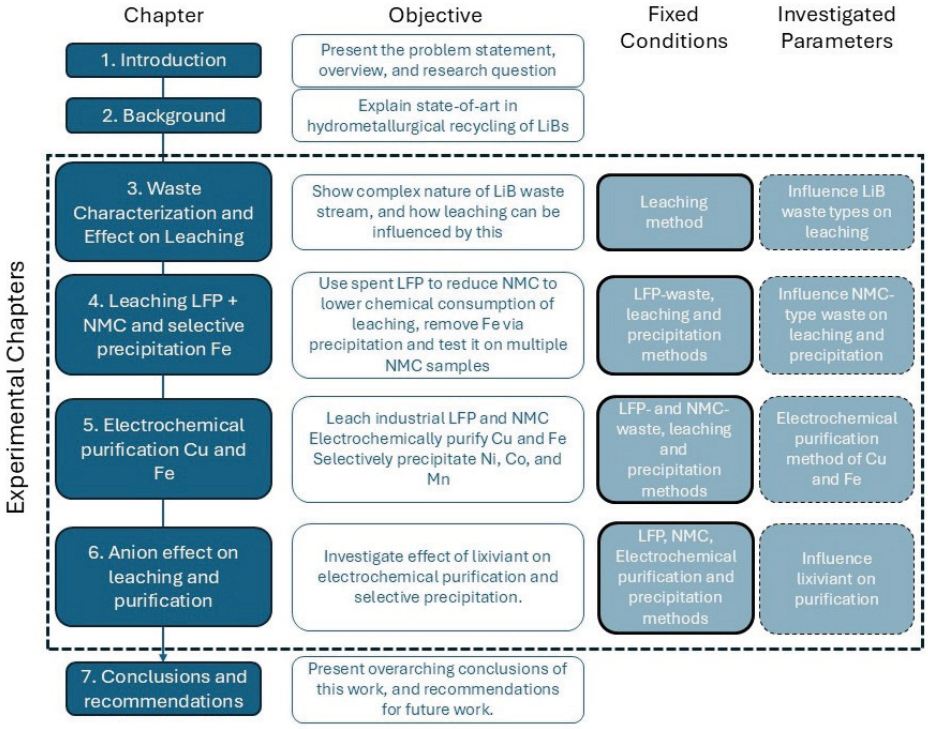


*Figure. 1.2: Thesis structure and overview of the chapters, their objectives and their experimental approach.*

In the first chapter, **Chapter 1**, the current limitations of Li-ion battery recycling, as well as the aim of this dissertation and its research question are formulated. **Chapter 2** provides a background of Li-ion battery recycling in both research and industry, with the aim of elaborating on the knowledge gap between state-of-the-art in research and large scale LiB-recycling. It discusses pre-treatment and provides a detailed coverage of the unit operations used in the experimental part of this research, including leaching and subsequent purification steps.

**Chapter 3** addresses the first two research questions by investigating the influence of LiB-waste composition on leaching. Various LiBs from consumer electronics are manually dismantled and analysed, providing clear insight into why industrially pre-treated black mass is prone to variation and contamination with impurities. Subsequently, pristine cathode materials, manually extracted cathode materials and industrial black masses are leached using the same conditions, enabling a detailed comparison of their leaching performance.

In recent years, the simultaneous recycling of NMC- and LFP-type LiBs gained increased interest due to their market prevalence, as well as its potential in lowering

the need for chemical reagents. However, former literature on leaching and further purification have largely excluded variations in material compositions. Therefore, **Chapter 4** investigates the use of LFP as a reductant for the leaching of multiple NMC-type wastes, including a complex industrial waste stream, followed further purification by precipitation. This chapter addresses the third sub question, while also answering the second sub question for a new leaching process.

Since the simultaneous leaching of LFP and NMC is promising, it is used as the starting point for detailed research on purification steps. To answer the fourth sub question, **Chapter 5** explores an original combination of selective precipitation with a novel electrochemical purification method as an alternative for conventional, energy and chemical intensive purification. An assessment of the resulting products in terms of recovery and grade is also provided.

In **Chapter 6**, the fifth sub question is aimed to be answered by investigating the effect of different lixiviants ($H_2SO_4$, HCl and $H_3PO_4$) on the in Chapter 5 developed leaching and purification process. The chapter provides a comparative evaluation of the leaching efficiency, as well as the composition of the recovered end products as a function of the applied lixiviant. The feasibility of electrochemical purification in all three systems is investigated.

**Chapter 7** presents overarching conclusions and practical recommendations for recycling industrially pre-treated LiB waste, considering its inherently complex and varying composition. The chapter synthesizes the findings from the research and answers found to the sub- and main research questions.

## REFERENCES


1. D. Stampatori, P.P. Raimondi, M. Noussan, Li-Ion Batteries: A Review of a Key Technology for Transport Decarbonization, *Energies 2020, Vol. 13, Page 2638* 13 (2020) 2638.
2. Y. Liang, C.Z. Zhao, H. Yuan, Y. Chen, W. Zhang, J.Q. Huang, D. Yu, Y. Liu, M.M. Titirici, Y.L. Chueh, H. Yu, Q. Zhang, A review of rechargeable batteries for portable electronic devices, *InfoMat* 1 (2019) 6–32.
3. I.Y.L. Hsieh, M.S. Pan, W.H. Green, Transition to electric vehicles in China: Implications for private motorization rate and battery market, *Energy Policy* 144 (2020) 111654.
4. J.C. Kelly, Q. Dai, M. Wang, Globally regional life cycle analysis of automotive lithium-ion nickel manganese cobalt batteries, *Mitig. Adapt. Strateg. Glob. Chang.* 25 (2019) 371–396.
5. M. Kamran, M. Raugei, A. Hutchinson, A dynamic material flow analysis of lithium-ion battery metals for electric vehicles and grid storage in the UK: Assessing the impact of shared mobility and end-of-life strategies, *Resour. Conserv. Recycl.* 167 (2021) 105412.
6. E.L. Schneider, W. Kindlein, S. Souza, C.F. Malfatti, Assessment and reuse of secondary batteries cells, *J. Power Sources* 189 (2009) 1264–1269.
7. M. Pagliaro, F. Meneguzzo, Lithium battery reusing and recycling: A circular economy insight, *Heliyon* 5 (2019) e01866.
8. J. Han, X. Gao, K. Gu, Lithium-ion batteries: Future market, challenges, and recycling, *Nanostructured Lithium-Ion Battery Materials: Synthesis, Characterization, and Applications* (2025) 587–620.
9. D. Deng, Li-ion batteries: basics, progress, and challenges, *Energy Sci. Eng.* 3 (2015) 385–418.
10. R. Korthauer, Lithium-ion batteries: Basics and applications, *Lithium-Ion Batteries: Basics and Applications* (2018) 1–413.
11. N. Nasajpour-Esfahani, H. Garmestani, M. Bagheritabar, D.J. Jasim, D. Toghraie, S. Dadkhah, H. Firoozeh, Comprehensive review of lithium-ion battery materials and development challenges, *Renewable and Sustainable Energy Reviews* 203 (2024) 114783.
12. A.K. Koech, G. Mwandila, F. Mulolani, P. Mwaanga, Lithium-ion battery fundamentals and exploration of cathode materials: A review, *S. Afr. J. Chem. Eng.* 50 (2024) 321–339.
13. O. Velázquez-Martínez, J. Valio, A. Santasalo-Aarnio, M. Reuter, R. Serna-Guerrero, A Critical Review of Lithium-Ion Battery Recycling Processes from a Circular Economy Perspective, *Batteries* 5 (2019) 68.
14. European Commission Directorate-General for Internal Market Industry Entrepreneurship and SMEs, M. Grohol, C. Veeh, Study on the critical raw materials for the EU 2023 – Final report, Publications Office of the European Union, 2023.
15. European Commission Directorate-General for Internal Market Industry Entrepreneurship and SMEs, D. Pennington, E. Tzimas, C. Baranzelli, J. Dewulf, S. Manfredi, P. Nuss, M. Grohol, A. Van Maercke, Y. Kayam, S. Solar, B. Vidal-Legaz, L. Talens Peirò, L. Mancini, C. Ciupagea, L. Godlewska, P. Dias, C. Pavel, D. Blagoeva, G. Blengini, V. Nita, C. Latunussa, C. Torres De Matos, F. Mathieux, A. Marmier, Methodology for establishing the EU list of critical raw materials – Guidelines, Publications Office, 2017.
16. W. Li, Review—An Unpredictable Hazard in Lithium-ion Batteries from Transition Metal Ions: Dissolution from Cathodes, Deposition on Anodes and Elimination Strategies, *J. Electrochem. Soc.* 167 (2020) 090514.

**17.** E. Bajraktarova-Valjakova, V. Korunoska-Stevkovska, S. Georgieva, K. Ivanovski, C. Bajraktarova-Misevska, A. Mijoska, A. Grozdanov, Hydrofluoric Acid: Burns and Systemic Toxicity, Protective Measures, Immediate and Hospital Medical Treatment, *Open Access Maced. J. Med. Sci.* 6 (2018) 2257.

**18.** A.A. Jensen, F. Tuchsen, Cobalt Exposure and Cancer Risk, *Crit. Rev. Toxicol.* 20 (1990) 427–439.

**19.** H. Guo, H. Liu, H. Wu, H. Cui, J. Fang, Z. Zuo, J. Deng, Y. Li, X. Wang, L. Zhao, Nickel Carcinogenesis Mechanism: DNA Damage, *Int. J. Mol. Sci.* 20 (2019) 4690.

**20.** X. Feng, M. Ouyang, X. Liu, L. Lu, Y. Xia, X. He, Thermal runaway mechanism of lithium ion battery for electric vehicles: A review, *Energy Storage Mater.* 10 (2018) 246–267.

**21.** S. Castillo, F. Ansart, C. Laberty-Robert, J. Portal, Advances in the recovering of spent lithium battery compounds, *J. Power Sources* 112 (2002) 247–254.

**22.** P. Zhang, T. Yokoyama, O. Itabashi, T.M. Suzuki, K. Inoue, Hydrometallurgical process for recovery of metal values from spent lithium-ion secondary batteries, *Hydrometallurgy* 47 (1998) 259–271.

**23.** C.K. Gupta, Chemical metallurgy: principles and practice, (2003) 811.

**24.** P. Hayes, Process Principles in Minerals and Materials Production with a Focus on Metal Production and Recycling, Fourth edition, Hayes Publishing Co, Sherwood, 2021.

**25.** J. Nan, D. Han, X. Zuo, Recovery of metal values from spent lithium-ion batteries with chemical deposition and solvent extraction, *J. Power Sources* 152 (2005) 278–284.

**26.** R.C. Wang, Y.C. Lin, S.H. Wu, A novel recovery process of metal values from the cathode active materials of the lithium-ion secondary batteries, *Hydrometallurgy* 99 (2009) 194–201.

**27.** P. Meshram, B.D. Pandey, T.R. Mankhand, Recovery of valuable metals from cathodic active material of spent lithium ion batteries: Leaching and kinetic aspects, *Waste Management* 45 (2015) 306–313.

**28.** M. Contestabile, S. Panero, B. Scrosati, A laboratory-scale lithium-ion battery recycling process, *J. Power Sources* 92 (2001) 65–69.

**29.** Z. Takacova, T. Havlik, F. Kukurugya, D. Orac, Cobalt and lithium recovery from active mass of spent Li-ion batteries: Theoretical and experimental approach, *Hydrometallurgy* 163 (2016) 9–17.

**30.** G. Dorella, M.B. Mansur, A study of the separation of cobalt from spent Li-ion battery residues, *J. Power Sources* 170 (2007) 210–215.

**31.** R. Sattar, S. Ilyas, H.N. Bhatti, A. Ghaffar, Resource recovery of critically-rare metals by hydrometallurgical recycling of spent lithium ion batteries, *Sep. Purif. Technol.* 209 (2019) 725–733.

**32.** X. Chen, H. Ma, C. Luo, T. Zhou, Recovery of valuable metals from waste cathode materials of spent lithium-ion batteries using mild phosphoric acid, *J. Hazard. Mater.* 326 (2017) 77–86.

**33.** C.K. Lee, K.I. Rhee, Reductive leaching of cathodic active materials from lithium ion battery wastes, *Hydrometallurgy* 68 (2003) 5–10.

**34.** G.P. Nayaka, J. Manjanna, K. V. Pai, R. Vadavi, S.J. Keny, V.S. Tripathi, Recovery of valuable metal ions from the spent lithium-ion battery using aqueous mixture of mild organic acids as alternative to mineral acids, *Hydrometallurgy* 151 (2015) 73–77.

**35.** Q. Meng, Y. Zhang, P. Dong, Use of glucose as reductant to recover Co from spent lithium ions batteries, *Waste Management* 64 (2017) 214–218.

**36.** S. Natarajan, A.B. Boricha, H.C. Bajaj, Recovery of value-added products from cathode and anode material of spent lithium-ion batteries, *Waste Management* 77 (2018) 455–465.

**37.** A.A. Nayl, M.M. Hamed, S.E. Rizk, Selective extraction and separation of metal values from leach liquor of mixed spent Li-ion batteries, *J. Taiwan Inst. Chem. Eng.* 55 (2015) 119–125.

**38.** L.P. He, S.Y. Sun, X.F. Song, J.G. Yu, Leaching process for recovering valuable metals from the $LiNi_1/_3Co_1/_3Mn_1/_3O_2$ cathode of lithium-ion batteries, *Waste Management* 64 (2017) 171–181.

**39.** Z. Dobó, T. Dinh, T. Kulcsár, A review on recycling of spent lithium-ion batteries, *Energy Reports* 9 (2023) 6362–6395.

**40.** A. Zanoletti, E. Carena, C. Ferrara, E. Bontempi, A Review of Lithium-Ion Battery Recycling: Technologies, Sustainability, and Open Issues, *Batteries* 10 (2024) 38.

**41.** S. Kim, J. Bang, J. Yoo, Y. Shin, J. Bae, J. Jeong, K. Kim, P. Dong, K. Kwon, A comprehensive review on the pretreatment process in lithium-ion battery recycling, *J. Clean. Prod.* 294 (2021) 126329.

**42.** A.M. Bernardes, D.C.R. Espinosa, J.A.S. Tenório, Recycling of batteries: a review of current processes and technologies, *J. Power Sources* 130 (2004) 291–298.

**43.** T. Zhao, W. Li, M. Traversy, Y. Choi, A. Ghahreman, Z. Zhao, C. Zhang, W. Zhao, Y. Song, A review on the recycling of spent lithium iron phosphate batteries, *J. Environ. Manage*. 351 (2024) 119670.

**44.** Y. Yao, M. Zhu, Z. Zhao, B. Tong, Y. Fan, Z. Hua, Hydrometallurgical Processes for Recycling Spent Lithium-Ion Batteries: A Critical Review, *ACS Sustain. Chem. Eng.* 6 (2018) 13611–13627.

**45.** A. Chagnes, B. Pospiech, A brief review on hydrometallurgical technologies for recycling spent lithium-ion batteries, *Journal of Chemical Technology & Biotechnology* 88 (2013) 1191–1199.

**46.** W. Lv, Z. Wang, H. Cao, Y. Sun, Y. Zhang, Z. Sun, A Critical Review and Analysis on the Recycling of Spent Lithium-Ion Batteries, *ACS Sustain. Chem. Eng.* 6 (2018) 1504–1521.

*Thus, the task is, not so much to see what no one has seen yet, but to think what nobody has thought yet, about that what everybody sees.*

Arthur Schopenhauer

# 2

# *Chapter 2*

## Fundamentals on Hydrometallurgical Recycling of Li-ion Batteries

In the introduction, the importance of Li-ion batteries in society was sketched. It was also established that they contain critical raw materials or CRMs, such as Li, Co and Mn, highlighting the need for recycling, with focus on hydrometallurgy. Chapter 2 aims to introduce the state-of-the-art in Li-ion battery recycling on both industrial and research level. The objective of this chapter is to briefly sketch how the LiBs are prepared for recycling on large scale and to compare the compositions of waste samples that are investigated in literature. Then, the main focus is to show the common practice in hydrometallurgical LiB-recycling, and what research has been conducted in the past years, leading to a better understanding of the knowledge gap presented in Chapter 1.

## 2.1. PROCESS FLOW OF LI-ION BATTERY RECYCLING

Recycling of LiBs has been plentifully researched and is also applied on large scale to some extent. Although variation between processes is seen, the general overview of a LiB-recycling process is shown in Fig. 2.1. The process typically begins with battery removal from end-of-life products, followed by a pre-treatment, in which the insides of the LiBs are exposed and their materials are separated based on their physical properties. These steps result in several fractions, of which the finest is known as black mass (BM). It contains the active electrode materials, i.e. most of the SRMs and CRMs, as well as contaminations of other fractions. This is followed by hydrometallurgical processing, starting from dissolution, or leaching, of the target elements into an aqueous solution, after which they are purified in subsequent steps with the aim to recover battery grade precursors [1–3]. This chapter describes this process in details, including the commonly applied unit operations in each recycling step, from the pre-treatment (section 2.1) and leaching (section 2.2), to purification and recovery (section 2.3). The most prevalent processes and unit operations reported in the literature, the steps which are part of the experimental parts (Chapter 3 – 6) of this thesis, as well as the current state of the art of industrial hydrometallurgical recycling are highlighted.

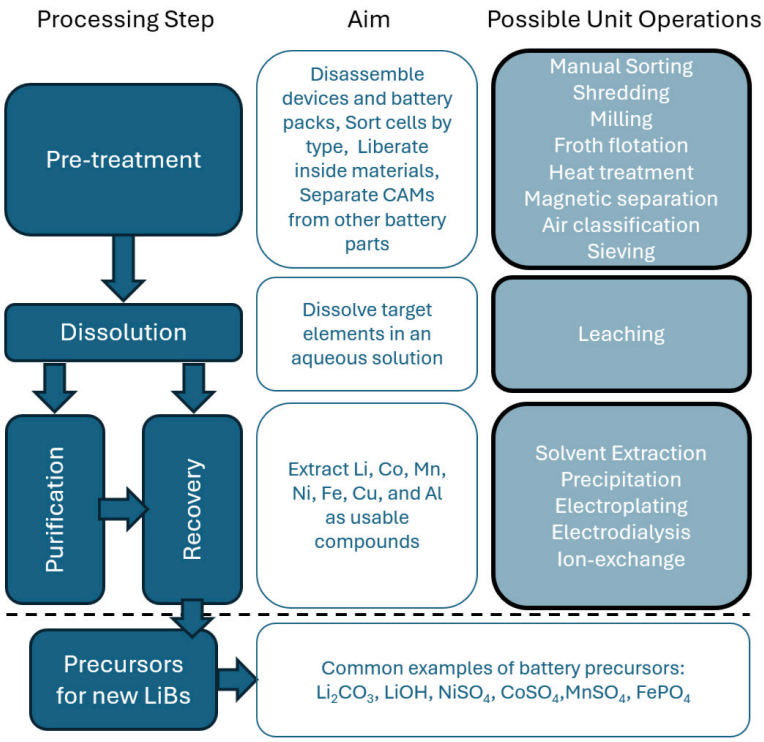


*Figure 2.1: Schematic overview of commonly practiced recycling steps for LiBs, their aim and corresponding unit operations.*

## 2.2. PRE-TREATMENT OF LIB-WASTE

Before the extraction of CRMs from LiBs is possible by hydrometallurgical recycling, the batteries must first undergo pre-treatment to liberate and separate the components from each other. LiBs generally have a strong casing that protects their internal components from damage and ensures safe operation, but this also makes the active materials (Li, Ni, Co and Mn) difficult to access. Hence, the batteries need to be disintegrated, either manually or via industrially sized unit operations. This chapter outlines the common approaches used for liberation of the cathode and anode materials. It highlights how these processes influence the composition of the resulting Black Mass. Three main types of unit operations are distinguished in the pre-treatment stage: manual, mechanical and thermal treatments.

### 2.2.1. Risk Mitigation Before & During Pre-treatment

Pre-treatment of LiBs is paired with major health and safety risks. Known dangers include the spontaneous combustion when LiBs are deformed or penetrated, as well as the toxicity of the compounds they contain [4,5]. To mitigate these risks, several precautionary measures can be taken during pre-treatment. At both research and industrial levels, some amount of manual labour is commonly applied, as according to EU-regulations LiBs in electronic products must be removed from their respective devices [6,7]. This requirement primarily aims to reduce fire risks, as well as avoid hazardous and toxic substances to end up in household waste. Hence, LiBs are manually removed from all portable electronic devices (PEDs) or dismantled from electric vehicles, resulting in a waste stream that ranges from individual cells to battery modules.

One way to mitigate the fire hazard during the subsequent pre-treatment is to discharge the batteries in a salt solution prior to disintegration. For example, they can be submerged in a NaCl or $K_2CO_3$ solution, resulting in controlled discharge from which the generated heat is absorbed by the aqueous solution [11]. However, especially in the case of the strongly corrosive NaCl solutions, this can result in electrolyte leakage, contaminating the solution with fluoride ions and organic solvents. Furthermore, such discharging typically takes 24 hours or more to complete, and is impractical for large scale operations. Despite this limitation, several industrial recycling processes, such as the Duesenfeld, Battery Resources and Onto technology processes still incorporate this step [3,8]. In academic research, this step is used often before manual opening of LiBs due to its simplicity [4,5].

Due to the practical limitations of the long discharge process, most current industrial settings make use of an inert atmosphere during size reduction to mitigate the fire hazard. Shredding of LiBs is carried out under Ar, $N_2$, or $CO_2$, or after cryogenic treatment with liquid $N_2$ [3–5]. These conditions suppress oxidation reactions and prevent thermal runaway. Such methods are used in the Duesenfeld, Retriev (Toxco) and Recupyl Valibat processes [3,8]. Working with closed systems also prevents toxic components from escaping [9,10]. A notable example is the fluorine containing electrolyte. When Li-salt ($LiPF_6$ or $LiBF_4$) comes into contact with water it can form HF, a very hazardous compound [11].

### 2.2.2. Mechanical Pre-treatment

The aim of mechanical treatment is to extract the active materials from the LiB-cells, resulting in a powder which is suitable for subsequent aqueous leaching. It pursues optimal separation of the components for further recovery in the safest achievable way. Hence, the mechanical pre-treatment concentrates the active materials into a black powder product called black mass. It typically involves a multitude of steps

such as crushing, shredding and sieving [4,5]. Fig. 2.2 shows the LiB-waste stream before and after mechanical treatment.

Firstly, the LiBs are submitted to an array of mechanical and physical unit operations, starting with a crushing step in which impact stresses are applied to the LiBs, leading to the breakage of the cells and exposure of the internal materials [4,5]. This can be achieved using rotary shear mills, hammer mills or cutting mills, yielding a coarse stream in which the battery materials remain recognisable. A second size reduction step further liberates the brittle CAMs, while the more ductile metals in the casing, collector foils (Al, Cu), and plastics largely retain their particle size. Subsequent steps make use of the physical properties of the components for their further separation. A magnetic separation removes steel and iron originating from cell casings and other parts, while sieving increases the content of Li, Co, Ni and Mn in the fine black mass fraction [3–5]. Furthermore, the differences in hydrophilicity between anode active materials (AAMs) and CAMs can be used to separate them. This is often done by froth flotation [12]. However, the organic binder that is used to attach active materials to their respective collector foil reduces their difference in hydrophilicity [12]. Occasionally, ultrasonic washing is applied to enhance liberation of the active materials from their collector foils [13,14]. This technique is aided by the use of solvents, which dissolve the binder and increase liberation, often achieving up to 99% of the active materials separation from the foils.



*Figure 2.2: LiB-waste before (left) and after (right) mechanical treatment as found in our research.*

### 2.2.3. Thermal Pre-treatment

For the black mass to have the desired properties for further recycling, mechanical operations are often combined with thermal treatments [15,16]. These treatments are commonly applied to remove binders and other organic materials, such as the separator, electrolyte and even surface coatings, avoiding contamination of aqueous

streams during downstream hydrometallurgical recycling. Thermal treatments are well-suited for industry use, as the equipment is widely available, and the practical execution is straightforward. A drawback, however, is the high energy consumption that is associated with these operations.

The binders in LiBs are often made of polyvinylidene fluoride (PVDF) [17]. Under an oxygen-containing atmosphere, it can start decomposing at temperatures from 350 °C [18]. For complete removal of organics, temperatures of 500 °C to 600 °C are generally applied. This results in splitting of polymeric chains to shorter units, and the subsequent detachment of active materials from collector foils [16]. This process can be enhanced by performing the heat treatment under vacuum. However, any leftover fluorine may generate hazardous by products such as HF [19], requiring appropriate scrubbing or cleaning systems. The carbon based components are not the only ones undergoing chemical transformation during heat treatment. At these high temperatures, the inorganic CAMs can be reduced by the graphite from the anode. This often also benefits downstream processing due to the better solubility of the resulting compounds [20].

### 2.2.4. Influence of Pre-treatment on Waste Composition

By combining the previously described unit operations, one can set up a variety of pre-treatment routes, all resulting in BM with varying composition and properties. While all BM typically contain the main target elements, including Li, Ni, Co, and Mn from NMC-type CAMs, or Li, Fe and $PO_4$ from LFP-type CAM, their oxidation state, types and amounts of impurities such as graphite, Al, and Cu differ. To illustrate this, the composition of a wide array of battery materials reported in literature on LiB-recycling is presented in Table 2.1. These are categorized into pristine materials, manually liberated materials and industrial BM samples. The pristine CAMs all have one common factor: the absence of impurities from other battery components, including organic contaminants and anode materials. Another interesting trait of pristine materials is that the composition does not always strictly match the nominal cathode type. For example, NMC 111 should theoretically have the equimolar amounts of Ni, Co and Mn. However, the NMC111 in the table diverts significantly form this ratio, since calculations come closer to a 4/3/3.5 ratio.

Overall, manually liberated materials contain more impurities than pristine materials. All of the reported samples typically include low amounts of Al and Cu, although some reach up to 8 wt.%. The impurity content is strongly dependent on the liberation process that is used to detach the active materials form the collector foils. For example, using solvent treatment to dissolve the binder, followed by filtration, generally results in low Al content, whereas grinding, heat treatment and sieving leads to higher contamination. Apart from Al and Cu, some samples

(excluding LFP) also show presence of Fe as impurity. Also noteworthy is the wide variation in the Ni/Co/Mn ratio observed in the reported waste samples. In the first instance, this depends on type of applied CAM chemistry, but some studies report mixing multiple CAMs together after liberation. Hence, when a LiB-waste sample is prepared manually, the amount of impurities are usually low, though the composition is still prone to variation and depends on the CAMs in the original LiBs.

In the lower part of Table 1, the compositions of industrial BM from various research papers are listed. A major difference compared to pristine and manually liberated samples is the general higher content of impurities. The contribution of metallic Al and Cu ranges from 0.16 to 11.7 wt.%, and from 0.48 to 4.6 wt.%, respectively, as a result of LiBs being shredded in their entirety. In contrast, manual liberation allows for careful removal of the cathode from other battery parts, which contain Cu (anode) and Fe (casing) as well as liberation of the CAMs from the cathode collector foil (Al). Fe is also present, ranging from 0.1 to 8.6 wt.%, likely coming from steel casing and/or LFP-type LiBs in the feed. Industrial BM is thus much more complex and typically contaminated with elements from the cell casings and anodes. Moreover, the total target metal concentration in the BMs is much lower than in pristine or manually liberated CAMs. This can be attributed to their “dilution” by graphite from the anode, which is a major component in industrial BM and is seldom reported, even though it is rarely completely removed [21,22]. Overall, table 1 demonstrates that BM composition can vary significantly, reflecting differences in pre-treatment methods, battery chemistries, and impurity levels. This variability highlights the importance of carefully characterizing BM for downstream recycling processes.

*Table 2.1: Elemental composition of LiB-waste samples from literature. "/" means that the presence of this element was not measured, while "0" means that this element was not detected.*

| Pre-treatment method | Main chemistry | Li | Co | Ni | Mn | Al | Fe | Cu | P | Reference |
|---|---|---|---|---|---|---|---|---|---|---|
| Pristine | NMC111 | 7.4 | 19.7 | 20.8 | 19.5 | / | / | / | / | [23] |
| Pristine | NMC111 | 7.8 | 20.5 | 23 | 16.6 | / | 0 | / | 0 | [24] |
| Pristine | LFP | 4.4 | / | / | / | / | 35.4 | / | 19.6 | [24] |
| Manual | Mix | 6.28 | 35.52 | 11.85 | 8.15 | 0.11 | / | / | / | [25] |
| Manual | 1 battery | 4.61 | 10.47 | 28.18 | 16.3 | 7.7 | 0.13 | 0.06 | / | [26] |
| Manual | Mix | 6.05 | 41.3 | 3.83 | 11.7 | 0.13 | 0.016 | 0.075 | / | [27] |
| Manual | Mix | 4 | 15 | 17 | 0.8 | 3.4 | 0.4 | 3.7 | / | [28] |
| Manual | LCO | 6.8 | 58.8 | 0.6 | 0 | 0.7 | / | / | / | [29] |
| Manual | NMC 532 | 7 | 12.7 | 30.7 | 18.7 | 0.64 | / | 0.02 | / | [30] |
| Manual | LFP | 5 | / | / | / | 4.4 | 25 | 7.6 | 12 | [31] |
| Manual | LMO | 4.5 | / | / | 26.5 | 5.2 | 2.3 | 5.4 | 3.1 | [31] |
| Manual | NMC | 4.2 | 15.6 | 15 | 20.5 | 4.8 | 0.5 | 8.1 | 1 | [31] |
| Manual | Mix | 5.8 | 41.3 | 3.8 | 11.4 | 0.2 | 0.02 | 0.07 | / | [32] |
| Manual | Mix | 7.6 | 20.5 | 19.4 | 19.5 | / | 0.1 | 0.004 | / | [33] |
| Industrial | Mix | 3.7 | 23.6 | 3.7 | / | 2.8 | 1.7 | 5.2 | / | [21] |
| Industrial | Mix | 5.2 | 6.5 | 22 | 7.3 | 3.7 | 0.01 | 4.8 | / | [22] |
| Industrial | Mix | 2.3 | 14.2 | 4.3 | 3.3 | 0.48 | 0.16 | 0.16 | / | [34] |
| Industrial | / | 4.1 | 8.7 | 15.8 | 8.4 | 2.4 | 0.1 | 2.3 | 9.8 | [24] |
| Industrial | / | 2.4 | 15.9 | 2.5 | 1.4 | 3.8 | 8.6 | 1.7 | 0.4 | [35] |
| Industrial | / | 3.9 | 26.5 | 2.7 | 1.7 | 1.6 | 0.6 | 2.7 | 0.5 | [35] |
| Industrial | Mix | 3.1 | 8.5 | 10.8 | 6.8 | 4.6 | 0.5 | 11.7 | / | [36] |
| Industrial | NMC 111 | 3.3 | 10 | 8.8 | 7.9 | 3.5 | 0.1 | 7.5 | / | [37] |

## 2.3. DISSOLVING CRITICAL ELEMENTS FROM LIB-WASTE: LEACHING

The first step in hydrometallurgical recycling of BM comprises of transferring the elements of interest from the solid material into a solution called the lixiviant, while preferably leaving impurities behind in the solid residue. Leaching has been used to extract metals from primary ores and secondary solid wastes for centuries [38,39] and is therefore a well-established process in industry. To quantify the amount a certain chemical element that dissolve compared to the feed material, the leaching efficiency ($\eta_L$) can be calculated according to equation (Eq. 2.1). In this equation, $\eta_L$ represents the leaching efficiency, $m^x_{PLS}$ the mass of element x that is dissolved to the pregnant leach solution (PLS), and $m^x_f$ the mass of that same element x originally present in the solid feed material. This is multiplied by 100, to result in a percentage.

$$\eta_L\,(\%) = \frac{m^x_{PLS}}{m^x_f} * 100 \qquad (2.1)$$



### 2.3.1. Acid Leaching & the Need for Reductive Conditions

Acid leaching is the most widely used method to dissolve Li, Ni, Mn and Co from LiB-waste [1,2,40,41]. The first leaching studies on LiB-waste dates from 1998, in which manually liberated LCO was subjected to leaching using three different lixiviants containing either $H_2SO_3$, $NH_2OH$*HCl or HCl [42]. The study found that increasing the acid concentration, temperature and contact time enhanced the dissolution of Li and Co. On the other hand, increasing the solid-to-liquid ratio (S/L) had negative effects on the dissolution [42]. These general trends have since been consistently observed in the literature for a variety of mineral acids [43–46]. For example, Meshram et al. [45] reported similar behaviour when leaching NMC-type waste in $H_2SO_4$. The overall reaction that was found to govern acid leaching, is shown in Eq. 2.2 [33]. In this equation, the sum of x, y and z equals to 1.

$$2LiNi_xMn_yCo_zO_2 + 6H^+ \rightarrow 2Li^+ + 2xNi^{2+} + 2yMn^{2+} + 2zCo^{2+} + 3H_2O + \frac{1}{2}O_2 \qquad (2.2)$$

In the study by Sattar et al. [33], acid leaching in 3 mol/L $H_2SO_4$ at 90 °C, with a solid to liquid ratio (S/L) of 60 g/L for 3 hours resulted in the dissolution of 95% of Li and Ni, 70 % Co and 35% Mn. Similar results were reported by Meshram et al. [45], who dissolved 93 % Li, 96% Ni, 50% Mn and 66% Co in 3 mol/L $H_2SO_4$ at 96 °C, 50 g/L over the course of 4 hours. These results show that with only an acid to drive dissolution of the CAMs, complete leaching is not achieved. This limitation arises because in CAMs such as $LiCoO_2$ and $LiNi_xMn_yCo_zO_2$, the transition metals (TMs)

are present in the average oxidation state +III [47]. In their delithiated or degraded form, these TMs are present in oxidation states +II, +III or +IV. To dissolve them effectively, these elements need to be reduced to their more soluble +II oxidation state [48]. Hence, there is a need for a reducing environment, a conclusion widely supported by subsequent research. Hence, many researchers combined mineral acids such as $H_2SO_4$, $HNO_3$, HCl and $H_3PO_4$ with additional reducing agents. Among the various reducing agents, $H_2O_2$ is most common, though $Fe^{2+}$ and $NaHSO_3$ have also been reported [26,33,48–56]. The resulting reaction during leaching is shown in Eq. 2.3. The general consensus is that the presence of a reducing agent is needed to approach complete dissolution of the TMs from the LiBs.

$$LiNi_xMn_yCo_zO_2 + 4H^+ + e^- \rightarrow Li^+ + xNi^{2+} + yMn^{2+} + zCo^{2+} + 2H_2O \quad (2.3)$$

Apart from mineral acids, organic acids, have also been reported plentifully in studies on LiB recycling, often with the aim to be a greener alternative [25,57–60]. Li et al. [60] reported leaching with acetic acid (1 mol/L), combined with $H_2O_2$ (6 v%), as well with maleic acid (2 mol/L) and $H_2O_2$ (4 v%). Both processes were conducted at 70°C for 60 min with an S/L of 20 g/L, resulting in 97 – 98% dissolution of Li, Ni, Co and Mn. In another study, Li et al. [59] showed that leaching with 0.5 mol/L citric acid and 1.5 v% $H_2O_2$ also resulted in near complete leaching. With 60 min of leaching at 90 °C and a S/L of 20 g/L, a result of > 95% leaching of Li, Ni, Co and Mn was achieved. These studies indicate that with these organic acids accompanied with a reducing agent, complete dissolution is still achievable. Such systems are often claimed to be environmentally friendlier due to lower secondary pollution and energy consumption compared to conventional mineral acids [25,58,59].

Other studies have explored organic reducing agents as substitutes for inorganic ones. For example, Pagnanelli et al. [61] demonstrated that glucose (50 g/L) can act as an effective reducing agent in combination with 2 mol/L $H_2SO_4$, achieving 88% dissolution of Co after 4 hours of leaching time at 80 °C, with a S/L of 35 g/L. Similarly , Chen et al. [62] used glucose (0.5 g/g of CAMs) together with citric acid (1.5 mol/L), achieving 99% dissolution of Li, and an average of 93% dissolution for Ni, Co and Mn after 2 hours at 80 °C. Other researchers investigated the use of waste tea leaves as replacement for $H_2O_2$ [29], alongside 1.5 mol/L citric acid. Using 0.4 g tea leaves per g of CAM and contact time of 2 hours at 90 °C, and S/L of and 30 g/L resulted in 98% Li and 96% Co dissolution. Similarly to replacing inorganic acids with organic ones, the replacement of inorganic reductants with organic compounds is generally deemed to be less hazardous and more environmentally friendly [29,61,62].

However, it is important to note that replacing inorganic reagents by organic ones does not necessarily improve the overall environmental impact of the

leaching process [63]. For example, the replacement of $H_2SO_4$ by citric acid may seem to improve circularity, since the latter can be produced by fermentation, is biodegradable, and is non-toxic [64,65]. However, $H_2SO_4$ is necessary in the production process of citric acid, rendering claims of replacement to be difficult to uphold [66]. Moreover, citric acid production requires large amounts of water and generates roughly 2.5 tons of waste per ton of acid. Additionally, leaching systems based on organic acids or reductants often employ lower S/L ratios, higher temperatures and longer leaching times [23,33,60,67–69], which can result in higher overall energy consumption. Therefore, leaching with inorganic acids and reducing agents remains an important area of research in Li-ion battery recycling.



### 2.3.2. Emerging Technologies for Sustainable Leaching

In an attempt to make the leaching process more sustainable, various methods have been explored, including the in-situ generation of reagents by microorganisms, reagent regeneration and process electrification. Instead of adding external reagents, the required acids can also be generated biologically by microorganisms. This approach is often regarded as less costly and more environmentally friendly, although it is time consuming and sensitive to environmental conditions and contamination [1]. Both fungi and bacteria can be used in this leaching method, therefore also named bioleaching. Fungi typically produce organic acids, while bacteria generate inorganic acids. In a study by Niu et al.[70], two bacterial species were used for in situ acid production. These cultures were pre-incubated in the presence of LiB waste for 30 days to develop tolerance to the metals present. Subsequentially, leaching with pulp density of 1%, 2% and 4% LiB waste was conducted. The researchers found that the bacterial culture was highly sensitive to high metal concentrations, as increasing the pulp density from 1 to 4 % decreased the leaching efficiencies of Li and Co from 80% to 37%, and from 52% to 10%, respectively. Zeng et al. [71], used bacteria (*Acidithiobacillus ferrooxidans)* in an aqueous solution of copper ions (0.75g/L) to leaching spent LiBs. A 99.9% leaching efficiency of Co was reached, but 6 days of contact time were necessary. Although the low need for starting chemicals, the overall long processing times in bioleaching make it a rather unattractive option for large scale Li-ion battery recycling. Moreover, the resulting low metal concentrations in the leachate make downstream processing challenging and result in a need for large reactor volumes to dissolve a relatively small amount of LiB-waste.

Another technique that makes use of an in-situ reagent generation is electrochemical leaching. In this process, the reducing agent needed for efficient dissolution of CAMs is generated directly in the leaching reactor by applying an electric current. Pei et al. [72] made use of a $CuSO_4$ solution which was electrolyzed

during the leaching reaction, which also contained the solid LiB-waste. This resulted in the reduction of $Cu^{2+}$ and the CAM at the cathode surface, resulting in $Cu^{+}$ and $Mn^{2+}$. The $Mn^{2+}$ released into the solution as a result of this, was oxidized to solid $MnO_2$ at the anode. Under conditions of 4.5h at 80 °C, a pH of 2.5, and current density of 50 $mA/m^2$, dissolution efficiencies of 92% Li, 89% Mn, 91% Co and 93% Ni were achieved. Zhong et al. [73] leached two CAM types, NMC and LFP ($LiFePO_4$), together in $H_2SO_4$ (1 mol/L) for 2 hours. A potential of 1V was applied, using NMC active material on carbon as cathode, and LFP active material on carbon as anode. This resulted in 98% dissolution of Li, Ni, Mn, Co, and Fe. Supported by other studies on electrochemical leaching [74–76], these results indicate that electrochemical leaching has the potential as a sustainable alternative to conventional acid leaching. However, further research is necessary to demonstrate its scalability and robustness against impurities and variation in composition of the waste feed.

Researchers have also explored different strategies to enhance leaching performance beyond optimizing the composition of the lixiviant. For instance, Li et al. [77] made use of an ultrasonic power of 90W for dissolution of Li and Co. They made use of 0.5 mol/L citric acid, 0.55M $H_2O_2$, a S/L of 25 g/L and a temperature of 60°C, and achieved 98% and 96% dissolution of Li and Co, respectively. Xu et al. [78] confirmed the positive effect of ultrasonic waves on leaching, stating that the local formation of voids results in extremely high pressure and temperature, as well as the in-situ formation of $H_2O_2$, which all lead to a higher leaching efficiency.

Alternative solvents have also been explored such as the use of deep eutectic solvents (DES) as potential lixiviants. Peeters et al. [79] synthesised a DES from water, choline chloride, and citric acid, which they used to dissolve LCO in presence of Al and Cu. With a S/L of 20 g/L and leaching time of 60 min at 40 °C, 98% of Co was dissolved. In the following years, many promising leaching research was published that made use of DES [80]. However, despite their promise, DES also come paired with significant drawbacks. While often portrayed as a more sustainable alternative to conventional acid dissolution processes, DES can suffer from limited chemical stability in metallurgical processes, high upscaling costs, difficulties with solvent recovery and re-use, and a lack of demonstration at pilot- and larger scales [81].

### 2.3.3. Solution Composition & Impurities in Acid Leaching Processes

Besides the leaching efficiency of the target elements (Li, Ni, Co and Mn) from the CAMs, the eventual composition, and hence the quality, of the PLS is also of high importance. The concentration of these target elements, as well as the level of contamination by impurities such as Al, Fe and Cu, all dictate what following

purification steps should be applied since new LiB precursors need to reach battery grade purity, usually 99.5% [82]. Moreover, even when similar leaching conditions are applied, the PLS composition can vary widely depending on the pre-treatment procedure, feed chemistry, and the leaching process conditions, such as the acid type and concentration. Table 2.2 demonstrates these aspects by showing the PLS compositions reported in various studies.

Firstly, one can see that no matter the pre-treatment type, impurities, i.e. Cu, Al, and Fe, are present in the PLS, effectively lowering the quality of the solution. These also differ strongly between studies. For example, Nan et al. [43] reported significant contamination by Cu (1.4 g/L), even though it only dissolved for 9%. They also found presence of Al (0.22 g/L), which is rather low due to their pre-treatment approach, in which they selectively removed the Al by alkaline leaching. When comparing this to the amount of target elements (22.2 g/L Li + Co) which leached for 98%, one can see that the presence of impurities is significant. Vieceli et al. [36] compared two leaching methods and reported large amounts of Al (2.5 – 7.5 g/L), a significant amount compared to the total amount of Li, Co, Ni and Mn (27.1 – 60.6 g/L total). Their Cu contamination was very minor, but contamination by Fe was found to be significant (0.29 – 0.43 g/L), resulting in the need for separation of the target elements from the dissolved impurities. Chen et al. [83] reported presence of Fe (1.96 g/L) and Cu (1.78 g/L) as impurities. The Li, Co, Ni and Mn had a total concentration of 19 g/L, again indicating a significant PLS quality loss due to a high presence of impurities compared to target elements.

Secondly, a strong difference is seen for the target elements among themselves, being Li, Ni, Co, and Mn. For example, the method of Peng et al. [84] results in a PLS containing 7 g/L Li, 44 g/L Co, 5 g/L Ni and 3 g/L Mn, while the PLS of Segura-Baillón et al. [85] contains 0.6 g/L Li, 0.5 g/L Co and 17.4 g/L Mn. This is a significant difference in PLS composition, which is not reflected in the average leaching efficiencies of Li, Ni, Co, and Mn in both studies, being 93% and 89%, respectively. Rather, the distinctions in PLS composition are a result of the difference in waste composition and the different leaching parameters. A large difference between the two PLS's from Gu et al. [30] and Gerold et al. [28], which both used manual CAM liberation, is also observed. These studies have a resulting PLS composition of 3.5 g/L Li, 6.3 g/L Co, 15.4 g/L Ni and 9.3 g/L Mn, versus 4 g/L Li, 12.7 g/L Co, 13.3 g/L Ni and 0.7 g/L Mn, respectively, indicating that these differences can also be large when using manually liberated CAMs. Vieceli et al. [36] also reported the concentration of all elements roughly doubled when comparing a S/L of 200 g/L to 100 g/L (L%), with the concentration of acid and reducing agent proportional to the S/L. However in other literature, increases of S/L are generally associated with lower leaching efficiency when reagent concentrations are not adjusted to accommodate

a higher feed concentration, as a result of reagent depletion [32,33,42,54,59]. In these cases, an increase in S/L can still result in increases of the concentrations of the elements from the LiB waste, albeit not linearly.

As concluded in section 2.5, the composition of the waste type depends on the chemistry of the cathodes from the LiB waste, and industrial pre-treatment results in dilution of these target elements compared to manual disassembly. Hence, together with the possible variation of S/L, this large variety will also be seen in the resulting PLS, even though the leaching efficiencies are similar. Understanding and controlling this variability is essential for two main reasons. First, impurities such as Fe, Al, or Cu could interfere with further recycling steps, leading to lower purity and yield of the recovered battery-grade precursors. Second, differences in the ratios of Li, Ni, Co, and Mn influence the design of subsequent hydrometallurgical processes, including pH control, reagent dosage, and solid–liquid separation strategies. Hence, achieving a predictable and well-characterized PLS composition is key to process optimization, scalability, and ensuring consistent product quality in a large-scale recycling process.

*Table 2.2: Concentrations of Li, Co, Ni, Mn, Al, Cu, and Fe (g/L) in the PLS from a selection of leaching studies.*

| Waste type | Lixiviant | T(°C) | t(min) | S/L (g/L) | Li | Co | Ni | Mn | Al | Fe | Cu | Reference |
|---|---|---|---|---|---|---|---|---|---|---|---|---|
| Manual | 2 mol/L $H_2SO_4$ + 1 mol. Eq. Glutathione | 65 | 60 | 100 | 3.5 | 6.3 | 15.35 | 9.3 | / | / | / | [30] |
| Manual | 2 mol/L $H_2SO_4$ | 80 | 240 | 100 | 4.1 | 12.7 | 13.3 | 0.7 | 2.1 | 0.3 | / | [28] |
| Manual | 3M $H_2SO_4$ | 70 | 360 | 200 | 2.06 | 20.1 | 0.04 | 0.002 | 0.22 | 0.01 | 1.42 | [43] |
| BM | 2M $H_2SO_4$ + 2 vol.% $H_2O_2$ | 80 | 60 | 50 | 1.78 | 7.18 | 4.29 | 5.68 | / | 1.96 | 1.78 | [83] |
| BM | 2M $H_2SO_4$ + 0.11M ascorbic acid | 80 | 90 | 200 | 6.98 | 44.14 | 4.96 | 3.2 | 5.59 | 1.29 | 0.11 | [84] |
| BM | 1m $H_2SO_4$ + 1.4 molar eq. hydrazine sulphate | 40 | 180 | 50 | 0.63 | 0.51 | 2.25 | 17.39 | 1.7 | 0.02 | 0.03 | [85] |
| BM | 2.5 mol/L $H_2SO_4$ + 0.3 mol//L $Na_2S_2O_5$ | 80 | 120 | 200 | 5.98 | 17.9 | 22.5 | 14.2 | 7.49 | 0.43 | 0.03 | [36] |
| BM | 1.25 mol/L $H_2SO_4$ + 0.15 mol//L $Na_2S_2O_5$ | 80 | 120 | 100 | 2.84 | 8.47 | 10.2 | 5.57 | 2.53 | 0.29 | 0.01 | [36] |
| BM | 2 mol/L $H_2SO_4$ + 6 vol.% $H_2O_2$ | 60 | 60 | 100 | 3 | 24.88 | 0.038 | 0.016 | 1.8 | 0.16 | 0.78 | [86] |

## 2.4. PURIFICATION AND RECOVERY OF NEW BATTERY MATERIALS

After dissolution into the PLS, the target elements have to be separated and purified for high-purity recovery. The synthesis of new CAMs such as NMC usually starts from Li-, Ni-, Co-, and Mn- carbonates or hydroxides [87]. Since these compounds are required to have purity of at least 99.5% [82], impurities such as Fe, Al, and Cu must be removed to facilitate the production of high-grade Li-, Ni-, Co-, and Mn-compounds. In the context of Li-ion battery recycling, the two most widely used unit operations for this purpose are solvent extraction (SX) and precipitation [1,2,88]. In addition to these well-stablished techniques, other means of purification are emerging in research on LiB recycling, such as electrochemical deposition, the sol-gel method, ion exchange and electrodialysis [1,2,88]. The most prevalent of these techniques are discussed and compared in this section.

### 2.4.1. Solvent Extraction

In SX, the aqueous PLS is brought into contact with an organic phase consisting of a solvent called the diluent, which contains an extractant [1,38,79,89]. This extractant is a molecule that preferably associates with one of the metals in the aqueous phase, forming an extractant-metal complex that subsequently transfers to the organic phase. This results in one element being selectively transferred to the organic solution, after which it can be recovered. In the context of LiBs, SX is often used to separate Ni, Co, or Mn from each other [89,90]. Industrial processes that incorporate SX in their flowsheets are the Brunp, GEM and JX Nippon Mining and Metals processes [91]. However, despite its potential, widespread adoption of this unit operation in LiB recycling is not yet achieved due to complex operating parameters and high investment costs [3,92]. Nonetheless, the method has been reported on plentifully in literature. Kang et al. [86] use an extractant called Cyanex® 272 to remove Co from a solution containing Ni and Li. They extracted 95 – 98% Co to the organic phase, together with merely 1% of the Ni. In another study, Chen et al.[83] made use of Mextral®272P to separate Co an Ni, reporting 97.8% Co extraction, while Chen et al [90] also achieved 97% Mn extraction from Li by using D2EHPA.

The benefit of SX is that when multiple stages are combined, often employing different parameters and extractants, high purity end products can be obtained [1,2]. This is crucial in the recycling of LiBs, as impurities in battery precursors can be detrimental to the electrochemical performance of CAMs. SX also offers short reaction times, typically around 30 minutes [1]. However, it suffers from high cost of the diluents, which are often petroleum-based solvents [38,93], as well as the extractant molecules themselves. Both extractants and diluents are also prone to

degradation, limiting their re-use over multiple cycles [94–97]. Moreover, precise pH control is required during the process, as it strongly influences the metals distribution between the organic and aqueous phases, resulting in complex operation [38,39]. Therefore, SX has potential to be a significant link in the LiB recycling chain should its environmental impact be mitigated and upscaling made more straight forward.

### 2.4.2. Precipitation

Precipitation involves transforming species in solution to a solid compound. This can be achieved through pH adjustment or by adding precipitation or complexing agents [38,93]. Selective precipitation exploits the different solubilities of metallic species in an aqueous solution to achieve separation. In LiB recycling, precipitation has been applied both to remove impurities such as Fe, Cu and Al from the PLS [98], and to convert Li, Co, Ni, or Mn into solid battery precursor [99,100]. For example, Chen et al. [90] applied pH adjustment to remove Fe and Cu from their PLS. A solution of 1 mol/L NaOH was added incrementally to increase the pH in steps of 0.5, starting at 1 and eventually reaching 5, at a temperature of 60°C. They found that by pH 3 Fe precipitated as $Fe(OH)_3$, following Eq.(2.4). Chernyaev et al. [101] employed both hydroxide and phosphate precipitation for removal of Fe and Al from a synthetic PLS at 60°C. They achieved 99% precipitation of Fe and Al at pH 3 in phosphate media (Eq. 2.5), while in hydroxide media a higher pH of 3.5 was required. Zou et al. [102] demonstrated that for a PLS obtained from combined LFP and NMC leaching, Fe removal of 97.8% is possible using NaOH at 60 °C and pH of 2. Further increase of the pH to 4.5 resulted in complete precipitation of Fe, accompanied by 91% precipitation of Al.

$$Fe^{3+} + 3OH^{-} \rightarrow Fe\left(OH\right)_{3(s)} \tag{2.4}$$

$$M^{3+} + PO_4^{3-} \rightarrow MPO_{4(s)} \left(M = Al, Fe\right) \tag{2.5}$$

In addition to impurity removal, Li, Ni, Co, and Mn can also be separately recovered from solution through precipitation. This is often done by adding salts such as $(NH_4)_2CO_3$ and $Na_2CO_3$, which readily form insoluble carbonates with these elements. The approach has been extensively demonstrated for Ni [40,67], Mn [56,103], Co [104], and Li [79,105] (Eqs. 2.6 and 2.7), and in some cases resulted in co-precipitates [105]. Phosphate salts have also been used as precipitation agents, either for the recovery of Li (Eq. 2.8) [106] or for transition metals such as Co (Eq. 2.9) [50]. Oxalates are another class of effective precipitants, which are primarily used to precipitate Co (Eq. 2.10) [43,56,107,108]. Oxalates and carbonates come with the additional benefit

of easy transformation to oxides by heat treatment, resulting in possible battery precursors [107].

$$M^{2+} + Na_2CO_{3(s)} \rightarrow MCO_{3(s)} + 2Na^{+} \left(M = Ni, Co, Mn\right) \quad (2.6)$$

$$2Li^{+} + Na_2CO_{3(s)} \rightarrow Li_2CO_{3(s)} + 2Na^{+} \quad (2.7)$$

$$3Li^{+} + Na_3PO_{4(s)} \rightarrow Li_3PO_{4(s)} + 3Na^{+} \quad (2.8)$$

$$3Co^{2+} + 2PO_4^{3-} \rightarrow Co_3(PO_4)_{2(s)} \quad (2.9)$$

$$Co^{2+} + H_2C_2O_{4(aq)} \rightarrow CoC_2O_{4(s)} + 2H^{+} \quad (2.10)$$

Although precipitation is a straightforward operation to separate metal species from a solution without the need for petroleum based solvents, it still has its shortcomings in the context of Li-ion battery recycling. Firstly, complete separation of Ni, Co and Mn is not possible without involving reagents such as oxalates, hypochlorites ($OCl^-$) or permanganates ($MnO_4^-$) [43,51,99,109], which drives up the process complexity and environmental footprint. On the other hand, one could coprecipitate these elements through pH adjustment with a simple base such as $Na_2CO_3$, but this has limited flexibility, since it results in a fixed Ni-Co-Mn ratio which subsequently results in one possible CAM-type that can be produced [110]. Secondly, the complete removal of impurities such as Fe, Al and Cu needs additional purification besides precipitation. In most cases, removing all of these elements by precipitation results in a loss of target elements, or treatments such as solvent extraction are needed to reach battery grade products [101,111,112]. Thirdly, precipitation often results in metal salts of which the anion, mainly resulting from the leaching acid or precipitation agent, needs to be replaced before re-use. This is the case for many sulphate, sulphide or chloride compounds of Ni, Co and Mn [54,86,113,114]. Lastly, the formation of waste salts from this process is a problem. Most prevalently, the sulphuric acid leaching followed by pH adjustment produces large amounts of $Na_2SO_4$ as waste product [114]. Although researchers have looked into recycling this into the respective acids and bases [115], this is still one of the major downsides of precipitation.

### 2.4.3. Electrochemical Purification

Beyond these two main purification and/or recovery methods, several emerging techniques have been increasingly reported in literature. Electrodeposition or electrowinning has been successfully applied to recover metals from solutions obtained after leaching of LiBs. Freitas et al. [116] report Co removal through

electrodeposition after leaching spent cathode materials in a combination of HCl and $H_2O_2$, resulting in a solution with 0.1 mol/L Li and Co each, which was adjusted to pH 5.4. With an applied potential of -1.00 V on an Al cathode, and a charge density 10.0 C/cm$^2$, they succeeded in plating pure Co with a charge efficiency of 96.9%. In a later study by Garcia et al. [117], a similar approach was taken with a stainless steel cathode and a potential of 1.7 V, resulting in Co plating with 96% efficiency. Other metals present in LiBs were also studied for their potential recovery through electrowinning. Moreover, the earlier study by Pei et al. [72] applied a second electrodeposition step that was aimed at $MnO_2$ recovery at the anode, and a Ni-Co alloy recovery at the cathode. At 70 °C and a current density of 40 mA/m$^2$, the Mn was recovered with 30% current efficiency after 10 h, and the Ni and Co were recovered with 72% current efficiency after 7 and 3 hours, respectively. A study by Rodrigues et al. [118] aims at the separation of Cu and Mn by application of -0.5V to a PLS obtained from spent LiBs. Over the course of 20 hours all of the Cu and Mn is reported to be removed from solution, with close to 100% purity Cu deposited at the cathode, and similar purity $MnO_2$ at the anode. The Ni and Co are unaffected by the electrochemical method.



Electrochemical purification techniques have also been applied outside Li-ion battery recycling in promising ways. For example, after leaching NdFeB-waste in HCl, Venkatesan et al. [119] oxidized $Fe^{2+}$ to $Fe^{3+}$ in situ using a large anode-to-cathode ratio, thereby increasing its separability from the rare-earth elements as oxalates, resulting in rare-earth products with >99% purity. Moreover, subsequent solution neutralization and electro-winning resulted deposition of Co metal. This approach holds potential relevance in LiB-recycling, as Fe is a common contamination in a PLS obtained from LiBs and Co is a main constituent of the CAMs. These studies show that electrochemical purification and recovery are promising approached in LiB recycling. However, their constraining long processing times and sometimes low current efficiencies leave more investigating work to be desired.

### 2.4.4. Other Purification & Recovery Methods

Another promising approach is the sol-gel method, in which the PLS undergoes chemical transformation to a gel form that entraps the desired elements. These processes often start with leaching with organic acids, which are preferred for their ability to form complexes with the desired elements. Through subsequent thermal treatments, called calcination, the required cathode active materials such as $LiCoO_2$ and $LiNi_xMn_yCo_zO_2$ (NMC) can be crystalized [120,121]. Although this method is relatively simple, the use of organic acids, long reaction times, and additional chemicals to adjust the PLS to a desired composition drive up the overall process costs [1,120]. Further research has also explored ion-exchange and electrodialysis

for purification and metal recovery [122,123]. However, these techniques are hard to implement at industrial scale due to high costs and complex operation.

## 2.5. CONCLUSIONS

The strong compositional variation and complexity of Li-ion battery waste, as well as its increasing volume, emphasises the need for an efficient recycling technology of critical raw materials such as Li, Ni, Co and Mn. The heterogeneous and inconsistent composition of this waste product pose significant hurdles for an effective recycling process. Effective pre-treatment and controlled leaching are essential to dissolve target elements into a pregnant leach solution (PLS) while minimizing impurities and reagent consumption. A range of lixiviants, from inorganic acids to organic and bio-based alternatives combined with reducing agents, have been investigated to achieve near complete dissolution while also attempting to minimize the environmental impact of the process.

Following leaching, purification and final recovery of the dissolved metals are essential to achieve the purity levels required for closed-loop recycling, enabling the use of the recovered products in new batteries. This requires a process that ensures overall efficiency, sustainability, and economic viability, while also possessing some form of adaptability and robustness to the varying composition akin to the LiB-waste. Conventional hydrometallurgical techniques, such as solvent extraction (SX) and precipitation, remain the most established routes, both in literature and in larger scale demonstrations. These unit operations are capable of achieving high-purity recovery of transition metals and Li. However, reliance on extensive use of reagents, sensitivity to operational parameters such as pH and temperature, as well as unknown robustness against varying waste compositions limit their industrial implementation.

These insights demonstrate that, while hydrometallurgical processing provides a technically mature foundation for LiB recycling, a deeper understanding of the underlying chemistry that links the waste composition, leaching efficiency, solution quality, separation, and purification is still needed. Bridging these aspects will be essential to design optimized and flexible recycling routes capable of handling the growing diversity of LiB chemistries on industrial scale. Therefore, there are urgent needs to establish a more robust and flexible hydrometallurgical recycling process with a low environmental footprint, ultimately contributing to a more circular and resilient battery value chain.

## REFERENCES


1. Z. Dobó, T. Dinh, T. Kulcsár, A review on recycling of spent lithium-ion batteries, *Energy Reports* 9 (2023) 6362–6395.
2. Y. Yao, M. Zhu, Z. Zhao, B. Tong, Y. Fan, Z. Hua, Hydrometallurgical Processes for Recycling Spent Lithium-Ion Batteries: A Critical Review, *ACS Sustain. Chem. Eng.* 6 (2018) 13611–13627.
3. O. Velázquez-Martínez, J. Valio, A. Santasalo-Aarnio, M. Reuter, R. Serna-Guerrero, A Critical Review of Lithium-Ion Battery Recycling Processes from a Circular Economy Perspective, *Batteries* 5 (2019) 68.
4. D. Yu, Z. Huang, B. Makuza, X. Guo, Q. Tian, Pretreatment options for the recycling of spent lithium-ion batteries: A comprehensive review, *Miner. Eng.* 173 (2021) 107218.
5. T. Gao, T. Dai, N. Fan, Z. Han, X. Gao, Comprehensive review and comparison on pretreatment of spent lithium-ion battery, *J. Environ. Manage.* 363 (2024) 121314.
6. Directive (EU) 2018/849 of the European Parliament and of the Council of 30 May 2018 amending Directives 2000/53/EC on end-of-life vehicles, 2006/66/EC on batteries and accumulators and waste batteries and accumulators, and 2012/19/EU on waste electrical and electronic equipment, *Official Journal* L 150 (2018) 93–99.
7. Directive 2012/19/EU of the European Parliament and of the Council of 4 July 2012 on waste electrical and electronic equipment (WEEE), *Official Journal* L 197 (2012) 38–71.
8. Ecofriendly recycling of lithium-ion batteries, (n.d.). https://www.duesenfeld.com/index.html (accessed July 23, 2025).
9. A.A. Jensen, F. Tuchsen, Cobalt Exposure and Cancer Risk, *Crit. Rev. Toxicol.* 20 (1990) 427–439.
10. H. Guo, H. Liu, H. Wu, H. Cui, J. Fang, Z. Zuo, J. Deng, Y. Li, X. Wang, L. Zhao, Nickel Carcinogenesis Mechanism: DNA Damage, *Int. J. Mol. Sci.* 20 (2019) 4690.
11. E. Bajraktarova-Valjakova, V. Korunoska-Stevkovska, S. Georgieva, K. Ivanovski, C. Bajraktarova-Misevska, A. Mijoska, A. Grozdanov, Hydrofluoric Acid: Burns and Systemic Toxicity, Protective Measures, Immediate and Hospital Medical Treatment, *Open Access Maced. J. Med. Sci.* 6 (2018) 2257.
12. S. Nazari, A.B. Vakylabad, K. Asgari, J. Li, H. Khoshdast, Y. He, A. Hassanzadeh, Bubbles to batteries: A review of froth flotation for sustainably recycling spent lithium-ion batteries, *J. Energy Storage* 84 (2024) 110702.
13. X. Ren, Z. Tong, Y. Dai, G. Ma, Z. Lv, X. Bu, M. Bilal, A.B. Vakylabad, A. Hassanzadeh, Effects of Mechanical Stirring and Ultrasound Treatment on the Separation of Graphite Electrode Materials from Copper Foils of Spent LIBs: A Comparative Study, *Separations* 10 (2023) 246.
14. J. Li, P. Shi, Z. Wang, Y. Chen, C.C. Chang, A combined recovery process of metals in spent lithium-ion batteries, *Chemosphere* 77 (2009) 1132–1136.
15. E. Mousa, X. Hu, L. Ånnhagen, G. Ye, A. Cornelio, A. Fahimi, E. Bontempi, P. Frontera, C. Badenhorst, A.C. Santos, K. Moreira, A. Guedes, B. Valentim, Characterization and Thermal Treatment of the Black Mass from Spent Lithium-Ion Batteries, *Sustainability (Switzerland)* 15 (2023) 15.
16. Y. Yang, G. Huang, S. Xu, Y. He, X. Liu, Thermal treatment process for the recovery of valuable metals from spent lithium-ion batteries, *Hydrometallurgy* 165 (2016) 390–396.
17. B. Chen, Z. Zhang, M. Xiao, S. Wang, S. Huang, D. Han, Y. Meng, Polymeric Binders Used in Lithium Ion Batteries: Actualities, Strategies and Trends, *ChemElectroChem* 11 (2024) e202300651.
18. C. Hanisch, T. Loellhoeffel, J. Diekmann, K.J. Markley, W. Haselrieder, A. Kwade, Recycling of lithium-ion batteries: a novel method to separate coating and foil of electrodes, *J. Clean. Prod.* 108 (2015) 301–311.
19. B. Wang, Y. Yin, H. Deng, H. Zhu, G. Li, W. He, Migration, transformation, and management of fluorine-containing substances in lithium-ion batteries during recycling − A review, *Sep. Purif. Technol.* 358 (2025) 130283.

**20.** N. Vieceli, R. Casasola, G. Lombardo, B. Ebin, M. Petranikova, Hydrometallurgical recycling of EV lithium-ion batteries: Effects of incineration on the leaching efficiency of metals using sulfuric acid, *Waste Management* 125 (2021) 192–203.

**21.** M. Aaltonen, C. Peng, B.P. Wilson, M. Lundström, Leaching of Metals from Spent Lithium-Ion Batteries, *Recycling* 2 (2017) 20.

**22.** E. Gerold, C. Schinnerl, H. Antrekowitsch, Critical Evaluation of the Potential of Organic Acids for the Environmentally Friendly Recycling of Spent Lithium-Ion Batteries, *Recycling* 7 (2022) 4.

**23.** L.P. He, S.Y. Sun, X.F. Song, J.G. Yu, Leaching process for recovering valuable metals from the $LiNi_{1/3}Co_{1/3}Mn_{1/3}O_2$ cathode of lithium-ion batteries, *Waste Management* 64 (2017) 171–181.

**24.** Y. Zou, A. Chernyaev, M. Ossama, S. Seisko, M. Lundström, Leaching of NMC industrial black mass in the presence of LFP, *Sci. Rep.* 14 (2024) 1–14.

**25.** L.P. He, S.Y. Sun, Y.Y. Mu, X.F. Song, J.G. Yu, Recovery of Lithium, Nickel, Cobalt, and Manganese from Spent Lithium-Ion Batteries Using l-Tartaric Acid as a Leachant, *ACS Sustain. Chem. Eng.* 5 (2016) 714–721.

**26.** S. Ghassa, A. Farzanegan, M. Gharabaghi, H. Abdollahi, The reductive leaching of waste lithium ion batteries in presence of iron ions: Process optimization and kinetics modelling, *J. Clean. Prod.* 262 (2020) 121312.

**27.** Y. Chen, D. Chang, N. Liu, F. Hu, C. Peng, X. Zhou, J. He, Y. Jie, H. Wang, B.P. Wilson, M. Lundstrom, Biomass-Assisted Reductive Leaching in H2SO4 Medium for the Recovery of Valuable Metals from Spent Mixed-Type Lithium-Ion Batteries, *JOM* 71 (2019) 4465–4472.

**28.** E. Gerold, S. Luidold, H. Antrekowitsch, Selective Precipitation of Metal Oxalates from Lithium Ion Battery Leach Solutions, *Metals (Basel).* 10 (2020) 1435.

**29.** X. Chen, C. Luo, J. Zhang, J. Kong, T. Zhou, Sustainable Recovery of Metals from Spent Lithium-Ion Batteries: A Green Process, *ACS Sustain. Chem. Eng.* 3 (2015) 3104–3113.

**30.** K. Gu, X. Gu, Y. Wang, W. Qin, J. Han, A green strategy for recycling cathode materials from spent lithium-ion batteries using glutathione, *Green Chemistry* 25 (2023) 4362–4374.

**31.** Y. Xin, X. Guo, S. Chen, J. Wang, F. Wu, B. Xin, Bioleaching of valuable metals Li, Co, Ni and Mn from spent electric vehicle Li-ion batteries for the purpose of recovery, *J. Clean. Prod.* 116 (2016) 249–258.

**32.** Y. Chen, N. Liu, F. Hu, L. Ye, Y. Xi, S. Yang, Thermal treatment and ammoniacal leaching for the recovery of valuable metals from spent lithium-ion batteries, *Waste Management* 75 (2018) 469–476.

**33.** R. Sattar, S. Ilyas, H.N. Bhatti, A. Ghaffar, Resource recovery of critically-rare metals by hydrometallurgical recycling of spent lithium ion batteries, *Sep. Purif. Technol.* 209 (2019) 725–733.

**34.** L.A. Diaz, M.L. Strauss, B. Adhikari, J.R. Klaehn, J.S. McNally, T.E. Lister, Electrochemical-assisted leaching of active materials from lithium ion batteries, *Resour. Conserv. Recycl.* 161 (2020) 104900.

**35.** J. Biswas, E. Esekheigbe, J. Partinen, L. Klemettinen, M. Lundström, A. Jokilaakso, Effect of In-Situ Catalyst on Co Extraction from Lithium-Ion Battery Scrap Via Selective Sulfation Roasting, *JOM* 77 (2025) 2244–2257.

**36.** N. Vieceli, C.A. Nogueira, C. Guimarães, M.F.C. Pereira, F.O. Durão, F. Margarido, Hydrometallurgical recycling of lithium-ion batteries by reductive leaching with sodium metabisulphite, *Waste Management* 71 (2018) 350–361.

**37.** J. Partinen, P. Halli, A. Varonen, B.P. Wilson, M. Lundström, Investigating battery black mass leaching performance as a function of process parameters by combining leaching experiments and regression modeling, *Miner. Eng.* 215 (2024) 108828.

**38.** P. Hayes, Process Principles in Minerals and Materials Production with a Focus on Metal Production and Recycling, Fourth edition, Hayes Publishing Co, Sherwood, 2021.

**39.** M.L. Free, Hydrometallurgy, Springer International Publishing, Salt Lake City, 2022.

**40.** A.A. Nayl, R.A. Elkhashab, S.M. Badawy, M.A. El-Khateeb, Acid leaching of mixed spent Li-ion batteries, *Arabian Journal of Chemistry* 10 (2017) S3632–S3639.

**41.** L. Brückner, J. Frank, T. Elwert, Industrial Recycling of Lithium-Ion Batteries—A Critical Review of Metallurgical Process Routes, *Metals (Basel).* 10 (2020) 1107.

**42.** P. Zhang, T. Yokoyama, O. Itabashi, T.M. Suzuki, K. Inoue, Hydrometallurgical process for recovery of metal values from spent lithium-ion secondary batteries, *Hydrometallurgy* 47 (1998) 259–271.

**43.** J. Nan, D. Han, X. Zuo, Recovery of metal values from spent lithium-ion batteries with chemical deposition and solvent extraction, *J. Power Sources* 152 (2005) 278–284.

**44.** Z. Takacova, T. Havlik, F. Kukurugya, D. Orac, Cobalt and lithium recovery from active mass of spent Li-ion batteries: Theoretical and experimental approach, *Hydrometallurgy* 163 (2016) 9–17.

**45.** P. Meshram, B.D. Pandey, T.R. Mankhand, Recovery of valuable metals from cathodic active material of spent lithium ion batteries: Leaching and kinetic aspects, *Waste Management* 45 (2015) 306–313.

**46.** S. Castillo, F. Ansart, C. Laberty-Robert, J. Portal, Advances in the recovering of spent lithium battery compounds, *J. Power Sources* 112 (2002) 247–254.

**47.** R. Korthauer, Lithium-ion batteries: Basics and applications, *Lithium-Ion Batteries: Basics and Applications* (2018) 1–413.

**48.** C.K. Lee, K.I. Rhee, Reductive leaching of cathodic active materials from lithium ion battery wastes, *Hydrometallurgy* 68 (2003) 5–10.

**49.** G. Dorella, M.B. Mansur, A study of the separation of cobalt from spent Li-ion battery residues, *J. Power Sources* 170 (2007) 210–215.

**50.** X. Chen, H. Ma, C. Luo, T. Zhou, Recovery of valuable metals from waste cathode materials of spent lithium-ion batteries using mild phosphoric acid, *J. Hazard. Mater.* 326 (2017) 77–86.

**51.** E.G. Pinna, M.C. Ruiz, M.W. Ojeda, M.H. Rodriguez, Cathodes of spent Li-ion batteries: Dissolution with phosphoric acid and recovery of lithium and cobalt from leach liquors, *Hydrometallurgy* 167 (2017) 66–71.

**52.** Q. Meng, Y. Zhang, P. Dong, Use of glucose as reductant to recover Co from spent lithium ions batteries, *Waste Management* 64 (2017) 214–218.

**53.** G.P. Nayaka, J. Manjanna, K. V. Pai, R. Vadavi, S.J. Keny, V.S. Tripathi, Recovery of valuable metal ions from the spent lithium-ion battery using aqueous mixture of mild organic acids as alternative to mineral acids, *Hydrometallurgy* 151 (2015) 73–77.

**54.** S. Natarajan, A.B. Boricha, H.C. Bajaj, Recovery of value-added products from cathode and anode material of spent lithium-ion batteries, *Waste Management* 77 (2018) 455–465.

**55.** W. Gao, X. Zhang, X. Zheng, X. Lin, H. Cao, Y. Zhang, Z. Sun, Lithium Carbonate Recovery from Cathode Scrap of Spent Lithium-Ion Battery: A Closed-Loop Process, *Environ. Sci. Technol.* 51 (2017) 1662–1669.

**56.** P. Meshram, B.D. Pandey, T.R. Mankhand, Hydrometallurgical processing of spent lithium ion batteries (LIBs) in the presence of a reducing agent with emphasis on kinetics of leaching, *Chemical Engineering Journal* 281 (2015) 418–427.

**57.** L. Li, E. Fan, Y. Guan, X. Zhang, Q. Xue, L. Wei, F. Wu, R. Chen, Sustainable Recovery of Cathode Materials from Spent Lithium-Ion Batteries Using Lactic Acid Leaching System, *ACS Sustain. Chem. Eng.* 5 (2017) 5224–5233.

**58.** L. Li, J. Lu, Y. Ren, X.X. Zhang, R.J. Chen, F. Wu, K. Amine, Ascorbic-acid-assisted recovery of cobalt and lithium from spent Li-ion batteries, *J. Power Sources* 218 (2012) 21–27.

**59.** L. Li, Y. Bian, X. Zhang, Y. Guan, E. Fan, F. Wu, R. Chen, Process for recycling mixed-cathode materials from spent lithium-ion batteries and kinetics of leaching, *Waste Management* 71 (2018) 362–371.

**60.** L. Li, Y. Bian, X. Zhang, Q. Xue, E. Fan, F. Wu, R. Chen, Economical recycling process for spent lithium-ion batteries and macro- and micro-scale mechanistic study, *J. Power Sources* 377 (2018) 70–79.

**61.** F. Pagnanelli, E. Moscardini, G. Granata, S. Cerbelli, L. Agosta, A. Fieramosca, L. Toro, Acid reducing leaching of cathodic powder from spent lithium ion batteries: Glucose oxidative pathways and particle area evolution, *Journal of Industrial and Engineering Chemistry* 20 (2014) 3201–3207.

**62.** X. Chen, B. Fan, L. Xu, T. Zhou, J. Kong, An atom-economic process for the recovery of high value-added metals from spent lithium-ion batteries, *J. Clean. Prod.* 112 (2016) 3562–3570.

**63.** K. Binnemans, Peter, T. Jones, Lindy Effect in Hydrometallurgy, *Journal of Sustainable Metallurgy* (2025) 1–18.

**64.** A.R. Angumeenal, D. Venkappayya, An overview of citric acid production, *LWT - Food Science and Technology* 50 (2013) 367–370.

**65.** M. Pazouki, T. Panda, Recovery of citric acid - A review, *Bioprocess Engineering* 19 (1998) 435–439.

**66.** R. Reena, R. Sindhu, P. Athiyaman Balakumaran, A. Pandey, M.K. Awasthi, P. Binod, Insight into citric acid: A versatile organic acid, *Fuel* 327 (2022) 125181.

**67.** A.A. Nayl, M.M. Hamed, S.E. Rizk, Selective extraction and separation of metal values from leach liquor of mixed spent Li-ion batteries, *J. Taiwan Inst. Chem. Eng.* 55 (2015) 119–125.

**68.** X. Chen, C. Guo, H. Ma, J. Li, T. Zhou, L. Cao, D. Kang, Organic reductants based leaching: A sustainable process for the recovery of valuable metals from spent lithium ion batteries, *Waste Management* 75 (2018) 459–468.

**69.** S.M. Shin, N.H. Kim, J.S. Sohn, D.H. Yang, Y.H. Kim, Development of a metal recovery process from Li-ion battery wastes, *Hydrometallurgy* 79 (2005) 172–181.

**70.** Z. Niu, Y. Zou, B. Xin, S. Chen, C. Liu, Y. Li, Process controls for improving bioleaching performance of both Li and Co from spent lithium ion batteries at high pulp density and its thermodynamics and kinetics exploration, *Chemosphere* 109 (2014) 92–98.

**71.** G. Zeng, X. Deng, S. Luo, X. Luo, J. Zou, A copper-catalyzed bioleaching process for enhancement of cobalt dissolution from spent lithium-ion batteries, *J. Hazard. Mater.* 199–200 (2012) 164–169.

**72.** S. Pei, S. Yan, X. Chen, J. Li, J. Xu, Novel electrochemical process for recycling of valuable metals from spent lithium-ion batteries, *Waste Management* 188 (2024) 1–10.

**73.** K. Zhong, M. Kang, Z. Ye, B. Meng, X. Hou, Z. Tian, K. Yang, Q. Wang, Z. Fang, $Fe^{2+}$/$Fe^{3+}$-Mediated synergistic electrochemical leaching of spent lithium-ion batteries under low voltage: a green chemistry approach, *Green Chemistry* 27 (2025) 5531–5545.

**74.** S. Lei, Y. Zhang, S. Song, R. Xu, W. Sun, S. Xu, Y. Yang, Strengthening Valuable Metal Recovery from Spent Lithium-Ion Batteries by Environmentally Friendly Reductive Thermal Treatment and Electrochemical Leaching, *ACS Sustain. Chem. Eng.* 9 (2021) 7053–7062.

**75.** S. Zhou, Y. Zhang, Q. Meng, P. Dong, X. Yang, P. Liu, Q. Li, Z. Fei, Recycling of spent $LiCoO_2$ materials by electrolytic leaching of cathode electrode plate, *J. Environ. Chem. Eng.* 9 (2021) 104789.

**76.** S. Li, X. Wu, Y. Jiang, T. Zhou, Y. Zhao, X. Chen, Novel electrochemically driven and internal circulation process for valuable metals recycling from spent lithium-ion batteries, *Waste Management* 136 (2021) 18–27.

**77.** L. Li, L. Zhai, X. Zhang, J. Lu, R. Chen, F. Wu, K. Amine, Recovery of valuable metals from spent lithium-ion batteries by ultrasonic-assisted leaching process, *J. Power Sources* 262 (2014) 380–385.

**78.** S.G. Zhu, W.Z. He, G.M. Li, X. Zhou, X.J. Zhang, J.W. Huang, Recovery of Co and Li from spent lithium-ion batteries by combination method of acid leaching and chemical precipitation, *Transactions of Nonferrous Metals Society of China* 22 (2012) 2274–2281.

**79.** N. Peeters, K. Binnemans, S. Riaño, Solvometallurgical recovery of cobalt from lithium-ion battery cathode materials using deep-eutectic solvents, *Green Chemistry* 22 (2020) 4210–4221.

**80.** A. Kityk, V. Pavlik, M. Hnatko, Reshaping the future of battery waste: Deep eutectic solvents in Li-ion battery recycling, *J. Energy Storage* 97 (2024) 112990.

**81.** K. Binnemans, P.T. Jones, Ionic Liquids and Deep-Eutectic Solvents in Extractive Metallurgy: Mismatch Between Academic Research and Industrial Applicability, *Journal of Sustainable Metallurgy* 9 (2023) 423–438.

**82.** G. Choe, H. Kim, J. Kwon, W. Jung, K.Y. Park, Y.T. Kim, Re-evaluation of battery-grade lithium purity toward sustainable batteries, *Nat. Commun.* 15 (2024) 1–10.

**83.** X. Chen, B. Xu, T. Zhou, D. Liu, H. Hu, S. Fan, Separation and recovery of metal values from leaching liquor of mixed-type of spent lithium-ion batteries, *Sep. Purif. Technol.* 144 (2015) 197–205.

**84.** C. Peng, J. Hamuyuni, B.P. Wilson, M. Lundström, Selective reductive leaching of cobalt and lithium from industrially crushed waste Li-ion batteries in sulfuric acid system, *Waste Management* 76 (2018) 582–590.

**85.** B. Segura-Bailón, G.T. Lapidus, G. Ramos-Sánchez, A comparative study of discharging and leaching of spent lithium-ion battery recycling, *Miner. Eng.* 218 (2024) 109012.

**86.** J. Kang, G. Senanayake, J. Sohn, S.M. Shin, Recovery of cobalt sulfate from spent lithium ion batteries by reductive leaching and solvent extraction with Cyanex 272, *Hydrometallurgy* 100 (2010) 168–171.

**87.** M. Malik, K.H. Chan, G. Azimi, Review on the synthesis of $LiNi_xMn_yCo_{1-x-y}O_2$ (NMC) cathodes for lithium-ion batteries, *Mater. Today Energy* 28 (2022) 101066.

**88.** A.M. Bernardes, D.C.R. Espinosa, J.A.S. Tenório, Recycling of batteries: a review of current processes and technologies, *J. Power Sources* 130 (2004) 291–298.

**89.** K.C. Sole, The Evolution of Cobalt–Nickel Separation and Purification Technologies: Fifty Years of Solvent Extraction and Ion Exchange, *Extraction* (2018) 1167–1191.

**90.** X. Chen, T. Zhou, J. Kong, H. Fang, Y. Chen, Separation and recovery of metal values from leach liquor of waste lithium nickel cobalt manganese oxide based cathodes, *Sep. Purif. Technol.* 141 (2015) 76–83.

**91.** E. Fan, L. Li, Z. Wang, J. Lin, Y. Huang, Y. Yao, R. Chen, F. Wu, Sustainable Recycling Technology for Li-Ion Batteries and Beyond: Challenges and Future Prospects, *Chem. Rev.* 120 (2020) 7020–7063.

**92.** W. Lv, Z. Wang, H. Cao, Y. Sun, Y. Zhang, Z. Sun, A Critical Review and Analysis on the Recycling of Spent Lithium-Ion Batteries, *ACS Sustain. Chem. Eng.* 6 (2018) 1504–1521.

**93.** C.K. Gupta, Chemical metallurgy: principles and practice, (2003) 811.

**94.** W.A. Rickelton, A.J. Robertson, J.H. Hillhouse, The Significance of Diluent Oxidation in Cobalt-Nickel Separation, *Solvent Extraction and Ion Exchange* 9 (1991) 73–84.

**95.** F. Principe, G.P. Demopoulos, The solubility and stability of organophosphoric acid extractants in $H_2SO_4$ and HCl media, *Hydrometallurgy* 68 (2003) 115–124.

**96.** M.A. Azam, S. Alam, F.I. Khan, The Solubility/Degradation Study of Organophosphoric Acid Extractants in Sulphuric Acid Media, *Journal of Chemical Engineering* 25 (2010) 18–21.

**97.** K.R. Barnard, Identification and characterisation of a Cyanex 272 degradation product formed in the Murrin Murrin solvent extraction circuit, *Hydrometallurgy* 103 (2010) 190–195.

**98.** Y. Zou, A. Chernyaev, S. Seisko, J. Sainio, M. Lundström, Removal of iron and aluminum from hydrometallurgical NMC-LFP recycling process through precipitation, *Miner. Eng.* 218 (2024) 109037.

**99.** S.P. Barik, G. Prabaharan, L. Kumar, Leaching and separation of Co and Mn from electrode materials of spent lithium-ion batteries using hydrochloric acid: Laboratory and pilot scale study, *J. Clean. Prod.* 147 (2017) 37–43.

**100.** X. Guo, X. Cao, G. Huang, Q. Tian, H. Sun, Recovery of lithium from the effluent obtained in the process of spent lithium-ion batteries recycling, *J. Environ. Manage.* 198 (2017) 84–89.

**101.** A. Chernyaev, J. Zhang, S. Seisko, M. Louhi-Kultanen, M. Lundström, $Fe^{3+}$ and $Al^{3+}$ removal by phosphate and hydroxide precipitation from synthetic NMC Li-ion battery leach solution, *Sci. Rep.* 13 (2023) 1–12.

**102.** Y. Zou, A. Chernyaev, S. Seisko, J. Sainio, M. Lundström, Removal of iron and aluminum from hydrometallurgical NMC-LFP recycling process through precipitation, *Miner. Eng.* 218 (2024) 109037.

**103.** M. Rezaei, A. Nekahi, A. Kumar M R, A. Nizami, X. Li, S. Deng, J. Nanda, K. Zaghib, A review of lithium-ion battery recycling for enabling a circular economy, *J. Power Sources* 630 (2025) 236157.

**104.** F. Pagnanelli, E. Moscardini, P. Altimari, T. Abo Atia, L. Toro, Cobalt products from real waste fractions of end of life lithium ion batteries, *Waste Management* 51 (2016) 214–221.

**105.** X. Lu, Y. He, Z. Huang, J. Li, Z. Qi, J. Qin, F. Wang, Recovering spent Li-ion batteries as $Li_2CO_3$ and NCM (nickel cobalt manganese) carbonate precursor by thermal reduction and co-precipitation combined process, *J. Environ. Chem. Eng.* 13 (2025) 118198.

**106.** Y. Song, Z. Zhao, Recovery of lithium from spent lithium-ion batteries using precipitation and electrodialysis techniques, *Sep. Purif. Technol.* 206 (2018) 335–342.

**107.** J.S. Sohn, D.H. Yang, S.M. Shin, J.G. Kang, Recovery of cobalt in sulfuric acid leaching solution using oxalic acid, *Geosystem Engineering* 9 (2006) 81–86.

**108.** L. Sun, K. Qiu, Organic oxalate as leachant and precipitant for the recovery of valuable metals from spent lithium-ion batteries, *Waste Management* 32 (2012) 1575–1582.

**109.** R.C. Wang, Y.C. Lin, S.H. Wu, A novel recovery process of metal values from the cathode active materials of the lithium-ion secondary batteries, *Hydrometallurgy* 99 (2009) 194–201.

**110.** X. Chen, C. Yang, Y. Yang, H. Ji, G. Yang, Co-precipitation preparation of Ni-Co-Mn ternary cathode materials by using the sources extracting directly from spent lithium-ion batteries, *J. Alloys Compd.* 909 (2022) 164691.

**111.** J. Shuai, W. Liu, S. Rohani, Z. Wang, M. He, C. Ding, X. Lv, Efficient extraction and separation of valuable elements from spent lithium-ion batteries by leaching and solvent extraction: A review, *Chemical Engineering Journal* 503 (2025) 158114.

**112.** K. Zhang, H. Liang, X. Zhong, H. Cao, R. Wang, Z. Liu, Recovery of metals from sulfate leach solutions of spent ternary lithium-ion batteries by precipitation with phosphate and solvent extraction with P507, *Hydrometallurgy* 210 (2022) 105861.

**113.** N. Peeters, S. Riaño, K. Binnemans, Conversion of Lithium Chloride into Lithium Hydroxide Using a Two-Step Solvent Extraction Process in an Agitated Kühni Column, *Journal of Sustainable Metallurgy* 10 (2024) 637–645.

**114.** J. Hu, J. Zhang, H. Li, Y. Chen, C. Wang, A promising approach for the recovery of high value-added metals from spent lithium-ion batteries, *J. Power Sources* 351 (2017) 192–199.

**115.** O.S.L. Bruinsma, D.J. Branken, T.N. Lemmer, L. van der Westhuizen, S. Rossouw, Sodium sulfate splitting as zero brine process in a base metal refinery: Screening and optimization in batch mode, *Desalination* 511 (2021) 115096.

**116.** M.B.J.G. Freitas, E.M. Garcia, Electrochemical recycling of cobalt from cathodes of spent lithium-ion batteries, *J. Power Sources* 171 (2007) 953–959.

**117.** E.M. Garcia, H.A. Tarôco, T. Matencio, R.Z. Domingues, J.A.F. Dos Santos, M.B.J.G. De Freitas, Electrochemical recycling of cobalt from spent cathodes of lithium-ion batteries: Its application as coating on SOFC interconnects, *J. Appl. Electrochem.* 41 (2011) 1373–1379.

**118.** B.V.M. Rodrigues, A. Bukowska, S. Opitz, M. Spiewak, S. Budnyk, P. Kuśtrowski, A. Rokicińska, A. Slabon, J. Piątek, Selective electrochemical recoveries of Cu and Mn from end-of-life Li-ion batteries, *Resour. Conserv. Recycl.* 197 (2023) 107115.

**119.** P. Venkatesan, Z.H.I. Sun, J. Sietsma, Y. Yang, An environmentally friendly electro-oxidative approach to recover valuable elements from NdFeB magnet waste, *Sep. Purif. Technol.* 191 (2018) 384–391.

**120.** L. Yu, X. Liu, S. Feng, S. Jia, Y. Zhang, J. Zhu, W. Tang, jingkang Wang, J. Gong, Recent progress on sustainable recycling of spent lithium-ion battery: Efficient and closed-loop regeneration strategies for high-capacity layered NCM cathode materials, *Chemical Engineering Journal* 476 (2023) 146733.

**121.** I.L. Santana, T.F.M. Moreira, M.F.F. Lelis, M.B.J.G. Freitas, Photocatalytic properties of $Co_3O_4$/$LiCoO_2$ recycled from spent lithium-ion batteries using citric acid as leaching agent, *Mater. Chem. Phys.* 190 (2017) 38–44.

**122.** A. Iizuka, Y. Yamashita, H. Nagasawa, A. Yamasaki, Y. Yanagisawa, Separation of lithium and cobalt from waste lithium-ion batteries via bipolar membrane electrodialysis coupled with chelation, *Sep. Purif. Technol.* 113 (2013) 33–41.

**123.** M.L. Strauss, L.A. Diaz, J. McNally, J. Klaehn, T.E. Lister, Separation of cobalt, nickel, and manganese in leach solutions of waste lithium-ion batteries using Dowex M4195 ion exchange resin, *Hydrometallurgy* 206 (2021) 105757.

*In the end we retain from our studies only that which we practically apply.*

Johann Wolfgang von Goethe

# 3

# Chapter 3

## A Closer Look at Lithium-Ion Batteries in E-waste & the Potential for a Universal Hydrometallurgical Recycling Process

We have now established that industrial black mass is associated with variance in composition and impurities. This can significantly influence the performance of hydrometallurgical recycling. However, this has not been quantitatively studied before. Hence, there is a need for a quantitative comparison of recycling performance of multiple waste types over one set of experimental parameters.

Chapter 3 focusses on explaining in detail the reason for the variance of black mass. It also shows that the composition of this black mass has an influence on the first step in hydrometallurgical recycling, and which chemical properties of the black mass are at the basis of this.

This study investigates the structure and composition of battery modules in common appliances such as laptops, power banks, smart watches, wireless earphones and mobile phones. The battery cells in the module are disassembled into cell casing, cathode, anode and separator, followed by detailed characterization of the cathode active materials (CAMs) with XRD-, SEM-, EDX- and ICP-OES-analysis. No direct link is found between the chemistry of the active materials (NMC, LCO, LMO, LFP etc.) and the application. Then, these materials are all subjected to the same leaching conditions (2 mol/L $H_2SO_4$, 50 °C, 2 hr, 60 g BM/L) with varying concentration of $H_2O_2$ (0-4 vol%). The leaching performance of these samples are compared, showing that only a part of the BMs dissolved completely at 4 vol% $H_2O_2$, which is attributed to the oxidation state of the transition metals (TMs). Exact determination of $H_2O_2$ consumption by redox titration confirms this hypothesis.

---

This chapter is published in Nature, Scientific Reports:
van de Ven, J. J. M. M., Yang, Y. & Abrahami, S. T. A closer look at lithium-ion batteries in E-waste and the potential for a universal hydrometallurgical recycling process. 14, 1–12 (2024).

## 3.1. INTRODUCTION

In the current society, batteries are widely used for storage of energy; from green technology applications, such as electric vehicles (EVs) and storage units for intermittent renewable energy sources (such as solar and wind), to consumer electronics such as mobile phones and laptops [1]. Rechargeable lithium-ion batteries (LiBs) are the most prevalent type of batteries in such applications, with their demand growing, while the supply of the necessary materials is under pressure [2,3]. The rapid pace of technological advancements and consumer preferences for frequent device upgrades have contributed to a significant increase in e-waste generation [4]. A substantial portion of this e-waste nowadays contains LiBs, which pose severe safety and environmental concerns when not properly managed [5–7]. Although batteries in consumer electronics are a relatively small fraction of the global market, all batteries are subject to European Union (EU) regulations and need to be (manually) removed from their devices for subsequent treatment before further e-waste processing and recycling [8–10].

LiBs contain many elements that are currently listed as critical raw materials (CRMs) according to the EU, such as cobalt, manganese and lithium [11–14]. Recycling can partly relieve pressure on primary resources, thereby reducing the reliance on import [14,15]. Although this already happens to some extent, industrial recycling processes that are in place focus on the most valuable elements, such as cobalt, nickel and copper [12,16,17]. Therefore, there is a need for recycling processes that aim to recover all elements. Most studies focussed on optimizing the hydrometallurgical recycling of a single black mass (BM, a mixture of LiB cathode materials and impurities) composition, obtained from dismantling batteries by hand or through simulated crushing processes [18–26]. For example, $H_2SO_4$ (1 – 3 M) is a widely used for the leaching of cathode materials [19,27]. However, complete dissolution is often not reached without high temperatures (up to 95 °C) and/or long reaction times (up to 6 hr). Also, additional reagents such as $H_2O_2$ are used to improve leaching for Li, Mn, Co and Ni at milder conditions [20,22,28]. For example, Sattar et al. [22] used a solution of 2 mol/L $H_2SO_4$ with 4 vol% $H_2O_2$, resulting in a leaching efficiency ≥ 98% for Li, Co, Ni and Mn (50 °C, 2 hr, S/L = ± 60 g/L). They used one mixture of heat treated CAMs from manually dismantled electronics as BM. In another study, He et al. [28] acquired ≥ 99.7 % leaching efficiency for these four elements with only 1 M $H_2SO_4$ and 1 vol% $H_2O_2$ (40 °C, 1 hr, S/L = 40 g/L), using pristine NMC 111 cathode powder. HCl solutions of up to 4 M are also used and result in high (≥99%) leaching efficiencies for Li, Ni, Mn and Co [18,25,26,29]. These processes required higher temperatures (80 °C) but differs in the required leaching time (1 – 2 hours), as well as in the reported S/L ratio (20 – 100 g/L). Other studies

describe leaching processes with $HNO_3$ [30,31] and $H_3PO_4$ [21,32], or organic acids such as oxalic acid [33,34], citric acid [24,35] and acetic acid [36,37], sometimes with additional reagents such as $H_2O_2$. Since the feed material differs per study; ranging from pristine materials to (a mixture of) cathode materials from used batteries, the influence of feed chemistry on leaching was not directly studied. Therefore, the reality of contemporary industrial e-waste and battery sorting and the following (mechanical) processing capabilities are not taken into account [38]. For example, it is not possible to distinguish the specific chemistry of a Li-ion battery by simple visual inspection of its casing, though new regulations regarding battery passport are predicted to change this in the next decade [39,40].

As a consequence, industrial scale BM preparation processes will inevitably process a mixture of the various types of LIBs available on the market. Also, despite the available technologies for mechanical separation, additional materials originating from different components of the module (e.g. metallic materials in the casing and battery management system) will likely introduce extra contaminates to the BM. This drastically increases the heterogeneity of input material to downstream recycling processes and may causes limitations in the achieved purity levels. To explore the potential of a flexible and universal hydrometallurgical recycling process, this paper reports on the first step in achieving such an aim by leaching various types of different BM compositions. Therefore, the present study begins with characterizing the structure of battery modules and cell chemistry in various small electronic appliances such as laptops, mobile phones, power banks, smart watches, and wireless earphones. Next, the influence of composition on the recycling process of the main present metals (Li, Ni, Co, and Mn) is investigated. Finally, the potential of establishing a more flexible and universal hydrometallurgical processing route is discussed.



## 3.2. MATERIALS & METHODS

### 3.2.1. Battery Retrieval & Discharging

To get an insight in the composition of battery waste from consumer electronics, a variety of end-of-life (EoL) devices were disassembled. These were provided by a local collector of batteries (Van Peperzeel B.V.). Removal of the batteries from their respective devices was rather straight forward. The devices could either be screwed, pried or in some cases cut open with a Dremel. Then, a battery module (cell(s) with casing, Battery Management System (BMS) etc.) was removed from its respective device. These were disassembled and their components were weighed, after which the weight percentages for all components were calculated.

The retrieved battery cells were then discharged by submerging them in an aqueous $K_2CO_3$ (≥99.0%, Sigma-Aldrich) solution of 10 wt.% for (at least) 24 hours [41]. Next, the cells were wiped off and dried in an oven at 50 °C for 8 hours. The voltage was measured before and after treatment to verify a successful discharge.

### 3.2.2. Cell Dismantling

Two cell types could be distinguished: cylindrical (18650) and pouch cells. The cylindrical cells have a nickel-plated steel casing and were opened by cutting the top and bottom of the battery with a pipe cutter, after which a longitudinal cut was made (Fig. A.1, Appendices). After this, the steel casing could be removed, revealing the cathode, separator, and anode. The pouch cells have plastic casings, which can be easily cut open with a knife. For both types of cells, the electrodes and separator were uncurled, after which they could be separated. All parts were weighed and compared to the initial cell weight to account for any losses during the dismantling process. The mass percentages for all components were also calculated. The electrolyte is not retrieved separately and mostly evaporates after opening the cell. It is accounted for in the “loss” category.

### 3.2.3. Preparation of Black Mass

After separation of the cathode from all other cell parts, it was cut into pieces of roughly 1.5 x 1.5 cm. These pieces were submerged in N-methyl-2-pyrrolidone (NMP) (99%, Thermo Scientific), which dissolved the binder. This process was done at 75 °C with ultrasonification (Emag Emmi-40HC ultrasound bath). Depending on the battery, this took between 1 to 3 hours. After NMP treatment, the solution was left to cool down and the aluminium foil pieces were filtered out. The NMP with cathode material in suspension was left to settle for at least 24 hours, after which it was decanted, leaving a dense slurry of NMP and BM (CAMs with impurities). Both the aluminium foil and BM were dried at 60 °C until no solvent was left. They were weighed and mass percentages compared to the total cathode weight were calculated. Around 65 – 80 wt.% of the cathode was retrieved as BM. The rest consists of the aluminium foil, as well as the removed binder and cathode material in suspension of NMP which could not be fully filtrated due to the small particle size. The retrieved BM samples were subjected to various characterization techniques, as described in section 2.4. In addition, Hanwa Europe B. V. provided an industrially pre-treated (mechanically processes and pyrolyzed) BM. Important to note here is that this method to retrieve BM differs substantially from the liberation methods used in industry [42]. Industrial pre-treatment results in BM with many impurities from other parts of the battery (cells), as shown later in this study. For research purposes

the aim is to minimise the amount of impurities in the BM, which is why a delicate liberation method is chosen. Pristine NMC 532 was bought from Nanographi.

### 3.2.4. Characterization Techniques

The different phases in the black mass were analysed through X-ray diffraction (XRD) analysis with a Bruker D8 Advance diffractometer with Bragg-Brentano geometry and a Lynxeye position sensitive detector, using Cu Kα radiation. The 2Θ range was 10 – 110 °, with a step size of 0.04° and a counting time of 2s per step. Bruker software DiffracSuite.EVA vs 6.0 was used for data analysis.

The morphologies and individual grain compositions of various black mass samples were investigated using a scanning electron microscope in combination with energy dispersive X-ray analysis (SEM-EDX). For this, a Jeol JSM-IT100 was used. A small amount of black mass was applied on a piece of carbon tape and placed on the sample holder.



Before analysing the black mass with ICP-OES, it was dissolved in aqua regia to ensure complete dissolution. Each black mass type was analysed three times to account for heterogeneity. 100 mL of aqua regia was prepared by combining 25 mL of $HNO_3$ solution (65%, VWR chemicals) with 75 mL HCl solution (37%, Merck). This was added to a triple necked round bottom flask with reflux cooler. In this, 1 gram of black mass was dissolved at 70 °C for 5 hours, while stirring at 500 rpm. This entire solution was filtered through a Whatman 595 ½ folded filter paper and diluted to 1L, using a volumetric flask. Samples from this solution, as well as the diluted PLS samples, were applied for ICP-OES analysis with a Spectro Arcos-EOP-device, with Modified Lichte nebulizer and mini cyclonic spray chamber. In order to verify complete dissolution of all metals, the residue was analysed with SEM in combination with EDX-analysis. In order to avoid any matrix effects during ICP-OES analysis, both the samples from digestion and leaching were diluted a second time with a 3 wt.% $HNO_3$ (65%, VWR chemicals) solution, with a dilution factor of 20.

### 3.2.5. Leaching

The lixiviant was prepared by adding concentrated sulfuric acid (95 – 97%, Sigma-Aldrich) to Milli-Q water in a glass vial of 30 mL. In some cases, $H_2O_2$ solution (30%, Sigma-Aldrich) was added as well. To account for bubble formation, the maximum total amount of lixiviant was kept at 16 mL and a small hole was made on the top of the screw cap. A magnetic stir bar was added, after which the black mass was weighed and added to the lixiviant. The glass vials containing the leaching system were then placed in an aluminium heating block on a stirring plate with a thermocouple, at 50 °C while stirring at 400 rpm. After 2 hours maximum dissolution is reached [22]. The leaching system was removed and a sample of the pregnant

leach solution (PLS) was taken. This was filtered with a syringe filter (Chromafil Xtra PFTE-45/25), after which 0.2 mL PLS was diluted to 10 mL and submitted to ICP-OES analysis. To ensure a minimal error due to water evaporation, the initial and remaining volume were compared. Also, the residue was analysed to ensure a correct mass balance. Each leaching experiment was done in triplicate.

To evaluate the leaching performance, the leaching efficiency ($\eta_L$) of each experiment was calculated according to equation (3.1). In this formula, $m^x_f$ represents the initial mass of element x in the feed and $m^x_{PLS}$ represents the mass of element x present in the PLS after leaching.

$$\eta_L = \frac{m^x_{PLS}}{m^x_f} * 100\% \tag{3.1}$$

### 3.2.6. $KMnO_4$ Titration

To determine and compare the necessary amount of $H_2O_2$ for full dissolution of the black mass samples, a leaching experiment was performed with an excess $H_2O_2$. The same leaching procedure was followed as described earlier, with 10 vol% of $H_2O_2$ solution. After leaching, 0.2 mL of the PLS was diluted and submitted to ICP-OES analysis. The remaining solution was diluted and directly titrated with a 0.3 mol/L $KMnO_4$ (EMSURE, ACS grade) solution to determine the remaining amount of $H_2O_2$ [43,44]. This was used to calculate the amount of $H_2O_2$ that was used in the dissolution.

## 3.3. RESULTS & DISCUSSION

### 3.3.1. Battery Modules Composition

Some very prevalent devices with LiBs are laptops, smartwatches, wireless earbuds, powerbanks and mobile (smart)phones [1]. From each of these applications, multiple battery modules have been disassembled. In Fig. 3.1, one example of a battery module (sometimes with respective device) can be seen for each mentioned application. The battery module is made of five major components: the battery cell(s), battery casing, the battery management system (BMS), wiring and separators or glues. The battery cells contain the active materials and are used for the storage of electrical energy. The wiring connects multiple cells to the BMS, which in turn ensures safe charge and discharge of the battery cells. The separators are used to avoid short circuiting by direct contact of the cells, and the glue keeps the cells in place during use. Lastly, the casing encapsulates and protects all other components. After disassembly, the average relative weights of all components from the battery modules were calculated. These are compared in Fig. 3.2 for the main five components.

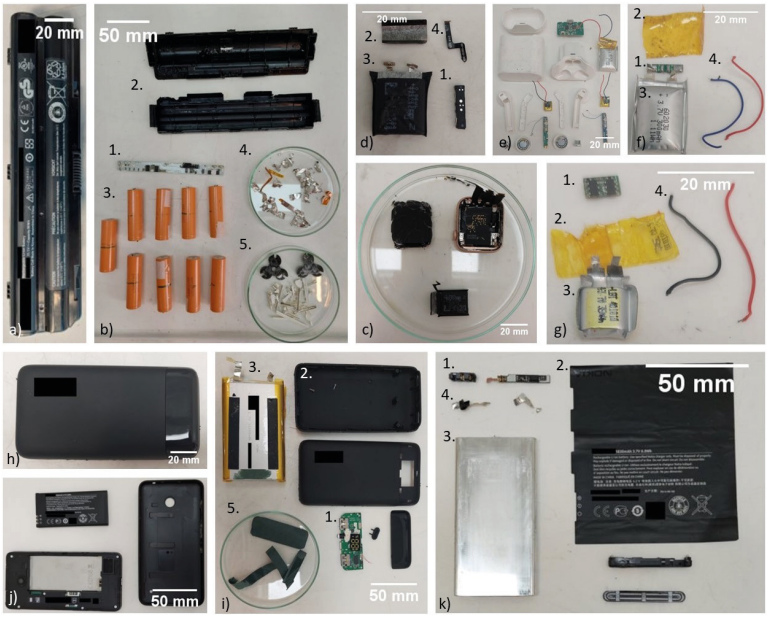


*Figure 3.1: Battery modules (some of which with device) before and after disassembly. Represented are a (disassembled) laptop battery module (a and b), smart watch (c and d), set of wireless earphones (e, f and g), powerbank (h and i) and mobile phone module (j and k). For all sub images, the numbers represent the same component: 1. BMS, 2. Battery casing, 3. Battery cells, 4. Wiring, 5. Glue and separating components.*

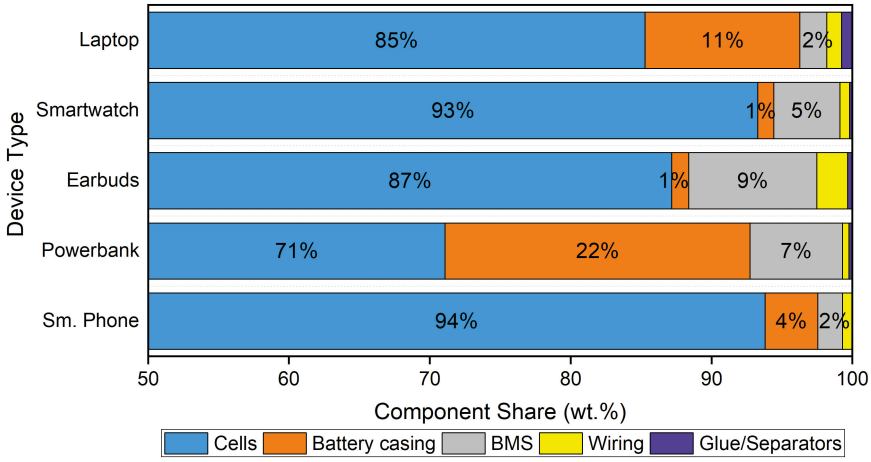


*Figure 3.2: Proportional composition of battery modules from laptops, smartwatches, earbuds, powerbanks, and (smart)phones (sm. phone). Note that the x-axis starts at 50 wt.%.*

The laptops (3 devices) researched in this study all included a rather easily removeable module, one of which is shown in Fig. 3.1a. Fig. 3.1b shows this same battery module after disassembly. For this application the cells, either 18650 type as seen in the picture or pouch type, take up most of the weight (85 wt.%). This is followed by the battery casing with 11 wt%. The BMS (1.5 wt.%), glue and separators (1.0 wt. %) and wiring (0.8 wt.%) are only minor components.

The disassembled smartwatches (4 devices) use a smaller battery module with one cell (Fig. 3.1c). These modules consist of a pouch type cell (93 wt.%), to which a BMS (5 wt.%) is attached. The battery casing consists of a plastic foil (1.2 wt.%) wrapped over the BMS. Hard plastic casings, such as seen in the laptop battery modules, are not present. The wiring and glue or separators have a very low relative weight of 0.7 and 0.2 wt.% respectively. An example of the disassembled module is shown in Fig. 3.1d.

All disassembled earbud sets (4 devices) (Fig. 3.1e) contain three battery modules: one large module (Fig. 3.1f) and two smaller modules (Fig. 3.1g). These mostly consist of a cell (87 wt.%) to which a BMS is attached (9 wt.%). It must be noted that the BMSs shown in Figs. 3.1f and g are not present in all modules that were retrieved. In two units, the cells are directly attached to the circuitry in the earplugs or the casing, avoiding the need for an extra BMS. The battery casing consists, similarly to the modules present in smartwatches, of a foil wrapped around the module (1.2 wt.%). The wiring and glue or separators contribute 2.2 and 0.3 wt.% respectively.

An example of a powerbank is shown in Fig. 3.1h. Fig. 3.1i shows this powerbank after disassembly. The disassembled powerbanks (5 devices) contain one to three cells, either 18650 or pouch type, which take up 71 wt.% on average. The casing and BMS take up 22 and 6.6 wt.% respectively. The wiring and glue or separators are only minor components, taking up 0.5 and 0.3 wt.% respectively.

The array of (smart)phones (10 devices) that were disassembled contain two types of battery modules, all with one single pouch type cell. One module type is similar to the modules found in the smartwatches and earbuds, albeit larger. The second type is shown in Fig. 3.1j and is easily removeable from the device. These were generally found in the older (smart)phones (2008-2015), but it also depended on the brand. The module after disassembly can be seen in Fig. 3.1k. The cell (94 wt.%) is similar in shape to the pouch cells seen in Fig. 3.1i, except for the connectors. Instead of a broad wire, flat connecting points are used on which the BMS (1.7 wt.%) is directly applied. Some modules such as the one shown make use of wiring (0.7 wt.%) to attach the BMS to (one of) the connecting points. The module casing consists of a sticker wrapped around the cell, in combination

with plastic parts to cap off the top and bottom of the module (3.7 wt.%). Glue and separators are used very scarcely (<0.1 wt.%).

When comparing the different applications with each other, major variations can be seen. The powerbanks and laptop battery modules have multiple cells which need to be kept in place, connected with wiring and isolated by rubber pads to avoid short circuiting. Therefore, the relative weight of the cells is lower (71 – 85 wt.%) than for applications with just one cell per module (87 – 94 wt.%). The smaller modules consist of one cell (87 - 94 wt.%) to which the other parts are attached. These modules are generally not easily removed from the device since they are kept in place by a glue. In this manner, the device itself also acts as protective cover. Therefore, the need for casing, internal wiring and separators is limited. This results in a large weight contribution of the battery casing in the applications with multiple cells (11 – 22 wt.%) compared to applications with one cell per module (1 – 4 wt.%). Divergent are the easily removable batteries from (older) mobile phones, as seen in Fig. 3.1j, of which the casing contains hard plastic parts to protect the BMS during removal and placement. This results in the higher casing contribution for the mobile phones. The BMS is relatively large for smaller modules, resulting in a high weight contribution for the earbuds (9.1 wt.%) and smartwatches (4.7 wt.%). The BMS contribution is lower for the larger modules from smartphones (1.7 wt.%) and laptops (1.9 wt.%). This does not hold for the powerbanks, since the BMS often also harbours a screen and multiple charging ports resulting in a higher relative weight. The two other components (wiring, glue and separators) are similar for all categories and mostly depend on the size of the module. It must be noted that the limited number of samples in this study provides a good illustration of the typical components in consumer e-waste stream containing LIBs, but is not exhaustive and further variation can be expected.



### 3.3.2. Battery Cells Composition

After removing the cells from the battery modules, they were placed in the salt electrolyte for discharging before disassembly. Three typical examples can be seen in Fig. 3.3, before and after disassembly. The two most popular types of cells, cylindrical (typically 18650) and pouch cells, are shown. Although battery cells vary in size and shape, their basic structure is identical. Generally, a battery cell consists of the cell casing, an anode (graphite (C) on copper foil), a cathode (lithium metal oxide on aluminium foil) and a polymer separator with a supporting electrolyte in which lithium ions move.[1] The electrode foils (Cu, Al) are present to transfer electrons from and to the electrode materials via an external circuit. All components are indicated by the numbers 1-4 in Fig. 3.3. The average proportional composition of both cell types is compared in Fig. 3.4.

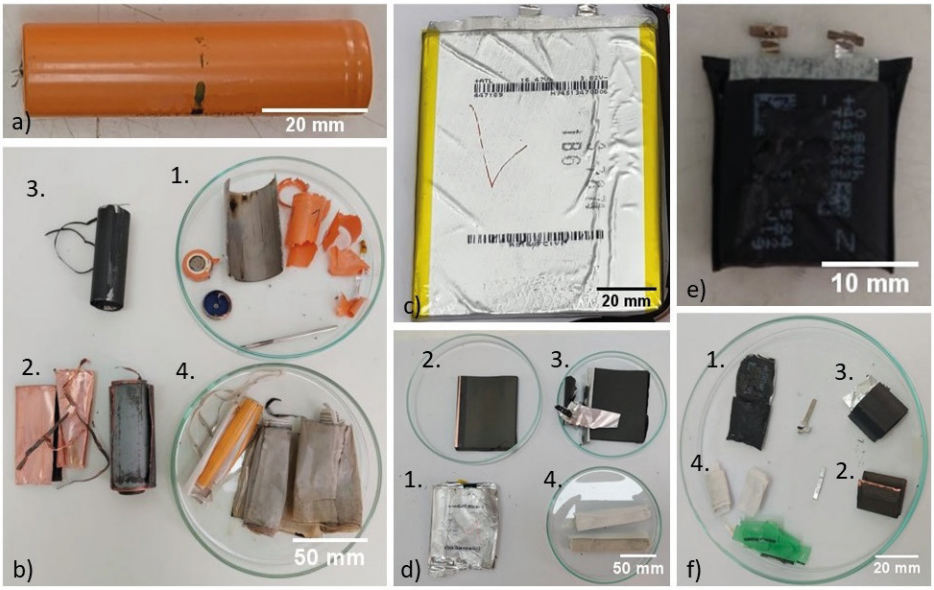


*Figure 3.3: 18650 type (a and b) and two pouch type (c-f) battery cells before and after disassembly. For all sub images, the numbers represent the same component. 1. Cell casing, 2. Anode, 3. Cathode, 4. Separator.*

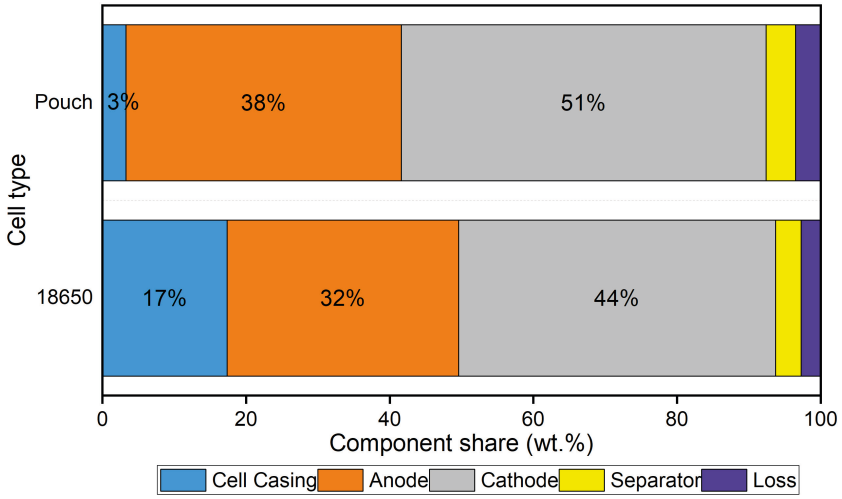


*Figure 3.4: Average proportional composition of pouch and 18650 type cells. Subtraction of the component weights from the initial cell weight results in the loss category. It includes evaporated electrolyte and potential loss of (active) materials during cell opening.*

Figs. 3.3a and b show a 18650 battery cell before and after disassembly, respectively. In these cells, the cathode is most prevalent (44 wt.%), followed by the anode (32 wt.%) and cell casing (17 wt.%). The separator and loss have a low contribution of 3.6 and 2.7 wt.%, respectively. Figs. 3.3c and e both show pouch type cells. Figs. 3.3d and f show these same cells after opening. Within these cells, the cathode has again the highest component share (51 wt.%), followed by the anode (38 wt.%). The cell casing, separator and loss all have a low contribution, being 3.3, 4.1 and 3.5 wt.%, respectively.

When comparing the two cell types, the main difference is found in the contribution of the cell casing. This is much larger for the 18650 cells, which have a steel casing, compared to the pouch cells, with a plastic one. When the cell casing is excluded, the relative share of the other components is the same for both cell types. The composition of the 18650 cells found here is in good agreement with earlier studies when considering the contribution of the cell casing and separator [41,45]. Differences are found when comparing the anode and cathode, as well as the electrolyte. The latter is not considered in our study, since it is impregnated on the separator, cathode and anode. Also, a part of it evaporates after opening the cells (this is incorporated in the “loss” category). The electrolyte is therefore not selectively removed and weighed. This results in the anode and cathode categories being larger since they include some remaining electrolyte. Also, the amount of cathode or anode material that is attached to the collector foil can vary amongst different manufacturers, resulting in a different component share [46].



### 3.3.3. Black Mass Composition & Morphology

To study the variety in composition and morphology of BM from Li-ion battery waste streams in consumer electronics, samples from the previously disassembled cells were characterized. The SEM results can be seen in Fig. 3.5. The explanation of these results, as well as the prevalent phases according to XRD, are presented in Table A.1 in the appendix. Their elemental compositions according to ICP-OES are depicted in Table 3.1.

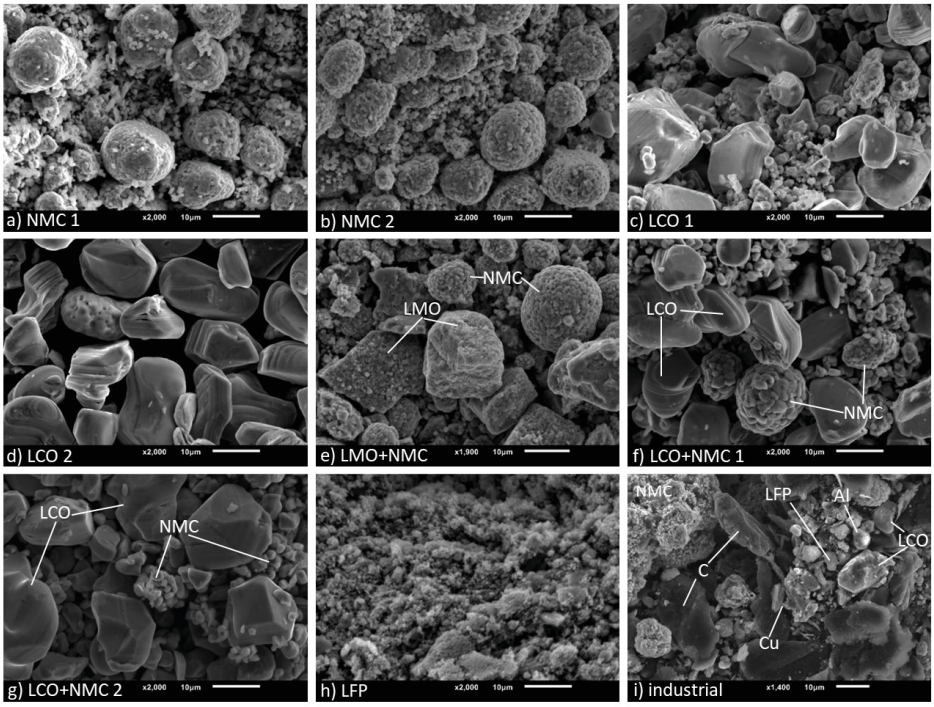


*Figure 3.5: SEM images of BM retrieved manually from batteries (a – h) and industry (i). Individual grains were characterised by SEM-EDX.*

*Table 3.1: Elemental composition (wt.%) according to ICP-OES analysis of various manually acquired BM types, and one industrial sample. "Other" category includes graphite, leftover binder and oxygen.*

| Sample name | Li | Co | Ni | Mn | Al | Fe | Cu | $PO_4$ | Other |
|---|---|---|---|---|---|---|---|---|---|
| NMC1 | 5.6 | 12.2 | 28.7 | 17.2 | 0.4 | 0.1 | / | / | 35.6 |
| NMC2 | 5.4 | 9.5 | 34.8 | 18.8 | 0.2 | 0.3 | / | / | 31.0 |
| LCO 1 | 6.6 | 57.5 | 0.0 | 0.0 | 3.5 | 0.0 | / | / | 32.4 |
| LCO 2 | 6.5 | 58.9 | 1.5 | 0.0 | 0.1 | 0.0 | / | / | 32.9 |
| LMO + NMC | 4.4 | 4.6 | 11.6 | 41.4 | 2.5 | 1.2 | / | / | 34.2 |
| LCO+NMC1 | 7.4 | 53.8 | 6.6 | 3.1 | 0.1 | 0.0 | / | / | 29.2 |
| LCO+NMC2 | 6.7 | 53.3 | 6.3 | 3.4 | 1.0 | 0.0 | / | / | 29.1 |
| LFP | 4.1 | 0.0 | 0.0 | 0.0 | 0.3 | 32.6 | / | 52.2 | 10.8 |
| Industrial | 4.2 | 18.1 | 12.3 | 4.7 | 2.8 | 0.4 | 2.1 | / | 55.4 |

The first two samples, which are shown in Figs. 3.5a and b and labelled NMC 1 and NMC 2 respectively, both consist of a mixed lithium metal (nickel, cobalt and manganese) oxide. They are present as small particles (1 – 4 µm), as well as larger coagulates of these particles (8 – 20 µm). XRD-analysis confirms the presence of a mixed lithium metal oxide in both NMC 1 and NMC 2. ICP-OES-analysis (Table 3.1) shows that Ni is the most prevalent element in both samples (29-35 wt.%), followed by Mn (17-18 wt.%) and Co (10-12 wt.%). The samples consist of around 5.5 wt.% Li. Al is present as impurity in both samples (0.2 – 0.4 wt.%). 31 – 36 wt.% is taken up by other compounds or elements, such as graphite, binder and O.

The samples shown in Figs. 3.5c and d consist of an oxide of Li and Co, labelled as LCO 1 and LCO 2, respectively. The grain size ranges from 2 to 40 µm in LCO 1, and from 10 to 30 µm in LCO 2. According to XRD-analysis, both samples consist of $LiCoO_2$, however LCO 1 also contains $CoO_2$. ICP-OES-analysis shows that cobalt is the most prevalent element in both BMs (58 - 59 wt.%), followed by Li (6.5 – 6.6 wt.%). LCO 1 contains a small amount of Al as impurity (3.5 wt.%), while LCO 2 contains some Ni (1.5 wt.%). Both samples also contain 32-33 wt.% of other compounds or elements.



Figs. 3.5e, f and g show samples that consist of blended cathode material, called LMO + NMC, LCO + NMC 1 and LCO + NMC 2 respectively. These blended cathode materials are a more recent development in LiB technology, and will therefore be increasingly expected in e-waste in the coming decades [47,48]. Cathode blending is done to complement positive aspects of certain cathode chemistries, while also mitigating their drawbacks [48]. XRD-analysis indicates that the first sample consists of $LiMn_2O_4$ + $Li_{1.2}Mn_{0.6}Ni_{0.2}O_2$, whereas the other two samples consist of $LiCoO_2$ and $LiNi_xMn_yCo_zO_2$. According to ICP-OES-analysis, LMO + NMC mostly consists of Mn (41 wt.%), followed by Ni (12 wt.%), Co (4.6 wt.%) and Li (4.4 wt.%). Al is present as impurity (2.5 wt.%). Both LCO + NMC samples mostly consist of Co (54 - 53 wt.%). Ni (6.6 – 6.3 wt.%) and Mn (3.1 – 3.4 wt.%) are present in lower amounts. Both also contain a small amount of Al (0.1 - 1 wt.%). Other compounds take up 34.2, 29.2 and 29.1 wt.% respectively.

Fig. 3.5h shows BM that is retrieved from lithium iron phosphate (LFP) battery cells. This type of cathode material is increasingly used due to its higher stability during charge and discharge and its lower cost [49,50]. However, its chemical properties also result in a lower capacity [49,50]. The grains look more like flakes and range from 1 to 15 µm in size. According to XRD-analysis, this sample consists of $LiFePO_4$, $FePO_4$ and graphite. ICP-OES-analysis shows that of the LFP black mass, 33 wt.% is Fe, and 52 wt.% is $PO_4$. Al is present as impurity (0.3 wt.%). 10.8 wt.% of the black mass is taken up by graphite, O, Li and others.

Lastly, an industrial BM is shown in Fig. 3.5i. Its pre-treatment differs from the one applied to earlier mentioned BMs; the battery cells are shredded entirely instead of disassembled manually (the latter including separation of anode and cathode). Also, the BM is pyrolyzed to remove organic components such as the binder and electrolyte components. Therefore, more impurities are to be expected. The BM consists of a multitude of compounds, such as NMC, LCO and LFP as well as graphite, which is used as anode active material and is not present in previous samples. Particles of Al and Cu foils are also present. These result from breakage of the cathode and anode collector foils, respectively. Al was present in some previous samples, whereas Cu was not. XRD-analysis confirms the presence of these phases, as well as $Cu_{0.2}MnNi_{5.8}O_8$, $Cu_{0.85}Fe_{0.1}O$ and $Li_2CO_3$. Also, a part of the Ni is present in metallic form. This is due to it being present in the metallic shell of the 18650 cells, which is not removed in industrial pre-treatment. According to ICP-OES-analysis, Co is the most prevalent element (18 wt.%) in the industrial sample, followed by Ni (12 wt.%), Mn (4.7 wt.%) and Li (4.2 wt.%). Al (2.8 wt.%) and Cu (2.1 wt.%) are both present in a small amount, as well as Fe (0.4 wt.%). Other compounds and elements, such as graphite, binder, and O take up 55.4 wt.%.

When comparing all these different BMs, it can be seen that there is a number of different cathode chemistries present in various electronic devices. Samples can be high in Co (LCO), Mn (LMO), Ni (NMC 1 and 2) or contain Fe and P (LFP). Sometimes, a blend of different chemistries is used (LMO + NMC, LCO + NMC 1 and 2). No direct link is found between the type of device and the cathode chemistry, suggesting that sorting per device will not reduce the variation in chemistries. Other elements such as Al are often present as impurities. It is important to note that large standard deviations of the Al content were found since in some batteries, the collector foil was so thin that it broke by the ultrasonic vibrations during the liberation process.

The industrial sample seems to be a mixture of all other investigated battery types, as Li, Co, Ni, Mn, Al, and Fe are all present. Mechanical processing and pyrolysis are generally able to remove most of the plastics originating from the module casings, glue and separating components as well as the pouch cell casings and separators [42]. The metallic Fe, which can originate from the cell casing of cylindrical cells, can be largely removed by magnetic separation [42]. In addition, it contains impurities of Cu and Al, likely from the current collectors. These are, on industrial scale, separated by multiple sieving steps and electrostatic separation, however, certain level of impurities is always present after mechanical processing [42]. Lastly, the industrial BM contains a lot of graphite, as seen on the SEM-image (Fig. 3.5i). This is the active material of the anode, which could be separated by

flotation or removed by heat-treatment [42]. Alternatively, it can also be removed as residue after leaching [42].

### 3.3.4. Effect of Black Mass Composition & $H_2O_2$ Addition on Leaching

A selection of BMs that were retrieved in the previous sections, as well as a pristine sample, were submitted to the same leaching conditions. This provides insight into the influence of BM composition on the leaching efficiency of the contained elements. The following conditions were chosen as a benchmark based on a literature survey [20,22,28,51]. All samples were submitted to a lixiviant with 2 mol/L $H_2SO_4$ for 2 hours at 50 °C and S/L of 60 g/L. The addition of $H_2O_2$ is varied from 0 to 4 vol% to study the required extent for a reductive agent, which improves dissolution of the TMs [52]. In order to perform leaching experiments on multiple BMs, only 0, 1 and 4 vol% of $H_2O_2$ addition were applied. The driving reaction in this leaching system is described in Eq. 3.2 [22]. Note that this reaction assumes an equal presence of Ni, Co and Mn, which is not always the case in this study.



$$6LiNi_{\frac{1}{3}}Mn_{\frac{1}{3}}Co_{\frac{1}{3}}O_{2\,s} + 9H_2SO_{4\,aq} + 3H_2O_{2\,aq}$$

$$\rightarrow 3Li_2SO_{4\,aq} + 2NiSO_{4\,aq} + 2CoSO_{4\,aq} + 2MnSO_{4\,aq} + 12H_2O + 3O_{2\,g} \qquad (3.2)$$

The results of the leaching experiments for the different chemistries are illustrated in Fig. 3.6. Since the chosen manual liberation method resulted in a generally low amount of impurities (mostly Al), only the leaching efficiencies of the relevant elements; Li, Ni, Mn and Co are shown. It is important to note that sometimes the leaching efficiency exceeds 100%, which is not possible in practice. Evaporation of water from the PLS during the experimental phase could lead to an overestimation of elemental concentrations. Also, while both initial composition and leaching results were performed multiple times, the inherent heterogeneous nature of BM leads to an estimated error of 4-5%.

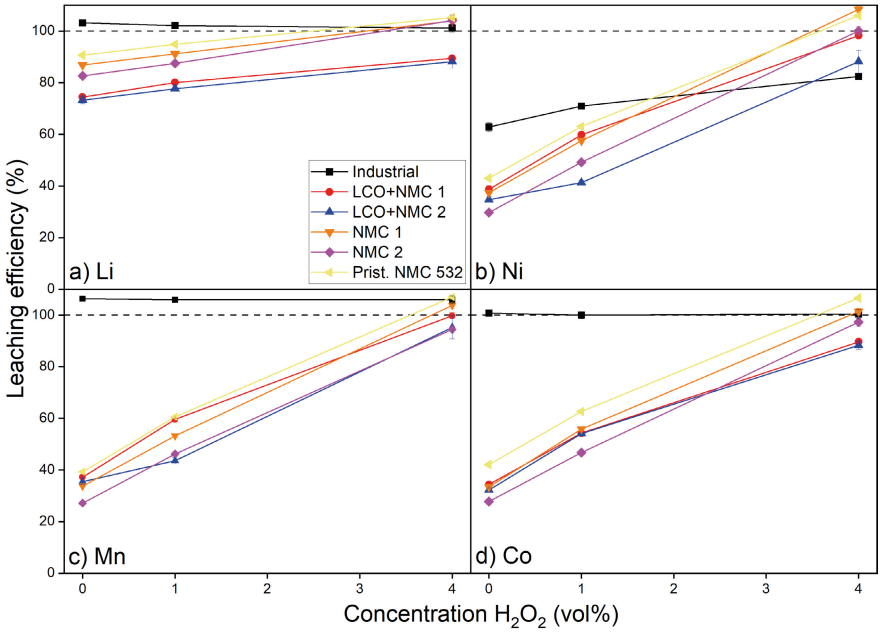


*Figure 3.6: Leaching efficiencies of Li, Ni, Mn and Co from different BM samples as a function of the amount of $H_2O_2$ addition. Other leaching conditions are 2 mol/L $H_2SO_4$, S/L = 60 g/L, T = 50 °C, t = 120 min.*

Without addition of $H_2O_2$, the leaching efficiency of all elements except Li is very poor. Li is leached between 68 and 90%, whereas dissolution of the TMs ranges between 25 and 45%. An increase in the $H_2O_2$ concentration generally improves the leaching efficiency of all relevant elements. This is already seen when 1 vol.% of $H_2O_2$ solution is added, at which point the leaching efficiencies increase from 72 to 95% for Li and from 40 to 70 % for the TMs. However, 100% leaching efficiency is not reached for all samples, despite their similar trends, even at 4 vol.% $H_2O_2$. This is observed in the leaching of both mixed LCO and NMC chemistries, showing much lower efficiencies (approx. 88%, 89%, 93% and 97% for Li, Co, Ni and Mn, respectively), but comparable to each other. On the other hand, the two NMC samples (NMC 1 and NMC 2) show much more promising results, but with a slight discrepancy between the two samples (100% and 95% leaching efficiency, respectively) for TMs, while Li is leached for 100% in both cases. The pristine NMC 532 shows the best leaching behaviour, even at low (or zero) $H_2O_2$ concentration. At 4 vol% $H_2O_2$, both the TMs and Li are fully leached.

The observed trend concerning the $H_2O_2$ concentration, as well as the distinct leaching behaviour of Li compared to the TMs is in agreement with earlier studies [22,28]. It is to be expected that 100% leaching efficiency will be achieved for all

BMs with further increase of the $H_2O_2$ concentrations [53]. Noticeably, however, the leaching trend of the industrial BM is completely different from all other BM samples. Strangely, Li, Co and Mn are fully leached without addition of any $H_2O_2$. However, at this point, Ni is only leached for 61 % and does not exceed 80% at 4 vol% $H_2O_2$ solution. The high observed leaching efficiencies can be attributed to the low metal concentration in the feed, as seen in Table 3.1. It contains a lot of graphite, which does not dissolve during leaching but does contribute to the S/L, which was kept constant in all leaching experiments. Therefore, the total amount of metals in the feed is much lower relative to other samples. This dilution of the target metals by other components, such as graphite, plastics, binder and current collectors (Al, Cu) is also reported in other studies [54]. Also, it is known that pyrolysis of BMs containing graphite can induce reactions between the present metals and graphite, causing pre-reduction of the TMs [55]. As a consequence, leaching efficiencies are much higher at a lower addition of $H_2O_2$. Ni is the only element that does not fully dissolve, which is a result of it being present in metallic form, as observed earlier.



Li leaching generally shows a slightly different trend compared to the transition metals. At lower $H_2O_2$ concentrations it is not completely leached, but it varies from 70 to 90%. This is due to the good solubility of $Li^+$ and the lower binding energy of Li and O, compared to the other TMs [28,56]. However, for Li to be fully leached, the solid particles need to be broken down first, enabling contact between the Li present inside these particles and the dissolving acid. On the other hand, the TMs dissolve most efficiently in oxidation state +II [31]. However, these are also present in state +III (Ni and Co) and +IV (Co and Mn) [57,58]. Hence, they need to be reduced before dissolution, which is manifested by the reaction with $H_2O_2$ [53]. When the average oxidation state is higher, a larger amount of $H_2O_2$ is needed to reduce the TMs to the +II state [31]. The leaching results suggest a different magnitude of $H_2O_2$ consumption for the tested BMs, and therefore a different distribution of the oxidation numbers of the TMs in these samples. To study this in more detail, some of these samples have been subjected to leaching with an excess of $H_2O_2$ in combination with $KMnO_4$-titration.

When leaching with 10 vol% $H_2O_2$ solution, all the Li and TMs in NMC 1, NMC 2, the industrial BM and the pristine NMC 532 were transferred to the PLS according to ICP-OES analysis. Afterwards, the remaining $H_2O_2$ was titrated with a $KMnO_4$ solution to calculate the $H_2O_2$ consumption, which is expressed as moles of $H_2O_2$ consumed per mole of TMs. Results show that the dissolution of NMC 2 consumes more $H_2O_2$ compared to NMC 1 (0.91 and 0.87, respectively). Dissolution of the industrial BM requires about 3 times more $H_2O_2$ (2.7 moles per mole of TMs). The dissolution of the pristine NMC 532 results in the lowest ratio (0.67). These differences in consumption of the reducing agent indicate, according to Eq. 2, the

difference in oxidation states of the TMs in the NMC samples. The fact that the industrial BM requires so much reducing agent compared to the other samples is unexpected. One explanation is the high content of impurities which can react with $H_2O_2$, such as Cu, Al and Fe [59–61]. Therefore, the high consumption is not only related to the oxidation number of the target TMs and cannot be directly compared with the other samples. The $H_2O_2$ consumption of NMC 2, NMC 1 and pristine (NMC 532) is in agreements with the leaching results observed earlier, as leaching efficiencies follows the same respective order NMC 2 > NMC 1 > pristine concluded for increasing oxidation states of TMs. The titration experiments suggest a higher average oxidation states of Ni and Co in the used samples (NMC 1 and 2) compared to pristine material, which directly influences their leaching efficiencies.

Generally, the leaching experiments show that it is possible to leach all the different chemistries together at high $H_2O_2$ concentration. It has to be noted that not all CAM chemistries available on the market were used in the leaching experiments. These may be present in an industrially processed BM, as is shown earlier, and lead to even more divergence in leaching efficiencies. To accommodate for variations in chemistries, a high amounts of reagents is needed, putting extra pressure on the sustainability of the recycling process as a whole. Also important to note is that in the leaching of the industrial BM, impurities end up in the PLS. Table A.2 in the appendices shows the composition of the PLS, acquired after leaching the industrial BM with 4 vol% $H_2O_2$-solution. It can be seen that Cu, Al and Fe contaminate this PLS. In order for any recycled Li, Co, Ni and Mn products to meet industrial standards, these elements need to be removed. There are various methods to serve this purpose, such as solvent extraction and subsequent stripping and scrubbing steps, precipitation and recrystallization or electrowinning[62]. However, these steps can be energy intensive and produce (indirect) emissions.

## 3.4. CONCLUSIONS

Li-ion batteries from a range of consumer electronics were systematically disassembled and characterized, highlighting possible sources of impurities that can contaminate the BM. Two main cell types were found: pouch- and 18650-cells. The main difference between them is the cell casing (consisting of plastic or steel, respectively). If the casing is excluded, the other components (separator, cathode and anode) have the same relative weight in both types of cells. The individual battery cells are the major component (>71 wt.%) of battery modules from consumer electronics. Internal wiring and glue/separating components take up a very small portion. The BMS takes up a larger relative weight in small modules and when

fulfilling other needs besides safe (dis)charging. The casing is larger for modules with multiple cells due to a greater need of structural integrity. Major impurities after industrial BM processing are Al, Cu and graphite. However, the presence of Ni in metallic form, assumably originating from the metal casing on 18650 cells, was also observed. Next, the CAMs were liberated from those old battery cells and characterized. Results show that there is no link between the CAM chemistry and the type of application. Various chemical compositions of CAMs have been found in consumer LiBs, sometimes with multiple chemistries combined in single battery cells. As expected, industrial BM is a combination of many different cathode chemistries, as well as earlier mentioned impurities.

With the aim of exploring the possibilities for a universal hydrometallurgical process, we researched the influence of chemical composition on the leaching behaviour of Li, Ni, Mn and Co under the same $H_2SO_4$ leaching conditions (2 mol/L, 50 °C, 2 hr, 400 rpm, 60 g BM /L) and a varying concentration of $H_2O_2$ (0-4 vol.%). Although samples with different chemistries generally exhibited similar trends, there is a difference in the amount of $H_2O_2$ required for complete dissolution of all the TMs. The leaching efficiencies of all studied elements generally increased with additions of $H_2O_2$, except for the industrial BM. Pristine NMC 532 and one of the used NMC BMs showed complete dissolution in the presence of 4 vol% $H_2O_2$-solution, whereas other BMs reached between 80 or 90% efficiency under the same conditions. The industrial BM showed distinct behaviour. All metals except Ni were leached completely without the need for $H_2O_2$. The low Ni leaching efficiency was attributed to the presence of metallic nickel from the nickel-plated steel battery cell casing. The high leaching efficiencies of Li, Co and Mn in the industrial BM is attributed to their relatively low content compared to other samples (due to the high non-metallic impurities such as graphite). Lastly, variations in the oxidation states of Ni and Co from EoL batteries were found to affect the leaching process. This was confirmed by leaching with an excess of $H_2O_2$ followed by titration. This study shows that a universal hydrometallurgical leaching process can be designed to deal with the high variety of available chemistries in mixed BM coming from EoL Li-ion batteries in consumer waste. Nevertheless, this requires excess amount of additional reducing agents, such as $H_2O_2$, to achieve high leaching efficiencies before further purification and recovery.

## REFERENCES


1. Y. Liang, C.Z. Zhao, H. Yuan, Y. Chen, W. Zhang, J.Q. Huang, D. Yu, Y. Liu, M.M. Titirici, Y.L. Chueh, H. Yu, Q. Zhang, A review of rechargeable batteries for portable electronic devices, *InfoMat* 1 (2019) 6–32.
2. G. Zubi, R. Dufo-López, M. Carvalho, G. Pasaoglu, The lithium-ion battery: State of the art and future perspectives, *Renewable and Sustainable Energy Reviews* 89 (2018) 292–308.
3. Y. Ding, Z.P. Cano, A. Yu, J. Lu, Z. Chen, Automotive Li-Ion Batteries: Current Status and Future Perspectives, *Electrochemical Energy Reviews* 2 (2019) 1–28.
4. P.R. Jadhao, E. Ahmad, K.K. Pant, K.D.P. Nigam, Environmentally friendly approach for the recovery of metallic fraction from waste printed circuit boards using pyrolysis and ultrasonication, *Waste Management* 118 (2020) 150–160.
5. A. Rensmo, E.K. Savvidou, I.T. Cousins, X. Hu, S. Schellenberger, J.P. Benskin, Lithium-ion battery recycling: a source of per- and polyfluoroalkyl substances (PFAS) to the environment?, *Environ. Sci. Process. Impacts* 25 (2023) 1015–1030.
6. A. V. Plakhotnyk, L. Ernst, R. Schmutzler, Hydrolysis in the system $LiPF_6$—propylene carbonate—dimethyl carbonate—$H_2O$, *J. Fluor. Chem.* 126 (2005) 27–31.
7. K. Gu, X. Gao, Y. Chen, W. Qin, J. Han, Closed-loop recycling of spent lithium-ion batteries based on selective sulfidation: An unconventional approach, *Waste Management* 169 (2023) 32–42.
8. A. Mayyas, K. Moawad, A. Chadly, E. Alhseinat, Can circular economy and cathode chemistry evolution stabilize the supply chain of Li-ion batteries?, *Extr. Ind. Soc.* 14 (2023) 101253.
9. Directive (EU) 2018/849 of the European Parliament and of the Council of 30 May 2018 amending Directives 2000/53/EC on end-of-life vehicles, 2006/66/EC on batteries and accumulators and waste batteries and accumulators, and 2012/19/EU on waste electrical and electronic equipment, *Official Journal* L 150 (2018) 93–99.
10. Directive 2012/19/EU of the European Parliament and of the Council of 4 July 2012 on waste electrical and electronic equipment (WEEE), *Official Journal* L 197 (2012) 38–71.
11. Regulation of the European Parliament and of the Council Establishing a Framework for Ensuring a Secure and Sustainable Supply of Critical Raw Materials and Amending Regulations (EU) 168/2013, (EU) 2018/858, 2018/1724 and (EU) 2019/1020, *Official Journal* COM 160 (2023).
12. O. Velázquez-Martínez, J. Valio, A. Santasalo-Aarnio, M. Reuter, R. Serna-Guerrero, A Critical Review of Lithium-Ion Battery Recycling Processes from a Circular Economy Perspective, *Batteries* 5 (2019) 68.
13. European Commission Directorate-General for Internal Market Industry Entrepreneurship and SMEs, D. Pennington, E. Tzimas, C. Baranzelli, J. Dewulf, S. Manfredi, P. Nuss, M. Grohol, A. Van Maercke, Y. Kayam, S. Solar, B. Vidal-Legaz, L. Talens Peirò, L. Mancini, C. Ciupagea, L. Godlewska, P. Dias, C. Pavel, D. Blagoeva, G. Blengini, V. Nita, C. Latunussa, C. Torres De Matos, F. Mathieux, A. Marmier, Methodology for establishing the EU list of critical raw materials – Guidelines, Publications Office, 2017.
14. European Commission Directorate-General for Internal Market Industry Entrepreneurship and SMEs, M. Grohol, C. Veeh, Study on the critical raw materials for the EU 2023 – Final report, Publications Office of the European Union, 2023.
15. G. Harper, R. Sommerville, E. Kendrick, L. Driscoll, P. Slater, R. Stolkin, A. Walton, P. Christensen, O. Heidrich, S. Lambert, A. Abbott, K. Ryder, L. Gaines, P. Anderson, Recycling lithium-ion batteries from electric vehicles, *Nature* 575 (2019) 75–86.
16. Y. Yang, E.G. Okonkwo, G. Huang, S. Xu, W. Sun, Y. He, On the sustainability of lithium ion battery industry – A review and perspective, *Energy Storage Mater.* 36 (2021) 186–212.

**17.** L. Brückner, J. Frank, T. Elwert, Industrial Recycling of Lithium-Ion Batteries—A Critical Review of Metallurgical Process Routes, *Metals (Basel).* 10 (2020) 1107.

**18.** P. Zhang, T. Yokoyama, O. Itabashi, T.M. Suzuki, K. Inoue, Hydrometallurgical process for recovery of metal values from spent lithium-ion secondary batteries, *Hydrometallurgy* 47 (1998) 259–271.

**19.** J. Nan, D. Han, X. Zuo, Recovery of metal values from spent lithium-ion batteries with chemical deposition and solvent extraction, *J. Power Sources* 152 (2005) 278–284.

**20.** G. Dorella, M.B. Mansur, A study of the separation of cobalt from spent Li-ion battery residues, *J. Power Sources* 170 (2007) 210–215.

**21.** X. Chen, H. Ma, C. Luo, T. Zhou, Recovery of valuable metals from waste cathode materials of spent lithium-ion batteries using mild phosphoric acid, *J. Hazard. Mater.* 326 (2017) 77–86.

**22.** R. Sattar, S. Ilyas, H.N. Bhatti, A. Ghaffar, Resource recovery of critically-rare metals by hydrometallurgical recycling of spent lithium ion batteries, *Sep. Purif. Technol.* 209 (2019) 725–733.

**23.** S.P. Barik, G. Prabaharan, L. Kumar, Leaching and separation of Co and Mn from electrode materials of spent lithium-ion batteries using hydrochloric acid: Laboratory and pilot scale study, *J. Clean. Prod.* 147 (2017) 37–43.

**24.** L. Li, J. Ge, F. Wu, R. Chen, S. Chen, B. Wu, Recovery of cobalt and lithium from spent lithium ion batteries using organic citric acid as leachant, *J. Hazard. Mater.* 176 (2010) 288–293.

**25.** M. Contestabile, S. Panero, B. Scrosati, A laboratory-scale lithium-ion battery recycling process, *J. Power Sources* 92 (2001) 65–69.

**26.** Z. Takacova, T. Havlik, F. Kukurugya, D. Orac, Cobalt and lithium recovery from active mass of spent Li-ion batteries: Theoretical and experimental approach, *Hydrometallurgy* 163 (2016) 9–17.

**27.** P. Meshram, B.D. Pandey, T.R. Mankhand, Recovery of valuable metals from cathodic active material of spent lithium ion batteries: Leaching and kinetic aspects, *Waste Management* 45 (2015) 306–313.

**28.** L.P. He, S.Y. Sun, X.F. Song, J.G. Yu, Leaching process for recovering valuable metals from the $LiNi_{1/3}Co_{1/3}Mn_{1/3}O_2$ cathode of lithium-ion batteries, *Waste Management* 64 (2017) 171–181.

**29.** R.C. Wang, Y.C. Lin, S.H. Wu, A novel recovery process of metal values from the cathode active materials of the lithium-ion secondary batteries, *Hydrometallurgy* 99 (2009) 194–201.

**30.** S. Castillo, F. Ansart, C. Laberty-Robert, J. Portal, Advances in the recovering of spent lithium battery compounds, *J. Power Sources* 112 (2002) 247–254.

**31.** C.K. Lee, K.I. Rhee, Reductive leaching of cathodic active materials from lithium ion battery wastes, *Hydrometallurgy* 68 (2003) 5–10.

**32.** E.G. Pinna, M.C. Ruiz, M.W. Ojeda, M.H. Rodriguez, Cathodes of spent Li-ion batteries: Dissolution with phosphoric acid and recovery of lithium and cobalt from leach liquors, *Hydrometallurgy* 167 (2017) 66–71.

**33.** X. Zeng, J. Li, B. Shen, Novel approach to recover cobalt and lithium from spent lithium-ion battery using oxalic acid, *J. Hazard. Mater.* 295 (2015) 112–118.

**34.** L. Sun, K. Qiu, Organic oxalate as leachant and precipitant for the recovery of valuable metals from spent lithium-ion batteries, *Waste Management* 32 (2012) 1575–1582.

**35.** G.P. Nayaka, J. Manjanna, K. V. Pai, R. Vadavi, S.J. Keny, V.S. Tripathi, Recovery of valuable metal ions from the spent lithium-ion battery using aqueous mixture of mild organic acids as alternative to mineral acids, *Hydrometallurgy* 151 (2015) 73–77.

**36.** S. Natarajan, A.B. Boricha, H.C. Bajaj, Recovery of value-added products from cathode and anode material of spent lithium-ion batteries, *Waste Management* 77 (2018) 455–465.

**37.** L. Li, Y. Bian, X. Zhang, Q. Xue, E. Fan, F. Wu, R. Chen, Economical recycling process for spent lithium-ion batteries and macro- and micro-scale mechanistic study, *J. Power Sources* 377 (2018) 70–79.

**38.** S. Kim, J. Bang, J. Yoo, Y. Shin, J. Bae, J. Jeong, K. Kim, P. Dong, K. Kwon, A comprehensive review on the pretreatment process in lithium-ion battery recycling, *J. Clean. Prod.* 294 (2021) 126329.

**39.** K. Berger, J.P. Schöggl, R.J. Baumgartner, Digital battery passports to enable circular and sustainable value chains: Conceptualization and use cases, *J. Clean. Prod.* 353 (2022) 131492.

**40.** Y. Bai, N. Muralidharan, Y.K. Sun, S. Passerini, M. Stanley Whittingham, I. Belharouak, Energy and environmental aspects in recycling lithium-ion batteries: Concept of Battery Identity Global Passport, *Materials Today* 41 (2020) 304–315.

**41.** J. Shaw-Stewart, A. Alvarez-Reguera, A. Greszta, J. Marco, M. Masood, R. Sommerville, E. Kendrick, Aqueous solution discharge of cylindrical lithium-ion cells, *Sustainable Materials and Technologies* 22 (2019) e00110.

**42.** D. Yu, Z. Huang, B. Makuza, X. Guo, Q. Tian, Pretreatment options for the recycling of spent lithium-ion batteries: A comprehensive review, *Miner. Eng.* 173 (2021) 107218.

**43.** N. V. Klassen, D. Marchington, H.C.E. McGowan, $H_2O_2$ Determination by the $I_3^-$ Method and by $KMnO_4$ Titration, *Anal. Chem.* 66 (1994) 2921–2925.

**44.** C.E. Huckaba, F.G. Keyes, The Accuracy of Estimation of Hydrogen Peroxide by Potassium Permanganate Titration, *J. Am. Chem. Soc.* 70 (1948) 1640–1644.

**45.** L.F. Guimarães, A.B. Botelho Junior, D.C.R. Espinosa, The Characterization of Li-ion Batteries and the Importance of the Recycling Processes, *JOM* 75 (2023) 3622–3631.

**46.** Y. Kim, M. Kim, T. Lee, E. Kim, M. An, J. Park, J. Cho, Y. Son, Investigation of mass loading of cathode materials for high energy lithium-ion batteries, *Electrochem. Commun.* 147 (2023) 107437.

**47.** T. Kobayashi, Y. Kobayashi, H. Miyashiro, Lithium migration between blended cathodes of a lithium-ion battery, *J. Mater. Chem. A Mater.* 5 (2017) 8653–8661.

**48.** S.B. Chikkannanavar, D.M. Bernardi, L. Liu, A review of blended cathode materials for use in Li-ion batteries, *J. Power Sources* 248 (2014) 91–100.

**49.** S.Y. Chung, J.T. Bloking, Y.M. Chiang, Electronically conductive phospho-olivines as lithium storage electrodes, *Nat. Mater.* 1 (2002) 123–128.

**50.** T. Kim, W. Song, D.Y. Son, L.K. Ono, Y. Qi, Lithium-ion batteries: outlook on present, future, and hybridized technologies, *J. Mater. Chem. A Mater.* 7 (2019) 2942–2964.

**51.** X. Chen, B. Xu, T. Zhou, D. Liu, H. Hu, S. Fan, Separation and recovery of metal values from leaching liquor of mixed-type of spent lithium-ion batteries, *Sep. Purif. Technol.* 144 (2015) 197–205.

**52.** L. Li, J. Ge, R. Chen, F. Wu, S. Chen, X. Zhang, Environmental friendly leaching reagent for cobalt and lithium recovery from spent lithium-ion batteries, *Waste Management* 30 (2010) 2615–2621.

**53.** N. Vieceli, P. Benjamasutin, R. Promphan, P. Hellström, M. Paulsson, M. Petranikova, Recycling of Lithium-Ion Batteries: Effect of Hydrogen Peroxide and a Dosing Method on the Leaching of LCO, NMC Oxides, and Industrial Black Mass, *ACS Sustain. Chem. Eng.* (2023).

**54.** C. Peng, J. Hamuyuni, B.P. Wilson, M. Lundström, Selective reductive leaching of cobalt and lithium from industrially crushed waste Li-ion batteries in sulfuric acid system, *Waste Management* 76 (2018) 582–590.

**55.** N. Vieceli, R. Casasola, G. Lombardo, B. Ebin, M. Petranikova, Hydrometallurgical recycling of EV lithium-ion batteries: Effects of incineration on the leaching efficiency of metals using sulfuric acid, *Waste Management* 125 (2021) 192–203.

**56.** Y. Koyama, I. Tanaka, H. Adachi, Y. Makimura, T. Ohzuku, Crystal and electronic structures of superstructural $Li_{1-x}[Co_{1/3}Ni_{1/3}Mn_{1/3}]O_2$ ($0 \leq x \leq 1$), *J. Power Sources* 119–121 (2003) 644–648.

**57.** M.C. Biesinger, B.P. Payne, A.P. Grosvenor, L.W.M. Lau, A.R. Gerson, R.S.C. Smart, Resolving surface chemical states in XPS analysis of first row transition metals, oxides and hydroxides: Cr, Mn, Fe, Co and Ni, *Appl. Surf. Sci.* 257 (2011) 2717–2730.

**58.** J.L. White, F.S. Gittleson, M. Homer, F. El Gabaly, Nickel and Cobalt Oxidation State Evolution at Ni-Rich NMC Cathode Surfaces during Treatment, *Journal of Physical Chemistry C* 124 (2020) 16508–16514.

**59.** A. Chernyaev, Y. Zou, B.P. Wilson, M. Lundström, The interference of copper, iron and aluminum with hydrogen peroxide and its effects on reductive leaching of $LiNi_{1/3}Mn_{1/3}Co_{1/3}O_2$, *Sep. Purif. Technol.* 281 (2022) 119903.

**60.** A. Chernyaev, J. Zhang, S. Seisko, M. Louhi-Kultanen, M. Lundström, $Fe^{3+}$ and $Al^{3+}$ removal by phosphate and hydroxide precipitation from synthetic NMC Li-ion battery leach solution, *Sci. Rep.* 13 (2023) 1–12.

**61.** A. Chernyaev, B.P. Wilson, M. Lundström, Study on valuable metal incorporation in the Fe–Al precipitate during neutralization of LIB leach solution, *Sci. Rep.* 11 (2021) 1–8.

**62.** J. Neumann, M. Petranikova, M. Meeus, J.D. Gamarra, R. Younesi, M. Winter, S. Nowak, Recycling of Lithium-Ion Batteries—Current State of the Art, Circular Economy, and Next Generation Recycling, *Adv. Energy Mater.* 12 (2022) 2102917.

*Nothing in life is to be feared, it is only to be understood. Now is the time to understand more, so that we may fear less.*

Marie Curie

# 4

# Chapter 4

## Simultaneous Recycling of Spent LFP & NMC Li-ion Batteries Under Mild Leaching Conditions

Chapter 3 clearly shows how hydrometallurgical recycling can be influenced by the composition of the LiB-waste. It also shows that when enough reagents are used, complete dissolution of the target metals (Li, Co, Ni and Mn) can be reached. However, the use of more reagents is also associated with a larger environmental footprint. Hence, it is desirable to limit the use of chemicals during recycling, by smartly designing each process.

Chapter 4 explores the possibility of lowering the chemicals consumption of Li-ion battery recycling, by replacing a commonly used reducing agent by a waste material from another Li-ion battery type: LFP. This is of utmost importance in order to recycle these batteries on a large scale in a sustainable way.

Leaching studies over time are conducted using stepwise additions of LFP and $H_2O_2$-solution (1 vol%) to a mild lixiviant of 0.63 mol/L $H_2SO_4$ at 50°C. For pristine NMC 532, ±95% leaching of Li, Ni, Co, and Mn is achieved. The divalent Fe present in LFP, as well as $H_2O_2$, act as a reductant for the dissolution of Ni, Co, and Mn. The Al and Cu present in industrially treated BM further enhance the dissolution of the transition metals via a catalysed reaction with Fe from LFP. This results in complete leaching of Li, Ni, Co, and Mn for mechanically pre-treated industrial black mass samples. However, the leaching residues acquired from these samples, which consist largely of $FePO_4$, get contaminated with graphite. Also, while pyrolysis of the black mass benefits the leaching of Co and Mn, it results in difficulties in subsequent removal of Fe from the pregnant leach solution. The chemical processes and their performance are described in this work.

---

This Chapter is published in Journal of Sustainable Metallurgy:
van de Ven, J. J. M. M., Teeuwisse, P. J., Hendrikx, R. W. A., Yang, Y. & Abrahami, S. T.. Simultaneous Recycling of Spent $LiFePO_4$ and $LiNi_xMn_yCoz O_2$ Li-Ion Batteries Under Mild Leaching Conditions. 1–12 (2025).

## 4.1. INTRODUCTION

In our current society, lithium-ion batteries (LiBs) are widely used to store electricity, thereby contributing to the energy transition [1]. They are used in many applications, such as electric vehicles (EVs), portable electronics and stationary energy storage [1]. LIBs contain many elements listed on the EU's critical raw materials (CRMs) list which are essential for their optimal functionality [2,3]. Well known examples of these are Co, Mn and Li [2,3]. These elements are mainly present as oxides in the cathode such as $LiCoO_2$ (LCO) or $LiNi_xMn_yCo_zO_2$ (NMC) [4]. Hence, they are also known as cathode active materials (CAMs). Due to a high demand and geopolitical concerns, the supply of these CRMs is under pressure, yet they are crucial for the European economy [5–7]. However, the global market for LiBs is projected to grow significantly in the coming years, resulting in the need for more of these CRMs [8]. Also, the LiBs are mostly produced in China, which means most countries will rely on import of these batteries [9]. Therefore, apart from sourcing more of these raw materials, recycling will play a significant role in meeting future demands [10]. Also, landfilling of LiBs can cause harmful substances to leak in the environment, further emphasizing the need for recycling [11].

Although there is a range of possible routes to recycle LiBs, hydrometallurgical processes are emerging as the future choice of technology due to its ability to recover more materials compared to the traditional pyrometallurgy [12]. In hydrometallurgy, materials are selectively dissolved and then purified using aqueous and/or non-aqueous solutions [13]. There are various examples of hydrometallurgical processes that aim to extract and purify Li, Ni, Co, and Mn from LiBs [14–19]. However, these studies still present many limitations. For the case of LiBs, the starting material for the hydrometallurgical process is black mass (BM), a mixture of both anode and cathode containing graphite, metal oxides (Li, Mn, Co, Ni) and impurities such as Fe, Al, and Cu. Acquiring this material requires an extensive initial pre-treatment. In addition, LIBs are a family of different chemistries, leading to a heterogeneous waste stream of which the composition is prone to variations [20,21]. Hence, there is a need for recycling processes capable to handle this complex waste stream[21].

Before recycling, the Ni, Co and Mn in the BM are typically present in the +II, +III or +IV oxidation states [22,23]. However, to efficiently dissolve these transition metals (TMs) during leaching they all need to be reduced to the divalent state [24–26]. Therefore, the lixiviant needs to have a reducing nature, resulting in the reaction illustrated in Eq. 4.1 [24–27]. This can be established by the presence of an acid with reducing capabilities such as HCl [15,28,29], or additional reducing agents such as $H_2O_2$, glucose or ascorbic acid [25–27,30–33]. In the study of Wang et al., 4 mol/L of HCl could both reduce and dissolve the elements in NMC cathode

materials [34]. When leached for 60 minutes at 80 °C and a solid-to-liquid ratio (S/L) of 20 g/L, this resulted in leaching efficiencies exceeding 99.5% for Li, Ni, Co and Mn. However, HCl comes with the drawback of chlorine gas formation during leaching, as well as high corrosiveness, which can result in damage to equipment [28]. Sattar et al., made use of 2 mol/L $H_2SO_4$, while adding $H_2O_2$ to create a reducing environment [25]. The experiments were conducted at 50 °C for 3 hours, with a S/L of ±60g/L. Without the reducing agent, leaching efficiencies did not exceed 45 % for Mn and Co, and around 80% for Li and Ni. However, addition of 4 vol% $H_2O_2$-solution increased these values to > 98%. Similar results were found in the systems of Meng et al. and Peng et al. [30,33], where glucose and ascorbic acid were added as reducing agents, respectively. However, the general drawback is that additional reagents are also accompanied by higher costs and extra indirect emissions. To lower the environmental footprint as well as some economic burdens of the recycling of LiBs, we need to find a way to reduce the consumption of chemicals without introducing any new impurities [35].



$$3LiNi_{1/3}Mn_{1/3}Co_{1/3}O_{2\,(s)} + 12H^{+}_{(aq)} + 3e^{-} \rightarrow 3Li^{+}_{(aq)} + Ni^{2+}_{(aq)} + Mn^{2+}_{(aq)} + Co^{2+}_{(aq)} + 6H_2O_{(l)} \quad (4.1)$$

$LiFePO_4$ (LFP) batteries are gaining popularity due to its high thermal and electrochemical stability, as well as a lower material cost [36,37]. Due to its chemical nature, it can also be used as a reducing agent in recycling, instead of adding additional reducing compounds [38–40]. After its dissolution in $H_2SO_4$ (Eq. 4.2), the present $Fe^{2+}$ can be oxidised, hence releasing electrons (Eq. 4.3) [38–40]. Jiang et al. showed that spent $LiFePO_4$ can be used as reagent in the leaching of LCO, which resulted in lower consumption of chemicals [38]. An acid concentration of only 0.5 mol/L ($H_2SO_4$) was used, with a leaching time of 20 minutes at 50°C and a total solid to liquid ratio of 30 g/L. These conditions resulted in over 99% extraction of Li, Fe, and $PO_4^{3-}$, and 92.4% for Co. Also, no additional reagents such as $H_2O_2$ were necessary. The $Fe^{3+}$ could be removed by pH adjustment, due to the limited solubility of $FePO_4$ above pH=2 [38]. Similar findings were presented by Chen et Al. [39] and Liu et Al. [40], who used spent NMC-type cathode materials instead of LCO. Chen et Al. found that a lixiviant composed of $H_3PO_4$ (2 mol/L) and 4 vol% $H_2O_2$ solution succeeded in leaching the Li, Ni, Co, and Mn from the waste cathode materials when reacting for 60 hours at 60 °C and an S/L of 50 g/L. The Fe from LFP was left behind in the residue. They also showed the possibility of subsequent purification and regeneration of the cathode materials[39]. Liu et Al. found that with 0.25 mol/L $H_2SO_4$ and an S/L of 32 g/L while leaching for 4 hours at 80 °C also resulted in complete dissolution of Li, Ni, Co, and Mn. They even added

5 g/L of $FePO_4$*$2H_2O$ seed crystals during leaching, which resulted in simultaneous recrystallization of Fe from the PLS as phosphate.

$$LiFePO_{4(s)} + 2H^{+}_{(aq)} \rightarrow Li^{+}_{(aq)} + Fe^{2+}_{(aq)} + H_2PO^{-}_{4(aq)} \quad (4.2)$$

$$Fe^{2+}_{(aq)} \rightarrow Fe^{3+}_{(aq)} + e^{-} \quad (4.3)$$

Using LFP to recycle other spent cathode materials is an elegant way to reduce the chemical consumption of the recycling process while increasing the recycling rates of both types of batteries, especially with simultaneous recovery of cathode materials. However, these proof-of-concept studies do not capture the complexity of the current industrial battery waste stream, especially coming from e-waste [21]. Consequently, the challenges arising from the heterogeneous composition of industrial battery waste are not addressed [41]. For example, the impact of impurities that are often present in black mass, such as graphite, Al and Cu, on the leaching and purification are not discussed. [42]

Therefore, in this paper we focus on recycling of various LiBs waste streams available on the current market. By studying the effect of varying waste composition and pre-treatment on the leaching using LFP from spent LiBs, the following research question can be answered: Is it possible to leach a mixed LiB-waste stream aided by LFP, with less need of chemicals and limited additional contamination? To answer this question, we designed and tested an experiment that aimed for full dissolution of Li, Co, Ni and Mn and monitored the reactions over time. This experimental procedure was then applied to 5 different types of battery waste, ranging from pristine NMC 532 to industrially pre-treated black masses. Next, we analysed the leaching residues to highlight the impact of impurities from industrial LiB-waste. Following leaching, we used pH adjustment to selectively remove the Fe introduced by LFP-addition from the pregnant leach solution (PLS). It was precipitated as $FePO_4$, which is also a precursor in the synthesis of new $LiFePO_4$.

## 4.2. MATERIALS & METHODS

### 4.2.1. Battery Materials

Within this study, we distinguish the terms cathode active material (CAM) and black mass (BM). CAMs are mixed oxides of Li, Co, Ni and Mn, directly purchased from a manufacturer or manually removed from a battery. The term black mass (BM) is used for the combination of CAMs with impurities, retrieved via industrial pre-

treatment. Industrial pre-treatment includes steps such as shredding, magnetic separation, milling and sieving.

In the leaching experiments, three types of battery products were used. The first material is a CAM with the chemical formula $LiNi_{0.5}Mn_{0.3}Co_{0.2}O_2$ (High power Li-ion Battery Cathode Application, Nanographi), and is called NMC 532. Two other samples were manually prepared from spent LiBs, originating from end-of-life (EoL) consumer electronics. One of them is a material similar to the pristine sample, so it is called "spent NMC 532". The $LiFePO_4$ (LFP) used in this study is also retrieved in this manner. To acquire these materials, pouch type battery cells were removed from their respective devices and discharged in a 10% $K_2CO_2$ (≥99.0%, Sigma-Aldrich) solution for 24 hours. Then, the cells were opened with a box cutter. This revealed a roll of cathode, anode and separator, which was removed and unrolled. The cathode foil was separated, since it contains the active materials used in this study. To liberate the cathode material from the aluminium foil, the cathode was cut into pieces of approximately 2 by 2 cm. These pieces were submerged in N-methyl-pyrrolidone (NMP) at 80 °C with ultrasonification to dissolve the binder. The slurry of NMP and cathode material was then allowed to settle for at least 24 hours, after which it was decanted, and the remaining solvent was dried. This left behind CAMs with a relatively low amount of impurities. Thirdly, various BMs from industry were used in this research. The composition of all CAMs and BMs together with their abbreviation are listed in Table 4.1.



*Table 4.1: Composition (wt.%) of all CAMs and BMs used in this study.*

| Abbreviation | Li | Co | Ni | Mn | Al | Fe | Cu | $PO_4^{3-}$ | Note |
|---|---|---|---|---|---|---|---|---|---|
| NMC 532 | 7.8 | 11.7 | 31.0 | 16.4 | 0.0 | 0.0 | 0.0 | - | Pristine NMC 532 |
| Spent NMC 532 | 5.2 | 11.5 | 28.5 | 15.4 | 0.4 | 0.0 | 0.0 | - | NMC 532 from spent LiBs |
| LFP | 4.0 | - | - | - | 0.3 | 32.6 | 0.0 | 52.2 | LFP form spent LiBs. |
| BM P | 4.2 | 17.8 | 12.0 | 4.5 | 2.8 | 0.4 | 2.1 | * | Industrial BM, Pyrolyzed |
| BM M | 3.3 | 6.8 | 16.7 | 6.7 | 0.5 | 1.1 | 1.0 | * | Industrial BM, mechanical ** |
| BM M+ | 4.5 | 7.9 | 22.0 | 8.0 | 1.3 | 0.9 | 3.0 | * | Industrial BM, mechanical *** |

*For industrial BMs the P from LFP batteries and P from electrolyte components could not be differentiated, and therefore was not included,

**Discharged LiBs, shredded, magnetic separation and sieving, *** = BM M with extra milling and sieving step.

### 4.2.2. Characterization Techniques

The present phases in the battery materials, as well as the leaching residues and $FePO_4$-precipitates, were characterized by X-ray diffraction (XRD) analysis. The analysis was carried out with a Bruker D8 Advance diffractometer with Bragg-

Brentano geometry and a Lynxeye position sensitive detector, using Cu Kα radiation. The 2Θ range was 10 – 110°, with a step size of 0.04° and a counting time of 2s per step. To analyse the data, the Bruker software DiffracSuite.EVA vs 6.0 was used.

To determine the elemental composition of the CAMs and BMs, they were analysed with ICP-OES. Therefore, the samples were digested with aqua regia for complete dissolution. To account for the heterogeneity, each sample was analysed at least three times, or at least four times when a high variance was seen. One gram of battery material was dissolved in 100 mL of aqua regia. This solution was prepared by combining 25 mL of $HNO_3$ (65%, VWR chemicals) with 75 mL HCl (37%, Merck). The digestion was carried out in a triple necked round bottom flask with reflux cooler, at 70 °C for 5 hours, while stirring at 500 rpm. After digestion, the solid residue was separated through a Whatman 595 ½ folded filter paper and the solution was diluted to 1L using a volumetric flask at 20 °C. A sample of 0.5 mL from this solution was sent to ICP-OES analysis.

ICP-OES analysis was carried out using a Spectro Arcos-EOP-device with Modified Lichte nebulizer and mini cyclon spray chamber. For verification of complete dissolution of all metals after aqua regia digestion, the residue was analysed to check any remaining residual metals with a Jeol JSM-IT100 scanning electron microscopy (SEM) in combination with energy dispersive X-ray (EDX) analysis. A small amount of the residue was applied on a piece of carbon tape and placed on the sample holder.

### 4.2.3. Leaching

For the extraction of Li, Ni, Co, and Mn from the black mass, a lab scale leaching setup with a 500 mL triple necked round bottom flask was used as shown in the appendix (Fig. B.1). The lixiviant had a total volume of 100 mL and contained $H_2SO_4$ (95.0 – 97.0 %, Sigma-Aldrich), diluted in Milli-Q water. The acid concentration was determined based on literature and preliminary experiments, and was 0.63 mol/L. The leaching was carried out for 2 hours while stirring at 400 rpm with a magnetic stirring bar. At the end of the reaction, the slurry was filtered through a Cytiva ME 25 membrane filter with 0.45 µm pore size. The residue was dried (50°C, 8 hours) and weighed, and the PLS was collected for further study on Fe precipitation. In one final leaching experiment with a lixiviant of 500 mL, a 1 L triple necked round bottom flask was used.

For the leaching experiments, monitoring the reactions over time was required. A syringe was used to extract 0.5 mL of the leaching system every 15 minutes. In order to separate the remaining solids, this slurry was filtered through a syringe filter (Chromafil Xtra PFTE-45/25), after which 0.1 mL was submitted to inductively coupled plasma optical emission spectroscopy (ICP-OES) analysis.

To compare the performance of different leaching experiments, the leaching efficiency ($\eta_L$) was calculated according to Eq. 4.4. In this formula, $m^x_f$ represents the initial mass of element x in the feed. This was determined from aqua regia digestion of the sample in triplicates and subsequent ICP-OES analysis. $m^x_{PLS}$ represents the mass of element x present in the pregnant leach solution (PLS) after leaching. This was determined by ICP-OES analysis of the PLS.

$$\eta_L = \frac{m^x_{PLS}}{m^x_f} * 100\% \tag{4.4}$$

### 4.2.4. Precipitation stripping of Fe

After filtration of the residue, the PLS was allowed to cool down for roughly 15 minutes. Then, its pH was measured, after which it was increased stepwise to 1.6, 2 and eventually 3 by the addition of a 1 mol/L NaOH solution. To correct the concentrations of the metals in the PLS, it was weighed before neutralisation, as well as after reaching the aforementioned pH values. At each dedicated pH value, a sample of 1 mL was taken with a syringe and filtered through a syringe filter (Chromafil Xtra PFTE-45/25). This was submitted to ICP-OES-analysis to calculate the percentage of remaining elements in the PLS. After reaching pH 3, the precipitates were filtered using a Whatman 595 ½ folded filter paper. The precipitates were then dried at 50 °C for 8 hours.

In the last leaching experiment with 500 mL PLS, this approach was altered slightly. A 2 mol/L LiOH-solution was used for neutralisation. The resulting precipitate from this experiment was, after drying, also submitted to heat treatment in order to manifest crystallization. This was done at 600 °C for 2 hours under $N_2$-atmosphere. Hence, the sample could be characterized by XRD-analysis.

## 4.3. RESULTS & DISCUSSION

Within this study, two types of experiments were conducted. Firstly, a leaching experiment was set up in which different battery materials were allowed to dissolve under mild leaching conditions while studying the reaction over time. The residues were then characterized to evaluate their purity, indicating of potential reuse in LiBs. Secondly, the iron that originated from the LFP was removed from the PLS by precipitation. The efficiency of the iron removal as well as the purity of the resulting precipitate was evaluated.

### 4.3.1. Influence of Black Mass Composition on Leaching with $LiFePO_4$

The reducing capability of Fe(II) in LFP for reductive acid leaching has been demonstrated in literature [38–40]. Here, we test the feasibility of this leaching process for industrial LiBs waste recycling. An LFP:NMC-ratio of 1:1 was chosen for this study. To ensure complete dissolution, 1 vol% of $H_2O_2$ solution is added during the last phase of leaching. To show the individual impact of LFP and $H_2O_2$ on leaching, they were added at different stages; LFP was added after 30 minutes, while $H_2O_2$ was added after 90 minutes of reaction time. Then, the solution was left to react further for 30 more minutes, for a total leaching time of 2 hours. To monitor the reaction progress, a sample was taken every 15 minutes. It was expected that LFP greatly benefits the dissolution of Ni, Co and Mn. This should be seen in the shape of a sharp increase in leaching efficiency at the 45-minute mark, 15 minutes after its addition. Addition of $H_2O_2$ at 90 minutes should result in an increased leaching efficiency of all metals at 105 and 120 minutes. After conducting this experiment on the pristine NMC532, it was also applied to the other BM samples of which the compositions can be found in Table 4.1.

Fig. 4.1 shows the results for the pristine NMC 532. It can be seen that the leaching efficiency of Ni, Co and Mn after 30 minutes is rather low, reaching around 37%, while Li is extracted for 75%. After the addition of LFP to the mixture, a sharp increase in leaching efficiency can be seen, after only 15 minutes of reaction time. Also, even though the feed concentration of Li almost doubles upon the addition of LFP, its leaching efficiency still increases to 89%. This indicates a fast dissolution of LFP, as well as an efficient reaction between $Fe^{2+}$ and the TMs in NMC. After the sharp initial increase, the leaching efficiency continues to climb, albeit more gradually. A total reaction time of 90 minutes, of which 60 minutes are in the presence of LFP, results in 99% extraction of Li and around 94% for the TMs. Furthermore, addition of $H_2O_2$ at the end further enhances the dissolution of Li, Ni, Co, and Mn to roughly 98%, which is expected since the reducing ability of $H_2O_2$ is well known. Fortunately, the extraction of the possibly contaminating iron is limited to 33%, with a concentration of 3.7 g/L in the PLS. This is a result of the limited solubility of $FePO_4$ [38,39]. After $Fe^{2+}$ is oxidised (Eq. 4.3), it largely precipitates as $FePO_4$, as indicated by Eq. 4.5 [38].

$$Fe^{3+}_{(aq)} + H_2PO^-_{4(aq)} \rightarrow FePO_{4(s)} + 2H^+_{(aq)} \tag{4.5}$$

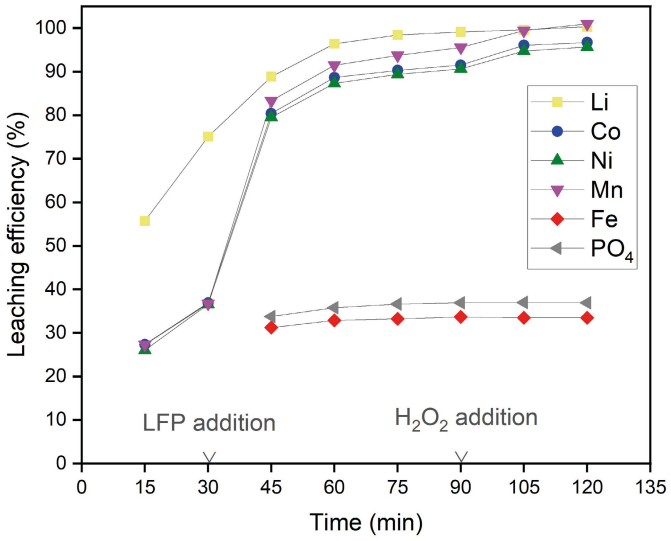


*Figure 4.1: Dependence of the leaching efficiency of Li, Ni, Co, Mn, Fe, and $PO_4^{3-}$ on time, as well as the presence of LFP and $H_2O_2$. LFP (34 g/L) and $H_2O_2$ (1 vol%) were added to the leaching system at 30 and 90 minutes, respectively. The S/L of NMC was 20 g/L.*



These results are in line with our expectation. Without the presence of LFP, the Ni, Mn and Co at higher oxidation states are not dissolved, resulting in the low leaching efficiency of approximately 35%. The presence of LFP from the 30 minute mark onwards provides Fe(II) as a reducing agent, thereby enhancing the leaching efficiencies. Li dissolves relatively easily, resulting in 75% leaching without LFP. The efficient leaching of lithium is attributed to the good solubility of $Li^+$, the lower binding energy between Li and O compared to the other metals and the fact that it does not need to be reduced before dissolution [26,42].

This leaching process was repeated on the other BMs which are included in Table 4.1. The results for BM P and BM M+ can be found in Fig 4.2. The spent NMC 532 and BM M show similar results compared to the pristine NMC 532 (Fig. 4.1) and BM M+ (Fig. 4.2a), and are therefore included in the appendix (Fig. B.2). For each experiment, the combined amount of Ni, Co, and Mn in the feed was kept constant at 0.2 mol, which was based on the experiment in Fig. 4.1. This was done to avoid a lower feed concentration of the target metals, which is a result of dilution by insoluble components such as graphite in industrial BM samples. As a result, the S/L ratio varies between the leaching experiments of the different BM samples, being between 54 and 73 g/L total (LFP + NMC-type waste). Also, leaching efficiency sometimes exceeds 100%. This is of course not possible in practice and is a result of experimental uncertainties and the inherent heterogeneous nature of the samples.

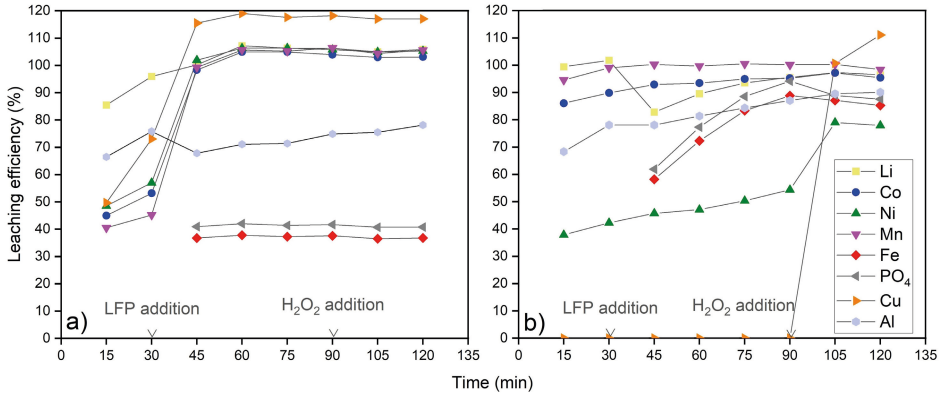


*Figure 4.2: Dependence of the leaching efficiency of Li, Ni, Co, Mn, Cu, Fe, Al, and $PO_4^{3-}$ on time, as well as the presence of LFP and $H_2O_2$, for two different black mass samples; a) BM M+ (30.5 g/L), b) BM P (33.5 g/L). LFP (34 g/L) and $H_2O_2$ (1 vol%) were added to the leaching system at 30 and 90 minutes, respectively.*

When comparing the results of all the analysed BM samples (Figs. 4.2 and B.2), similar trends emerge. Addition of either LFP or $H_2O_2$ results in a better leaching performance, albeit to a higher or lower extent. However, the various treatments applied to BMs as well as the different impurities they contain result in more complex leaching systems yielding different results.

Fig. 4.2a depicts the results for BM M+. The leaching behaviour is similar compared to the pristine NMC 532, but important differences are also present. After 30 minutes, Ni, Co and Mn are extracted for around 50%, whereas Li reached 93%. At this point, the Cu and Al are extracted for 74%. When LFP is added it first dissolves according to Eq. 4.2. After 30 minutes of $Fe^{2+}$ being present, the leaching of the Li, Ni, Co, and Mn is at 100% (Eqs. 4.1 and 4.3). When $Fe^{2+}$ is oxidised to $Fe^{3+}$, it mostly precipitates again as iron phosphate (Eq. 4.5), which can be seen by its maximum leaching efficiency of 38% as well as by XRD-analysis of the leaching residue (Fig. 4.4 in section 4.3.3).

Since Al is also present in the LFP, its feed concentration increased at 30 minutes from 0.4 to 0.5 g/L. This results in a seemly lower leaching efficiency after 45 minutes, although its total concentration in the PLS increases (0.30 g/L at 30 minutes, 0.34 g/L at 45 minutes). Al reacts slower, and its dissolution in sulfuric acid is already described in literature (Eq. 4.6) [43]. However, both the dissolution of Al and Cu are facilitated by the presence of $Fe^{3+}$ in the solution. The latter is produced from the oxidation of $Fe^{2+}$ originating from LFP. The reduction of Al and Cu can be found in Eqs. 4.7 and 4.8, respectively [43]. As a consequence, the dissolution of Al and Cu leads to reduction of Ni, Co, and Mn, through catalysis by the $Fe^{3+}/Fe^{2+}$-couple.

This explains the higher leaching efficiency of Ni, Co, and Mn for the industrial BM M+ (Fig 4.2a), compared to pristine NMC 532 (Fig. 4.1). The latter has no reducing capacity that is generated by the dissolution of Al and Cu. It is important to note that the Cu is already partially extracted (73%) before LFP addition. This is most likely the result of Fe impurities present in the industrially processed feed, which can also reduce the Co, Ni and Mn and hence start catalysing the dissolution of Cu and Al. As a result, addition of $H_2O_2$ is not needed in this case. The dissolution of Al, Fe and $PO_4^{3-}$ after 120 minutes total reaction time reaches 77, 37 and 41% respectively.

$$2Al_{(s)} + 3H_2SO_{4\,(aq)} \rightarrow 2Al^{3+}_{(aq)} + 3SO^{2-}_{4\,(aq)} + 3H_{2\,(g)} \quad (4.6)$$

$$Al_{(s)} + 3Fe^{3+}_{(aq)} \rightarrow Al^{3+}_{(aq)} + 3Fe^{2+}_{(aq)} \quad (4.7)$$

$$Cu_{(s)} + 2Fe^{3+}_{(aq)} \rightarrow Cu^{2+}_{(aq)} + 2Fe^{2+}_{(aq)} \quad (4.8)$$



Fig. 4.2b depicts the leaching process of industrial BM P. The dissolution behaviour of this BM differs significantly from all the other samples. Under the applied mild chemical conditions, Li, Mn, and Co are dissolved quickly, without any additional reducing agent. They reach leaching efficiencies of 102, 99, and 90%, respectively, which is very high compared to the other samples. This is most probably a result of the high temperature treatment the BM received. The industrial samples also contain graphite from the anode of LiBs. At high temperature, this can cause pre-reduction of the TMs [44]. Therefore, the reaction according to Eq. 4.1 has already been completed to a large extent before the leaching process. Ni, on the other hand, is only extracted for 42%. According to XRD-analysis (Fig. B.4), it is present as both NiO and metallic Ni. Hence, one part is already soluble (NiO) and another part needs to be oxidised (Ni), for which no reagents are present during the first 30 minutes.

Addition of LFP does not have a significant impact on the dissolution of Ni, Co, and Mn. An increase of Li in the feed from 1.4 to 2.8 g/L leads to a lower leaching efficiency for this element (83 % at 45 minutes), although the concentration in solution increases from 1.4 to 2.3 g/L. At 90 minutes, Li, Co, Mn, and Ni are extracted for 96, 95, 100, and 54%, respectively. It is unclear whether additional reaction time or the presence of LFP is causing this gradual increase in dissolution. Distinct behaviour of Fe and $PO_4^{3-}$ is also seen. The extraction of these entities is far greater than in the other experiments, reaching around 89% at maximum. This indicates that the Fe(II) from the LFP dissolves well (Eq. 4.2). However, the target metals are already dissolved due to the pre-reduction during pyrolysis and $Fe^{2+}$ is

not required to act as a reducing agent. Thus, it remains in solution and does not turn into the less soluble $Fe^{3+}$ (Eq. 4.3), hampering precipitation as $FePO_4$ (Eq. 4.5).

After adding $H_2O_2$ and reacting for another 30 minutes, the Ni extraction eventually reaches 78%. This increase is the result of metallic Ni being oxidised by $H_2O_2$, which can also act as an oxidising agent according to Eq. 4.9 [45]. Addition of $H_2O_2$ also results in a small amount of oxidation of $Fe^{2+}$ to $Fe^{3+}$ (Eq. 4.10) [46]. This has several consequences for the leaching system. Firstly, a small portion of the Fe and $PO_4^{3-}$ precipitates, reducing their leaching efficiencies to around 85%. Secondly, the presence of $Fe^{3+}$ kickstarts the dissolution of Cu according to Eq. 4.8.

It is important to note that $H_2O_2$ can engage in many side reactions, especially after forming radicals in combination with $Fe^{3+}$-ions such as shown in Eq. 4.11 [43,46]. To verify that the Cu dissolution is truly a result of catalysis by $Fe^{3+}/Fe^{2+}$, this experiment was repeated with addition of pristine NMC 532 after 90 minutes, instead of $H_2O_2$ (Fig. B.3). The added CAMs should be able to react with the remaining $Fe^{2+}$-ions in solution, hence forming $Fe^{3+}$ (Eqs. 4.1 and 4.3), without the risk of side reactions. Subsequently, the Cu could then be dissolved according to Eq. 4.8. It can be seen in these results that the leaching efficiency of Cu increases to 29% upon addition of the pristine NMC 532. This confirms that the dissolution of Cu is indeed the result of its oxidation by $Fe^{3+}$, which was generated from the reaction of $Fe^{2+}$ with the pristine NMC 532.

$$H_2O_{2(aq)} + 2H^+_{(aq)} + Ni_{(s)} \rightarrow 2H_2O_{(l)} + Ni^{2+}_{(aq)} \left(E^0 = 2.02V\right) \tag{4.9}$$

$$H_2O_{2(aq)} + Fe^{2+}_{(aq)} \rightarrow OH^-_{(aq)} + OH^{\cdot}_{(aq)} + Fe^{3+}_{(aq)} \tag{4.10}$$

$$H_2O_{2(aq)} + Fe^{3+}_{(aq)} \rightarrow H^+_{(aq)} + HO^{\cdot}_{2(aq)} + Fe^{2+}_{(aq)} \tag{4.11}$$

Fig. B.2a shows the leaching results for the spent NMC 532. The trend looks very similar to the one seen for the pristine NMC 532 (Fig. 4.1), and the results and discussion are therefore part of the appendix. It is interesting to note, however, that this sample requires more reducing agents in the form of LFP and $H_2O_2$ compared to the pristine 532. This is presumably the result of TMs being present in compounds formed by side reactions during the use phase of these LiBs, as we previously have shown [21].

Fig. B.2b shows the leaching behaviour of BM M, which looks similar to the behaviour of BM M+. The difference rises from the higher amount of graphite in BM M, resulting in a higher S/L ratio (38.4 compared to 30.5 g/L). Hence, the dissolution goes slower. A detailed description can be found in the appendix. The leaching behaviour of Li is however noteworthy, since it does not reach full dissolution. This

is likely because of its presence in the relatively large amount of graphite, which originates from the anodes in LiBs. These particles do not dissolve, resulting in the need for Li to migrate out of these particles. Hence, the leaching efficiency of Li is lower.

Overall, the leaching trends of these BM samples are similar. Addition of LFP greatly improves the dissolution of Ni, Co, and Mn and also benefits the dissolution of Li. However, samples such as the spent NMC 532 have a higher need for additional reducing agent. According to literature, this is largely the result of the oxidation state of the TMs in the BM, which are dependent on side reactions of the CAMs during use of the batteries [21]. Also, the Al and Cu which are present in industrial black mass samples have reducing capabilities, if catalysed by $Fe^{3+}/Fe^{2+}$. When these elements were not present, additional $H_2O_2$ was needed to complete dissolution. Since it is usual for industrially pre-treated BM to contain Cu and Al impurities, the use of $H_2O_2$ can be minimized or avoided, reducing the need for additional chemicals in recycling.



### 4.3.2. Analysis of the Leaching Residues

Besides the content of the PLS, the purity of the leaching residue is of great importance in hydrometallurgical recycling. Hence, semi-quantitative XRD-analysis with Rietveld refinement and ICP-OES analysis were performed on the leaching residues resulting from the experiments presented in Figs 4.1, 4.2 and B.2. The results can be found in Table 4.2.

*Table 4.2: Results of XRD-analysis ($FePO_4$ and Graphite) and ICP-OES analysis (Al, Cu, and Li + Ni + Mn + Co) of leaching residues, reported in wt.%.*

| Fig. | BM sample | $FePO_4$ | Graphite | Al | Cu | Li, Ni, Mn, Co |
|---|---|---|---|---|---|---|
| 4.1 | NMC 532 | Main component | < 1 | 0.0 | 0.0 | 0.4 |
| B.2a | Spent NMC 532 | 83 | 1 | 0.1 | 0.0 | 4.6 |
| 4.2b | BM P | 13 | 74 | 2.0 | 0.8 | 6.6 |
| B.2b | BM M | 72 | 28 | 0.0 | 0.0 | 0.3 |
| 4.2a | BM M+ | 72 | 28 | 0.1 | 0.1 | 0.1 |

For the experiments using pristine and spent NMC 532, the residues primarily consist of $FePO_4$ (>83 wt.%) with minimal contamination from graphite, Al and Cu (≤1 wt.%). This low level of impurities can be attributed to the high purity of the starting materials. Pristine NMC 532, purchased directly from a supplier, contains very few impurities that could carry over to the residue. Similarly, the spent NMC

532 was manually liberated from a LiB and the CAMs directly removed from the cathode. Incomplete leaching, however, results in some CAMs still remaining in the residue, as is shown by the larger presence of Li, Ni, Co, and Mn (4.6 wt.% total). The small amount of graphite that is present in these cases, likely results from the carbon coatings of the CAMs which is applied to improve their conductivity during use [47]. For industrial black mass samples, impurities from other components of the LiB cells persist in the leaching residues. For the pyrolyzed BM, the residue primarily consist of graphite (74 wt.%), followed by Al (2 wt.%) and Cu (0.8 wt.%). This is a result of the low amount of $FePO_4$ precipitation during leaching, as well as the poor leaching of Al and Cu. There is also a significant amount of elements from the CAMs present (6.6 wt.%), as leaching was not complete. In mechanically pre-treated samples, the residue mostly consists of reprecipitated $FePO_4$ (72 wt.%). However, graphite remains a significant contaminate, constituting of 28 wt.%. Unlike the pyrolyzed BM, Al and Cu dissolved during leaching, which is why the residue from BM M+ contains only 0.1 wt.% of Al and Cu.

These results show that when industrial pre-treatment is absent, and the BM sample contains few impurities, the resulting residue is of higher purity. Previous studies conclude that such leaching residues are suitable for re-used in batteries, with minimal additional purification steps. However, our findings indicate that this is not possible in practice. Depending on the pre-treatment, Al and Cu often remain in the leaching residues and must be removed before $FePO_4$ can be repurposed. Moreover, the recovered $FePO_4$ is amorphous, so it would need to be recrystallised before being used in new LiBs. Apart from that, there is significant contamination by graphite. As the primary anode active material, graphite is always present in LiBs, and will inevitably contaminate the leaching residues unless completely removed during pre-treatment. While the removal of graphite has been studied by methods such as froth flotation, implementing this step in a practical and economically viable manner remains challenging [48]. Therefore, it is essential to address the presence of these impurities to ensure residue quality and viability for reuse.

### 4.3.3. Precipitation Stripping of Fe

As is seen in the previous sections, the Fe(II) present in LFP is able to act as a reducing agent in the leaching of various NMC-based black mass samples. However, one very important aspect still needs to be studied: the use of LFP as a reducing agent should not be accompanied by the introduction of additional impurities. Therefore, the removal of Fe from the PLS is investigated. This was done by increasing the pH of the PLS by the addition of NaOH to precipitate the remaining $Fe^{3+}$ as $FePO_4$ [38]. The precipitation experiment was conducted on all previously reported systems, but most of them yielded similar results to the pristine

NMC 532. Therefore, Fig. 4.3 only depicts the precipitation stripping results for the experiments on the pristine NMC 532 (Fig. 4.1) and BM P (Fig. 4.2b). The rest of the results can be found in Figs. B.5-B.7 in the appendix.

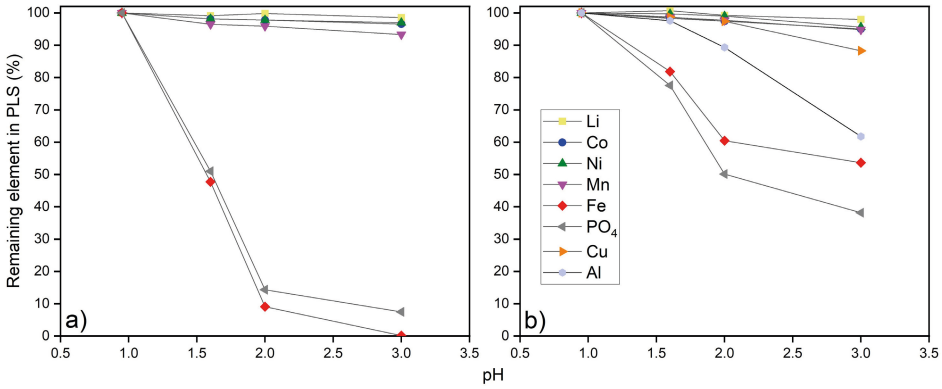


*Figure 4.3: Precipitation stripping of Li, Ni, Co, Mn, Fe, Al, Cu, and $PO_4^{3-}$, after leaching of NMC 532 (a) and BM P (b), by pH adjustment.*

The precipitation stripping from the PLS retrieved after leaching pristine NMC 532 can be seen in Fig. 4.3a. These results show that Li, Ni, Co, and Mn are only slightly removed (around 4% on average) from the PLS during this process. The Fe, however, is completely removed from the PLS at pH=3. The $PO_4^{3-}$ follows the same trend as the Fe but is slightly more persistent. The resulting precipitate was dried and submitted to aqua regia digestion and ICP-OES analysis (Table 4.2). This showed that 8% of the precipitate consists of $SO_4^{2-}$. It could be that $PO_4^{3-}$ is not completely removed because it is partly substituted by $SO_4^{2-}$ from the lixiviant. Also, a combined 1.3 wt.% of Li, Ni, Co, and Mn was found in the precipitate. These elements are not likely to co-crystallize since they do not precipitate at pH=3, but are rather present as physical inclusions in the fast-forming $FePO_4$ or leftover PLS that is dried together with the precipitate [49–51]. To verify these theories, the precipitate of the next pH-adjustment experiment was washed with demineralised water a few times (± 50 mL total) after filtration.

Fig 4.3b shows the precipitation of Fe from the PLS acquired after the leaching of BM P, which yields drastically different results. Although the Li, Ni, Co, and Mn are only slightly removed from the PLS (5% average), the removal of Fe is very inefficient. At a pH of 3, 54% of the Fe remains in the solution. This can be attributed to the fact that a large percentage of Fe was not used to reduce any TMs from the BM during leaching (as in Eq. 4.3). Therefore, a large portion of the Fe is still present in the divalent state instead of the less soluble trivalent state. This hampers its precipitation stripping by pH adjustment. Precipitation of Cu (12% removed),

and Al (38% removed) is also seen. The precipitate was filtered and washed with demineralised water. This resulted in a far lower amount of Li, Ni, Co, and Mn in the $FePO_4$-precipitate, being 0.3 wt. % in total (Table 4.3). This indicates that these elements are most likely not co-crystallized. Also interesting to see is that Al (1.5 wt.%) and Cu (0.3 wt.%) are not washed out of the precipitate. This indicates that these elements can co-crystallize with, and hence contaminate, the $FePO_4$.

*Table 4.3: Elemental composition (wt.%) of the resulting precipitates from the pH-adjustment experiment in Fig. 4.3. It is also indicated whether the precipitates were washed with demineralised water directly after filtration.*

| BM sample | Precipitation study | Washing | Li | Co | Ni | Mn | Al | Fe | Cu | $PO_4^{3-}$ | $SO_4^{2-}$ |
|---|---|---|---|---|---|---|---|---|---|---|---|
| NMC 532 | Fig. 4.3a | x | 0.2 | 0.2 | 0.5 | 0.4 | 0 | 22.9 | 0 | 35.6 | 7.7 |
| BM P | Fig. 4.3b | ✓ | 0.02 | 0.1 | 0.1 | 0.1 | 1.5 | 21.8 | 0.3 | 44.8 | 0.6 |

In order to research the transformation of LFP to $FePO_4$ in more detail, a larger experiment with 500 mL PLS using BM M+ was set up. After stripping, the precipitate was calcinated to manifest crystallization, enabling characterization by XRD-analysis. Also, it was investigated if pH adjustment with a 2 mol/L LiOH solution worked as well. In this way, the complexity of the PLS does not increase by adding another ion-type. The resulting PLS after Fe removal can be found in Table B.1. This shows that Fe is almost completely removed, and only Al and Cu impurities remain. Also, the Li, Ni, Co, and Mn are present in a large amount compared to these other impurities.

After heat treatment (600 °C, 2 hours, $N_2$-atmosphere), the precipitate was again submitted to XRD-analysis. The diffractograms of LFP before reaction, the leaching residue and the precipitate can be found in Fig. 4.4. This shows that before leaching, the recovered LFP from spent batteries is indeed mostly $LiFePO_4$. In the residue, this is converted to $FePO_4$. The calcinated precipitate consists of $FePO_4$ as well. Hence, it is shown that the LFP added during leaching indeed transforms to $FePO_4$. However, this product contains impurities regardless of whether a washing step is applied and would require further purification before it can be re-used in a new LiB.

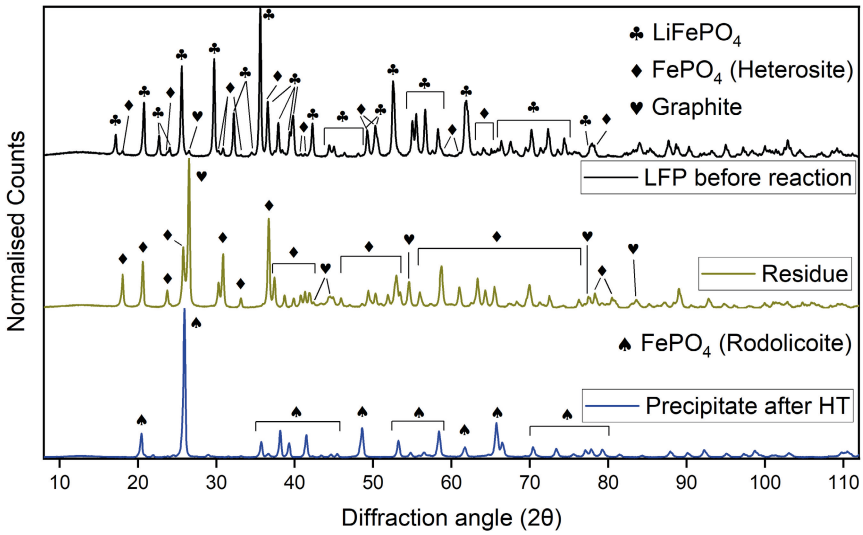


*Figure 4.4: XRD-diffractograms of the LFP before reaction, the residue after leaching and the heat treated precipitate.*



## 4.4. CONCLUSIONS

Our findings demonstrate that the simultaneous recycling of LFP and NMC provides substantial benefits in terms of chemical consumption. At optimal conditions, this approach eliminates the need for an additional reducing agent, enabling an effective dissolution of Ni, Co, and Mn at mild conditions (0.63 mol/L $H_2SO_4$, 50°C) from various battery waste compositions. By repurposing LFP, a waste product with limited economical value, as a reagent, the method not only minimizes chemical usage but also offers a sustainable solution to recycle LFP without requiring prior separation.

LFP acts as an efficient reducing agent in reductive acid leaching by dissolving in $H_2SO_4$, releasing $Fe^{2+}$, which facilitates the dissolution of the tri- or tetravalent Ni, Co, and Mn. Key results are:

When leaching **Pristine NMC 532** without any reducing agent, dissolution of Ni, Mn and Co reached 36% in 30 minutes. Upon addition of LFP, this increased to about 80% in just 15 minutes. Leaching of **Spent NMC 532** yielded similar results. **Mechanically pre-treated BM** exhibited slightly higher efficiencies compared to pristine and spent NMC 532, achieving complete leaching within 30 minutes with LFP. The presence of Cu and Al impurities in this BM enhances the leaching efficiencies of TMs through catalysis with $Fe^{3+}/Fe^{2+}$. Pre-reduction of Ni, Co, and Mn during pyrolysis **in the pyrolyzed BM** resulted in 90-100% leaching

efficiencies without any additional reducing agent. Consequently, adding LFP did not significantly affect metals extraction.

Consequently, Fe introduced via LFP can be effectively removed by pH adjustment with NaOH or LiOH, yielding $FePO_4$ precipitates with minimal losses of Li, Co, Ni and Mn (0.3 wt.% in total) after washing. Residue analysis revealed differences in impurity levels based on the starting waste composition. Leaching pristine or manually liberated NMC 532 produced residue primarily consisting of $FePO_4$, while residue from industrially pre-treated BMs contained up to 74 wt.% graphite and smaller amounts (0.1 to 2 wt.%) of Al and Cu, necessitating further purification steps. However, challenges remain. In pyrolyzed BM, unutilized $Fe^{2+}$ from LFP remains in the PLS at pH = 3, complicating PLS purification from iron.

## REFERENCES


1. Y. Liang, C.Z. Zhao, H. Yuan, Y. Chen, W. Zhang, J.Q. Huang, D. Yu, Y. Liu, M.M. Titirici, Y.L. Chueh, H. Yu, Q. Zhang, A review of rechargeable batteries for portable electronic devices, *InfoMat* 1 (2019) 6–32.
2. S. Megahed, B. Scrosati, Lithium-ion rechargeable batteries, *J. Power Sources* 51 (1994) 79–104.
3. J.W. Fergus, Recent developments in cathode materials for lithium ion batteries, *J. Power Sources* 195 (2010) 939–954.
4. F. Schipper, E.M. Erickson, C. Erk, J.-Y. Shin, F.F. Chesneau, D. Aurbach, Review—Recent Advances and Remaining Challenges for Lithium Ion Battery Cathodes, *J. Electrochem. Soc.* 164 (2016) A6220.
5. Regulation of the European Parliament and of the Council Establishing a Framework for Ensuring a Secure and Sustainable Supply of Critical Raw Materials and Amending Regulations (EU) 168/2013, (EU) 2018/858, 2018/1724 and (EU) 2019/1020, *Official Journal* COM 160 (2023).
6. European Commission Directorate-General for Internal Market Industry Entrepreneurship and SMEs, D. Pennington, E. Tzimas, C. Baranzelli, J. Dewulf, S. Manfredi, P. Nuss, M. Grohol, A. Van Maercke, Y. Kayam, S. Solar, B. Vidal-Legaz, L. Talens Peirò, L. Mancini, C. Ciupagea, L. Godlewska, P. Dias, C. Pavel, D. Blagoeva, G. Blengini, V. Nita, C. Latunussa, C. Torres De Matos, F. Mathieux, A. Marmier, Methodology for establishing the EU list of critical raw materials – Guidelines, Publications Office, 2017.
7. European Commission Directorate-General for Internal Market Industry Entrepreneurship and SMEs, M. Grohol, C. Veeh, Study on the critical raw materials for the EU 2023 – Final report, Publications Office of the European Union, 2023.
8. Y. Ding, Z.P. Cano, A. Yu, J. Lu, Z. Chen, Automotive Li-Ion Batteries: Current Status and Future Perspectives, *Electrochemical Energy Reviews* 2 (2019) 1–28.
9. E. Kallitsis, J.J. Lindsay, M. Chordia, B. Wu, G.J. Offer, J.S. Edge, Think global act local: The dependency of global lithium-ion battery emissions on production location and material sources, *J. Clean. Prod.* 449 (2024) 141725.
10. S. Jin, D. Mu, Z. Lu, R. Li, Z. Liu, Y. Wang, S. Tian, C. Dai, A comprehensive review on the recycling of spent lithium-ion batteries: Urgent status and technology advances, *J. Clean. Prod.* 340 (2022) 130535.
11. M. Kayla Kilgo, A. Anctil, M.S. Kennedy, B.A. Powell, Metal leaching from Lithium-ion and Nickel-metal hydride batteries and photovoltaic modules in simulated landfill leachates and municipal solid waste materials, *Chemical Engineering Journal* 431 (2022) 133825.
12. Z.J. Baum, R.E. Bird, X. Yu, J. Ma, Lithium-Ion Battery Recycling─Overview of Techniques and Trends, *ACS Energy Lett.* 7 (2022) 712–719.
13. C.K. Gupta, Chemical metallurgy : principles and practice, (2003) 811.
14. W. Gao, X. Zhang, X. Zheng, X. Lin, H. Cao, Y. Zhang, Z. Sun, Lithium Carbonate Recovery from Cathode Scrap of Spent Lithium-Ion Battery: A Closed-Loop Process, *Environ. Sci. Technol.* 51 (2017) 1662–1669.
15. S.P. Barik, G. Prabaharan, L. Kumar, Leaching and separation of Co and Mn from electrode materials of spent lithium-ion batteries using hydrochloric acid: Laboratory and pilot scale study, *J. Clean. Prod.* 147 (2017) 37–43.
16. B. Wang, X.Y. Lin, Y. Tang, Q. Wang, M.K.H. Leung, X.Y. Lu, Recycling $LiCoO_2$ with methanesulfonic acid for regeneration of lithium-ion battery electrode materials, *J. Power Sources* 436 (2019) 226828.
17. N. Peeters, K. Binnemans, S. Riaño, Solvometallurgical recovery of cobalt from lithium-ion battery cathode materials using deep-eutectic solvents, *Green Chemistry* 22 (2020) 4210–4221.

**18.** E. Asadi Dalini, G. Karimi, S. Zandevakili, Treatment of valuable metals from leaching solution of spent lithium-ion batteries, *Miner. Eng.* 173 (2021) 107226.

**19.** P. Meshram, B.D. Pandey, T.R. Mankhand, Extraction of lithium from primary and secondary sources by pre-treatment, leaching and separation: A comprehensive review, *Hydrometallurgy* 150 (2014) 192–208.

**20.** W. Lv, Z. Wang, H. Cao, Y. Sun, Y. Zhang, Z. Sun, A Critical Review and Analysis on the Recycling of Spent Lithium-Ion Batteries, *ACS Sustain. Chem. Eng.* 6 (2018) 1504–1521.

**21.** J.J.M.M. van de Ven, Y. Yang, S.T. Abrahami, A closer look at lithium-ion batteries in E-waste and the potential for a universal hydrometallurgical recycling process, *Sci. Rep.* 14 (2024) 1–12.

**22.** M.C. Biesinger, B.P. Payne, A.P. Grosvenor, L.W.M. Lau, A.R. Gerson, R.S.C. Smart, Resolving surface chemical states in XPS analysis of first row transition metals, oxides and hydroxides: Cr, Mn, Fe, Co and Ni, *Appl. Surf. Sci.* 257 (2011) 2717–2730.

**23.** J.L. White, F.S. Gittleson, M. Homer, F. El Gabaly, Nickel and Cobalt Oxidation State Evolution at Ni-Rich NMC Cathode Surfaces during Treatment, *Journal of Physical Chemistry C* 124 (2020) 16508–16514.

**24.** C.K. Lee, K.I. Rhee, Reductive leaching of cathodic active materials from lithium ion battery wastes, *Hydrometallurgy* 68 (2003) 5–10.

**25.** R. Sattar, S. Ilyas, H.N. Bhatti, A. Ghaffar, Resource recovery of critically-rare metals by hydrometallurgical recycling of spent lithium ion batteries, *Sep. Purif. Technol.* 209 (2019) 725–733.

**26.** L.P. He, S.Y. Sun, X.F. Song, J.G. Yu, Leaching process for recovering valuable metals from the $LiNi_{1/3}Co_{1/3}Mn_{1/3}O_2$ cathode of lithium-ion batteries, *Waste Management* 64 (2017) 171–181.

**27.** N. Vieceli, P. Benjamasutin, R. Promphan, P. Hellström, M. Paulsson, M. Petranikova, Recycling of Lithium-Ion Batteries: Effect of Hydrogen Peroxide and a Dosing Method on the Leaching of LCO, NMC Oxides, and Industrial Black Mass, *ACS Sustain. Chem. Eng.* (2023).

**28.** Z. Takacova, T. Havlik, F. Kukurugya, D. Orac, Cobalt and lithium recovery from active mass of spent Li-ion batteries: Theoretical and experimental approach, *Hydrometallurgy* 163 (2016) 9–17.

**29.** P. Zhang, T. Yokoyama, O. Itabashi, T.M. Suzuki, K. Inoue, Hydrometallurgical process for recovery of metal values from spent lithium-ion secondary batteries, *Hydrometallurgy* 47 (1998) 259–271.

**30.** Q. Meng, Y. Zhang, P. Dong, Use of glucose as reductant to recover Co from spent lithium ions batteries, *Waste Management* 64 (2017) 214–218.

**31.** F. Pagnanelli, E. Moscardini, G. Granata, S. Cerbelli, L. Agosta, A. Fieramosca, L. Toro, Acid reducing leaching of cathodic powder from spent lithium ion batteries: Glucose oxidative pathways and particle area evolution, *Journal of Industrial and Engineering Chemistry* 20 (2014) 3201–3207.

**32.** G.P. Nayaka, J. Manjanna, K. V. Pai, R. Vadavi, S.J. Keny, V.S. Tripathi, Recovery of valuable metal ions from the spent lithium-ion battery using aqueous mixture of mild organic acids as alternative to mineral acids, *Hydrometallurgy* 151 (2015) 73–77.

**33.** C. Peng, J. Hamuyuni, B.P. Wilson, M. Lundström, Selective reductive leaching of cobalt and lithium from industrially crushed waste Li-ion batteries in sulfuric acid system, *Waste Management* 76 (2018) 582–590.

**34.** R.C. Wang, Y.C. Lin, S.H. Wu, A novel recovery process of metal values from the cathode active materials of the lithium-ion secondary batteries, *Hydrometallurgy* 99 (2009) 194–201.

**35.** K. Binnemans, P.T. Jones, The Twelve Principles of Circular Hydrometallurgy, *Journal of Sustainable Metallurgy 2022 9:1* 9 (2022) 1–25.

**36.** T. Kim, W. Song, D.Y. Son, L.K. Ono, Y. Qi, Lithium-ion batteries: outlook on present, future, and hybridized technologies, *J. Mater. Chem. A Mater.* 7 (2019) 2942–2964.

**37.** S.Y. Chung, J.T. Bloking, Y.M. Chiang, Electronically conductive phospho-olivines as lithium storage electrodes, *Nat. Mater.* 1 (2002) 123–128.

**38.** Y. Jiang, X. Chen, S. Yan, S. Li, T. Zhou, Pursuing green and efficient process towards recycling of different metals from spent lithium-ion batteries through Ferro-chemistry, *Chemical Engineering Journal* 426 (2021) 131637.

**39.** X. Chen, J. Li, D. Kang, T. Zhou, H. Ma, A novel closed-loop process for the simultaneous recovery of valuable metals and iron from a mixed type of spent lithium-ion batteries, *Green Chemistry* 21 (2019) 6342–6352.

**40.** Y. Liu, W. Lv, X. Zheng, D. Ruan, Y. Yang, H. Cao, Z. Sun, Near-to-Stoichiometric Acidic Recovery of Spent Lithium-Ion Batteries through Induced Crystallization, *ACS Sustain. Chem. Eng.* 9 (2021) 3183–3194.

**41.** A. Porvali, M. Aaltonen, S. Ojanen, O. Velazquez-Martinez, E. Eronen, F. Liu, B.P. Wilson, R. Serna-Guerrero, M. Lundström, Mechanical and hydrometallurgical processes in HCl media for the recycling of valuable metals from Li-ion battery waste, *Resour. Conserv. Recycl.* 142 (2019) 257–266.

**42.** Y. Koyama, I. Tanaka, H. Adachi, Y. Makimura, T. Ohzuku, Crystal and electronic structures of superstructural $Li_{1-x}[Co_{1/3}Ni_{1/3}Mn_{1/3}]O_2$ ($0 \leq x \leq 1$), *J. Power Sources* 119–121 (2003) 644–648.

**43.** A. Chernyaev, Y. Zou, B.P. Wilson, M. Lundström, The interference of copper, iron and aluminum with hydrogen peroxide and its effects on reductive leaching of $LiNi_{1/3}Mn_{1/3}Co_{1/3}O_2$, *Sep. Purif. Technol.* 281 (2022) 119903.

**44.** N. Vieceli, R. Casasola, G. Lombardo, B. Ebin, M. Petranikova, Hydrometallurgical recycling of EV lithium-ion batteries: Effects of incineration on the leaching efficiency of metals using sulfuric acid, *Waste Management* 125 (2021) 192–203.

**45.** M. Weller, T. Overton, J. Rourke, F. Armstrong, Inorganic Chemistry, 6th ed., Oxford University Press, Oxford, 2014.

**46.** E. Neyens, J. Baeyens, A review of classic Fenton's peroxidation as an advanced oxidation technique, *J. Hazard. Mater.* 98 (2003) 33–50.

**47.** Y. Meng, J. Xia, L. Wang, G. Wang, F. Zhu, Y. Zhang, A comparative study on $LiFePO_4$/C by in-situ coating with different carbon sources for high-performance lithium batteries, *Electrochim. Acta* 261 (2018) 96–103.

**48.** D. Yu, Z. Huang, B. Makuza, X. Guo, Q. Tian, Pretreatment options for the recycling of spent lithium-ion batteries: A comprehensive review, *Miner. Eng.* 173 (2021) 107218.

**49.** R.D. Crapnell, C.E. Banks, Electroanalytical overview: The determination of manganese, *Sensors and Actuators Reports* 4 (2022) 100110.

**50.** L.F. Huang, M.J. Hutchison, R.J. Santucci, J.R. Scully, J.M. Rondinelli, Improved Electrochemical Phase Diagrams from Theory and Experiment: The Ni-Water System and Its Complex Compounds, *Journal of Physical Chemistry C* 121 (2017) 9782–9789.

**51.** E.M. Garcia, J.S. Santos, E.C. Pereira, M.B.J.G. Freitas, Electrodeposition of cobalt from spent Li-ion battery cathodes by the electrochemistry quartz crystal microbalance technique, *J. Power Sources* 185 (2008) 549–553.

*Nature is our kindest friend and best critic in experimental science if we only allow her intimations to fall unbiased on our minds.*

Michael Faraday

# 5

# Chapter 5

## Leaching and Electrochemical Purification of Mixed Industrial LFP-and NMC type Lithium-ion Battery Waste

In the previous chapter, it was shown that simultaneous leaching of spent LFP and NMC enhances the reductive dissolution of NMC while lowering the overall chemical consumption. However, this method remains untested on feed materials exclusively from industrial origin, and the increased Fe, Cu, and Al introduced by this leaching method remained largely unaddressed. These impurities must be removed prior to downstream recovery of high-purity battery precursors, requiring a flexible strategy capable of accommodating the variation in impurity and target element concentrations typical for industrial black mass. Chapter 5 explores the applicability of the leaching method presented in Chapter 4 on industrially pre-treated black mass, and the possibility of removing the two main impurities from the leach solution: Cu and Fe.

The chapter starts by applying the simultaneous leaching conditions from Chapter 4 to industrial LFP and NMC BM, followed by direct precipitation of Co, Ni, Mn, Fe, Al and Cu. Results indicate that without targeted purification steps, effective separation of the target metals from impurities is not achieved. Consequently, the leaching method is adapted to industrial BM feed through stepwise LFP addition, optimisation of the LFP to NMC ratio, an increase in acid concentration to 1 mol/L. These modifications allow complete dissolution of the target metals without any external reducing agent. Additionally, increase of feed concentration to 125 g/L total LFP and NMC BM was done to more closely represent industrially relevant conditions.

To assess the feasibility of electrochemically removing Fe, electro-oxidation experiments are first tested on a model $FeSO_4$-solution and a simple LFP-leachate, followed by its application to the more complex LFP and NMC PLS. These studies confirm that oxidizing $Fe^{2+}$ to the less soluble $Fe^{3+}$, followed by its precipitation at suitable pH, is a viable strategy for Fe removal. In practice, however, it is limited by competing side reactions involving Cu in the complex PLS. To address this

Submitted for journal publication:
van de Ven, J. J.M.M. Anghel, M. A., Teeuwisse, P. J., Yang, Y. & Abrahami, S. T., Leaching and Electrochemical Purification of Mixed Industrial LFP- and NMC type Lithium-ion Battery Waste

limitation, electrochemical purification process involving Cu electrodeposition combined with Fe electro-oxidation is developed. The impact of this approach on downstream product purity is subsequently evaluated by precipitation study. As a result of this combined electrotechnical purification, Ni, Co, and Mn precipitates with impurity levels as low as 0.1 – 0.6 wt.% are obtained.

## 5.1. INTRODUCTION

Lithium-ion batteries (LiBs) are a crucial technology for electricity storage and play an essential role in the energy transition, with applications ranging from stationary energy storage to electric vehicles (EVs) and portable electronic devices (PEDs) [1–4]. These batteries rely on materials classified by the EU as critical raw materials (CRMs), such as Li, Co, and Mn, as well as the strategic raw materials (SRMs) Cu and Ni [1,5,6]. However, while the demand for LiBs is expected to rise significantly in the coming years [3,4,7], the geopolitical supply risks associated with these elements are growing due to geographic concentration of primary production and growing international competition for these resources [6,8]. Therefore, recycling will be an essential contributor to meet future demand, while also preventing landfilling or stockpiling of LiBs [9].

Among the wide variety of techniques available for the recycling of LiBs, hydrometallurgy enables the recovery of a broad range of materials with high purities alongside limited energy intensity, making it the preferred route for future recycling [10–13]. Hydrometallurgical recycling of LiBs typically requires an extensive pre-treatment that starts by shredding the batteries, producing a powder known as black mass (BM) that contains the majority of desired elements, including Li, Ni, Co, and Mn [14]. Afterwards, the black mass is leached, typically in an acidic environment, to extract the metals into the liquid phase, called the *pregnant leach solution* (PLS) [15–18]. Researchers have found mineral acids such as HCl, $H_2SO_4$ and $HNO_3$ to be particularly effective for this purpose, with studies reporting more than 99% dissolution of Li, Ni, Co, and Mn [19–22].

Although promising results are reported with acid leaching, most studies emphasize the need to provide reducing conditions to dissolve Ni, Co, and Mn present in the cathode active materials (CAMs) [23–26]. This is because the average oxidation state of these elements in the solid CAMs is (III), while they are most soluble in state (II) [25–27]. Therefore, most hydrometallurgical routes rely on additional reducing agents, most commonly $H_2O_2$, $Na_2S_2O_5$, or ascorbic acid, to enable complete dissolution of Ni, Co, and Mn [23,28–34]. However, this is often accompanied by increased dissolution of impurities that are preset in BM, including Fe, Al, and

Cu. Moreover, the use of additional reagents increases the environmental footprint of the recycling process [35]. Consequently, recent studies have shown that Fe(II) from spent $LiFePO_4$ (LFP) batteries can serve as an alternative to these reducing agents, which can avoid the need for additional reducing agents and strong acidic solutions [24,36,37].

After leaching, Li, Ni, Co, and Mn must be effectively separated from Fe, Al, and Cu to create high grade battery precursors [38]. A technique frequently applied in hydrometallurgy, and particularly in LiB-recycling, is selective precipitation [15,18,39,40]. For example, Kang et al. [41] used a solution containing 4 mol/L NaOH and 50 wt.% $CaCO_3$ to precipitate over 99% of Fe, Al, and Cu as hydroxides at pH 6.5 . However, this purification step also resulted in a significant loss of Li, Ni, Co, and Mn (2%, 19%, 7%, and 15%, respectively). Chernyaev et al. [42] demonstrated that carrying out Fe and Al precipitation at lower pH values of 3.5 for hydroxides and 3 for phosphates can minimize the coprecipitation of these valuable metals in a synthetic LiB PLS. In a later study, Zou et al. [43] showed that 97.8% Fe removal is possible at a low pH of 2 in the presence of phosphates from simultaneous leaching of industrial NMC with pristine LFP, provided that iron is present as $Fe^{3+}$, rather than the soluble $Fe^{2+}$. A higher pH value of 4.5 allowed the removal of Fe together with Al and Cu but also induced substantial coprecipitation of Li, Ni, Co, and Mn. These results show that separation of Fe, Al, and Cu from Li, Ni, Co, and Mn by precipitation only could only be achieved when, apart from a base to adjust pH, additional reagents such as phosphates or carbonates are used, since processes without such reagents reported major loss of the target elements.

In our previous study [24] on simultaneous leaching of LFP and NMC presented in Chapter 4, Fe removal efficiency was found to be lower when industrially pre-treated BM was used, which is a result of variations in need for reducing agents by industrial NMC BM, resulting in a PLS that contains both $Fe^{2+}$ and $Fe^{3+}$ ions. While $Fe^{3+}$ can be readily removed at lower pH, any remaining $Fe^{2+}$ remains soluble until higher pH, potentially coprecipitating with Ni, Co, and Mn products that are formed at a later stage of the recycling process [44]. Given the high complexity of industrial BM which has a variable need for reducing agents as result of varying oxidation states of Ni, Co, and Mn, and hence a resulting PLS with a fluctuating $Fe^{2+}$ to $Fe^{3+}$ ratio, a controlled and flexible processing step to oxidize any remaining $Fe^{2+}$ is necessary before efficient removal can be achieved. While oxidation by air or pure oxygen is thermodynamically feasible, the reaction in acidic media is sluggish [45,46] and therefore alternative methods need to be explored.

For both Cu and Fe, electrochemical methods offer a potentially more environmentally friendly approach for purification [47], although they have not yet been applied in the context of LiBs. After all, electrowinning of Cu has been

extensively demonstrated in literature and in industry, both in primary production, as well as for the recycling of e-waste and other Cu-containing waste streams [48]. Similarly, electrochemical methods for Fe removal have been demonstrated in other context, such as by Venkatesan et al. [49] for recycling of NdFeB magnets. After leaching the magnets in HCl, an electrochemical setup with a large anode and small cathode was used to oxidize Fe from the NdFeB alloy to $Fe^{3+}$, enabling its removal as $FeCl_3$. These examples suggest that electrochemical removal of Cu and Fe could be a promising approach for a sustainable purification method, as it aligns with circular hydrometallurgical principles [47].

In this study, we investigate the combined use of electrochemical and precipitation-based purification approaches and assess their application for industrially relevant conditions. We begin with optimizing the simultaneous leaching procedure for LFP and NMC [24] using both industrially pre-treated BM of NMC and LFP. Next, we study the electrochemical oxidation of excess $Fe^{2+}$ to $Fe^{3+}$ and electro-deposition of Cu. Its effectiveness was compared for three different solutions: a synthetic $FeSO_4$-solution, a PLS from industrial LFP and a PLS from industrial LFP and NMC, allowing assessment of process efficiency as a function of PLS complexity. We then determine the optimal pH of these processes by comparing the composition of the purified PLS and the precipitates that form upon pH adjustments with and without prior electrochemical purification. This study provides crucial insights into the applicability of electrodeposition and electro-oxidation for LiBs recycling.

## 5.2. MATERIALS & METHODS

### 5.2.1. Battery Materials

The battery materials used in this research were obtained from industrial partners and produced by mechanical pre-treatment, without additional heat treatment. Applied unit operations include shredding, sieving, magnetic separation, and grinding. Three different materials were used in this study. The NMC BM was used directly as received from the supplier. The LFP BM was also used as received in the first leaching experiment, but for the remainder of the experiments it was used after an additional size classification step that was performed in our lab (500 µm sieve retention) to decrease the amount of graphite, Al and Cu in this BM. Therefore, the as-received LFP BM is referred to as LFP BM and the sieved BM is referred to as LFPs BM. The composition of all BMs shown in Table 5.1. It should be noted that BM composition may change slightly over time due to the reactivity of its components. Therefore, these compounds were regularly analysed. The table represents the composition of the BMs at the beginning of the experiments

*Table 5.1: Composition (wt.%) of all BMs used in this study as determined by aqua regia digestion and ICP-OES analysis. Other contains oxygen, graphite, and organic impurities.*

| Material Name | Li | Co | Ni | Mn | Al | Fe | Cu | $PO_4^{3-}$ | Other | Note |
|---|---|---|---|---|---|---|---|---|---|---|
| NMC BM | 3.8 | 6.7 | 16.8 | 6.5 | 0.5 | 0.9 | 0.9 | - | 63.9 | BM containing NMC CAM |
| LFP BM | 2.1 | - | - | - | 2.5 | 16.9 | 3 | 31.8 | 43.6 | BM containing LFP CAM before sieving |
| LFPs BM | 1.8 | - | - | - | 1.6 | 17.7 | 1.8 | 33.9 | 43.2 | BM containing LFP CAM after sieving |

### 5.2.2. Characterization Techniques

The elemental compositions of the BM samples, leaching solutions, and precipitates were determined by inductively coupled plasma-optical emission spectroscopy (ICP-OES) using a Spectro Arcos-EOP device with Modified Lichte nebulizer and mini cyclonic spray chamber. Calibration curves were made using 1000 mg/L ICP standards from each corresponding element. From the BM, 1 g of each sample was digested in 100 mL aqua regia, a combination of 25 mL $HNO_3$ (65%, VWR chemicals) and 75 mL HCl (37%, Merck). The digestion was carried out in a triple necked round bottom flask with reflux cooler, for 5 h at 70°C. After this, the residue was separated through a Whatmann 595 ½ filter. The filtrate was diluted to 1L in a volumetric flask and a sample of 0.5 mL from this solution was submitted to ICP-OES analysis. Each digestion was carried out at least three times. Over the course of the experiments, this characterization was repeated to ensure that changes in BM composition due to oxidation over time were accounted for.

The ferrozine method was used to determine the $Fe^{2+}/Fe^{3+}$ ratio in aqueous solutions [50]. A solution containing ferrozine (4.9 g/L, monosodium salt hydrate, 97%, Sigma-Aldrich) was used to form a Fe-complex measurable with UltraViolet-Visible spectrophotometry (UV-Vis). Using a Shimadzu UV-2600 apparatus, the absorption at 562 nm was measured, after which a reducing solution of 1.4 mol/L hydroxylamine hydrochloride (99%, Sigma-Aldrich) and 2 mol/L HCl (37%, Merck) was added. After 10 min reaction, a pH buffer containing 10 mol/L $CH_3COONH_4$ (97%, Alfa Aesar), which was adjusted to pH 9.5 with $NH_3$-solution (25%, VWR chemicals), was added and the absorption at 562 nm was measured again. Comparing the difference in absorption before and after reduction, provides the $Fe^{2+}/Fe^{3+}$ ratio.

For characterization of BM, Cu deposits, and precipitates, identification of chemical phases was required, for which X-ray diffraction (XRD) analysis was conducted. A Bruker D8 Advance diffractometer with Bragg-Brentano geometry

and Lynxeye-XE-T position sensitive detector was used for the analysis, with Cu Kα radiation. The 2θ range was 5 - 110°, with a step size of 0.03 and 1s per step. Data analysis was done via the Bruker software DiffracSuite.EVA vs 7.2.

### 5.2.3. $H_2SO_4$ Leaching of LFP & NMC

Leaching was performed to optimize the dissolution of Li, Ni, Co, and Mn from NMC in presence of LFP, as well as to acquire a solution suited for further purification. The laboratory scale leaching setup consisted of a 1L round bottom flask, which was placed in a heating mantle on a stirring and heating plate as shown in Chapter 4. A temperature probe was inserted through one of the necks for temperature control and a reflux cooler was attached to another neck. Stirring was achieved with a magnetic stir bar. The lixiviant had a total volume of 500 mL and contained $H_2SO_4$ (95.0 – 97.0 %, Sigma-Aldrich), diluted in Milli-Q water. The process was carried out for 2 h total with 600 rpm stirring. After this reaction, the slurry was filtered in two steps, once through a vacuum filtration with a Whatmann 113 filter (90 mm diameter, 30 µm pore size), followed by membrane filtration through a Cytiva ME 25 membrane filter with 0.45 µm pore size. The residue was dried for 8 h at 55°C, and the PLS was collected for further study.

In the first leaching experiment (Fig 5.1), NMC BM was leached in 0.63 mol/L $H_2SO_4$ at 50°C. The solid-to-liquid (S/L) ratio of the NMC BM is 38.4 g/L, which was based on the amount of Ni, Co and Mn that was present in the solutions of van de Ven et al. [51] After 30 min, one molar equivalent of LFP BM was added, which is based on the ratio of the sum of (Ni + Co + Mn) in NMC BM compared to Fe in LFP BM, resulting in a S/L for LFP BM of 65.6 g/L. Then, at a total time of 90 min, 1 vol% of $H_2O_2$-solution (30% Sigma-Aldrich) is added to ensure complete leaching, after which it is allowed to react for 30 more mins. This brings the total reaction time to 2h.

In the following leaching experiments (Fig. 5.3), 1 mol/L $H_2SO_4$ was used at 50°C together with the sieved LFPs BM. A lower molar ratio of 0.75 LFP:NMC was used due to the presence of Cu and Al which, together with Fe, exhibit catalytic reducing effect [24]. The total S/L was also increased to more closely resemble industrial conditions, resulting in 57.6 g/L NMC BM and 67.7 g/L LFPs BM. The LFPs BM was added in three equal steps at 30, 60, and 90 minutes of leaching, after which it was allowed to react for 30 more minutes, resulting in 2 h total. No $H_2O_2$ was added.

The leaching progress over time was studied by sampling 1.5 mL at each 15 minutes interval, after which the slurry was filtered with a syringe filter (Fisherbrand PTFE 0.45 µm). Of this filtrate, 0.1 mL was submitted to ICP-OES analysis.
To assess the effectiveness of the leaching process, the leaching efficiency ($\eta_L$) of the elements of interest was calculated according to Eq. 5.1. In this formula, $m^x_f$ represents the initial mass of element x in the feed, which was determined by

the analysis of the BM as described in section 2.2. $m^x_{PLS}$ represents the mass of element x present in the PLS after leaching. This was determined by ICP-OES analysis of the PLS.

$$\eta_L = \frac{m^x_{PLS}}{m^x_f} * 100\% \tag{5.1}$$

### 5.2.4. Selective Precipitation

After leaching or electrochemical treatment, selective precipitation by pH adjustment was applied. This was done using a 2 mol/L LiOH solution (Monohydrate, ≥99%, Fischer Scientific). After the first leaching experiment without electrochemical treatment, to account for concentration changes in the PLS caused by dilution, the solution was weighed before and after LiOH addition. In all other experiments, including after electrochemical treatment, the dilution was accounted for by measuring the initial volume each step with a volumetric cylinder and the LiOH solution was added using a Metrohm 775 dosimat. At each desired pH, the solution suspension was filtered with a vacuum filtration pump using a Büchner funnel and Whatmann 542 filter paper (90mm diameter, 2.7 µm pore size). The filtrate (0.1mL) was diluted in 3 wt.% $HNO_3$ and submitted to ICP-OES analysis. The remaining filtrate was weighed again, after which the following pH adjustment was done.

After these steps were carried out for all applied pH increments, the collected precipitates were dried (55°C, 8 h), and weighed. Then, 0.1 g of each precipitate sample was dissolved in 5 wt.% $HNO_3$, sometimes assisted by the addition of $H_2O_2$ (35% solution, Thermo Scietific) in a 100 mL volumetric flask. Of this solution, 0.5 mL was submitted to ICP-analysis.

### 5.2.5. Electrochemical Techniques

For all electrochemical purification experiments, a Parstat 4000 (Ametek, UK) potentiostat was used, controlled with the Versastudio software. For the electro-oxidation, a Pt basket of 5 * 11 cm was used as anode (working electrode), while a Pt wire was used as cathode (counter electrode). This results in an anode-to-cathode surface ratio of roughly 35:1. Electro-oxidation was carried out using the chronopotentiometry method, at 1.2A resulting in a current density of 21.8 mA/cm$^2$. The setup is visualised in Fig. C.1 in the appendix. The first electro-oxidation test was conducted on a $FeSO_4$-solution which contained 0.18 mol/L Fe, similar to the PLS from simultaneous leaching (0.173 mol/L Fe), while LFP PLS was obtained by leaching the LFPs BM with the same conditions as in the combined leaching, but in absence of NMC BM, resulting in 0.2 mol/L Fe.

In the Cu deposition experiments, a 0.5cm wide Pt plate anode was used as counter electrode, while a steel plate of 4 cm wide submerged for 4 cm was used as cathode (counter electrode). The anode-to-cathode-ratio was 1:8, and a current of 0.2A (12.5 mA/cm$^2$) was applied on the cathode through chronopotentiometry. The setup is visualised in Fig. C.2 in the appendix. Both experiments made use of a triple electrode setup with a saturated Ag/AgCl electrode as a reference electrode. All reported potentials in this work are relative to the standard hydrogen electrode (SHE). The experiments were performed in a beaker with 250 mL of solution, magnetically stirred at 400 rpm and room temperature. During electrochemical purification, samples of 1.5 mL were taken at regular intervals and filtered through a syringe filter (Fisherbrand PTFE 0.45 µm). A sample of 0.1 mL from this solution was submitted to ICP-OES analysis, while 0.03 mL was submitted to UV-Vis analysis.

## 5.3. RESULTS & DISCUSSION

### 5.3.1. Simultaneous Leaching of NMC- & LFP Black Mass Followed by pH-controlled Precipitation

The effect of $Fe^{2+}$ on NMC leaching has been demonstrated in our previous study [24]. However, this was conducted using a manually liberated LFP cathode material. To bring the method one step closer to practical conditions, industrially pre-treated samples were used in the present study. The results of leaching efficiency as function of time for different elements/species are illustrated in Fig. 5.1.

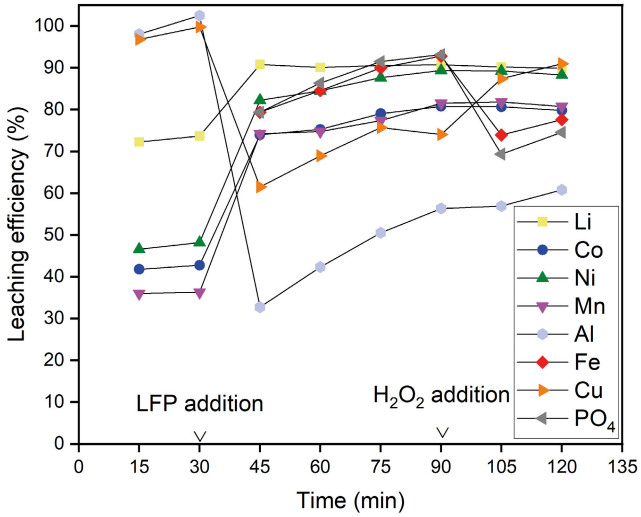


*Figure 5.1: Dependence of the leaching efficiency (0.63 mol/L $H_2SO_4$, 50°C) of Li, Co, Ni, Mn, Cu, Fe, Al, and $PO_4^{3-}$ from NMC BM (38.4 g/L) on time, as well as the presence of LFP BM (65.5 g/L) and $H_2O_2$ (1 vol%).*

These results show that the initial dissolution of NMC BM in 0.63 mol/L $H_2SO_4$ is low (around 40% Ni, Co, and Mn and 74% for Li), while the low amounts of Al and Cu impurities that are present in the NMC BM completely dissolve. This behaviour is well-known in the literature and arises because Ni, Co and Mn in a higher oxidation state must first be reduced to their divalent state to dissolve [23,27,29,34,52]. Only under such conditions, the dissolution of NMC BM follows the reaction presented in Eq. 5.2, resulting in efficient dissolution. Addition of LFP BM after 30 minutes results in the presence of $Fe^{2+}$ in solution, according to Eq. 5.3, which can act as a reducing agent according to Eq. 5.4. This leads to a rapid increase, followed by a more gradual increase in the leaching efficiencies of Ni, Co, and Mn, reaching 89%, 81%, and 81% after a total reaction time of 90 min (of which 60 min with LFP BM), respectively, while also 91 % of Li is dissolved, even though its feed concentration almost doubles upon LFP BM addition. The leaching efficiencies of Cu and Al are lowered (74% Cu and 56% Al) due to their increased concentration after LFP BM addition (from 0.2 to 1.2 g/L for Cu, and from 0.2 to 1.8 g/L for Al).

The addition of $H_2O_2$ at the 90 min mark increases the dissolution of Cu and Al to 91% and 61%, respectively, as a result of their oxidation. Moreover, about 20% of the Fe and $PO_4^{3-}$ in solution is removed upon $H_2O_2$ addition, which can be attributed to the oxidation of the $Fe^{2+}$ by $H_2O_2$. Although this reaction involving free radicals is complex and unpredictable, the overarching reactions are shown in Eqs. 5.5 and 5.6 [53]. Due to the low solubility of $Fe^{3+}$ in the presence of $PO_4^{3-}$, $FePO_4$ precipitates according to Eq. 5.7 [24]. This behaviour was not observed in the previous research reported in Chapter 4, as $H_2O_2$ reacts with unoxidized $Fe^{2+}$ in presence of reduced Ni, Co and Mn (Fig. 4.2b), as well as with unreduced Ni, Co, and Mn in presence of oxidized $Fe^{3+}$ (Figs. 4.1 and B.2a). Since both unoxidized Fe and unreduced Ni, Co, and Mn are present in the current study, and $H_2O_2$ is a stronger oxidizing agent than a reducing agent [54], it favours Fe oxidation (Eqs. 5.5 and 5.6) rather than the reduction of Ni, Co, and Mn. As a result, the leaching of Ni, Co, and Mn is unaffected by $H_2O_2$ addition.



$$3LiNi_{1/3}Mn_{1/3}Co_{1/3}O_{2(s)} + 12H^+_{(aq)} + 3e^- \rightarrow 3Li^+_{(aq)} + Ni^{2+}_{(aq)} + Mn^{2+}_{(aq)} + Co^{2+}_{(aq)} + 6H_2O_{(l)} \quad (5.2)$$

$$LiFePO_{4(s)} + 2H^+_{(aq)} \rightarrow Li^+_{(aq)} + Fe^{2+}_{(aq)} + H_2PO^-_{4(aq)} \quad (5.3)$$

$$Fe^{2+}_{(aq)} \rightarrow Fe^{3+}_{(aq)} + e^- \quad (5.4)$$

$$H_2O_{2(aq)} + H^+_{(aq)} + Fe^{2+}_{(aq)} \rightarrow H_2O_{(l)} + HO^{\cdot}_{(aq)} + Fe^{3+}_{(aq)} \quad (5.5)$$

$$HO^{\cdot}_{(aq)} + H^{+}_{(aq)} + Fe^{2+}_{(aq)} \rightarrow H_2O_{(l)} + Fe^{3+}_{(aq)} \quad (5.6)$$

$$Fe^{3+}_{(aq)} + H_2PO^{-}_{4\,(aq)} \rightarrow FePO_{4\,(s)} + 2H^{+}_{(aq)} \quad (5.7)$$

It is important that the introduced Fe, Al, and Cu should not contaminate any Ni, Co, and Mn compounds aimed to be recovered downstream. Selective precipitation is a widely used purification technique in hydrometallurgy, is straight forward, can directly result in battery precursors, and is therefore attractive in LiB recycling. To study the applicability of this technique after simultaneous leaching of LFP and NMC, the PLS from this experiment was subjected to precipitation by incremental pH adjustments. This was done by adding a 2 mol/L LiOH solution to the PLS until a desired pH, after which the solution was filtered and analysed on remaining elements.

Fig. 5.2 shows the percentages of elements remaining in the PLS vs. pH, after correcting for dilution. Increasing the pH from 1.7, the final pH of the PLS, to pH 4.0 causes most of the Al to precipitate from the solution. This can be seen by its steep decrease in concentration, resulting in 10.5% of the initial concentration remaining at pH 4.0. Cu exhibits a similar trend, with only 3.5% remaining at pH 4.5. At this pH, roughly 97% of the Ni, Co, and Mn remain in solution, indicating a 3% loss of these valuable elements. A further pH increase shows that Co and Ni mainly precipitate between pH 5.5 and pH 9.0, as the concentrations decline steeply within this pH range, while Mn precipitates above pH 9.0. In contrast, Fe does not show a sharp decrease within a narrow pH window but exhibits a gradual decrease over the entire pH range, resulting in significant Fe contamination in all precipitates. This is confirmed by analysis of the precipitates which shows a minimum Fe content of 4 wt.% across all pH steps. $PO_4^{3-}$ shows the largest decrease of all elements between pH 1.7 and 2.5, resulting in 22% being precipitated. Subsequentially, it keeps declining alongside Al, Cu, and Fe, respectively. Especially after pH 4.5, the trend is nearly identical to that of Fe. The results for Ni, Co, and Mn are similar to what Wang et al. [55] found when precipitating Li, Ni, Co, Mn, Cu, Al, and Fe from a PLS of industrial NMC BM, through pH increase with NaOH. However, Cu and Al precipitate between pH 2 and 5 in the current research, presumably due to phosphate presence lowering the solubility of these two impurities, while in the study of Wang et al. they precipitate between pH 3 and 6. Moreover, the Fe in the study of Wang et al. precipitates entirely by pH 4.5, which is a result of its low feed concentration (0.3 wt.% in the BM) compared to the current research, in which it is present for 16.9% in the LFP BM. As Fe coprecipitates in the entire pH

range, potentially resulting in low quality Ni, Co, and Mn products, further process optimization to minimize Fe-contamination is necessary.

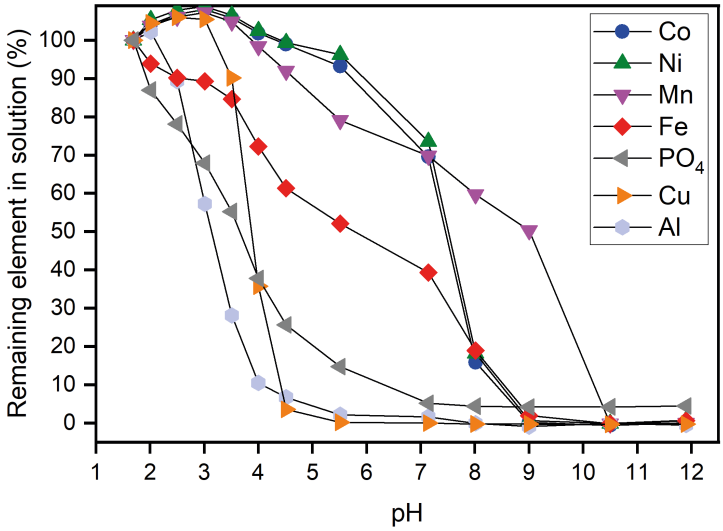


*Figure 5.2: The remaining elemental concentration compared to the PLS at different pH values, as achieved by stepwise precipitation after simultaneous leaching of NMC BM and LFP BM.*

Important to note is that with exception of Al, Fe, and $PO_4^{3-}$, the concentration of all elements seems to increase at the beginning of the precipitation. This can be mainly attributed to the nature of the correction by dilution by the LiOH-solution, which is done by solution mass increase. However, experimental uncertainties and different density of the PLS and LiOH-solution make complete correction impossible. Hence in any following experiment, the dilutions were measured by volume, making correction far more accurate. Another important point to be made is that the precipitates that are formed are largely amorphous, apart from the presence of $Li_2SO_4$ and a minor amount of $FePO_4$, as shown by XRD-analysis. As examples, the diffractograms of the precipitates formed at pH 2.0, 4.0, and 8.0 are shown in the appendix (Fig. C.3). Amorphous, or homogeneous, precipitation causes impurities to absorb on the surface of the formed precipitates, hence removing them from the solution [56]. This is why the concentration of Ni, Co and Mn lowers already from pH 4 onwards, as these are lost in the homogeneous precipitates of Fe, Al and Cu.

The reason for the wide precipitation range of Fe is most likely the result of the two oxidation states in which it is present. While $Fe^{3+}$ has low solubility above pH 2, $Fe^{2+}$ remains soluble at higher pH from 5 even up to 11 as a result of ion pair formation with hydroxides, resulting in soluble $FeOH^+$ [44,57,58]. Hence,

$Fe^{2+}$ contaminates any precipitates that are formed at pH 3 and above. Moreover, presence of metals such as Cu and Al in industrially pre-treated BM lead to additional redox reactions with $Fe^{3+}$ during leaching, as described in Chapter 4 and other literature [24,59]. This essentially increases the reducing capacity of LFP BM beyond the calculated amount based on TMs (Ni, Co, Mn) and Fe molar ratios. Another point of interest is the $PO_4^{3-}$ precipitating faster than Fe. Together with the analysis of the formed precipitates, which indicate the presence of Al, Cu, and $PO_4^{3-}$, this suggests precipitation of $AlPO_4$ and $Cu_3(PO_4)_2$.

To avoid an excess of $Fe^{2+}$ in the PLS, improvements were made to the reagents and leaching procedure. Firstly, size classification (sieving), a commonly practiced method in industry, lowers the amount of graphite, Al, and Cu in the as-received LFP BM. Secondly, the molar ratio of LFPs BM to NMC BM was lowered from 1 to 0.75 to account for the “excess” reducing capability of Cu and Al. Thirdly, the LFPs BM was added in three steps of 0.25 molar ratio at 30, 60, and 90 min of leaching, as this can avoid high initial S/L while being a relatively simple process control parameter. Fourthly, raising the acid concentration to 1 mol/L $H_2SO_4$ accommodated a higher total S/L of 122.8 g/L, which is closer to industrially relevant conditions compared to the initial leaching procedure. As a result, leaching could be completed without the need for $H_2O_2$, as is shown in the leaching results over time in Fig. 5.3a. The subsequent precipitation and corresponding precipitate compositions are shown in Fig. 5.3b and c, respectively.

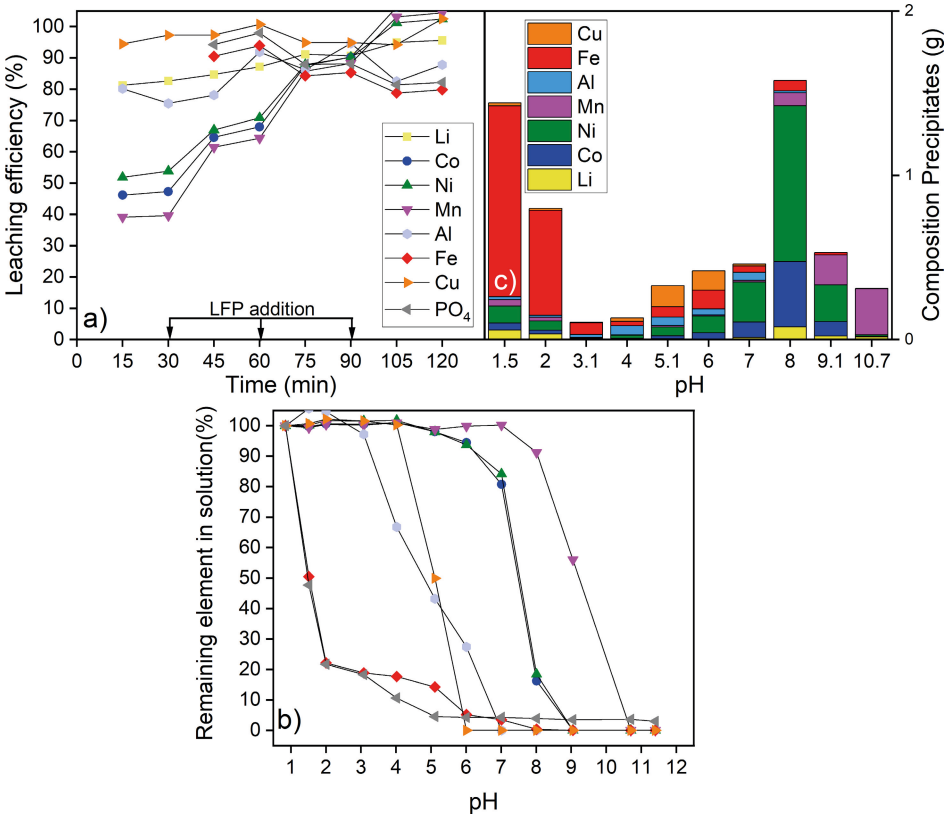


*Figure 5.3: a) Leaching efficiency of Li, Ni, Co, Mn, Fe, Al, Cu, and $PO_4^{3-}$ from NMC BM (57.6 g/L) as a function of time, with stepwise addition of LFPs BM (65.2 g/L). b) remaining elemental concentration compared to the PLS at different pH values, as achieved by stepwise precipitation after simultaneous leaching of NMC BM and LFPs BM. c) composition of resulting precipitates.*

The leaching efficiencies of the target elements at the start of the experiment are slightly higher (6-7%) compared to the ones observed in the previous conditions (Fig. 5.1), with an average of 46% Co, Ni and Mn dissolved and 83% of Li. This is most likely due to the higher acid concentration (1 mol/L instead of 0.63 mol/L), which compensates for the higher S/L of the NMC BM (57.6 vs. 38.4 g/L).

At 45 minutes (15 min after the first dose of LFPs BM), the dissolution of Ni, Co, and Mn rises to 68% on average, while for Li it rises to 87% despite its increased feed concentration from 1.6 to 1.9 g/L. Similar increases of approx. 18% are seen after the second and third dose of LFPs BM addition, which are all a result of Fe(II) from LFP readily dissolving (Eq. 5.3), promoting the reduction of Ni, Co, and Mn from the NMC BM. Finally, after 2 h of total leaching, Ni, Co, and Mn are completely dissolved, with the efficiency of Li reaching 95%. Around 95% of Cu and 88% Al

dissolve throughout the leaching process according to the mechanism described earlier in this research. The leaching efficiencies of Fe and $PO_4^{3-}$ are always high, starting at 92%, 15 min after LFPs BM addition (45 min mark) and dropping to 80% at the end of the leaching experiment, as a result of the increasing S/L of LFPs BM.

With the leaching process further optimized, it is necessary to evaluate its influence on the subsequential purification by pH adjustment. The composition of the remaining PLS at different pH values can be seen in Fig. 5.3b, while the composition of the resulting precipitates is shown in Fig. 5.3c. Compared to the previous precipitation results (Fig. 5.2), there is a significant improvement in the separation of Fe, Al, and Cu from Li, Ni, Co, and Mn. Upon reaching pH 2.0, 78% of the Fe is removed, as the $Fe^{2+}$ from the dissolved LFPs BM was consumed in the reduction of Ni, Co, and Mn, to a greater extent as a result of leaching parameter optimization and feed material sieving, resulting in a high amount of poorly soluble $Fe^{3+}$ in the PLS. At pH 5.1, only 10% of Fe and $PO_4^{3-}$ is left in solution, while the Cu and Al remain for 50% and 43%, respectively. As a result, the precipitates formed at pH 1.5, 2.0 and 3.1 mainly consist of Fe and $PO_4^{3-}$, whereas the precipitates at pH 4.0 and 5.1 also contain Al and Cu. However, Ni and Co start to precipitate from pH 5.1 onwards, as can be seen by their steeper decrease in concentration beyond this point. As the higher degree of $FePO_4$ precipitation between pH 1.5 and 3.1 leaves less $PO_4^{3-}$ available to precipitate with Al and Cu, there is a significant overlap in the precipitation of these impurities with Ni and Co, which is also confirmed by precipitate analysis in Fig. 5.3c. It shows that the precipitates formed at pH 6.0 and pH 7.0 are a mixture of Ni, Co, Fe, Al and Cu. Moreover, even the precipitate formed at pH 8.0, which contains the largest amount of Ni and Co, is contaminated with Fe. The remaining Ni and Co precipitate at pH 9.1, whereas the Mn precipitates between pH 8 and 10.7.

Due to the higher removal of Fe by merit of the more carefully controlled leaching process, these precipitates are significantly less contaminated with impurities. However, large amounts of contamination in the precipitates formed between pH 5.1 and pH 8.0 show that solely adjusting leaching does not result in sufficient separation of Cu, Al, and Fe from Li, Ni, Co, and Mn, and that there is a need for further purification steps, starting with the oxidation and removal of Fe.

### 5.3.2. Electrochemical Oxidation of $Fe^{2+}$ to $Fe^{3+}$ after Leaching

To investigate the electrochemical oxidation of Fe as function of PLS complexity, we start by oxidizing the Fe in a simple, synthetic, solution made of $FeSO_4$ in 1 mol/L $H_2SO_4$. This is performed in an electrochemical cell with a large anode to cathode ratio, thereby promoting the Fe oxidation at the anode, according to Eq. 5.4, with hydrogen gas formation at the cathode, resulting in the overall cell reaction in Eq. 5.8. After this initial test, we repeated the process on a PLS made from leaching

of LFPs BM alone. This simplified PLS is used to test the process on industrial BM without interference from additional metal ions originating from NMC BM. Next, the method is repeated on the optimized PLS resulting from simultaneous leaching of LFPs BM and NMC BM (Fig. 5.3a). A comparison of the measured potential in the three described solutions over time is shown in Fig. 5.4, together with the $Fe^{3+}$ vs total Fe percentage at selected measurement points.

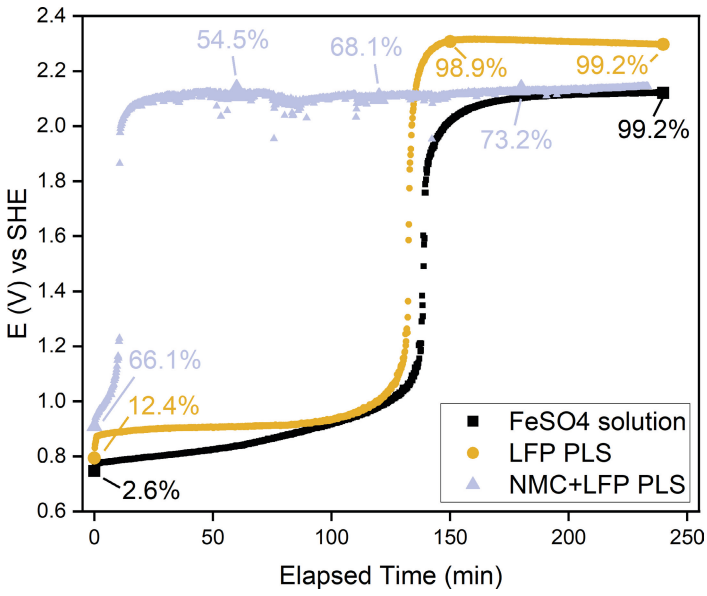


*Figure 5.4: Evolution of the anode potential over time during chronopotentiometry (1.2A) performed on a $FeSO_4$-solution (0.18 mol/L), LFPs BM-PLS, and NMC BM + LFPs BM-PLS. Percentages of $Fe^{3+}$ compared to total Fe concentration are indicated.*

$$2H^{+}_{(aq)} + 2Fe^{2+}_{(aq)} \rightarrow H_{2(g)} + 2Fe^{3+}_{(aq)} \left(\Delta E = 0.77V\right) \tag{5.8}$$

The cell potential of the $FeSO_4$-solution starts at E < 0.77 V vs. SHE, which is the standard potential of $E^0$ = 0.77 V for the oxidation of $Fe^{2+}$ to $Fe^{3+}$ but very soon reaches 0.78 V. Over the course of 125 min, the potential gradually increases to 1.05 V, after which it sharply rises to 2.1 V, where it stabilizes around that value (± 0.1 V). A similar curve is observed for the PLS containing only LFPs BM, starting at a slightly higher potential of 0.9 V for the first 120 min, before it suddenly increases to 2.3 V, a few minutes earlier than in the $FeSO_4$-solution. The curve for the PLS from simultaneous leaching (NMC BM + LFPs BM) also starts around 0.9 V, but it sharply increases after 10 min, rising to an anode potential of 2.1 V, where it stabilizes over the remaining 230 min. The shape of these curves reflects the decrease in $Fe^{2+}$ concentration, accompanied by an increase in $Fe^{3+}$ concentration,

in accordance with the Nernst equation in Eq. 5.9, where $R$ is the ideal gas constant, $T$ the temperature, $n$ the number of electrons, and $F$ the Faraday constant. It has to be noted that in Eq. 5.9, the activity coefficients of $Fe^{3+}$ and $Fe^{2+}$ are approximated by their concentrations. The dependence of the Fe oxidation on the cell potential is visualized in the appendix, Fig C.4.

$$E = E^0 + \frac{RT}{nF} * ln \frac{\left[Fe^{3+}\right]}{\left[Fe^{2+}\right]} \tag{5.9}$$

Once the concentration of $Fe^{2+}$ has dropped significantly, the solution no longer has sufficient $Fe^{2+}$ to sustain the redox process and a sharp increase in anode potential toward 2V marks the transition from $Fe^{2+}$ oxidation to water electrolysis. At this point, the oxygen evolution reaction (OER) becomes the dominant anodic process, which is also indicated by gas formation at the anode. This trend is also confirmed by $Fe^{3+}/Fe^{2+}$ ratio analysis using UV-Vis. Before electro-oxidation, only 2.4% of the Fe in $FeSO_4$-solution was in the $Fe^{3+}$ state. This increased to 99.2% after 240 min of electro-oxidation. In the simple LFPs BM PLS, 12.4% of the Fe was initially present as $Fe^{3+}$, which possibly oxidized during the processing of the BM, leaching or due to battery aging. This number increased to 98.9% after 150 min, and 99.1% after 240 min of electro-oxidation. The shapes of the potential curves for the $FeSO_4$-solution and the LFPs BM PLS are both similar to the curves in the study of Venkatesan et al. [49], who also investigated a relatively simple solution containing predominantly $Fe^{2+}$ and $Nd^{3+}$ in HCl. Hence, it is clear that electro-oxidation is an effective method to oxidize $Fe^{2+}$ in solutions containing predominantly Fe, and monitoring the anode potential provides a reliable indication for the oxidation progress.

The distinct curve of the electro-oxidation in the PLS containing LFP- and NMC BM can be attributed to multiple factors. Firstly, the amount of Fe that was already in the oxidized state, $Fe^{3+}$, directly after leaching was significantly higher (66.1%). This is due to redox reaction with the Ni, Co and Mn from the NMC BM, which are reduced by the $Fe^{2+}$ during leaching. Secondly, after 180 min the oxidation to $Fe^{3+}$ increased by a mere 7% (to 73.2%). This was accompanied by the deposition of a red-brown coloured deposit at the cathode, which XRD-analysis revealed to contain Cu and $Cu_2O$ (Fig. C.5). $Cu^{2+}$ in solution makes its reduction on the cathode ($E^0$ = 0.34 V, Eq. 5.21, Table 5.2) thermodynamically more favoured compared to the hydrogen evolution under the applied conditions. Moreover, the deposits also increase the surface area of the cathode which, together with the increasing $Fe^{3+}$ concentration in solution now leads to its reduction back to $Fe^{2+}$ becoming more favoured ($E^0$ = 0.77 V), leading to reaction “loop” and low overall oxidation efficiency. Thirdly, any deposited Cu can react with $Fe^{3+}$ through the same reaction as during leaching, essentially resulting in a zero net operation. Fourthly, apart from Cu, reduction of other elements

at the cathode such as Al, Mn, Fe, Co, and Ni according to Eqs. 5.11 to 5.15 are plausible at such high cell potentials. ICP-OES analysis of a cathode deposit in a later experiment confirms the presence of all of these elements. This suggests that these can interfere with efficient Fe oxidation since their metallic deposits can react with $Fe^{3+}$, similarly to the leaching reactions, producing $Fe^{2+}$ again. Lastly, side reactions at the anode, such as the oxidation of $Co^{2+}$ to $Co^{3+}$ (Eq. 5.29, +1.92V) and $Mn^{2+}$ to $Mn^{3+}$ (Eq 5.27, +1.51V), can lead to further efficiency losses. These reactions compete with $Fe^{2+}$ oxidation, since the potential reaching 2.1V provides sufficient driving force. While these trivalent cations can still facilitate $Fe^{2+}$ oxidation by reacting with it in solution, the formation of insoluble oxides such as $NiO_2$ (Eq 5.28), $CoO_2$ (Eq 5.26), or $MnO_2$ (Eq. 5.25) is detrimental to the process. Analysis of the anode deposit in a later experiment confirms the presence of Mn, Ni, and Co alongside Fe, confirming the formation of insoluble oxides.

*Table 5.2: Reduction half reactions relevant for the LFPs + NMC PLS*

| Reduction Half Reaction | E° (V) [54] | Eq. nr. |
|---|---|---|
| $Li^+ + e^- \rightarrow Li$ | -3.04 | (5.10) |
| $Al^{3+} + 3e^- \rightarrow Al$ | -1.676 | (5.11) |
| $Mn^{2+} + 2e^- \rightarrow Mn$ | -1.18 | (5.12) |
| $Fe^{2+} + 2e^- \rightarrow Fe$ | -0.44 | (5.13) |
| $Co^{2+} + 2e^- \rightarrow Co$ | -0.282 | (5.14) |
| $Ni^{2+} + 2e^- \rightarrow Ni$ | -0.257 | (5.15) |
| $H_3PO_4 + 2H^+ + 2e^- \rightarrow H_3PO_3 + H_2O$ | -0.276 | (5.16) |
| $Fe^{3+} + 3e^- \rightarrow Fe$ | -0.044 | (5.17) |
| $2H^+ + 2e^- \rightarrow H_2$ | 0 | (5.18) |
| $HSO_4^- + 3H^+ + 2e^- \rightarrow H_2SO_3 + H_2O$ | +0.158 | (5.19) |
| $Cu^{2+} + e^- \rightarrow Cu^+$ | +0.159 | (5.20) |
| $Cu^{2+} + 2e^- \rightarrow Cu$ | +0.340 | (5.21) |
| $Cu^+ + e^- \rightarrow Cu$ | +0.520 | (5.22) |
| $Fe^{3+} + e^- \rightarrow Fe^{2+}$ | +0.77 | (5.23) |
| $O_2 + 4H^+ + 4e^- \rightarrow 2H_2O$ | +1.23 | (5.24) |
| $MnO_2 + 4H^+ + 2e^- \rightarrow Mn^{2+} + 2H_2O$ | +1.23 | (5.25) |
| $CoO_2 + 4H^+ + e^- \rightarrow Co^{3+} + 2H_2O$ | +1.4 | (5.26) |
| $Mn^{3+} + e^- \rightarrow Mn^{2+}$ | +1.51 | (5.27) |
| $NiO_2 + 4H^+ + 2e^- \rightarrow Ni^{2+} + 2H_2O$ | +1.59 | (5.28) |
| $Co^{3+} + e^- \rightarrow Co^{2+}$ | +1.92 | (5.29) |

### 5.3.3. Electrodeposition of Cu & Subsequent Electro-oxidation of Fe

While the presence of $Cu^{2+}$ interferes with the complete oxidation of $Fe^{2+}$, it also presents an interesting opportunity to remove Cu electrochemically and recover it

in its metallic state. To maximize Cu and Fe removal after simultaneous leaching, we investigated a purification strategy that includes pH adjustment to 2, 3 or 4, followed by a two-step electrochemical purification process consisting of Cu electrodeposition and Fe oxidation (Fig. 5.5). Table 5.3 shows the concentration of all elements in the solution at different steps of the process, including after the pH increase, Cu deposition, and Fe oxidation.

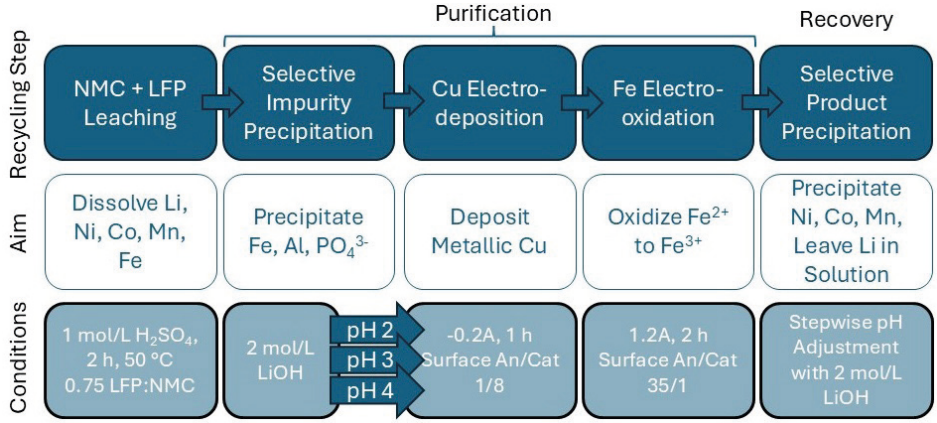


*Figure 5.5: Overview of recycling approach. Cu-deposition, Fe-oxidation, and subsequent selective precipitation were carried out three times, at pH 2, 3, and 4.*

*Table 5.3: Concentration of elements in solution at the end of different stages in the recycling process, measured by ICP-OES. Decreases in concentration which are not due to dilution (volume increase is indicated as "V*x") are highlighted in green, together with the corresponding percentages between brackets (relative to the initial PLS). For comparison, the solution after leaching industrial BM + spent LFP and precipitating to pH 3 from Fig 4.3b is also reported.*

| | | Species concentration after recycling step (g/L) | | | | | | | |
|---|---|---|---|---|---|---|---|---|---|
| **pH** | **Process stage** | **Li** | **Co** | **Ni** | **Mn** | **Al** | **Fe** | **Cu** | **$PO_4^{3-}$** |
| 2 | Leaching | 3.29 | 3.65 | 9.99 | 3.59 | 1.42 | 9.96 | 1.76 | 18.44 |
| | Precipitation (V*1.32) | 5.41 | 2.75 (100%) | 7.57 (100%) | 2.69 (99%) | 0.92 (85%) | 1.04 (14%) | 1.32 (99%) | 2.46 (18%) |
| | Cu-deposition (1h, 0.2A) | 5.41 | 2.75 | 7.58 | 2.69 | 0.91 | 1.03 | 0.68 (51%) | 2.43 |
| | Fe-oxidation (2h, 1.2A) | 5.49 | 2.77 | 7.65 | 2.70 | 0.91 | 0.97 (13%) | 0.68 | 2.34 (17%) |
| 3 | Leaching | 3.29 | 3.65 | 9.99 | 3.59 | 1.42 | 9.96 | 1.76 | 18.44 |
| | Precipitation (V*1.38) | 5.58 | 2.63 (99%) | 7.24 (100%) | 2.54 (98%) | 0.70 (68%) | 0.74 (10%) | 1.10 (86%) | 1.45 (11%) |
| | Cu-deposition (1h, 0.2A) | 5.66 | 2.60 | 7.23 | 2.55 | 0.69 | 0.73 | 0.59 (46%) | 1.41 |
| | Fe-oxidation (2h, 1.2A) | 5.75 | 2.65 | 7.36 | 2.54 | 0.71 | 0.35 (5%) | 0.59 | 0.79 (6%) |
| 4 | Leaching | 3.08 | 3.63 | 10.05 | 3.57 | 1.35 | 9.99 | 1.77 | 18.65 |
| | Precipitation (V*1.41) | 5.47 | 2.52 (97%) | 7.02 (99%) | 2.41 (95%) | 0.48 (51%) | 0.68 (10%) | 0.70 (55%) | 0.94 (7%) |
| | Cu-deposition (1h, 0.2A) | 5.49 | 2.44 | 7.02 | 2.40 | 0.47 | 0.63 | 0.34 (27%) | 0.87 |
| | Fe-oxidation (2h, 1.2A) | 5.65 | 2.52 | 7.25 | 2.40 | 0.48 | 0.51 (7%) | 0.35 | 0.71 (5%) |
| 3 | Solution Chapter 4 [51] | 2.55 | 5.33 | 3.83 | 1.91 | 0.60 | 7.35 | 0.28 | 11.07 |

Comparing the concentration of Fe and $PO_4^{3-}$ after the first precipitation step, we can conclude that about 86% of the present Fe precipitates as $FePO_4$ at pH 2, similarly to the results shown in Fig. 5.3. Precipitation increases at higher pH, reaching 89.7 % at pH 3 and 90.4 % at pH 4. Apart from dilution, Cu is not affected by adjusting the solution to pH 2, while 15% of Al precipitates at this point. However, 32 % of Al and 14% of the Cu precipitate at pH 3, while roughly 47% of both Cu and Al are removed by adjusting the solution to pH 4. Important to note as well is that raising the pH to 2 causes no significant loss of Ni, Co, and Mn due to coprecipitation, while raising to pH 3 or 4 only results in roughly 1% and 2.5% loss of these elements on average, respectively.

During the second purification step, Cu deposition results in 49% of Cu removal at pH 2, while at pH 3 and 4, 53% and 73% are removed, respectively. For all three pH values, the concentrations of Ni, Co, and Mn do not change in the process. These findings indicate that Cu deposition is reasonably efficient at all tested pH values, which is a result of the low anode-to-cathode surface ratio (1:8), promoting Cu deposition at the larger cathode, and limiting the premature oxidation of $Fe^{2+}$ to $Fe^{3+}$ at the smaller anode, in favour of the oxygen evolution reaction (Eq. 5.24). Also, since the pH is increased, any Fe that does oxidize to $Fe^{3+}$ precipitates, avoiding interference with Cu deposition and resulting in high selectivity for Cu. This is apparent from the fact that the concentration of all other species during Cu deposition is nearly unaffected, and that qualitative ICP-OES analysis of the deposits on the cathode shows few impurities at pH 2 and 3. However, the deposit at pH 4 also contains a significant amount of Co and Ni. Qualitative analysis shows a ratio of 1:2 for Co:Cu, and 1:4 for Ni:Cu. When looking at Eqs. 5.14 and 5.15 in Table 5.2, this can be easily explained. The cathode potential (vs. SHE) during deposition starts at -1.7V, and eventually reaches -1.4V, as can be seen in Fig C.6 in the appendix. This is sufficient to reduce $Ni^{2+}$ and $CO^{2+}$ to their metallic form ($E^0$= -0.26 and -0.28, resp.).

During subsequent $Fe^{2+}$ oxidation, little changes in the elemental concentrations are measured, with a 1-5% decrease of Fe and $PO_4^{3-}$. The system at pH 2 only shows a 1% decrease in Fe and $PO_4^{3-}$ concentration, since this pH is too low for any oxidized Fe to precipitate. The same process at pH 3 also only shows a change in Fe and $PO_4^{3-}$ concentration, from 10.5% to 5.5% on average, lowering the concentration from 0.73 to 0.35 g/L and 1.41 to 0.79 g/L, respectively. Surprisingly, the oxidation at pH 4 only decreases Fe by 2% or 0.12 g/L. This could be a result of the lower $PO_4^{3-}$ concentration at the start of the oxidation due to prior $AlPO_4$ precipitation. Also, the pH after the Fe oxidation decreased from 4 to 2.4, resulting in higher solubility of $Fe^{3+}$, thereby lowering the efficiency of its removal. The Ni and Co concentrations are unaffected throughout all experiments, but the

Mn concentration lowers by 1% during the electro-oxidation at pH 4. ICP-OES analysis of the deposit on the anode shows the presence of Mn.

When comparing the resulting solution obtained after electrochemical purification at pH 4 with the one obtained by van de Ven et al. [51] (Chapter 4, Fig. 4.3b) through leaching of an industrial NMC BM with spent LFP and subsequent pH adjustment to 3.0, the effectiveness of the presented recycling approach is further established. Improved leaching conditions result in a higher amount of Ni, Co, and Mn in total, being 12.17 g/L (after 40% dilution by pH increase) rather than 11.07 g/L, while Li numbers are hard to compare due to different pH adjustment media (LiOH vs NaOH). Cu and Al concentrations are similar in the current research versus the results of Chapter 4, being 0.35 vs 0.28 g/L Cu, and 0.48 vs 0.60 g/L Al, both despite a much higher leaching efficiency in the current leaching method. Most importantly however, the Fe concentration in the current research is significantly lower, being 0.51 vs 7.35 g/L, as a result of electrochemical purification.

### 5.3.4. Selective Precipitation of Ni, Co, & Mn after Electrochemical Purification



Besides the impurity removal efficiency, the composition and purity of the recovered target element compounds are of great importance in a hydrometallurgical process. In our case, the target elements Ni, Co, and Mn are recovered by a second precipitation through pH adjustment, which was conducted after electrochemical treatments at different pH values, analogous to the selective precipitation in Fig. 5.3, leaving Li in solution. To emphasise the purity of the resulting precipitates rather than the remaining elemental concentration over the pH increase, only the composition of the precipitates formed as a result this procedure are shown in Fig. 5.6. To compare how the purity of the precipitates is influenced by the pH at which electrochemical purification is conducted (2, 3 or 4), the impurity content of the precipitates on metal basis is calculated according to Eq. 5.30. The mass components in this equation represent the mass of the corresponding element that is present in the precipitate obtained at pH X. These values are reported above the respective bar in in Fig. 5.6.

$$Impurity\ content = 100 * \frac{m_x^{Fe} + m_x^{Al} + m_x^{Cu}}{m_x^{Fe} + m_x^{Al} + m_x^{Cu} + m_x^{Ni} + m_x^{Co} + m_x^{Mn} + m_x^{Li}} \tag{5.30}$$

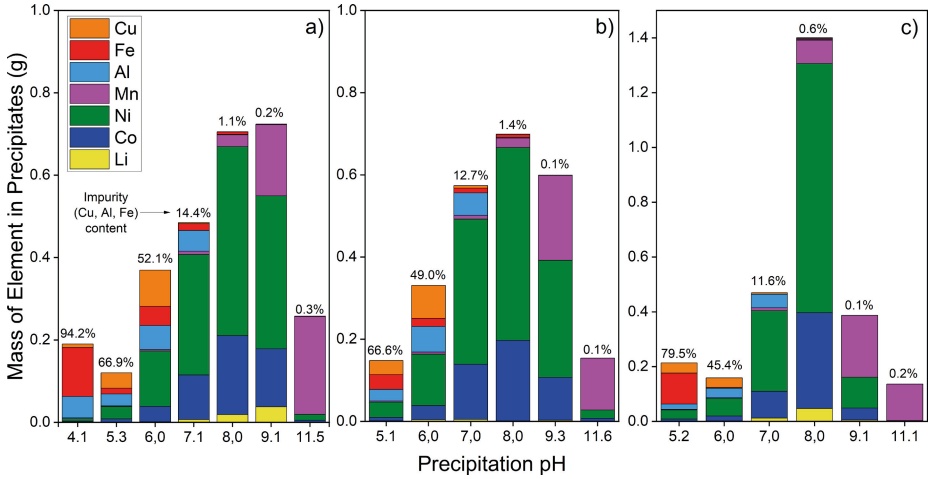


*Figure 5.6: Composition of the precipitates formed through selective precipitation after electrochemical purification at pH 2 (a), pH 3 (b), and pH 4 (c). Above each bar, impurity content on metal basis according to Eq. 5.30 is shown.*

Fig. 5.6a shows the compositions of the precipitates formed after electrochemical purification at pH 2. The first precipitate at pH 4.1 mostly consists of Fe, Al and Cu impurities (94.2%) while the precipitate at pH 5.3 contains significantly less, being 66.9%. At this point, having such high impurity content is desirable since the selective precipitation is targeted at removing Fe, Al, and Cu, rather than recovering Ni, Co, and Mn. However, the precipitate at pH 5.3 containing 33.1% target elements indicates a significant loss. Further raising the pH to 6.0, at which the target elements Ni and Co start precipitating significantly, results in a precipitate containing 52.1% impurities, while the following precipitate at pH 7.1 mostly contains target elements and only 14.4% impurities. The precipitates at pH 8.0, 9.1, and 11.5 represent the main recoveries of the target elements, and merely consist of 1.1%, 0.2% and 0.3% impurities, respectively. This is already a significant improvement to the selective precipitation without prior electrochemical purification, as presented in Fig. 5.3c, which produced precipitates at pH 8.0, 9.1, and 10.7 containing 4.7%, 2.8%, and 0.5%, respectively. However, more improvement is left to be desired when comparing to precipitation studies such as the one from Kang et al.[41], who achieved 99% precipitation of Fe, Al, and Cu associated with a loss of 19% Ni, 7% Co, and 15% Mn, while the present results show 99% precipitation of Fe, Al, and Cu alongside a nearly 30% loss of Ni and Co.

In Fig. 5.6b, the precipitates after electrochemical purification at pH 3 are presented. The solids formed at pH 5.5 and 6.1 are similar to their counterparts from Fig. 5.6a, and contain much contamination by Fe, Al, and Cu, being 66.6% and 49.0%, respectively. The precipitate at pH 7.0 has a large amount of Ni and

Co, but still contains 12.7% impurities of which most is Al, which is problematic regarding the high amount of Ni and Co that is hence lost. Beyond this point, the precipitates are of good quality, showing 1.4%, 0.1% and 0.1% impurities at pH 8.0, 9.3, and 11.6, respectively.

In Fig 5.6c, the compositions of the precipitates acquired after electrochemical purification at pH 4 are shown. Here, the precipitate formed at pH 5.2 again shows the largest presence of Fe, Al, and Cu, totalling 79.5%. The solids formed at pH 6.0 and 7.0 show lower impurity contents of 45.4% and 11.6%, respectively. Similarly to the other two scenarios, this results in a large loss of target elements due to overlap between target element and impurity coprecipitation. Further precipitates at pH 8.0, 9.1, and 11.1 merely contain 0.6%, 0.1%, and 0.2% impurities, respectively, showing the highest purity of the main target element precipitates.

Comparing the three sets of precipitates leads to the conclusion that electrochemical purification at higher pH leads to precipitates with less impurities. Although the metal basis purities at pH 8.0 for the experiments at pH 2, 3, and 4 are 96.3%, 98.5%, and 96.0% (not shown in graph), respectively, also looking at impurities, which make up 1.1%, 1.4%, and 0.6%, respectively, vouches for this trend. The precipitates around pH 9 also have lower impurity content in case of electrochemical purification at pH 2, 3, and 4 with values of 0.2%, 0.1%, and 0.1%. This again shows that selective precipitation after electrochemical treatment at pH 4 produces the purest precipitate. Conversely, at pH 5 or lower, high impurity content is desired indicating good removal of Fe, Al, and Cu with minimal loss of target elements. The differences in impurity contents at pH 5 in Fig. 5.6a, b, and c (66.9%, 66.6%, and 79.5%) again indicate electrochemical purification at pH 4 being superior, since it results in the precipitate with the highest impurity content of 79.5%.



## 5.4. CONCLUSIONS

This study developed an improved method to simultaneously leach mechanically pre-treated industrial LFP- and NMC- BM, achieving complete dissolution of Ni, Co, and Mn at lower chemical consumption. Al and Cu impurities from the current collectors regenerate $Fe^{2+}$ via redox reactions, increasing the reducing capabilities of the LFPs BM. However, this also increases Al and Cu contamination in the PLS. Additional measures, including sieving steps to lower the Al and Cu content of LFP BM, as well as optimization of leaching parameters, limit this effect while still achieving complete leaching of Ni, Co, and Mn without any external reducing agent. These optimized parameters are 1 mol/L $H_2SO_4$ (98 g/L), 65.2 g/L LFPs BM and

57.6 g/L NMC BM (0.75 molar ratio), and a total leaching time of 2 h. The LFPs BM is added stepwise in three equal portions at 30, 60, and 90 minutes.

Although $Fe^{3+}$ can be readily removed from the PLS at pH 2, the $Fe^{2+}$ that is not used as reducing agent during leaching does not precipitate until pH 8, and contaminates any Ni, Co, and Mn precipitates as a result of coprecipitation. Therefore, electrochemical oxidation of $Fe^{2+}$ was explored as a subsequent purification step to convert the remaining $Fe^{2+}$ to the less soluble $Fe^{3+}$using a large anode and small cathode (35:1) and a current density of 21.8 mA/$cm^2$ (1.2A). While electrochemical purification was effective in simple media, such as a $FeSO_4$-solution or a PLS of LFPs BM, oxidizing 99.2% of the present $Fe^{2+}$ in 240 min, it also offers the major advantage of in-situ monitoring of Fe oxidation progress due to the potential being dependant on the $Fe^{3+}/Fe^{2+}$- ratio, as described by the Nernst equation. However, other elements present in the complex PLS of simultaneous LFP and NMC leaching hinder electrochemical oxidation of $Fe^{2+}$. Most importantly, Cu deposits on the cathode, where it can react with $Fe^{3+}$ to regenerate $Fe^{2+}$ and $Cu^{2+}$, drastically lowering the oxidation efficiency. Moreover, the potential oxidation of Ni, Co, and Mn at the anode results further reduces the effectiveness of Fe-oxidation, which reaches only 73.2% after 240 min.

This electrochemical reaction loop can be avoided by first precipitating the present $Fe^{3+}$ in the form of $FePO_4$ by increasing the pH, after which Cu is removed via electrodeposition at 0.2A (12.5 mA/$cm^2$), followed by the $Fe^{2+}$ electro-oxidation. This sequence of processing steps was investigated as a function of solution pH (2, 3 and 4), with the most efficient results obtained at pH 4, for which 93% of the Fe, and 73% of the Cu were removed. The process at pH 3 resulted in the highest Fe removal of 95.2% after the full electrochemical purification, but was limited by the lower Cu removal of 54%. Subsequently, selective precipitation resulted in improved separation of the remaining Fe, Al, and Cu from the target elements, with the system electrochemically purified at pH 4 resulting in Ni, Co, and Mn precipitation products containing a maximum of 0.6% impurities, while leaving Li in solution. While this work presents a significant step towards more eco-friendly LiB-recycling, further optimization is needed to improve Cu removal, and address Al, which remained the primary contaminant of the Co, Ni, and Mn end products.

## REFERENCES


1. Y. Liang, C.-Z. Zhao, H. Yuan, Y. Chen, W. Zhang, J.-Q. Huang, D. Yu, Y. Liu, M.-M. Titirici, Y.-L. Chueh, H. Yu, Q. Zhang, A review of rechargeable batteries for portable electronic devices, *InfoMat* 1 (2019) 6–32.
2. J.C. Kelly, Q. Dai, M. Wang, Globally regional life cycle analysis of automotive lithium-ion nickel manganese cobalt batteries, *Mitig. Adapt. Strateg. Glob. Chang.* 25 (2019) 371–396.
3. Y. Ding, Z.P. Cano, A. Yu, J. Lu, Z. Chen, Automotive Li-Ion Batteries: Current Status and Future Perspectives, *Electrochemical Energy Reviews* 2 (2019) 1–28.
4. G. Zubi, R. Dufo-López, M. Carvalho, G. Pasaoglu, The lithium-ion battery: State of the art and future perspectives, *Renewable and Sustainable Energy Reviews* 89 (2018) 292–308.
5. Directive 2012/19/EU of the European Parliament and of the Council of 4 July 2012 on waste electrical and electronic equipment (WEEE), *Official Journal* L 197 (2012) 38–71.
6. European Commission Directorate-General for Internal Market Industry Entrepreneurship and SMEs, M. Grohol, C. Veeh, Study on the critical raw materials for the EU 2023 – Final report, Publications Office of the European Union, 2023.
7. S. Jin, D. Mu, Z. Lu, R. Li, Z. Liu, Y. Wang, S. Tian, C. Dai, A comprehensive review on the recycling of spent lithium-ion batteries: Urgent status and technology advances, *J. Clean. Prod.* 340 (2022) 130535.
8. European Commission Directorate-General for Internal Market Industry Entrepreneurship and SMEs, D. Pennington, E. Tzimas, C. Baranzelli, J. Dewulf, S. Manfredi, P. Nuss, M. Grohol, A. Van Maercke, Y. Kayam, S. Solar, B. Vidal-Legaz, L. Talens Peirò, L. Mancini, C. Ciupagea, L. Godlewska, P. Dias, C. Pavel, D. Blagoeva, G. Blengini, V. Nita, C. Latunussa, C. Torres De Matos, F. Mathieux, A. Marmier, Methodology for establishing the EU list of critical raw materials – Guidelines, Publications Office, 2017.
9. M. Kayla Kilgo, A. Anctil, M.S. Kennedy, B.A. Powell, Metal leaching from Lithium-ion and Nickel-metal hydride batteries and photovoltaic modules in simulated landfill leachates and municipal solid waste materials, *Chemical Engineering Journal* 431 (2022) 133825.
10. J. Ordoñez, E.J. Gago, A. Girard, Processes and technologies for the recycling and recovery of spent lithium-ion batteries, *Renewable and Sustainable Energy Reviews* 60 (2016) 195–205.
11. J. Shuai, W. Liu, S. Rohani, Z. Wang, M. He, C. Ding, X. Lv, Efficient extraction and separation of valuable elements from spent lithium-ion batteries by leaching and solvent extraction: A review, *Chemical Engineering Journal* 503 (2025) 158114.
12. P. Meshram, B.D. Pandey, T.R. Mankhand, Extraction of lithium from primary and secondary sources by pre-treatment, leaching and separation: A comprehensive review, *Hydrometallurgy* 150 (2014) 192–208.
13. G. Tian, G. Yuan, A. Aleksandrov, T. Zhang, Z. Li, A.M. Fathollahi-Fard, M. Ivanov, Recycling of spent Lithium-ion Batteries: A comprehensive review for identification of main challenges and future research trends, *Sustainable Energy Technologies and Assessments* 53 (2022) 102447.
14. D. Yu, Z. Huang, B. Makuza, X. Guo, Q. Tian, Pretreatment options for the recycling of spent lithium-ion batteries: A comprehensive review, *Miner. Eng.* 173 (2021) 107218.
15. A.M. Bernardes, D.C.R. Espinosa, J.A.S. Tenório, Recycling of batteries: a review of current processes and technologies, *J. Power Sources* 130 (2004) 291–298.
16. O. Velázquez-Martínez, J. Valio, A. Santasalo-Aarnio, M. Reuter, R. Serna-Guerrero, A Critical Review of Lithium-Ion Battery Recycling Processes from a Circular Economy Perspective, *Batteries* 5 (2019) 68.
17. A. Chagnes, B. Pospiech, A brief review on hydrometallurgical technologies for recycling spent lithium-ion batteries, *Journal of Chemical Technology & Biotechnology* 88 (2013) 1191–1199.

**18.** P. Hayes, Process Principles in Minerals and Materials Production with a Focus on Metal Production and Recycling, Fourth edition, Hayes Publishing Co, Sherwood, 2021.

**19.** J. Nan, D. Han, X. Zuo, Recovery of metal values from spent lithium-ion batteries with chemical deposition and solvent extraction, *J. Power Sources* 152 (2005) 278–284.

**20.** P. Zhang, T. Yokoyama, O. Itabashi, T.M. Suzuki, K. Inoue, Hydrometallurgical process for recovery of metal values from spent lithium-ion secondary batteries, *Hydrometallurgy* 47 (1998) 259–271.

**21.** R.C. Wang, Y.C. Lin, S.H. Wu, A novel recovery process of metal values from the cathode active materials of the lithium-ion secondary batteries, *Hydrometallurgy* 99 (2009) 194–201.

**22.** S. Castillo, F. Ansart, C. Laberty-Robert, J. Portal, Advances in the recovering of spent lithium battery compounds, *J. Power Sources* 112 (2002) 247–254.

**23.** J.J.M.M. van de Ven, Y. Yang, S.T. Abrahami, A closer look at lithium-ion batteries in E-waste and the potential for a universal hydrometallurgical recycling process, *Sci. Rep.* 14 (2024) 1–12.

**24.** J.J.M.M. Van De Ven, · Patrick, J. Teeuwisse, · Ruud, W.A. Hendrikx, Y. Yang, S.T. Abrahami, Simultaneous Recycling of Spent $LiFePO_4$ and $LiNi_xMn_yCo_zO_2$ Li-Ion Batteries Under Mild Leaching Conditions, *Journal of Sustainable Metallurgy* (2025) 1–12.

**25.** M.C. Biesinger, B.P. Payne, A.P. Grosvenor, L.W.M. Lau, A.R. Gerson, R.S.C. Smart, Resolving surface chemical states in XPS analysis of first row transition metals, oxides and hydroxides: Cr, Mn, Fe, Co and Ni, *Appl. Surf. Sci.* 257 (2011) 2717–2730.

**26.** J.L. White, F.S. Gittleson, M. Homer, F. El Gabaly, Nickel and Cobalt Oxidation State Evolution at Ni-Rich NMC Cathode Surfaces during Treatment, *Journal of Physical Chemistry C* 124 (2020) 16508–16514.

**27.** N. Vieceli, R. Casasola, G. Lombardo, B. Ebin, M. Petranikova, Hydrometallurgical recycling of EV lithium-ion batteries: Effects of incineration on the leaching efficiency of metals using sulfuric acid, *Waste Management* 125 (2021) 192–203.

**28.** G. Dorella, M.B. Mansur, A study of the separation of cobalt from spent Li-ion battery residues, *J. Power Sources* 170 (2007) 210–215.

**29.** R. Sattar, S. Ilyas, H.N. Bhatti, A. Ghaffar, Resource recovery of critically-rare metals by hydrometallurgical recycling of spent lithium ion batteries, *Sep. Purif. Technol.* 209 (2019) 725–733.

**30.** C.K. Lee, K.I. Rhee, Reductive leaching of cathodic active materials from lithium ion battery wastes, *Hydrometallurgy* 68 (2003) 5–10.

**31.** G.P. Nayaka, J. Manjanna, K. V. Pai, R. Vadavi, S.J. Keny, V.S. Tripathi, Recovery of valuable metal ions from the spent lithium-ion battery using aqueous mixture of mild organic acids as alternative to mineral acids, *Hydrometallurgy* 151 (2015) 73–77.

**32.** C. Peng, J. Hamuyuni, B.P. Wilson, M. Lundström, Selective reductive leaching of cobalt and lithium from industrially crushed waste Li-ion batteries in sulfuric acid system, *Waste Management* 76 (2018) 582–590.

**33.** K. Tanong, L. Coudert, M. Chartier, G. Mercier, J.F. Blais, Study of the factors influencing the metals solubilisation from a mixture of waste batteries by response surface methodology, *Environmental Technology (United Kingdom)* 38 (2017) 3167–3179.

**34.** J. Wang, M. Chen, H. Chen, T. Luo, Z. Xu, Leaching Study of Spent Li-ion Batteries, *Procedia Environ. Sci.* 16 (2012) 443–450.

**35.** R.F. Maritz, R.F. van Schalkwyk, N. Elginöz, G. Akdogan, C. Dorfling, Using life cycle assessment to aid process development for hydrometallurgical recycling of end-of-life lithium ion batteries, *Waste Management* 200 (2025) 114763.

**36.** Y. Jiang, X. Chen, S. Yan, S. Li, T. Zhou, Pursuing green and efficient process towards recycling of different metals from spent lithium-ion batteries through Ferro-chemistry, *Chemical Engineering Journal* 426 (2021) 131637.

**37.** X. Chen, J. Li, D. Kang, T. Zhou, H. Ma, A novel closed-loop process for the simultaneous recovery of valuable metals and iron from a mixed type of spent lithium-ion batteries, *Green Chemistry* 21 (2019) 6342–6352.

**38.** A. Chernyaev, Y. Zou, B.P. Wilson, M. Lundström, The interference of copper, iron and aluminum with hydrogen peroxide and its effects on reductive leaching of $LiNi_{1/3}Mn_{1/3}Co_{1/3}O_2$, *Sep. Purif. Technol.* 281 (2022) 119903.

**39.** Z. Dobó, T. Dinh, T. Kulcsár, A review on recycling of spent lithium-ion batteries, *Energy Reports* 9 (2023) 6362–6395.

**40.** C.K. Gupta, Chemical metallurgy : principles and practice, (2003) 811.

**41.** J. Kang, G. Senanayake, J. Sohn, S.M. Shin, Recovery of cobalt sulfate from spent lithium ion batteries by reductive leaching and solvent extraction with Cyanex 272, *Hydrometallurgy* 100 (2010) 168–171.

**42.** A. Chernyaev, J. Zhang, S. Seisko, M. Louhi-Kultanen, M. Lundström, $Fe^{3+}$ and $Al^{3+}$ removal by phosphate and hydroxide precipitation from synthetic NMC Li-ion battery leach solution, *Sci. Rep.* 13 (2023) 1–12.

**43.** Y. Zou, A. Chernyaev, S. Seisko, J. Sainio, M. Lundström, Removal of iron and aluminum from hydrometallurgical NMC-LFP recycling process through precipitation, *Miner. Eng.* 218 (2024) 109037.

**44.** F.E. Furcas, B. Lothenbach, O.B. Isgor, S. Mundra, Z. Zhang, U.M. Angst, Solubility and speciation of iron in cementitious systems, *Cem. Concr. Res.* 151 (2022) 106620.

**45.** W. Stumm, G.F. Lee, Oxygenation of Ferrous Iron, *Ind. Eng. Chem.* 53 (2002) 143–146.

**46.** S.M. Park, S.Y. Shin, J.S. Yang, S.W. Ji, K. Baek, Selective Recovery of Dissolved Metals from Mine Drainage Using Electrochemical Reactions, *Electrochim. Acta* 181 (2015) 248–254.

**47.** K. Binnemans, P.T. Jones, The Twelve Principles of Circular Hydrometallurgy, *Journal of Sustainable Metallurgy* 9 (2022) 1–25.

**48.** E.C. Gugua, C.O. Ujah, C.O. Asadu, D.V. Von Kallon, B.N. Ekwueme, Electroplating in the modern era, improvements and challenges: A review, *Hybrid Advances* 7 (2024) 100286.

**49.** P. Venkatesan, Z.H.I. Sun, J. Sietsma, Y. Yang, An environmentally friendly electro-oxidative approach to recover valuable elements from NdFeB magnet waste, *Sep. Purif. Technol.* 191 (2018) 384–391.

**50.** E. Viollier, P.W. Inglett, K. Hunter, A.N. Roychoudhury, P. Van Cappellen, The ferrozine method revisited: Fe(II)/Fe(III) determination in natural waters, *Applied Geochemistry* 15 (2000) 785–790.

**51.** J.J.M.M. van de Ven, P.J. Teeuwisse, R.W.A. Hendrikx, Y. Yang, S.T. Abrahami, Data underlying the publication: Simultaneous Recycling of Spent $LiFePO_4$ and $LiNi_xMn_yCo_zO_2$ Li-Ion Batteries Under Mild Leaching Conditions, (2025).

**52.** N. Vieceli, P. Benjamasutin, R. Promphan, P. Hellström, M. Paulsson, M. Petranikova, Recycling of Lithium-Ion Batteries: Effect of Hydrogen Peroxide and a Dosing Method on the Leaching of LCO, NMC Oxides, and Industrial Black Mass, *ACS Sustain. Chem. Eng.* (2023).

**53.** S. Goldstein, D. Meyerstein, G. Czapski, The Fenton reagents, *Free Radic. Biol. Med.* 15 (1993) 435–445.

**54.** M. Weller, T. Overton, J. Rourke, F. Armstrong, Inorganic Chemistry, 6th ed., Oxford University Press, Oxford, 2014.

**55.** H. Wang, B. Friedrich, Development of a Highly Efficient Hydrometallurgical Recycling Process for Automotive Li–Ion Batteries, *Journal of Sustainable Metallurgy* 1 (2015) 168–178.

**56.** G.P. Demopoulos, Aqueous precipitation and crystallization for the production of particulate solids with desired properties, *Hydrometallurgy* 96 (2009) 199–214.

**57.** T. Vander Hoogerstraete, B. Blanpain, T. Van Gerven, K. Binnemans, From NdFeB magnets towards the rare-earth oxides: a recycling process consuming only oxalic acid, *RSC Adv.* 4 (2014) 64099–64111.

**58.** R.M. Cornell, U. Schwertmann, The Iron Oxides: Structure, Properties, Reactions, Occurences and Uses, wiley, 2004.

**59.** A. Porvali, A. Chernyaev, S. Shukla, M. Lundström, Lithium ion battery active material dissolution kinetics in Fe(II)/Fe(III) catalyzed Cu-$H_2SO_4$ leaching system, *Sep. Purif. Technol.* 236 (2020) 116305.

*Healthy scepticism is the basis of all accurate observation.*

Arthur Conan Doyle - *The Vital Message* - (1919)

# 6

# Chapter 6

## Influence of Lixiviant on Recycling of Industrial LFP- & NMC-type Li-ion Battery Waste

In Chapter 5, we demonstrated that combining selective precipitation and electrochemical purification effectively removes most impurities from the PLS. Cu was removed by electro-deposition, while Fe was removed via electro-oxidation and subsequent precipitation. However, precipitation by pH increase still resulted in coprecipitation of remaining Fe, Al, and Cu, with Ni, Co, and Mn despite electrochemical purification (0.1 – 0.6% total impurities). Hence, there is a need for further research to develop improved strategies for impurity removal.

Chapter 6 explores the effect of the lixiviant used to dissolve industrial LFP- and NMC-type black mass on leaching performance, electrochemical purification and selective precipitation of Ni, Co, and Mn. Three different mineral acids are studied: $H_2SO_4$, $H_3PO_4$, and HCl under the same conditions as in Chapter 5, showing complete dissolution of Li, Ni, Co, and Mn under the applied conditions of 1 mol/L acid and 50°C is only achieved in $H_2SO_4$, whereas HCl and $H_3PO_4$ results in average leaching efficiencies of 71% and 58%, respectively. The pH of each PLS is then increased incrementally to assess the effectiveness of selective precipitation to separate Cu, Fe and Al from Ni, Co, and Mn, leaving Li behind in solution. Results indicate major coprecipitation of all elements except Li in all three lixiviant types without additional purification. To study the performance of electrochemical purification for Fe and Cu removal, the PLS was adjusted to pH 3.5 ($H_3PO_4$) or 4 ($H_2SO_4$, HCl) followed by two-step electrochemical purification, after which the pH of the resulting solution is increased further to precipitate any remaining Fe, Al, and Cu separately from Ni, Co, and Mn, resulting in improved separation in all three lixiviant types. This provides crucial insights on the performance of selective precipitation and electrochemical purification as a function of the anions present in solution. $H_2SO_4$ is shown to be the most effective overall, combining high leaching efficiency with good electrochemical purification, resulting in Ni, Co, and Mn precipitates containing merely 0.1% - 0.6% Fe, Al, and Cu in total.

---

In preparation for journal submission:
van de Ven, J. J. M. M., Teeuwisse, P. J., Yang, Y., & Abrahami, S. T., Influence of Lixiviant type on Recycling of Industrial LFP-and NMC-type Li-ion Battery Waste

## 6.1. INTRODUCTION

Within our daily lives, lithium-ion batteries (LIB) are widely applied for electricity storage. Moreover, they are essential for the energy transition, since they are used in stationary energy storage and electric vehicles (EVs) [1]. These types of batteries rely on chemical elements, such as Co, Mn and Li, which are classified as critical raw materials (CRMs) by the EU [2,3]. They are present in the form of oxides, such as $LiNi_xMn_yCo_zO_2$ (NMC) or $LiCoO_2$ (LCO), in the cathode, resulting in their name *cathode active materials* (CAMs) [4]. The supply of CRMs in these CAMs is currently under pressure, since they are high in demand, associated with geopolitical concerns while being crucial for the European economy [5–7]. Additionally, the global market for LiBs is projected to grow significantly in the coming years, which will drive the demand for those CRMs even further [8]. As LiBs manufacturing remain predominantly concentrated in China, most countries will continue to rely on imports [9]. Given these trends, increasing the recycling capacity within the EU will be crucial to meet future demands and increase supply resilience [10].

Hydrometallurgy is becoming the preferred option for LiB-recycling, as it can recover high purity materials by making use of aqueous or non-aqueous solutions to selectively dissolve and extract chemical elements [11,12]. After prior shredding and other mechanical preparation steps, the fine fraction of LIB waste called black mass (BM) is subjected to leaching, which aims to dissolve Li, Ni, Co, and Mn, while leaving impurities such as graphite, Fe, Al, and Cu behind [13–15]. Over the past years, many studies were conducted on this dissolution step using mineral acids such as HCl [16], $H_2SO_4$ [17,18] and $HNO_3$ [19], as well as organic acids including citric acid [20,21], acetic acid [22,23], and oxalic acid [24]. Although the general consensus is that acid concentration, time, temperature, and stirring speed positively influence leaching efficiency, the effect of the anion from the lixiviant further in the recycling process is seldomly considered.

Many of these studies also showed that apart from acids, reducing conditions are necessary in order to effectively dissolve LiB-waste, resulting in the use of reducing agents such as $H_2O_2$ [17,25–27], $Na_2S_2O_5$ [28,29] or ascorbic acid [30] to enhance the dissolution of Ni, Co, and Mn. However, the need for reducing agents will increase the environmental footprint of said recycling processes. Hence, the replacement of a reducing agent by a waste cathode material, $LiFePO_4$, was reported in more recent literature as well as in Chapter 4 and 5 of this dissertation, which showed that the Fe(II) present in LFP can effectively reduce Ni, Co, and Mn from NMC-type LiB waste [25,31]. However, simultaneous leaching of industrially pre-treated LFP and NMC results in a pregnant leach solution (PLS) with increased Cu, Al, and especially Fe content [25,32,33]. As a result, additional purification steps are required to enable

high-purity recovery of the target elements as battery precursors, which usually need at least 99.5% purity [34].

A relatively straight forward and widely applied purification technique is selective precipitation, which uses chemical agents to manipulate the solubility of the target elements [11,12]. Literature reports the use of oxalic acid to precipitate Ni or Co [35,36], NaOH to precipitate Fe as $Fe(OH)_3$ [36], $KMnO_4$ to precipitate $Mn^{2+}$ as $Mn_2O_3$ and $MnO_2$ [36], or $Na_3PO_4$ to precipitate Li as $Li_3PO_3$[36]. Nayl et al.[37] precipitated Mn and Ni with a $Na_2CO_3$ solution resulting in $MnCO_3$ and $NiCO_3$, but prior solvent extraction was necessary to remove Fe, Al, and Cu, in order to reach 99.7% and 99.4% product purity, respectively. Similarly, Co was precipitated with NaOH, leading to $Co(OH)_2$ with >99% purity, while Li was retrieved as a carbonate, with a 99.6% purity. Lastly, Wang et Al. [38] explored possible separation of Fe, Al, and Cu, as well as Li, Ni, Co, and Mn, by NaOH addition. They found that while Fe, Al, and Cu can be nearly completely precipitated at pH 5.8, it comes at the expense of 18% Ni, Co, and Mn loss on average, whereas precipitation with $Na_2CO_3$ instead slightly decreased this loss to 15%. In industrial LiB recycling, precipitation steps are also widely applied, such as in the Accurec and Recupyl Valibat processes to precipitate $Li_2CO_3$, and in the Battery Resources process to precipitate Cu, Al and Fe with NaOH [13].

These results show that precipitation can be an effective way to recover Li, Ni, Co, and Mn into battery precursors, since purities of over 99.5% have been reported. However, the need for additional reagents increases the carbon footprint of a recycling process and results in large amounts of by-products, of which $Na_2SO_4$ is the most prevalent example. It is a product consisting of the lixiviant anion, often from $H_2SO_4$, which is later neutralized with NaOH [39]. Additionally, selective precipitation usually needs to be combined with an additional prior purification step such as solvent extraction, or needs to be targeted at only one of the elements in solution such as in the case of Mn precipitation by oxidation, or in the case of Li by addition of phosphate anions to precipitate $Li_3PO_4$, to consistently reach the required purity [36,37]. Since anionic species, such as phosphates or carbonates, are often used to selectively remove cations of interest, such has Li, Ni, Co, or Mn, researching the effect of the anionic species in a PLS, originating from the lixiviant, on subsequent precipitation steps is a major point of interest.

An alternative option to separate impurities from target metals without the need for additional chemicals are electrochemical processes, which allow carrying out redox-reactions without adding any reducing or oxidizing agents [11,12,40]. A well-known example of this is the electrodeposition of Cu, which has been widely used in the recycling of e-waste, resulting in pure Cu products [41,42]. Hence, we explore its applicability in the context of LiB recycling, similarly to Chapter 5 of this dissertation,

in which two separate electrochemical purification steps succeeded in removal of Cu through deposition in metallic form, and oxidation of $Fe^{2+}$ to $Fe^{3+}$ followed by iron precipitation.

In this chapter we aim to combine selective precipitation, electro-oxidation and electro-reduction for the purification of the PLS as demonstrated in Chapter 5 of this thesis, while investigating the influence of the present anionic species. This is done by leaching LFP and NMC BM with three different acids: HCl, $H_2SO_4$, or $H_3PO_4$. Subsequently, without any electrochemical purification, the pH of the resulting PLS is incrementally increased to achieve selective precipitation, as described in Chapter 5. This provides a first insight into how the anions in the solution affect precipitation behaviour of Fe, Al, Cu, Li, Ni, Co, and Mn. In the following set of experiments, the three types of untreated PLS are adjusted to pH 4, (3.5 for $H_3PO_4$), followed by two electrochemical purification steps that aim to remove the Cu by electrodeposition, as well as to oxidise the Fe and decrease its solubility, followed again by selective precipitation. This experimental approach leads to fundamental knowledge on the anionic effects on the following electrochemical purification, as well as resulting precipitation products, in LiB recycling. Because of the industrial nature of the BM, it also shows the potential of these strategies in industrial context.

## 6.2. MATERIALS & METHODS

### 6.2.1. Battery Materials

The materials used in this research were kindly provided by industrial partners. They underwent mechanical pre-treatment steps without pyrolysis before arriving at the lab, including shredding, sieving, magnetic separation, and grinding. Two types of materials were used in the experiments: 1) NMC-type BM and 2) LFP-type BM. The NMC-type BM, called ‘NMC BM’ was used as received. The ‘LFP-BM’ was sieved through a 500 µm sieve before use to increase the cathode active material (CAM) content. Due to their reactivity and heterogeneity, each BM was characterized three times at the beginning of the study, as well as regularly during the period of the experiments to ensure consistency. In Table 6.1, the composition of the BMs as analysed in the beginning of the experiments is listed.

*Table 6.1: Composition (wt.%) of BMs used in this study as analysed by ICP-OES after aqua regia digestion. Other contains oxygen, graphite, and organic impurities.*

| Material Name | Li | Co | Ni | Mn | Al | Fe | Cu | $PO_4^{3-}$ | Other |
|---|---|---|---|---|---|---|---|---|---|
| NMC BM | 3.1 | 6.4 | 16.3 | 6.3 | 0.5 | 0.9 | 0.9 | - | 65.5 |
| LFP BM | 2.1 | - | - | - | 1.8 | 17.5 | 1.8 | 32.6 | 44.2 |

### 6.2.2. Characterization Techniques

To determine the elemental composition of the BMs, the same procedure as described in Chapter 5 was applied.

ICP-OES characterization was carried out with a Spectro Arcos-EOP-device with Modified Lichte nebulizer and mini cyclonic spray chamber. Calibration samples were made using 1000 mg/L ICP standards from each corresponding element.

X-ray diffraction (XRD) analysis was applied to investigate the present phases on the deposits formed during the electrochemical experiments. The deposits were scraped off the electrodes, after which they were deposited on a Si510 zero-background wafer. The analysis was carried out using a Bruker D8 Advance diffractometer with Bragg-Brentano geometry, a graphite monochromator and a Vantec position sensitive detector. Co Kα radiation of 40 kV and 4 mA was used. The 2θ range was 10 - 90°, with a step size of 0.035°, 1s per step. The data was analysed with the Bruker software DiffracSuite.EVA vs 7.3.



### 6.2.3. Leaching

Three leaching experiments were performed to compare the effectiveness of three lixiviant types, and to prepare solutions suited for further purification. Leaching was performed in a triple necked 1L round bottom flask placed in a heating mantle on a heating and stirring plate, similarly to Chapter 5. The lixiviants consisted of 1 mol/L solutions of $H_2SO_4$ (95.0 – 97.0 %, Sigma-Aldrich), HCl (37%, Merck), or $H_3PO_4$ (85%, EMSURE), with a total volume of 500 mL. The leaching experiments were carried out at a stirring speed of 600 rpm for 2 hours. At the start of the leaching process, the NMC BM was added with a solid-to-liquid (S/L) ratio of 57.6 g/L. Subsequently, LFP BM was added stepwise in increments of 21.7 g/L each after 30, 60, and 90 min, resulting in a total S/L of 65.2 g/L. This results in a 0.75 molar ratio of Fe in the LFP BM to Ni, Co, and Mn total in the NMC BM.

During leaching, the lixiviant was periodically sampled to monitor the leaching over time. 1.5mL of slurry was collected every 15 min and filtered through a 0.45 µm PTFE syringe filter (Fisherbrand). After leaching, the slurry was filtered twice, once through a vacuum filtration with a Büchner funnel and Whatmann 113 filter (90 mm diameter, 30 µm pore size), and once through a membrane filtration setup with a Cytiva ME 25 membrane filter with 0.45 µm pore size. The residues were dried at

55 °C for 8 hours to remove excess water before analysis through dissolution and ICP-OES, while the pregnant leach solution (PLS) was collected for further study.

To compare the leaching processes with each other, the leaching efficiencies ($\eta_L$) of the elements of interest were calculated according to Eq. 6.1. The initial mass of element x in the feed ($m^x_f$) was determined by ICP-OES analysis of the BM according to the method described in section 6.1.2. $m^x_{PLS}$ represents the mass of element x present in the PLS as also determined by ICP-OES analysis of the solution.

$$\eta_L = \frac{m^x_{PLS}}{m^x_f} * 100\% \tag{6.1}$$

### 6.2.4. Selective Precipitation

After leaching, selective precipitation by pH adjustment was applied to selectively remove Fe, Al, and Cu from solution, as well as to recover Ni, Co, and Mn from the PLS, leaving Li behind. The pH increase was achieved by adding a 2 mol/L LiOH solution (Monohydrate, ≥99%, Fischer Scientific), as described in Chapter 5. Once the target pH was reached, the suspension (precipitates) was filtered under vacuum using a Büchner funnel and Whatmann 542 filter paper (90mm diameter, 2.7 µm pore size). The solution volume before and after each pH adjustment was recorded to account for dilution when calculating elemental concentrations.

The precipitates acquired after pH adjustments were dried for 8 hours at 55°C. This was followed by dissolving 0.1g of each solid in 5 wt.% $HNO_3$, sometimes assisted by addition of $H_2O_2$ (35% solution, Thermo Scientific). A 100 mL volumetric flask was used for volume determination.

### 6.2.5. Electrochemical Purification Techniques

In this research, two types of electrochemical purification steps were carried out: Cu deposition and Fe oxidation. All electrochemical tests were conducted using a triple-electrode setup with an Ag/AgCl as reference electrode and a Parstat 4000 (Ametek, UK) potentiostat controlled with the Versastudio software, as visualised and described in Chapter 5 (Figs. C.1 and C.2).

The Cu plating step was designed to selectively remove Cu from the solution Chronopotentiometry was performed by applying a constant current of 0.2A (14.3 $mA/cm^2$) for 1 hour, while magnetically stirring at 400 rpm. A stainless-steel plate of 4 by 3.5 cm was used as the cathode (and working electrode), while a 0.5 by 3.5 cm Pt anode was used as anode (and counter electrode).

The Fe oxidation step was designed to oxidize all the remaining $Fe^{2+}$ in the solution into $Fe^{3+}$, which subsequently precipitates at lower pH. A Pt basket was

used as an anode and working electrode, while a Pt wire was used as a cathode and counter electrode. Chronopotentiometry was used to apply a current of 1.2A (21.8 mA/cm$^2$) for 2 hours, while magnetically stirring at 400 rpm.

## 6.3. RESULTS & DISCUSSION

This study compares three leaching approaches, in which a combination of NMC and LFP BM are leached in three different lixiviants of 1 mol/L: $H_2SO_4$ (same as Chapter 5), HCl, and $H_3PO_4$. This results in three solutions containing Li, Ni, Co, Mn, Fe, Al, Cu, and $PO_4^{3-}$, in addition to the anionic species resulting from either $H_2SO_4$ or HCl. After the initial leaching step, two different recycling routes are followed: one direct precipitation approach, which opts for separation of target elements (Li, Ni, Co, and Mn) from impurities (Fe, Al, and Cu) only through selective precipitation by pH adjustment, and one electrochemical approach, which involves raising the PLS to pH 4 (3.5 for $H_3PO_4$) to remove Fe and Al, followed by Cu deposition and Fe oxidation before subsequent selective Ni, Co, and Mn precipitation, leaving Li in solution. Both approaches are schematically visualized in Fig. 6.1.



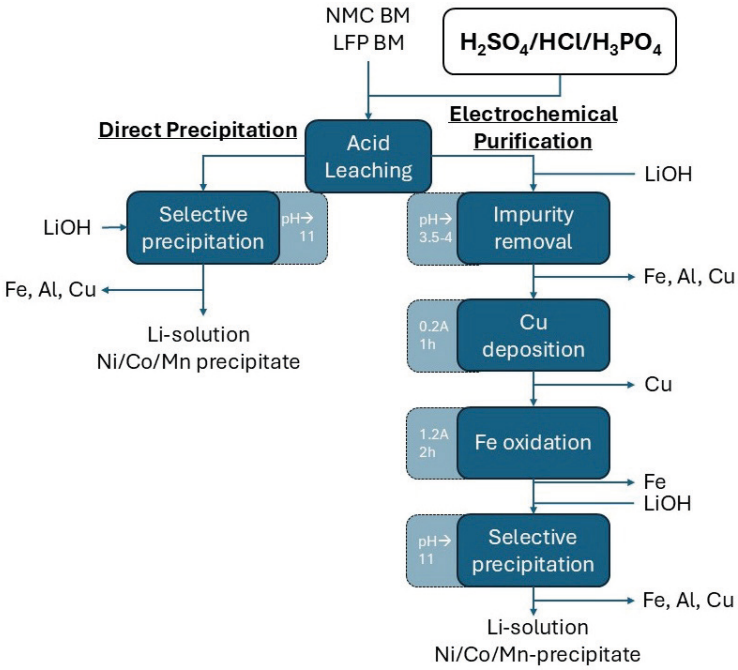


*Figure 6.1: Overview of the two parallelly investigated purification approaches. Leaching was carried out in three lixiviants of 1 mol/L acid: $H_2SO_4$, HCl, or $H_3PO_4$.*

### 6.3.1. Comparison of Simultaneous Leaching of NMC & LFP in $H_2SO_4$, HCl or $H_3PO_4$

Previous studies have shown that $H_2SO_4$, HCl, and $H_3PO_4$ are all capable of dissolving Ni, Co, Mn, and Li from LiB-waste. In this work, these acids are applied in the simultaneous leaching of two BMs: NMC and LFP. This is achieved through a stepwise process in which LFP BM is added in three steps. A comparison of the leaching efficiencies of the three different acids under the same conditions (1 mol/L acid, 2h, 50°C) can be seen in Fig. 6.2.

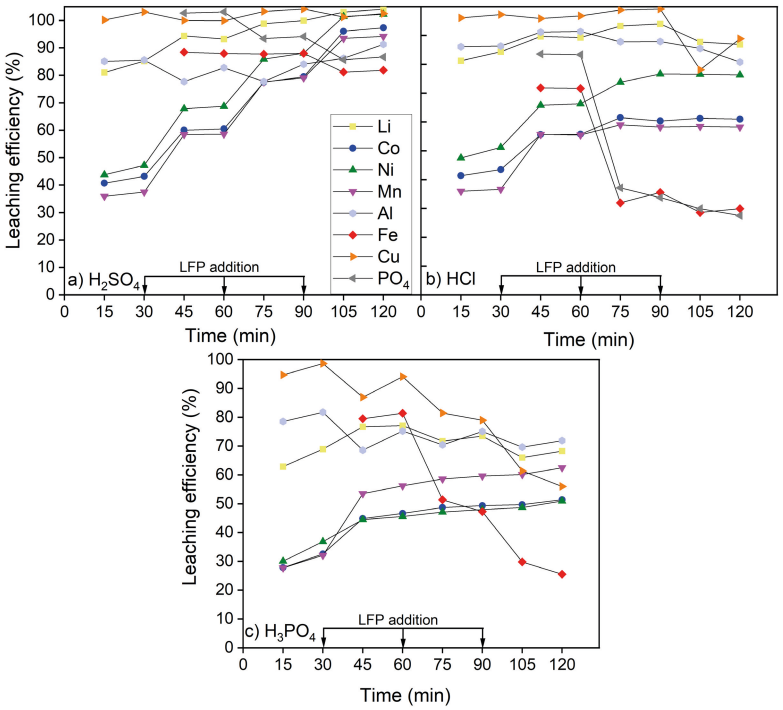


*Figure. 6.2: Influence of acid type of the leaching efficiency of Li, Ni, Co, Mn, Cu, Fe, Al, and $PO_4^{3-}$ from NMC BM (57.6 g/L) and LFP BM (65.2 g/L) over time. Lixiviant: $H_2SO_4$ (a), HCl (b), $H_3PO_4$ (c).*

The first graph (Fig. 6.2a) shows the leaching efficiency of the elements from the LFP and NMC BMs over time, similarly to Fig. 5.3a in Chapter 5, in the 1 mol/L $H_2SO_4$ lixiviant. Fig 6.2a, shows that after 30 min of leaching, on average 40% of the Ni, Co, and Mn, and 81% of the Li are dissolved. Cu is completely dissolved at this point, followed by 86% of the Al. The three LFP BM additions are all followed by a consistent increase in the leaching efficiencies of Ni, Co, and Mn, which eventually reach 97% on average. Li is completely leached after 2h, even though

its feed concentration increases from 1.7 g/L at the start, to 2.9 g/L at 90 min. Cu is eventually completely dissolved, together with 91% of Al. The Fe and $PO_4$, which mainly originate from the LFP BM, reach a leaching efficiency of 85% on average.

These results are consistent with our previous findings [32] and well documented in the literature [31,43]. Slight differences (of 4% – 8%) shown here are a result of the inherent heterogeneous nature and reactivity of the BMs, which were characterized again for this set of experiments. The moderate leaching of Ni, Co, and Mn after 30 min originates from the limited reducing capability of the lixiviant and the high oxidation states of these metals in battery waste [25,44,45]. Hence, external reducing agents improve their dissolution drastically (Eq. 6.2), as indicated by the immediate increases of Ni, Co, and Mn leaching seen after the addition of LFP BM portions. The LFP dissolves according to Eq 6.3, after which the $Fe^{2+}$ that is hence introduced can act as reducing agent as is shown in Eq. 6.4, causing the increase of the leaching efficiencies of Ni, Co, and Mn that are seen in Fig. 6.2a. Additionally, both of the solid feed materials contain Cu and Al impurities. These two metals dissolve well in the presence of $Fe^{3+}$, as described in Eqs. 6.5 and 6.6, forming more $Fe^{2+}$, and hence lead to a high leaching efficiency of Ni, Co, and Mn, but come with the drawback that Cu and Al also need to be removed from the resulting pregnant leach solution (PLS).



$$3LiNi_{1/3}Mn_{1/3}Co_{1/3}O_{2(s)} + 12H^{+}_{(aq)} + 3e^{-} \rightarrow 3Li^{+}_{(aq)} + Ni^{2+}_{(aq)} + Mn^{2+}_{(aq)} + Co^{2+}_{(aq)} + 6H_2O_{(l)} \quad (6.2)$$

$$LiFePO_{4(s)} + 2H^{+}_{(aq)} \rightarrow Li^{+}_{(aq)} + Fe^{2+}_{(aq)} + H_2PO^{-}_{4(aq)} \quad (6.3)$$

$$Fe^{2+}_{(aq)} \rightarrow Fe^{3+}_{(aq)} + e^{-} \quad (6.4)$$

$$Al_{(s)} + 3Fe^{3+}_{(aq)} \rightarrow Al^{3+}_{(aq)} + 3Fe^{2+}_{(aq)} \quad (6.5)$$

$$Cu_{(s)} + 2Fe^{3+}_{(aq)} \rightarrow Cu^{2+}_{(aq)} + 2Fe^{2+}_{(aq)} \quad (6.6)$$

Fig. 6.2b shows the results of the leaching process using 1 mol/L HCl. The results are similar to $H_2SO_4$ in the first 30 min, as about 42% of the Ni, Co, and Mn are leached, while the Li leached for 84%. At this point, the Cu and Al are dissolved for 97% and 86%, respectively. The addition of LFP BM at 30 min increases the leaching efficiency of Ni, Co, and Mn to 59% after an additional 30 min, similar to $H_2SO_4$, while further additions of LFP BM at 60 and 90 min do not provide similar improvements. While the second addition still increases the leaching efficiency of Ni, Co, and Mn by approx. 6%, the third addition shows to have little to no influence. This change in the observed trend is accompanied by a drastic decrease in the

dissolution of Fe and $PO_4^{3-}$, from 87% after 30 min to 28% on average after 2h. The Cu and Al are only slightly affected during the entire leaching procedure, with final leaching efficiencies of 89% and 81%, respectively.

The differences for Ni, Co, Mn, Fe and $PO_4^{3-}$ in the HCl results compared to $H_2SO_4$ are likely the consequence of acid strength and redox capabilities. Table 6.2 contains the relevant acid dissociation constants ($pK_a$'s) for the lixiviants used in this work. HCl is the strongest acid of the three, but since it is a monoprotic acid and the molar concentration is the same compared to the $H_2SO_4$-case (1 mol/L), this results in limited capacity of the lixiviant to maintain low pH during leaching. This explains why the leaching of Fe and $PO_4^{3-}$ is rather low, as LFP consumes $H^+$ during dissolution according to Eq. 6.3, and as predicted by the pKa-values of $HPO_4^{2-}$ and $H_2PO_4^-$ in Table 6.2. Hence, LFP dissolution increases the pH, resulting in lower LFP solubility. Once LFP cannot dissolve further, the reduction of Ni, Co, and Mn (Eq. 6.2) can no longer proceed. This is confirmed by the final pH of the PLS which is 2.09 in the HCl system, which is significantly higher compared to the $H_2SO_4$ system (1.08). Furthermore, the oxygen that is present in NMC ($LiNi_xCo_yMn_zO_2$) can also no longer be converted into $H_2O$, since there is not enough $H^+$ present, hampering Ni, Co, Mn, and Li leaching even further.

*Table 6.2: Acid dissociation constants for the acids used in this work.*

| Acid | Dissociation constant (pKa)* [46] |
|---|---|
| $H_2SO_4$ | -2 |
| $HSO_4^-$ | 1.92 |
| HCl | -7 |
| $H_3PO_4$ | 2.12 |
| $H_2PO_4^-$ | 7.21 |
| $HPO_4^{2-}$ | 12.67 |

*Lower pKa is a result of higher acid dissociation and hence higher acidic strength

The final graph presented in Fig. 6.2c shows the leaching results for the 1 mol/L $H_3PO_4$-solution. Since the lixiviant itself contains a high concentration of $PO_4^{3-}$, this species is not reported in the results. In the first 30 min, $H_3PO_4$ shows the lowest leaching performance of the three tested acids, which is logical due to it being the weakest acid, with a $pKa_1$ value of 2.12. Ni, Co, and Mn are leached for 32-37%, while Li is leached for 69% and Cu and Al dissolve for 82% and 99%, respectively. The first batch of LFP BM, added after 30 min, dissolves effectively, with the leaching efficiency of Fe reaching 81% and causes increases of the leaching to 46% for Ni, 47% for Co, and 56% for Mn, while later additions of LFP BM do not cause significant further increases. These later additions also decrease the leaching efficiency of Fe, indicating poor dissolution of LFP as well as re-precipitation of

$FePO_4$, leading to a final Fe leaching of 26%. The cause of these observations is that although $H_3PO_4$ is triprotic, resulting in more $H^+$ available for donation to other species during the leaching process, the lower acidic strength compared to HCl and $H_2SO_4$ likely results in a lower dissolution rate of LFP (Eq. 6.3). Consequently, the oxidation of $Fe^{2+}$ (Eq. 6.4) is also slower, resulting in lower reduction and dissolution rate of NMC BM (Eq. 6.2). At the end of the leaching procedure, the pH was measured to be 2.3, the highest of all experiments, supporting this theory. Also, because presumably most of the formed $Fe^{3+}$ precipitates as $FePO_4$ at this pH, the Cu and Al have fewer opportunities to reduce $Fe^{3+}$ back to $Fe^{2+}$ (Eqs. 6.5 and 6.6), leading to their lower leaching efficiency.

Overall, under the same conditions, $H_2SO_4$ results in the most complete leaching. This is because it is a strong acid, while also being diprotic. However, this also comes with the drawback of dissolving the most Fe, Al, and Cu impurities. To investigate the potential of selective precipitation to remove Cu, Al, and Fe from the target elements, Li, Ni, Co, and Mn, all three PLS's are subjected to a controlled pH increase.

### 6.3.2. Comparison of Direct Selective Precipitation after Leaching in $H_2SO_4$, HCl or $H_3PO_4$



To investigate the effect of the lixiviant on precipitation of Li, Ni, Co, and Mn, the three PLS samples obtained in the previous step (section 6.3.1) were subjected to selective precipitation through stepwise pH adjustment by a 2 mol/L LiOH solution. The remaining concentration of each element present in the PLS at the pH intervals are presented in Fig. 6.2.

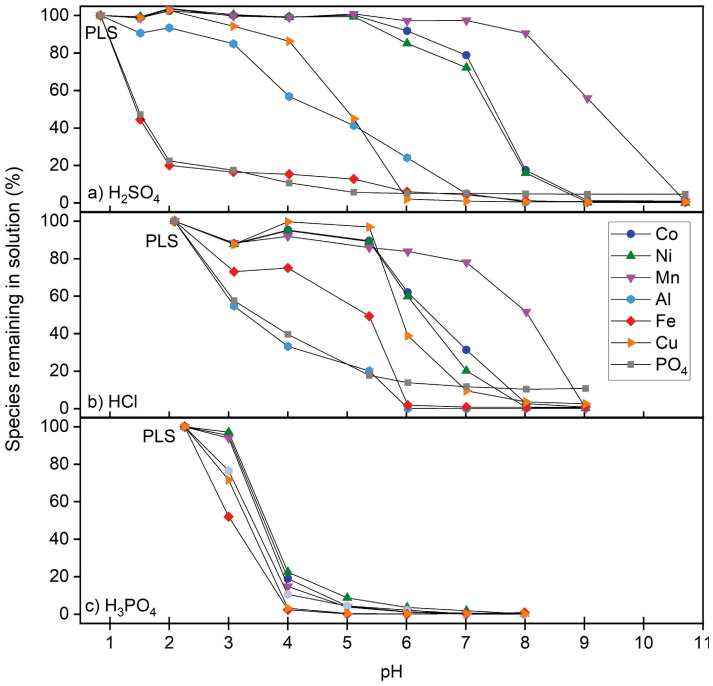


*Figure. 6.3: Selective precipitation of Li, Ni, Co, Mn, Fe, Al, Cu, and $PO_4^{3-}$ from the PLS, obtained after leaching with lixiviant $H_2SO_4$ (a, remeasured experiment from Chapter 5 of this thesis), HCl (b), and $H_3PO_4$ (c).*

In Fig. 6.3a of the graph, the precipitation results for the $H_2SO_4$-based PLS are shown, which contain remeasurements of the results in Fig. 5.3a (and hence the slightly differs). The precipitation can still be divided in three stages: pH 1-2, pH 3-5, and pH 6-10.5. Raising the pH of the PLS from 0.8 to 2.0 resulted in the in precipitation of 78% of Fe and $PO_4^{3-}$. When the pH is further increased to 5.1, 57% of the Cu and Al precipitates without any significant loss of target elements. In the last phase, between pH 6.0 and 10.5, the remaining concentrations of Co and Ni decreased to 16% at pH 8.0. Mn is more persistent in the solution, with approx. 90% remaining dissolved at this pH. Further increase to pH 10.5 results in complete precipitation of all the remaining Ni, Co, and Mn.

These results are in good agreement with earlier studies [35,36,38] and indicate that only rough separation can be achieved through direct precipitation via pH increase. The $Fe^{3+}$ precipitates at pH 2 due to its low solubility, whereas any Fe present above this pH is likely in the $Fe^{2+}$ state, as noted by previous research [31,32,38,47], and contaminates precipitates formed at higher pH. In addition to Fe, Al, and Cu also act as contaminants, since their precipitation overlaps with that of $FePO_4$,

as well as with the desired Ni, Co, and Mn compounds. In the previous chapter of this thesis, as well as in literature, it was shown that the cross contamination during precipitation is a result of adsorption of foreign elements on the surface of the formed amorphous solids [48], emphasizing the need for additional purification for the complete removal of Cu, Al, and Fe before precipitation of any Ni, Co, and Mn compounds.

In Fig. 6.3b the remaining elemental concentrations as a function of pH is shown for the HCl leaching system. Here, we cannot make the same distinction in terms of pH ranges as in the $H_2SO_4$-based system, but there are still 2 pH regions that can be differentiated. In the region between pH 2.1 and 5.4, Fe, $PO_4^{3-}$, and Al are the main precipitating species, which at pH 5.4 remain for 49%, 18%, and 20%, respectively. Unlike the $H_2SO_4$ system, Al and $PO_4^{3-}$ follow the same trend, rather than Fe and $PO_4^{3-}$. From pH 5.4 onwards, the remaining elements precipitate, starting with Cu, Co and Ni and eventually Mn. The remaining concentration of Co and Ni at pH 8.0 are 3% and 0.5%, respectively, whereas only 4% of Cu remains. For Mn to be removed, the pH needs to be increased to 9.0, resulting in its complete removal.

In comparison with the $H_2SO_4$-system, coprecipitation of target elements and impurities has increased, consequently resulting in lower selectivity. Al precipitates as a phosphate at low pH, whereas Fe is more soluble in this system. This could be a result of the low total Fe content in the PLS, which in turn is a result of the lower acidity of the lixiviant. The Fe in solution is largely in the more soluble $Fe^{2+}$ state, leaving a significant amount of $PO_4^{3-}$ that can precipitate with Al. As a result, the Fe and Cu only precipitate at pH 6.0, which coincides with Co and Ni precipitation, causing significant contamination. Moreover, most of the Co and Ni already precipitate by reaching pH 7.0, instead of pH 8.0 as in the $H_2SO_4$ system, while the Mn precipitates at pH 9.0 instead of 10.5, further increasing the coprecipitation with Cu and Fe.

Lastly, the precipitation study of the $H_3PO_4$-based leaching system is shown in Fig. 6.3 c. Although 50% Fe, 28% Cu, and 23% Al precipitate at pH 3 with only 3% loss of target elements on average, nearly all of the remaining Cu, Al, and Fe coprecipitate with the Ni, Co, and Mn between pH 3.0 and 5.0. Further increase to pH 7.0 leads to near complete removal of all these elements, whereas increase to pH 8.0 caused the ions from lixiviant and pH adjustment solution to precipitate together as $Li_3PO_4$, as is shown by the steep Li decrease at this point (not shown). Although the possibility of $Li_3PO_4$ recovery could be attractive, the rest of these observations make the $H_3PO_4$-based system rather inefficient, offering little separation between the desired elements and contaminants. This is not surprising, since the limited solubility of phosphates in general is a well-known phenomenon [49–52].

Overall, these results show that selective precipitation does not result in precipitates of sufficient purity without a suitable solution purification strategy in any of the tested lixiviants. While $Fe^{3+}$ can be reasonably separated in the presence of phosphates by pH adjustment, the precipitation of Cu and Al overlaps with that of Ni, Co, and Mn in all systems. This overlap is the smallest for the $H_2SO_4$-system, and the largest for the $H_3PO_4$-system. Hence, a different approach is required to remove impurities before the recovery of Ni, Co, and Mn by precipitation. Considering the goal of minimizing chemical consumption during further recycling steps, electrochemical purification, as described in Chapter 5, is a promising sustainable approach [53]. Hence, a three step process involving pH adjustment, Cu deposition, and Fe oxidation is applied to the three PLS types obtained in section 6.2.1.

### 6.3.3. Electrochemical Purification of the $H_2SO_4$, HCl & $H_3PO_4$-based PLS Systems

The electrochemical removal of Cu and Fe is well described in the literature, yet it is more complex in the context of lithium-ion battery recycling. When these two elements are present in the leaching solution, they can interfere in each other's electro-purification, as is explained in detail in Chapter 5. In short, $Fe^{3+}$ that is formed at the anode could react with the Cu that is reduced and deposited at the cathode, similar to the reaction in Eq. 6.6 that partially drives leaching [32,54]. To overcome this reversible reaction during purification, a stepwise treatment process was developed.

As first purification step, the pH of the PLS is increased to 4 for the $H_2SO_4$ and HCl systems, and to 3.5 for the $H_3PO_4$ system, resulting in precipitation of the $Fe^{3+}$ and, hence, a lower interference with subsequent Cu electrodeposition. These pH values were selected based on the results in Fig. 6.2, showing that at pH 4 most of the target elements in the $H_3PO_4$-sytem will already precipitate, while in the other two systems part of the Fe, Al, and Cu can be removed with limited coprecipitation of target elements. The second purification step targets Cu removal by its electrodeposition on a steel cathode that is 8 times larger than the anode, enhancing Cu reduction. The third step aims to oxidise the remaining $Fe^{2+}$ to the less soluble $Fe^{3+}$ using a large anode (Pt basket) to cathode (Pt wire) surface area ratio (35:1). This configuration promotes Fe-oxidation at the anode while minimizing hydrogen evolution reaction (HER) at the cathode. Finally, the pH is increased incrementally to selectively remove the remaining Cu, Fe, and Al, as well as to recover the Ni, Co, and Mn as precipitates, while leaving Li in the solution. The concentrations of Li, Ni, Co, Mn, Cu, Al, Fe, and $PO_4^{3-}$ as a result of the operations are presented in Table 6.3.

*Table 6.3: Change in concentration of Li, Co, Ni, Mn, Al, Fe, Cu, and $PO_4^{3-}$ from leaching in $H_2SO_4$, HCl, or $H_3PO_4$, over the course of pH adjustment and electrochemical purification. Decreases in impurity concentration which are not result of dilution (volume increase is indicated after pH, as "V*x"), are highlighted in green, while analogue decreases of target elements are highlighted in blue, together with the percentage of species compared to the PLS between brackets.*

| | | Species concentration after recycling step (g/L) | | | | | | | |
|---|---|---|---|---|---|---|---|---|---|
| **pH** | **Recycling stage** | **Li** | **Co** | **Ni** | **Mn** | **Al** | **Fe** | **Cu** | **$PO_4^{3-}$** |
| | PLS $H_2SO_4$ | 3.08 | 3.63 | 10.05 | 3.57 | 1.35 | 9.99 | 1.77 | 18.65 |
| | Precipitation (V*1.41) | 5.47 | 2.52 (97%) | 7.02 (99%) | 2.41 (95%) | 0.48 (51%) | 0.68 (10%) | 0.70 (55%) | 0.94 (7%) |
| 4 | Cu deposition (1h, 0.2A) | 5.49 | 2.44 | 7.02 | 2.40 | 0.47 | 0.63 (9%) | 0.34 (27%) | 0.87 |
| | Fe oxidation (2h, 1.2A) | 5.65 | 2.52 | 7.25 | 2.40 | 0.48 | 0.51 (7%) | 0.35 | 0.71 (5%) |
| | PLS HCl | 2.57 | 2.31 | 7.50 | 2.22 | 1.24 | 3.44 | 1.59 | 6.25 |
| | Precipitation (V*1.04) | 2.84 | 2.07 (93%) | 6.70 (93%) | 1.92 (90%) | 0.39 (32%) | 2.43 (73%) | 1.49 (97%) | 2.33 (39%) |
| 4 | Cu deposition (1h, 0.2A) | 2.84 | 2.08 | 6.72 | 1.92 | 0.38 | 1.84 (56%) | 0.45 (29%) | 1.34 (22%) |
| | Fe oxidation (2h, 1.2A) | 2.89 | 2.05 | 6.73 | 1.41 (66%) | 0.38 | 0.29 (9%) | 0.44 | 0.61 (10%) |
| | PLS $H_3PO_4$ | 1.97 | 1.88 | 4.91 | 2.31 | 1.04 | 2.83 | 0.89 | - |
| | Precipitation (V*1.13) | 3.04 | 1.39 (83%) | 3.90 (90%) | 1.57 (77%) | 0.64 (69%) | 0.67 (27%) | 0.28 (35%) | - |
| 3.5 | Cu deposition (1h, 0.2A) | 3.06 | 1.30 | 3.80 | 1.49 | 0.60 | 0.20 (8%) | 0.13 (17%) | - |
| | Fe oxidation (2h, 1.2A) | 2.40 (65%) | 1.08 (73%) | 3.19 (61%) | 1.26 (61%) | 0.53 (58%) | 0.17 (7%) | 0.11 (14%) | - |

By adjusting the pH of the $H_2SO_4$ PLS to 4 and taking dilution into account, 49% Al, 90% Fe and 45% Cu precipitate, while the Ni, Co, and Mn stay in solution, indicating effective separation of Fe and reasonable removal of Cu and Al. During the 60 min of Cu deposition that follows, the Cu concentration decreases with 50% (0.34 g/L) compared to the pH adjusted solution, whereas the concentrations of Li, Ni, and Mn remain largely unaffected. XRD analysis reveals the formation of metallic Cu, $Cu_2O$, and a Fe-Co mixed hydroxide on the cathode, the latter being consistent with the slight Fe and Co removal seen after the Cu deposition step. While the Al concentration remains unchanged, the concentrations of Fe and $PO_4^{3-}$ exhibit a slight decline of approx. 7%. This indicates that Cu deposition is effective, is paired with some Fe and $PO_4$ precipitation but comes with a slight (3%) Co loss. In the subsequent Fe oxidation step, slight increases are observed in the concentration of Al, Cu, Li, Ni, and Co, which presumably are a result of water electrolysis and subsequent solution volume decrease (qualitatively observed), which for the case of Mn is compensated by its oxidation and precipitation on the anode, according to Eq 6.7. However, the Fe and $PO_4^{3-}$ contents decrease an additional 18% and 17%, respectively, on top of the 7% precipitation (per element) achieved during Cu deposition.

$$MnO_2 + 4H^+ + 2e^- \rightarrow Mn^{2+} + 2H_2O \left(E^0 = 1.23V\right) \tag{6.7}$$

Adjustment of the HCl PLS to pH 4 precipitates 68% Al, 27% Fe, and 2% Cu, at the expense of 7% Co, 7% Ni, and 10% Mn due to coprecipitation. Compared to the pH adjusted solution, Cu deposition removes a larger share of Cu (70%) compared to the $H_2SO_4$-system (50%), although the final Cu concentration is higher (0.45 g/L). This occurs simultaneously to precipitation of $FePO_4$, with the amount of Fe and $PO_4$ decreased by 24% and 43%, respectively. XRD analysis confirms the presence of metallic Cu and $Cu_2O$, as well as $Cu_2(OH)_3Cl$ on the cathode, with the latter resulting from CuCl formation in solution, followed by oxidation with $O_2$ and water [55]. Compared to the $H_2SO_4$-system, the HCl-system produces a cathodic Cu product of higher metallic purity, as XRD shows no presence of other elements. Just as in the $H_2SO_4$-system, the Li, Ni, Co, Mn, and Al concentrations remain unaffected, again indicating an effective Cu removal step. Subsequent Fe oxidation is effective as well, as Fe and $PO_4^{3-}$ removal is increasing from 24% to 88%, and 43% to 74%, respectively. However, this step also causes a 26% loss of Mn, likely resulting from oxidation according to Eq. 6.7 due to the high voltage at the anode, which is 1.9V on average though other elements remain unaffected.

Adjusting the $H_3PO_4$-system to pH 3.5 results in precipitation of 31% Al, 73% Fe and 65% Cu, at the expense of 16% Co, 10% Ni and 23% Mn being lost through

coprecipitation. The Cu deposition step removes 52% of Cu that remained in solution after pH adjustment, resulting in the highest Cu removal out of the three systems, alongside 70% of Fe. XRD analysis of the cathode products shows only metallic Cu, the purest of the three systems, while decrease of the Fe concentration indicates $FePO_4$ precipitation. The subsequent Fe oxidation produces a thick precipitate at the cathode, which is analysed to be $Li_3PO_4$, coprecipitated with amorphous hydroxides of Ni, Co, Mn, Fe, Al and Cu. Such precipitates can form as a result of hydrogen evolution at the cathode, which locally increases the pH, rendering this step unsuitable in the $H_3PO_4$-system. Therefore, extending the Cu deposition step could achieve complete Fe and Cu removal without the need for an additional Fe oxidation step.

These results emphasise that electrochemical Cu deposition and Fe oxidation are promising strategies for Cu and Fe removal from a PLS from recycled LiBs, as also concluded in Chapter 5 of this dissertation, although the current research shows that the effectiveness of these steps is strongly dependent on the choice of lixiviant. In a $H_2SO_4$-system, two separate steps are required to achieve removal of Cu and Fe, both of which are effective but take significant time to complete. In the HCl-system, Cu deposition removes a larger amount of Cu and simultaneously removes part of the Fe. Additional Fe electro-oxidation is prone to side reactions, resulting in insoluble $MnO_2$ due to the high potential. Cu deposition in the $H_3PO_4$-system is effective, with simultaneous removal of Fe, while the Fe oxidation step should be avoided due to side reactions of the target elements. With the strengths and weaknesses of electrochemical purification in these three lixiviants now established, it is of importance to address the quality of the products formed in the following precipitation step.



### 6.3.4. Influence of Electrochemical Purification on Selective Precipitation

The electrochemical purification presented in the previous section is followed by selective precipitation through incremental pH adjustments using the same method as in Fig. 6.3, with the aim of removing any leftover Cu and Fe, as well as Al, separately from Ni, Co, and Mn, while leaving Li in solution. The results of this procedure are presented in Fig. 6.4, in which the remaining concentration of the different species in solution compared to the PLS is plotted as function of pH.

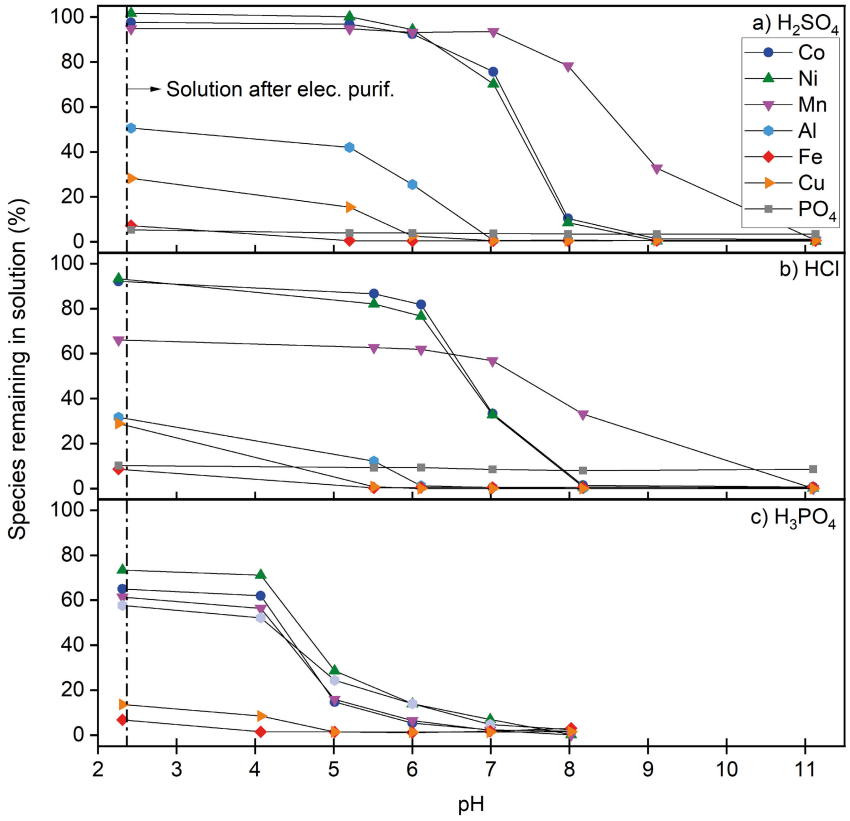


*Figure. 6.4: Selective precipitation of Li, Ni, Co, Mn, Fe, Al, Cu, and $PO_4^{3-}$ from the PLS after electrochemical purification, after leaching with lixiviant $H_2SO_4$ (a, reproduced from Chapter 5), HCl (b), and $H_3PO_4$ (c). (100% = concentration in PLS)*

In Fig. 6.4a, the precipitation process for the $H_2SO_4$-system after the electrochemical purification is shown, starting from pH 2.42, which decreased during the electrochemical process presumably as a result of $FePO_4$ precipitation (Chapter 5, Eq. 5.7) and the oxygen evolution reaction. When raised to 5.2, a sufficient amount of precipitate formed for filtration for analysis and 7% Fe, 13% Cu, and 8% Al are removed compared to the PLS after electrochemical purification. Over the next two steps the pH is raised from 5.2 to 7.0, causing the remaining Al to precipitate, although at this point 24% of the Co and 30% of the Ni are lost as well. When the pH is further increased to 11.1, the remainder of the Co and Ni precipitates, as well as all Mn.

Fig. 6.4b shows the results of selective precipitation in the HCl-system after electrochemical purification, where the pH prior to precipitation was 2.26, again

increased during electrochemical purification, and 34% Mn was already lost during the first pH adjustment and electrochemical purification. In the first step, the pH was increased to 5.5, resulting in total removal of 29% Cu and 9% Fe, which were left in solution after electrochemical purification, whereas Al removal progressed from 32% to 12%. Unfortunately, this was paired with coprecipitation of 7% each of Ni and Co and 3% of the Mn. Increase to pH 6.1 leads to complete precipitation of Al, but also causes more losses of Ni, Co, and Mn, which combined with electrochemical purification reach total losses of 23%, 18% and 38% at pH 6.1. Further increasing the pH to 8.0 recovers all remaining Co and Ni, while Mn is fully precipitated at pH 11.1.

Lastly, Fig. 6.4c shows the results for stepwise precipitation in the $H_3PO_4$-system after electrochemical purification, starting from pH 2.31 as result of increase during electrochemical purification, at which on average 37% of the target elements is already lost. Since the purification steps were carried out at pH 3.5 (rather than pH 4), the first measuring point is at pH 4.1, where another 5% each of Fe, Al, and Cu is removed, resulting in near complete removal of Fe and Cu, whereas 52% of the Al stays in solution. Upon further increasing the pH to 5.0, most species begin to precipitate, with 43% Ni, 47% Co, and 40% Mn recovered from solution, together with 28% of the Al. The remainder of the Ni, Co, Mn, and Al precipitates together at pH 7, while at pH 8 Li (originating from LFP and the pH adjustment solution) and $PO_4^{3-}$ (originating from LFP and the lixiviant) precipitate together as $Li_3PO_4$.



Comparing the results of Fig. 6.4 with the precipitation graphs in Fig. 6.3, it is apparent that the separation of Cu, Al, and Fe from the other elements has improved due to the electrochemical purification. Since the concentration of these impurities is much lower after electrochemical purification compared to the PLS, the quality of the subsequently precipitated Ni, Co, and Mn products is improved. To show this, the compositions of the compounds obtained through selective precipitation after electrochemical purification is plotted in Fig. 6.5. Additionally, the impurity content of the precipitates on metal basis is calculated to facilitate direct comparison of precipitate quality between the different lixiviant systems, according to Eq. 6.8. Each mass component in Eq. 6.8 represents the mass of the corresponding element that is present in the precipitate formed at pH X. These values are reported above the respective bar in in Fig. 6.5.

$$Impurity\ content = 100 * \frac{m_x^{Fe} + m_x^{Al} + m_x^{Cu}}{m_x^{Fe} + m_x^{Al} + m_x^{Cu} + m_x^{Ni} + m_x^{Co} + m_x^{Mn} + m_x^{Li}} \tag{6.8}$$

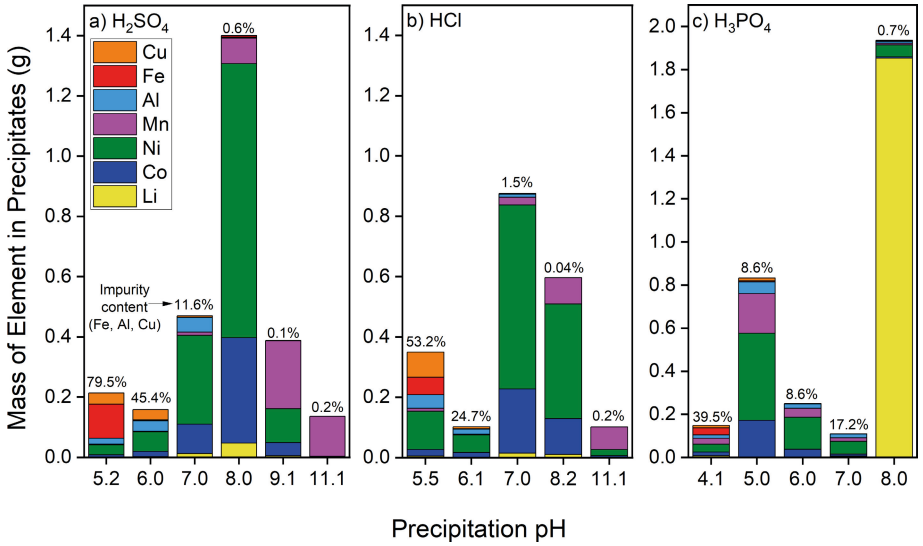


*Figure 6.5: Compositions of the precipitates formed after pH adjustment with prior electrochemical purification in $H_2SO_4$ (a), HCl (b) or $H_3PO_4$ (c) as lixiviant. Impurity content according to Eq. 6.8 is indicated above the respective bar.*

Fig. 6.5a shows the precipitate compositions of the $H_2SO_4$-system after prior electrochemical treatment. The precipitates formed at pH 5.2 and 6.0 contain a high total amount of impurities, being 79.5% and 45.4%, respectively, which should be as high as possible since the target elements mainly precipitate at a later stage, though it does indicate some loss of these elements during selective precipitation. The precipitate at pH 7.0 contains 11.6% impurities, which is expected as Fig. 6.4a indicates simultaneous Al, Co, and Ni removal when the solution pH is increased from 6.0 to 7.0. The following precipitates at pH 8.0, 9.1, and 11.1 show even lower presence of impurities, totaling 0.6%, 0.1% and 0.2%, respectively, indicating good quality precipitates. Hence, although some contaminants remain in the precipitates, the quality improves significantly after electrochemical purification, as also concluded in Chapter 5. Extending the duration of electrochemical purification could further lower contamination, thereby improving the purity of subsequent precipitates. Noteworthy is also that Li coprecipitation is seen in the precipitates from pH 6.0 to pH 9.1, indicating some loss of Li in the selective precipitation process. Unfortunately, Al contamination remains problematic regardless of the electrochemical purification. This is likely a result of complexation reactions keeping this element soluble, either with $H_2O$ and, through hydrolysis, $OH^-$, or with traces of $F^-$ present in the solution, making this element hard to precipitate [47,56,57].

Fig. 6.5b shows that the first two precipitates in the HCl system, at pH 5.5 and pH 6.1, have a lower presence of impurities, 53.2% and 24.7% respectively, than their

counterparts in the $H_2SO_4$ system, indicating a larger loss of target elements in the HCl system. Although this might partially result of the higher pH values at which they were acquired (5.2 and 6.0 in $H_2SO_4$), the fact that the precipitate at pH 7.0 consists of the main Ni and Co fraction indicates that these two elements precipitate at lower pH in the HCl system compared to the $H_2SO_4$ system. The precipitates at pH 7.0 have lower impurity content than its counterpart in the $H_2SO_4$ system, being 1.5% instead of 11.6%. The following precipitate formed at pH 8.2 contains merely 0.04% impurities, while the precipitate at pH 11.1 contains only 0.2%, indicating successful separation from impurities. The maximum amount of Li found in the precipitates (metal basis) is 1.7% at pH 8.2, indicating a minor loss of this element, and an improvement compared to the $H_2SO_4$ system (3.4% Li at pH 8.0) in this regard.

Fig. 6.5c shows the precipitates obtained from the $H_3PO_4$ system. The first precipitate was taken after pH 4 was reached, and contains 39.5% impurities, suggesting a significant overlap with Ni, Co, and Mn. The following precipitate at pH 5 is the main Ni, Co, and Mn containing compound but also contains 8.6% impurities, which is substantially higher compared to impurities in the main target element precipitates of the other two systems (1.5% and 0.6%). At pH 6.0 and 7.0, precipitates containing 8.6% and 17.2% Cu, Al and Fe are formed, which together with the pH 5.0 precipitate show that the $H_3PO_4$ system performs the worst in separating Ni, Co, and Mn from Cu, Fe and Al, out of the three tested lixiviants. Increasing the pH to 8 in the last step results in the precipitation of $Li_3PO_4$ containing merely 0.7% impurities, which is unique amongst the three lixiviants. From this set of results, it can be concluded that although the $H_3PO_4$-system benefits slightly from the Cu plating and Fe oxidation steps as seen in the first data point in Fig 6.4, precipitation itself in this system is still not effective in separating Ni, Co, and Mn from Cu, Al, and Fe. Therefore, a $H_3PO_4$ based recycling system relies heavily on the performance of electrochemical purification steps, which requires further optimization.

It is also important to consider the anions present in the formed precipitates, as shown in Fig D.1 in the appendix. In the $H_2SO_4$ and HCl systems, the firstly formed precipitates contain a significant amount of $PO_4^{3-}$, suggesting coprecipitation with $Fe^{3+}$ and $Al^{3+}$. Since $FePO_4$ could serve as precursor for new LFP CAM, this would be a desired outcome. However, the Ni, Co, and Mn precipitates, all contain traces of the anions found from the lixiviants. These would need to be replaced by hydroxides or carbonates, since these are the starting materials typically required by industry [58].

### 6.3.5. Overall Process Assessment

This work studied a recycling strategy for Li-ion batteries that involves leaching, selective precipitation and electrochemical purification for three lixiviant types: $H_2SO_4$, HCl, and $H_3PO_4$. The leaching efficiencies, element removal during the four purification steps, and purity of the mixed Ni, Co, and Mn precipitates are compared in Fig 6.6. A more detailed explanation of the calculations can be found in the appendix (Fig. D.2).

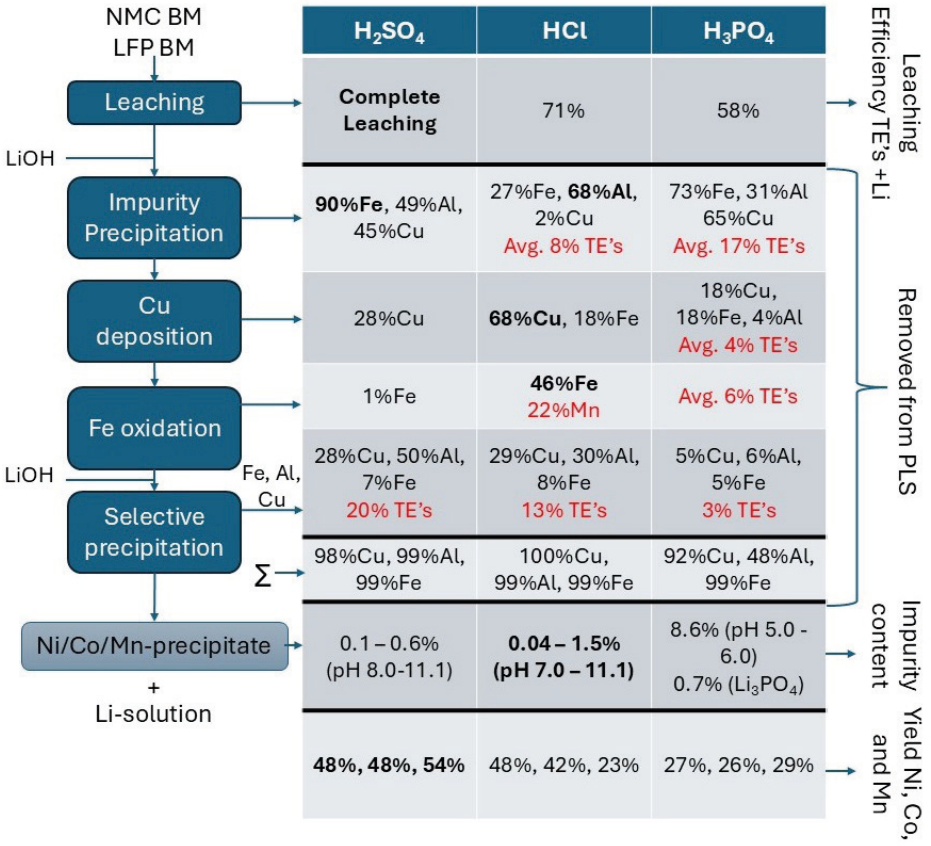


*Figure 6.6: Comparison of the performance of leaching efficiency of target elements (Ni, Co, Mn) and Li, elemental removal during purification, and impurity content (metal basis) for the three tested lixiviant types. Yield is calculated by comparing target elements in BM versus target element in the Ni/Co/Mn precipitates with <1.5% impurities.*

For the overall process efficiency, the leaching step, as well as the selectivity of the electrochemical purification and precipitation steps are all crucial. While $H_2SO_4$ is the most effective lixiviant for dissolving the target elements, achieving complete dissolution of Li, Ni, Co, and Mn, HCl results in a lower leaching (71%)

of the target elements, and $H_3PO_4$ performs even less effectively (58%). On the other hand, $H_2SO_4$ also dissolves the most impurities, leading to lower selectivity in downstream purification.

In the following impurity removal of the $H_2SO_4$ system, 90% of the Fe precipitates, alongside 49% Al and 45% Cu, with little coprecipitation of target elements, after which another 28% Cu is removed during Cu deposition. Subsequent Fe oxidation has little effect, while a second pH increase, to pH 7, removes 28% Cu, 50% Al and 7% Fe, resulting in their total removal of 98%, 75% and 99%, respectively, with a loss of 20% of the target elements due to coprecipitation (Fig. 6.5a, pH 6.0 and 7.0). Raising the pH of the HCl system to 4 after leaching results in 68% Al precipitation, along with 27% Fe and 2% Cu, at the cost of on average 8% per target elements. The following Cu deposition is the most successful of all systems, removing 68% Cu alongside 18% Fe as separate precipitate, while the subsequent Fe oxidation removes another 46% Fe together with 22% of Mn, which is a large loss of target elements. The final selective precipitation removes another 29% Cu, 30% Al and 8% Fe, at the expense of 13% target elements in total, which is the largest loss due to coprecipitation in the final purification stage of the three tested lixiviants, resulting in a total of 100% Cu, 99% Fe and 99% Al removal. Raising the pH to 3.5 in the $H_3PO_4$ system results in 73% Fe, 31% Al and 65% Cu precipitation, which is accompanied by the largest target element loss out of the three lixiviants, of 17% in total. The Cu deposition step removes 18% Cu and Fe each, results in the purest Cu deposit of the three systems, also results in 4% Al removal, but is paired with another loss of 4% TEs on average. Subsequent Fe oxidation only results in target element loss of 6%, and is, hence, undesirable, while increasing the pH to 4 after electrochemical purification results in another 5% removal of Cu and Fe, and 6% Al, paired with 3% loss per target element, which results in total to 92% Cu, 99% Fe, and 48% Al removal.

Hence, it is apparent that although all three systems succeed in removing >98% Cu and Fe as a result of the electrochemical purification, combined with the two selective precipitation steps, the Al stays a major contaminant in all three systems, coprecipitating with any target element in the product precipitation step. The HCl system is the only system removes 68% Al during impurity removal, with the $H_2SO_4$ and $H_3PO_4$ systems removing 49% and 31%, respectively. The $H_2SO_4$ results in the least target element loss during purification (20% per target element), followed by HCl (21 % Co and Ni, 43% Mn) and lastly $H_3PO_4$ (30% per target element).

Comparing the impurities in the recovered Ni, Co, and Mn precipitates, the HCl results in the highest quality, containing 0.04% - 1.5% impurities, followed by $H_2SO_4$ at 0.1% - 0.6% and $H_3PO_4$ at 0.7% - 8.6%, which comes with the additional advantage of $Li_3PO_4$ precipitation with low (0.7%) impurities. Taking all steps into

consideration, $H_2SO_4$ can be deemed the most proficient lixiviant under the tested conditions due to its high leaching efficiency, efficient Fe and Cu removal and low target element loss, although Al remains a problematic contaminant for the Ni, Co, and Mn products. It also results in the highest yield of Ni, Co, and Mn recovery, at 48%, 48% and 54%, respectively, recovered as precipitates between pH 8.0 and 11.1, while the remaining target elements are either lost during purification or co-precipitated with impurities. It should be noted, however, that the $H_2SO_4$ system was more carefully optimized compared to the other two acids, as part of the research in Chapter 5. While the HCl system excels in impurity removal, the leaching procedure needs optimization and the system presents a higher target element loss compared to the $H_2SO_4$-system, with total yields of Ni, Co, and Mn 48%, 42% and 23%, respectively. Lowering the Mn loss during Fe oxidation could already improve this process significantly. Similarly, leaching with $H_3PO_4$ also needs additional optimization, but the low purity precipitates, together with large target element loss makes the system undesirable as a whole, especially considering the low yields of Ni, Co, and Mn which are 27%, 26%, and 29%, respectively.

## 6.4. CONCLUSIONS

This study compared the leaching, purification and subsequent recovery of mixed LFP and NMC BM in three different lixiviant systems: $H_2SO_4$, HCl, and $H_3PO_4$, leading to the following insights and conclusions:

**Leaching:** Acidic strength and anion type associated with the three acids strongly influence leaching efficiency. HCl and $H_2SO_4$ each dissolve approx. 40% of the Ni, Co, and Mn after 30 min of leaching in the absence of LFP, while $H_3PO_4$ showed a lower leaching efficiency of 33%. The addition of LFP BM enhanced NMC dissolution in all systems, with complete leaching of Ni, Co, Mn, and Li achieved only in the $H_2SO_4$-system.

**Selective Precipitation without prior purification:** Consequent purification by precipitation through pH increase was ineffective for separating Fe, Al, and Cu impurities, resulting in large Ni, Co, and Mn losses during Cu, Al and Fe removal, as well as low-grade Ni, Co, and Mn precipitates. In the $H_2SO_4$-system, around 95% removal of Cu, Al and Fe was only achieved by raising the pH up to 7.0. This was accompanied by losses of 28% Ni, 21% Co, and 3% Mn, and resulted in coprecipitation of the remaining impurities with the Ni, Co, and Mn products. Separation of Fe, Al and Cu from the target elements in the HCl-system process even more challenging. At pH 6.0, 98% of Al, 98% of Fe, and only 61% of Cu are precipitated, combined with a loss of 40% Ni, 40% Co, and 16% Mn, again

resulting in substantial coprecipitation with Ni, Co, and Mn at higher pH. In the $H_3PO_4$ system, 48% Fe, 28% Cu and 23% Al were removed at pH 3, yet increasing the pH to 4 induced coprecipitation of all species except Li, resulting in the poorest separation between target elements and impurities. Nonetheless, this system offers the advantage of enabling direct Li recovery as $Li_3PO_4$.

**Electrochemical purification:** Electrochemical purification at elevated pH (3.5 for $H_3PO_4$ and HCl) prior to precipitation stripping significantly diminished the presence of Cu and Fe impurities in all systems. In the $H_2SO_4$-system, Cu and Fe are removed separately, during the dedicated Cu electrodeposition and Fe electro-oxidation steps. The HCl system enabled faster Cu removal by deposition, with simultaneous Fe precipitation. However, the process aimed at Fe oxidation caused significant Mn loss (26 %). In the $H_3PO_4$ system, Cu deposition resulted in the only pure Cu amongst all systems according to XRD-analysis, while also showing simultaneous Fe precipitation. However, Fe-oxidation caused undesirable coprecipitation of all species at the anode, resulting in 13% loss of Ni, Co, and Mn.

**Product precipitation after prior purification:** After electro-purification, selective precipitation achieved through pH adjustment significantly decreased contamination of the desired combined Ni-Co-Mn products with Fe, Al, and Cu impurities. In the $H_2SO_4$-system, selective precipitation between pH 8.0 and 11.1, following electrochemical purification, produces Ni-Co-Mn precipitates containing only 0.1-0.6% impurities). In the HCl system, the main Ni, Co, and Mn products contained 0.4–1.5% impurities at pH 7.0 – 11.1, though this came at the expense of 13% average target element loss during prior precipitation of Cu, Al and Fe at pH 5.5 – 6.1. The $H_3PO_4$ system showed the highest degree of coprecipitation of both impurities and target elements, with the main Ni, Co, and Mn product at pH 5.0 containing 8.6% impurities. However, the $H_3PO_4$-system has as a unique advantage that Li can be recovered in the form of $Li_3PO_4$ directly, with only 0.7% impurities while in the $H_2SO_4$ and HCl systems, Li remains in solution at the final pH, requiring an additional recovery step. While complete removal of Cu, Fe and Al was not achieved under any of the applied conditions, further optimization of the electrochemical purification is expected to enhance the purity of the precipitates significantly. Moreover, since Al cannot be addressed electrochemically, it continues to coprecipitate with the Ni, Co, and Mn after electrochemical purification, highlighting a potential area for further study.

**Assessment of overall process:** Looking at the overall process, the $H_2SO_4$ system is the most effective system among the three acids under the applied conditions. It combines efficient leaching with effective electrochemical purification, ultimately producing Ni, Co, and Mn precipitates containing a total of no more than 0.6% Cu, Fe, and Al combined. This system also provides the highest yields of

Ni, Co, and Mn in the recovered precipitates, at 48%, 48% and 54%, respectively, with the remaining losses occurring during impurity precipitation, electrochemical purification, or contamination by Cu, Fe, and Al. The HCl system allows for more effective electrochemical purification, however, it is paired with unwanted $Cl_2$ formation. Under the applied conditions, the yields of Ni, Co, and Mn are 48%, 42%, and 23%, respectively. With optimized leaching conditions, this system could become a viable option, although HCl-based lixiviants are very corrosive to equipment. The $H_3PO_4$-system, on the other hand, exhibits the poorest leaching and precipitation performance, with Ni, Co, and Mn yields reaching only 27%, 26%, and 29%, respectively. The possibility for $Li_3PO_4$ recovery could be attractive if complete Cu, Fe and Al removal is achieved during electrochemical purification. While still not perfect, the results demonstrate that electrochemical purification is an effective strategy for the separation of Cu, Fe impurities from Ni, Co, Mn, and Li, although Al remains to be addressed separately. These processes are straightforward to execute, can be monitored in situ by measuring the voltage, and requires minimal additional chemicals, making it a promising route for Li-ion battery recycling.

## REFERENCES


1. Y. Liang, C.Z. Zhao, H. Yuan, Y. Chen, W. Zhang, J.Q. Huang, D. Yu, Y. Liu, M.M. Titirici, Y.L. Chueh, H. Yu, Q. Zhang, A review of rechargeable batteries for portable electronic devices, *InfoMat* 1 (2019) 6–32.
2. S. Megahed, B. Scrosati, Lithium-ion rechargeable batteries, *J. Power Sources* 51 (1994) 79–104.
3. J.W. Fergus, Recent developments in cathode materials for lithium ion batteries, *J. Power Sources* 195 (2010) 939–954.
4. F. Schipper, E.M. Erickson, C. Erk, J.-Y. Shin, F.F. Chesneau, D. Aurbach, Review—Recent Advances and Remaining Challenges for Lithium Ion Battery Cathodes, *J. Electrochem. Soc.* 164 (2016) A6220.
5. Regulation of the European Parliament and of the Council Establishing a Framework for Ensuring a Secure and Sustainable Supply of Critical Raw Materials and Amending Regulations (EU) 168/2013, (EU) 2018/858, 2018/1724 and (EU) 2019/1020, *Official Journal* COM 160 (2023).
6. European Commission Directorate-General for Internal Market Industry Entrepreneurship and SMEs, D. Pennington, E. Tzimas, C. Baranzelli, J. Dewulf, S. Manfredi, P. Nuss, M. Grohol, A. Van Maercke, Y. Kayam, S. Solar, B. Vidal-Legaz, L. Talens Peirò, L. Mancini, C. Ciupagea, L. Godlewska, P. Dias, C. Pavel, D. Blagoeva, G. Blengini, V. Nita, C. Latunussa, C. Torres De Matos, F. Mathieux, A. Marmier, Methodology for establishing the EU list of critical raw materials – Guidelines, Publications Office, 2017.
7. European Commission Directorate-General for Internal Market Industry Entrepreneurship and SMEs, M. Grohol, C. Veeh, Study on the critical raw materials for the EU 2023 – Final report, Publications Office of the European Union, 2023.
8. Y. Ding, Z.P. Cano, A. Yu, J. Lu, Z. Chen, Automotive Li-Ion Batteries: Current Status and Future Perspectives, *Electrochemical Energy Reviews* 2 (2019) 1–28.
9. E. Kallitsis, J.J. Lindsay, M. Chordia, B. Wu, G.J. Offer, J.S. Edge, Think global act local: The dependency of global lithium-ion battery emissions on production location and material sources, *J. Clean. Prod.* 449 (2024) 141725.
10. S. Jin, D. Mu, Z. Lu, R. Li, Z. Liu, Y. Wang, S. Tian, C. Dai, A comprehensive review on the recycling of spent lithium-ion batteries: Urgent status and technology advances, *J. Clean. Prod.* 340 (2022) 130535.
11. C.K. Gupta, Chemical metallurgy: principles and practice, (2003) 811.
12. P. Hayes, Process Principles in Minerals and Materials Production with a Focus on Metal Production and Recycling, Fourth edition, Hayes Publishing Co, Sherwood, 2021.
13. O. Velázquez-Martínez, J. Valio, A. Santasalo-Aarnio, M. Reuter, R. Serna-Guerrero, A Critical Review of Lithium-Ion Battery Recycling Processes from a Circular Economy Perspective, *Batteries* 5 (2019) 68.
14. A.M. Bernardes, D.C.R. Espinosa, J.A.S. Tenório, Recycling of batteries: a review of current processes and technologies, *J. Power Sources* 130 (2004) 291–298.
15. Z. Dobó, T. Dinh, T. Kulcsár, A review on recycling of spent lithium-ion batteries, *Energy Reports* 9 (2023) 6362–6395.
16. P. Zhang, T. Yokoyama, O. Itabashi, T.M. Suzuki, K. Inoue, Hydrometallurgical process for recovery of metal values from spent lithium-ion secondary batteries, *Hydrometallurgy* 47 (1998) 259–271.
17. R. Sattar, S. Ilyas, H.N. Bhatti, A. Ghaffar, Resource recovery of critically-rare metals by hydrometallurgical recycling of spent lithium ion batteries, *Sep. Purif. Technol.* 209 (2019) 725–733.
18. P. Meshram, B.D. Pandey, T.R. Mankhand, Recovery of valuable metals from cathodic active material of spent lithium ion batteries: Leaching and kinetic aspects, *Waste Management* 45 (2015) 306–313.

**19.** C.K. Lee, K.I. Rhee, Reductive leaching of cathodic active materials from lithium ion battery wastes, *Hydrometallurgy* 68 (2003) 5–10.

**20.** L. Li, J. Ge, F. Wu, R. Chen, S. Chen, B. Wu, Recovery of cobalt and lithium from spent lithium ion batteries using organic citric acid as leachant, *J. Hazard. Mater.* 176 (2010) 288–293.

**21.** L. Li, Y. Bian, X. Zhang, Y. Guan, E. Fan, F. Wu, R. Chen, Process for recycling mixed-cathode materials from spent lithium-ion batteries and kinetics of leaching, *Waste Management* 71 (2018) 362–371.

**22.** L. Li, Y. Bian, X. Zhang, Q. Xue, E. Fan, F. Wu, R. Chen, Economical recycling process for spent lithium-ion batteries and macro- and micro-scale mechanistic study, *J. Power Sources* 377 (2018) 70–79.

**23.** S. Natarajan, A.B. Boricha, H.C. Bajaj, Recovery of value-added products from cathode and anode material of spent lithium-ion batteries, *Waste Management* 77 (2018) 455–465.

**24.** L. Sun, K. Qiu, Organic oxalate as leachant and precipitant for the recovery of valuable metals from spent lithium-ion batteries, *Waste Management* 32 (2012) 1575–1582.

**25.** J.J.M.M. van de Ven, Y. Yang, S.T. Abrahami, A closer look at lithium-ion batteries in E-waste and the potential for a universal hydrometallurgical recycling process, *Sci. Rep.* 14 (2024) 1–12.

**26.** G. Dorella, M.B. Mansur, A study of the separation of cobalt from spent Li-ion battery residues, *J. Power Sources* 170 (2007) 210–215.

**27.** E.G. Pinna, M.C. Ruiz, M.W. Ojeda, M.H. Rodriguez, Cathodes of spent Li-ion batteries: Dissolution with phosphoric acid and recovery of lithium and cobalt from leach liquors, *Hydrometallurgy* 167 (2017) 66–71.

**28.** J. Wang, M. Chen, H. Chen, T. Luo, Z. Xu, Leaching Study of Spent Li-ion Batteries, *Procedia Environ. Sci.* 16 (2012) 443–450.

**29.** K. Tanong, L. Coudert, M. Chartier, G. Mercier, J.F. Blais, Study of the factors influencing the metals solubilisation from a mixture of waste batteries by response surface methodology, *Environmental Technology (United Kingdom)* 38 (2017) 3167–3179.

**30.** G.P. Nayaka, J. Manjanna, K. V. Pai, R. Vadavi, S.J. Keny, V.S. Tripathi, Recovery of valuable metal ions from the spent lithium-ion battery using aqueous mixture of mild organic acids as alternative to mineral acids, *Hydrometallurgy* 151 (2015) 73–77.

**31.** Y. Jiang, X. Chen, S. Yan, S. Li, T. Zhou, Pursuing green and efficient process towards recycling of different metals from spent lithium-ion batteries through Ferro-chemistry, *Chemical Engineering Journal* 426 (2021) 131637.

**32.** J.J.M.M. Van De Ven, P. J. Teeuwisse, R.W.A. Hendrikx, Y. Yang, S.T. Abrahami, Simultaneous Recycling of Spent $LiFePO_4$ and $LiNi_xMn_yCo_zO_2$ Li-Ion Batteries Under Mild Leaching Conditions, *Journal of Sustainable Metallurgy* (2025) 1–12.

**33.** J. Partinen, P. Halli, A. Varonen, B.P. Wilson, M. Lundström, Investigating battery black mass leaching performance as a function of process parameters by combining leaching experiments and regression modeling, *Miner. Eng.* 215 (2024) 108828.

**34.** G. Choe, H. Kim, J. Kwon, W. Jung, K.Y. Park, Y.T. Kim, Re-evaluation of battery-grade lithium purity toward sustainable batteries, *Nat. Commun.* 15 (2024) 1–10.

**35.** E. Gerold, S. Luidold, H. Antrekowitsch, Selective Precipitation of Metal Oxalates from Lithium Ion Battery Leach Solutions, *Metals (Basel).* 10 (2020) 1435.

**36.** X. Chen, B. Xu, T. Zhou, D. Liu, H. Hu, S. Fan, Separation and recovery of metal values from leaching liquor of mixed-type of spent lithium-ion batteries, *Sep. Purif. Technol.* 144 (2015) 197–205.

**37.** A.A. Nayl, M.M. Hamed, S.E. Rizk, Selective extraction and separation of metal values from leach liquor of mixed spent Li-ion batteries, *J. Taiwan Inst. Chem. Eng.* 55 (2015) 119–125.

**38.** H. Wang, B. Friedrich, Development of a Highly Efficient Hydrometallurgical Recycling Process for Automotive Li–Ion Batteries, *Journal of Sustainable Metallurgy 2015 1:2* 1 (2015) 168–178.

**39.** O.S.L. Bruinsma, D.J. Branken, T.N. Lemmer, L. van der Westhuizen, S. Rossouw, Sodium sulfate splitting as zero brine process in a base metal refinery: Screening and optimization in batch mode, *Desalination* 511 (2021) 115096.

**40.** Michael Faraday, VI. Experimental researches in electricity.-Seventh Series, *Philos. Trans. R. Soc. Lond.* 124 (1834) 77–122.

**41.** A. Fathima, J.Y.B. Tang, A. Giannis, I.M.S.K. Ilankoon, M.N. Chong, Catalysing electrowinning of copper from E-waste: A critical review, *Chemosphere* 298 (2022) 134340.

**42.** W. Jin, Y. Zhang, Sustainable Electrochemical Extraction of Metal Resources from Waste Streams: From Removal to Recovery, *ACS Sustain. Chem. Eng.* 8 (2020) 4693–4707.

**43.** Y. Zou, A. Chernyaev, M. Ossama, S. Seisko, M. Lundström, Leaching of NMC industrial black mass in the presence of LFP, *Sci. Rep.* 14 (2024) 1–14.

**44.** N. Vieceli, R. Casasola, G. Lombardo, B. Ebin, M. Petranikova, Hydrometallurgical recycling of EV lithium-ion batteries: Effects of incineration on the leaching efficiency of metals using sulfuric acid, *Waste Management* 125 (2021) 192–203.

**45.** N. Vieceli, P. Benjamasutin, R. Promphan, P. Hellström, M. Paulsson, M. Petranikova, Recycling of Lithium-Ion Batteries: Effect of Hydrogen Peroxide and a Dosing Method on the Leaching of LCO, NMC Oxides, and Industrial Black Mass, *ACS Sustain. Chem. Eng.* (2023).

**46.** M. Weller, T. Overton, J. Rourke, F. Armstrong, Inorganic Chemistry, 6th ed., Oxford University Press, Oxford, 2014.

**47.** Y. Zou, A. Chernyaev, S. Seisko, J. Sainio, M. Lundström, Removal of iron and aluminum from hydrometallurgical NMC-LFP recycling process through precipitation, *Miner. Eng.* 218 (2024) 109037.

**48.** G.P. Demopoulos, Aqueous precipitation and crystallization for the production of particulate solids with desired properties, *Hydrometallurgy* 96 (2009) 199–214.

**49.** J.R. Klaehn, M. Shi, L.A. Diaz, D.E. Molina, S.M. Reich, O. Palasyuk, R. Repukaiti, T.E. Lister, Removal of impurity Metals as Phosphates from Lithium-ion Battery leachates, *Hydrometallurgy* 217 (2023) 106041.

**50.** A. Chernyaev, J. Zhang, S. Seisko, M. Louhi-Kultanen, M. Lundström, $Fe^{3+}$ and $Al^{3+}$ removal by phosphate and hydroxide precipitation from synthetic NMC Li-ion battery leach solution, *Sci. Rep.* 13 (2023) 1–12.

**51.** D.J. Shin, S.H. Joo, D. Lee, S.M. Shin, Precipitation of lithium phosphate from lithium solution by using sodium phosphate, *Canadian Journal of Chemical Engineering* 100 (2022) 3760–3767.

**52.** J.R.. Rumble, D.R.. Lide, T.J.. Bruno, CRC handbook of chemistry and physics : a ready-reference book of chemical and physical data, CRC Press, 2018.

**53.** K. Binnemans, P.T. Jones, The Twelve Principles of Circular Hydrometallurgy, *Journal of Sustainable Metallurgy* 9 (2022) 1–25.

**54.** A. Chernyaev, J. Partinen, L. Klemettinen, B.P. Wilson, A. Jokilaakso, M. Lundström, The efficiency of scrap Cu and Al current collector materials as reductants in LIB waste leaching, *Hydrometallurgy* 203 (2021) 105608.

**55.** H.W. Richardson, Handbook of Copper Compounds and Applications, CRC Press, 1997.

**56.** D.R. Parker, ALUMINUM SPECIATION, *Encyclopedia of Soils in the Environment* 4 (2005) 50–56.

**57.** F. Giacobello, V. Mollica-Nardo, C. Foti, R.C. Ponterio, F. Saija, S. Trusso, J. Sponer, G. Cassone, O. Giuffrè, Hydrolysis of $Al^{3+}$ in Aqueous Solutions: Experiments and Ab Initio Simulations, *Liquids* 2 (2022) 26–38.

**58.** M. Malik, K.H. Chan, G. Azimi, Review on the synthesis of $LiNi_xMn_yCo_{1-x-y}O_2$ (NMC) cathodes for lithium-ion batteries, *Mater. Today Energy* 28 (2022) 101066.

*Jij hebt de dingen niet nodig*
*om te kunnen zien*
*De dingen hebben jou nodig*
*om gezien te kunnen worden*

K. Schippers – *liefdesgedicht* – Een vis zwemt uit zijn taalgebied (1976)

# 7

# *Chapter 7*

## Conclusions & Recommendations

## 7.1. CONCLUSIONS

This dissertation examined how the complex nature of lithium-ion battery waste affects commonly applied hydrometallurgical recycling steps and developed a new leaching and purification process that minimizes the environmental impact of recycling, while enabling the treatment of mixed and varying LiBs waste streams, thereby introducing flexibility into the recycling process. The research provided the answers to the research questions presented in Chapter 1.

**Sub question 1: What compositional variabilities can be expected in mixed end-of-life Li-ion battery waste streams?**

Chapter 3 shows no clear link between CAM type and LiB application, with sometimes multiple CAM-types present in one single cell. Moreover, it is not possible to differentiate between different CAM-types from the outside of the LiB-cells, making sorting difficult. Hence, industrial black mass (BM) typically contains multiple CAM-types, in combination with impurities from other battery parts such as Fe, Cu, Al, and graphite. Moreover, the nature of the pre-treatment, either manual, mechanical, or involving heat treatment, determines the average oxidation states of the Ni, Co, and Mn.

**Sub question 2: What is the influence of black mass composition on leaching?**

Comparing the leaching behaviour of Li, Ni, Co, and Mn from pristine CAMs, manually liberated CAMs and industrial BMs have indicated that, although leaching efficiencies generally follow similar trends, the required amount of reducing agents, either $H_2O_2$ (Chapter 3) or $Fe^{2+}$ from dissolved $LiFePO_4$ (Chapter 4), for complete dissolution varies significantly. A higher average oxidation state of the transition metals (Ni, Co, and Mn) present in the waste increases the demand for reducing conditions, whereas prior high temperature pre-treatment can pre-reduce these metals, decreasing the need for strong reducing conditions during leaching. Overall, the study demonstrates that a universal leaching process can be designed for diverse LiB-waste streams, as long as the fluctuating need for a reducing environment is accommodated. However, it is also evident that maintaining excessive reducing environment using external chemical reagents increases reagent consumption, and promotes the dissolution of impurities such as Fe, Al, and Cu.

**Sub question 3: How can the chemical consumption during leaching of mixed Li-ion battery waste be decreased?**

Spent $LiFePO_4$ (LFP) can act as an effective reducing agent, offering a viable alternative to the commonly used $H_2O_2$. The divalent Fe present in LFP promotes the dissolution of high oxidation states (+III or +IV) Ni, Co, and Mn by their reduction to the more soluble +II state, as shown in the results of Chapter 4. In addition, Al and Cu impurities present in industrial BM can act as reducing agents through catalytic reactions with the dissolved $Fe^{2+}$. By carefully tuning the molar ratio of LFP to NMC during leaching of industrially pre-treated LFP and NMC BM, complete leaching of Li, Ni, Co, and Mn can be achieved (as shown in Chapter 5). For our battery materials, optimal leaching was achieved using 1 mol/L $H_2SO_4$, 50 °C, 2 hours and a 0.75 LFP to NMC molar ratio, of which the LFP was added in three equal steps. Leaching residue analysis indicates that most of the $Fe^{2+}$ was consumed and oxidized to $Fe^{3+}$, enabling its precipitation in the form of $FePO_4$ during leaching. Furthermore, additional $Fe^{3+}$ in the PLS can be removed by increasing the pH to 3 using LiOH or NaOH, also forming LFP precursor $FePO_4$. However, any remaining $Fe^{2+}$, either not having undergone oxidation, or a result of re-reduction by Al or Cu, hampers subsequent purification due to its higher solubility, persisting in solution up to pH 8. Moreover, Cu and Al impurities in the PLS also persist in solution beyond pH 7, resulting in contamination of the subsequently precipitated Ni, Co, and Mn products from pH 8 onwards by 0.5% - 5%. Therefore, further purification needs to handle fluctuating impurity levels, while also preserving the environmental benefit of replacing external reducing agents with spent LFP.

**Sub question 4: What purification approach enables low chemical consumption alongside flexibility towards varying and heterogeneous waste streams?**

Due to its flexible nature and absence of additional chemical reagents, electrochemical purification was selected in Chapter 5 as a strategy to oxidize $Fe^{2+}$ in the PLS to the less soluble $Fe^{3+}$, enabling its removal via precipitation as the LFP precursor $FePO_4$. Applying a 1.2 A current with a high anode to cathode ratio on a simplified solution containing only $Fe^{2+}$, or a simple PLS containing only LFP BM, enabled oxidation of 99.2% of the $Fe^{2+}$ in 4 hours. Monitoring the potential provides a method to track the progression of this reaction, consistent with the Nernst equation, allowing for in-situ process control. However, in the PLS containing leached LFP and NMC BMs, the presence of impurities, prominently Cu, interferes with efficient $Fe^{2+}$ oxidation. Raising the pH to 4 prior to electrochemical treatment

improves purification, since available $Fe^{3+}$ can precipitate due to its low solubility above pH 3. Based on these findings, a four-step purification route is proposed which is also visualised in Fig. 7.1:

1. $Fe^{3+}$, as well as partial Cu and Al precipitation by raising the pH to 4.
2. Cu deposition using a large cathode and a small anode.
3. Electro-oxidation of $Fe^{2+}$ with a large anode and a small cathode.
4. Selective precipitation of the remaining metals, namely Ni, Co, and Mn.

This newly developed recycling route, including simulations LFP and NMC leaching, results in high purity products, as the fourth purification step results in significantly higher purity Ni, Co and Mn precipitates (0.1 – 0.6% impurities) compared to the products without prior electrochemical treatment. Therefore, it can be concluded that electrochemical treatment is a very promising purification technique for LiB-recycling, since it does not require large amounts of reagents and can be a flexible step in the recycling process, accommodating composition variations. However, this method was only tested on a $H_2SO_4$-based PLS, and acid type can have major influence on downstream purification.

**Sub question 5: How can the choice of lixiviant impact downstream recycling?**

As part of further studying the proposed recycling route, the approach from Chapter 5 with $H_2SO_4$ as lixiviant was repeated with HCl and $H_3PO_4$ in Chapter 6. Leaching LFP and NMC BM with $H_2SO_4$, HCl, or $H_3PO_4$, shows that acidic strength and protic value are important factors in leaching efficiency, with complete leaching achievable only with $H_2SO_4$ under the investigated conditions. Without electrochemical treatment, selective purification does not result in effective separation of Fe, Al, and Cu impurities from the target elements (Li, Ni, Co, and Mn) in any of these acids. Hence it is clear that only replacing the lixiviant in absence of electrochemical purification does not pose any benefits to product purity. Adjusting the PLS of the $H_2SO_4$- and HCl- systems to pH 4, or of the $H_3PO_4$ system to pH 3.5, combined with the previously proposed electrochemical treatment, results in overall removal of up to 90% of both Cu and Fe. However, in the HCl system it is paired with significant (22%) Mn loss, and in the $H_3PO_4$-system a gel-type precipitate of Ni, Co and Mn forms. Conversely, when the electrochemically treated solutions are subjected to selective precipitation, co-precipitation of Fe, Al, and Cu with Ni, Co, and Mn drastically lowers for all three lixiviants, resulting in high purity products (0.1 – 0.6% impurities for $H_2SO_4$). The average yields of the target elements for the $H_2SO_4$, HCl and $H_3PO_4$ systems are 50%, 38% and 27%, respectively, with

the remainder of the Ni, Co, and Mn either not leached, or lost during purification. Although the phosphates based system has the additional advantage of Li-precipitation as $Li_3PO_4$, enabling directly recovery of this element , it is deemed the least effective lixiviant under the tested conditions due to the low leaching efficiency (58%) and low overall yield (27% target elements). The HCl system shows higher leaching efficiency (71%) and yield (38%), but has the major drawback of chlorine gas formation during electrochemical purification. The most efficient recovery of Ni, Co, and Mn was in the $H_2SO_4$ system, as it combined complete dissolution during leaching with good Cu, and Fe removal during electrochemical purification and Al removal during selective precipitation. This system also shows potential for further yield improvement through optimization of the electrochemical purification steps. This leads to the answer to the general research question:

***How can hydrometallurgical recycling be applied to a mixture of industrially pre-treated lithium-ion-battery waste, resulting in comprehensive recovery of high quality products with minimal environmental impact?***

The thesis developed a sustainable leaching method that makes use of LFP battery waste as a reagent in the leaching of high value metals present in NMC, LCO, and LMO type batteries to enable leaching of mixed battery waste streams at low acid concentration and no additional external chemical reagents. An electrochemical purification method was investigated offering a new way to remove Fe and Cu impurities. The proposed recycling route (Fig. 7.1) enables the treatment of mixed LiBs waste streams with good recovery of the CRMs and minimal environmental footprint. It consists of simultaneous leaching of LFP and NMC, followed by impurity removal by precipitation at pH 4, Cu electro-deposition, Fe electro-oxidation and product precipitation. The variable need for reducing agents to dissolve NMC could be offset by an excess of LFP during leaching, followed by electrochemical removal of the non-oxidized Fe and dissolved Cu. Since the progress of electrochemical treatment can be monitored in-situ, it provides a flexible step within the recycling chain. Finally, selective precipitation of Ni, Co, and Mn products yields high-grade precursors suitable for the production of new batteries alongside a Li-rich solution, resulting in a closed loop recycling process.

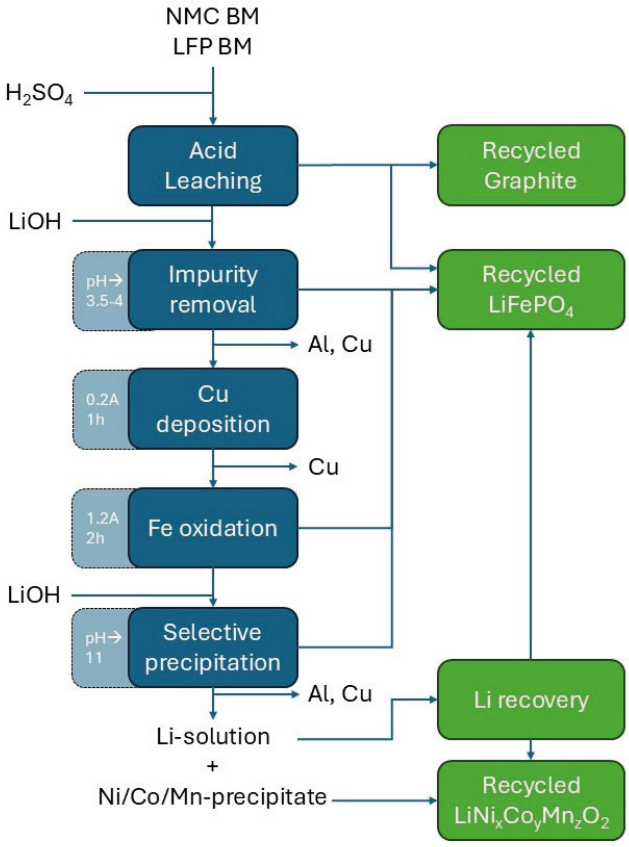


*Figure 7.1: Schematic overview of the proposed recycling strategy (blue) and future recommendations for resource recovery (green).*

## 7.2. RECOMMENDATIONS

This thesis presents crucial information on the complex nature of LiB-waste and how it can be efficiently recycled through a newly developed hydrometallurgical recycling process. However, further research and optimization of the proposed process are needed to fully realize its potential.

While electrochemical purification of Cu and Fe impurities was effective in lowering their co-precipitation with Ni, Co, and Mn, it did not result in their complete removal under the investigated conditions. Further optimization, such as in-situ pH monitoring and adjustment of the electrochemical purification, including optimized cell design, as well as thorough investigation of the influence of process parameters could further improve the quality of the resulting Ni, Co, and Mn co-precipitates.

In addition, process robustness should be tested by leaching a larger variety of LFP BMs with NMC, LCO, LMO and other lithium-metal oxide BMs, after which the electrodeposition of Cu and electrooxidation of Fe should be investigated in detailed to assess its in-situ controllability and sensitivity to additional variations in composition. Also, Al was the most persistent impurity during the selective precipitation, as Al cannot be targeted by electrochemical reduction due to its high tendency to oxidize ($E^0$= -1.68V). However, complete removal of Cu and Fe during electrochemical purification might result in more efficient Al removal during precipitation, as this leads to availability of $PO_4^{3-}$ that would otherwise precipitate with Cu.

While the replacement of commonly used chemical reducing agents during leaching by LFP, was presumed to result in a lower environmental impact compared to SoA hydrometallurgical processes, quantification of the energy consumption and environmental footprint should be carried out to verify this and quantify the impact.

Moreover, it is important to test the recycled products, listed in green along the recycling flowsheet in Fig. 7.1, and their performance in new Li-ion battery cells, incl. the **re-use of graphite** . The mild leaching environment might limit substantial chemical and morphological changes, resulting in a possibility for direct re-use, which could be tested by manufacturing battery cells with the recovered graphite and comparing their charging and discharging performance with cells containing pristine materials. Moreover, the recovered $FePO_4$, either during leaching, subsequent impurity removal, or by selective precipitation, has the potential as precursor for $LiFePO_4$ manufacturing. Therefore, we recommend separating the $FePO_4$ and graphite from each other by dissolving the phosphate again in mild acidic environment, followed by filtration of the graphite and subsequent re-precipitation of $FePO_4$ and combination with the other two $FePO_4$ streams. When combined with products from comprehensive **Li-recovery** from the purified solution, **recycled LFP** could be synthesised and tested in new cells. Similarly, the precipitates of Li, Ni, Co, and Mn could be manufactured into new **recycled NMC**-type cathode active materials, to be tested and benchmarked with pristine materials. Such tests are needed to ensure the extent of impurity removal suffices, as EU regulations require a recycled content of 12% Li, 15% Ni and 26% Co by 2036 and hence manufacturers need to be convinced that including recycled precursors not compromise the functionality of new LiBs.

# Appendix A

## SUPPLEMENTARY INFORMATION CHAPTER 3

*Figure A.1: 18650-type cell after removal of top and bottom and making a longitudinal cut.*

*Table A.1: Explanation of the sub images in Fig. 3.5. In addition, the XRD results of the corresponding depicted BMs are shown.*

| Image | Black mass name | Compound | Grain size | XRD results |
|---|---|---|---|---|
| a) | NMC 1 | NMC | 1 – 4 µm Individual<br>8 – 20 µm Coagulated | $LiNi_xMn_yCo_zO_2$ |
| b) | NMC 2 | NMC | 1 – 4 µm Individual<br>8 – 20 µm Coagulated | $LiNi_xMn_yCo_zO_2$ |
| c) | LCO 1 | LCO | 2 – 40 µm | $LiCoO_2 + CoO_2$ |
| d) | LCO 2 | LCO | 10 – 30 µm | $LiCoO_2$ |
| e) | LMO + NMC | NMC | 1 – 4 µm Individual<br>8 – 20 µm Coagulated | $LiMn_2O_4 + Li_{1.2}Mn_{0.6}Ni_{0.2}O_2$ |
| | | LMO | 7 – 40 µm | |
| f) | LCO + NMC 1 | NMC | 1 – 4 µm Individual<br>8 – 20 µm Coagulated | $LiCoO_2 + LiNi_xMn_yCo_zO_2$ |
| | | LCO | 10 – 30 µm | |
| g) | LCO + NMC 2 | NMC | 1 – 4 µm | $LiCoO_2 + LiNi_xMn_yCo_zO_2$ |
| | | LCO | 3 – 30 µm | |
| h) | LFP | LFP | 1 – 15 µm | $LiFePO_4 + FePO_4 + C$ |
| i) | Industrial | C | 10 – 25 µm | C + Ni + CoO + |
| | | NMC | 10 – 50 µm | $Cu_{0.2}MnNi_{5.8}O_8$ + |
| | | LCO | 10 – 20 µm | $LiMn_{0.8}Ni_{1.2}O_4$ + |
| | | LFP | 4 – 8 µm | $Cu_{0.85}Fe_{0.1}O + Li_2CO_3$ + |
| | | Al, Cu | Variable | $Li_3PO_4$ |

XRD suggests an equal molar distribution of the TMs in NMC 1 and NMC 2, as well as the mixed oxide in LCO + NMC 1 and LCO + NMC 2. This contradicts the XRF measurements. However, distinguishing NMC cathode powers with different ratios of TMs (111, 532, 811 etc.) by XRD-analysis is very difficult due to their nearly identical diffractograms. Therefore, only the ICP-OES-results are considered for distinguishing the exact cathode chemistry.

*Table A.2: Elemental concentrations (g/L) of Li, Co, Ni, Mn, Al, Fe and Cu in the PLS after leaching industrial BM. Leaching conditions were 2 mol/L $H_2SO_4$, 4 vol% $H_2O_2$-solution, S/L = 60 g/L, T = 50 °C and t = 120 min.*

| Element | Li | Co | Ni | Mn | Al | Fe | Cu |
|---|---|---|---|---|---|---|---|
| Concentration (g/L) | 2.6 | 10.8 | 5.9 | 3.0 | 1.8 | 0.36 | 0.86 |

# Appendix B

## SUPPLEMENTARY INFORMATION CHAPTER 4

### Leaching Setup

A triple necked round bottom flask of 500 mL with magnetic stirrer was used as a reaction vessel. This was placed on a stirring and heating plate. In the middle neck of the flask, a reflux cooler was placed. This was connected to the cooling water. The three necks allowed for addition of reagents while the leaching was carried out. The setup is shown in Fig. B.1. It was determined before leaching that a probe temperature of 54 °C resulted in a lixiviant temperature of 50 °C.


*Figure B.1: Lab scale leaching setup that was used in for the 100 mL leaching systems.*

## Additional Leaching Results

The following leaching results belong to the used NMC 532 (Fig. B.2a) and BM M (Fig. B.2b). They have not been included in the main manuscript because these results are very similar to what has been seen in the other results. They are briefly discussed in the main manuscript, and more in detail in the supplementary information.

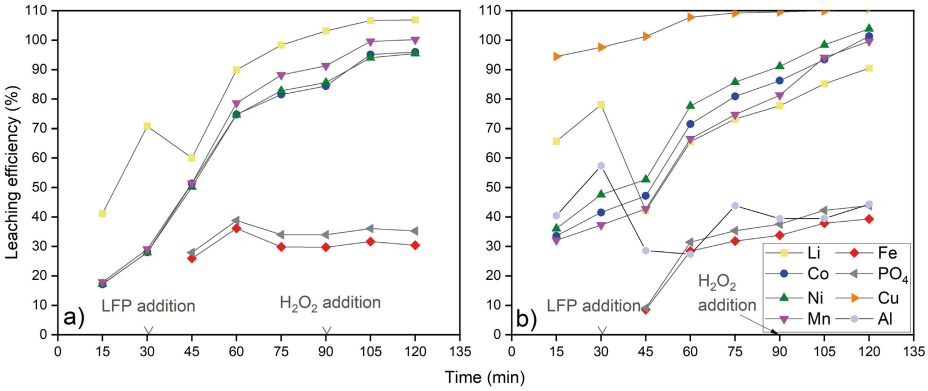


*Figure B.2: Dependence of the leaching efficiency of Li, Co, Ni, Mn, Cu, Fe, Al and $PO_4$ on time, as well as the presence of LFP and $H_2O_2$, for two different black mass samples; a) Used NMC 532 (20 g/L) and b) BM M (38.4 g/L). LFP (34 g/L) and $H_2O_2$ (1 vol%) were added to the leaching system at 30 and 90 min, respectively. Other conditions are 0.6 mol/L $H_2SO_4$, 50 °C and a total volume of 100 mL.*

Fig B.2a shows the leaching behaviour of the used NMC 532, which is similar compared to the pristine material. However, the leaching efficiency after 30 minutes is slightly lower, being ±28 % for the Ni, Co, and Mn and 71 % for Li. Addition of LFP shows an increase in the dissolution of the TMs, which raised by ± 23% in 15 mins, but slower than what is seen for the pristine NMC, which raised by ±43 % in the same time frame. Moreover, the leaching efficiency of Li decreased slightly because of the increase in its feed concentration, also indicating a slower reaction. At 90 minutes of leaching, the Ni, Co, and Mn are dissolved for ±87%, whereas Li is dissolved completely. The value for Li does not differ much compared to the pristine NMC, but the leaching efficiency for Co, Mn and Ni are 8, 5 and 5% lower, respectively. Addition of $H_2O_2$ leads to ± 97 % leaching of Ni, Co, and Mn. Fe and $PO_4^{3-}$ reach maximum leaching at 60 minutes, being 37%. After 2 hours, these elements are dissolved for 33%, similarly to the case of pristine NMC. The reactions found in this system are the same as in the case of pristine NMC 532. The slightly slower leaching efficiencies is attributed to the presence of harder to leach metal oxides, in which the metals have higher oxidation states (+III or +IV). These are a result of side reactions during use of the LiBs.

Fig. B.2b shows the leaching process performed on industrial BM M, a mixture of mainly NMC 622 and 532 batteries which were discharged and shredded. This sample represents BM M+ without additional milling and sieving steps for an additional removal of impurities. Its behaviour is comparable to the dissolution of used NMC 532. After 30 minutes, the leaching efficiencies of Ni, Co, and Mn are 48, 42 and 37% respectively. The extraction of Li is more efficient, being 78%. Addition of LFP does eventually increase the leaching efficiency of these elements, but the reaction goes slower than in the previous leaching experiments. When compared to BM M+ (Fig. 4.2a), complete extraction of all elements took 75 minutes longer. This can be attributed to the high S/L ratio (38.4 g/L compared to 30.5 for BM M+) which is a result of the high share of insoluble components in this BM. This lowers the contact surface between the particles of the CAMs and the leaching liquor. From the experiment, it is not clear if the complete extraction at 120 minutes is a result of $H_2O_2$-addition or an extra 30 minutes of reaction time. The behaviour of Li is distinct compared to the other experiments and it only reaches 90% at maximum. This is probably the result of the high S/L ratio, with more Li present in the graphite, originating from battery anodes. Graphite itself does not dissolve during the leaching. Therefore, the Li has to migrate out of the particles. The high S/L will limit the effectiveness of the agitation in the leaching system, hence slowing down this process. The slower leaching is also reflected in the extraction results of Fe and $PO_4^{3-}$. 15 minutes after its addition, only 9% is dissolved. Eventually, these elements reach a dissolution of ± 42%, which is similar to the first two leaching experiments. Cu dissolves efficiently after only 15 minutes and is extracted completely after 45 minutes. Al is extracted at a slower pace, and its leaching efficiency decreases at 45 minutes because of the increased feed concentration after LFP addition. Eventually after 120 minutes, 44% is extracted.

To verify if the dissolution of copper was the result of direct reaction with $H_2O_2$ or a reaction with Fe(III), the experiment in Fig 4.2b using BM P was redone. However, instead of $H_2O_2$-addition at 90 minutes, pristine NMC 532 was added. If Cu is indeed reacting with Fe(III), this should be seen as an increase in Cu extraction at 105 and 120 min. If Cu was reacting with $H_2O_2$, this increase should not be seen in this new experiment. The results can be found in Fig B.3.

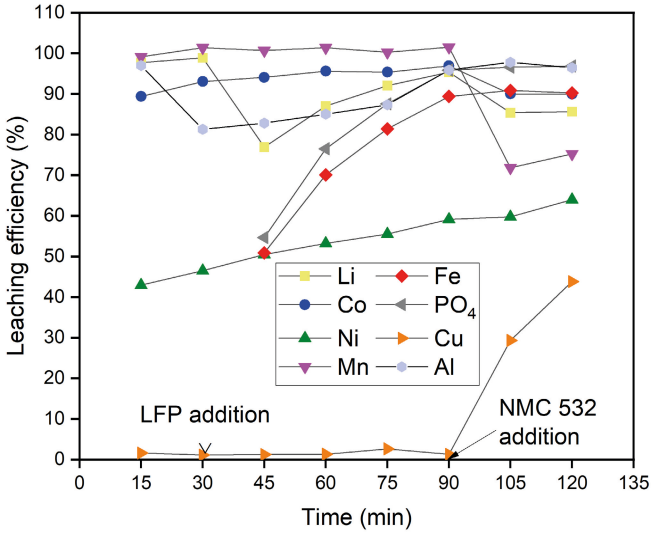


*Figure B.3: Dependence of the leaching efficiency of Li, Co, Ni, Mn, Cu, Fe, Al and $PO_4^{3-}$ on time as well as the presence of LFP and pristine NMC 532. LFP (34 g/L) and NMC 532 (10 g/L) were added to the leaching system at 30 and 90 min, respectively. Other conditions are 0.6 mol/L $H_2SO_4$, 50 °C, 33.5 g/L BM P and a total volume of 100 mL.*

As is also highlighted in the main text, it is clear that Cu dissolution is a result of the reaction with $Fe^{3+}$ according to Eq. 4.8. Just as in the experiment seen in Fig. 4.2b, dissolution of Co, Mn, and Li goes very efficiently. Ni extraction is slow. Addition of LFP does not seem to influence the extraction of these elements. Li extraction only changes because the increase in its feed concentration. Fe and $PO_4^{3-}$ are extracted very efficiently, indicating that the $Fe^{2+}$ cannot react according to Eq. 4.3. Hence, the formation of $Fe^{3+}$ and subsequently a $FePO_4$ precipitate are hampered. When pristine NMC 532 is added, an increase in Cu-extraction can be seen. It is not as fast as in Fig. 4.2b, but nevertheless shows that the formation of Fe(III) through the combination of Eqs. 4.1 and 4.3 goes efficiently. Then, the Cu is dissolved according to Eq. 4.8.

## XRD results

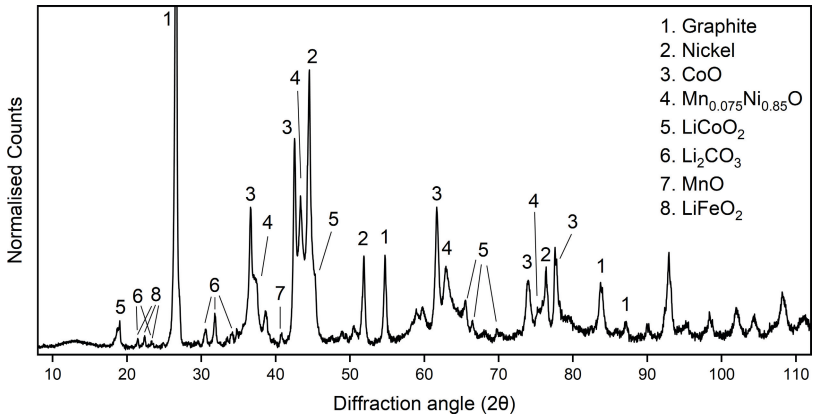


*Figure B.4: XRD diffractogram of BM P. It shows the presence of Ni(0), as well as the pre-reduced oxides of Ni, Co, and Mn (II).*

## Results precipitation Stripping

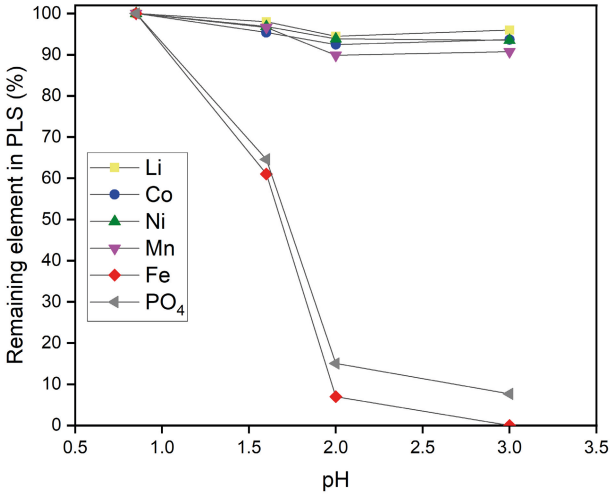


*Figure B.5: Precipitation stripping of Li, Ni, Co, Mn, Fe, Al, Cu, and $PO_4^{3-}$, after leaching of used NMC 532, by pH adjustment.*

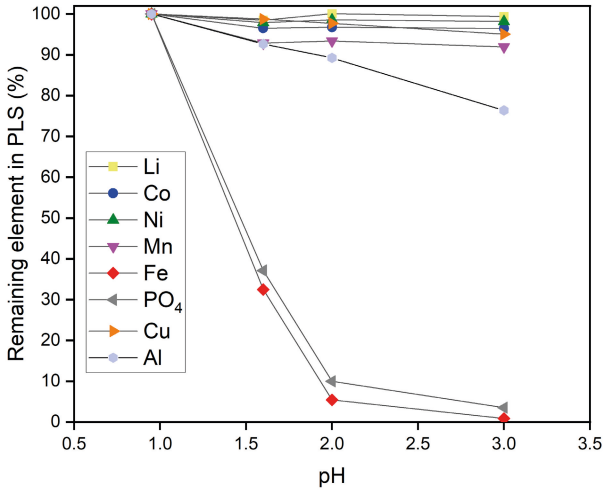


*Figure B.6: Precipitation stripping of Li, Ni, Co, Mn, Fe, Al, Cu and $PO_4^{3-}$, after leaching of BM M+, by pH adjustment.*

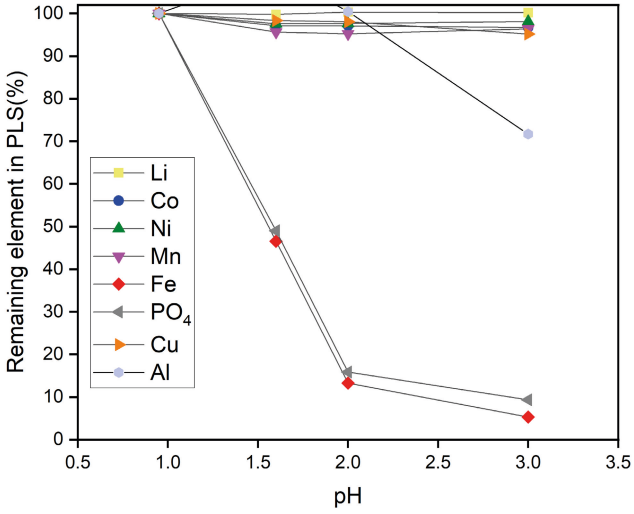


*Figure B.7: Precipitation stripping of Li, Ni, Co, Mn, Fe, Al, Cu, and $PO_4^{3-}$, after leaching of BM M, by pH adjustment.*

## PLS content of the 500 mL leaching system

The last leaching experiment was carried out using BM M+ and LFP. After leaching, the solution was neutralized with a 2 mol/L LiOH-solution. This results in a very high Li concentration. The Fe was almost completely removed. The Al and Cu persist in the solution. $PO_4^{3-}$ also seemingly stays behind, although analysis of the residue tells us it is there.

*Table B.1: Content of the PLS of the 500 mL leaching system after Fe removal (g/L)*

| Element/Ion | Li | Co | Ni | Mn | Al | Fe | Cu | $PO_4^{3-}$ |
|---|---|---|---|---|---|---|---|---|
| Concentration in PLS after Fe removal | 4.35 | 2.08 | 5.77 | 2.11 | 0.30 | 0.04 | 0.82 | 1.70 |

# Appendix C

## SUPPLEMENTARY INFORMATION CHAPTER 5

### Electrochemical Setups

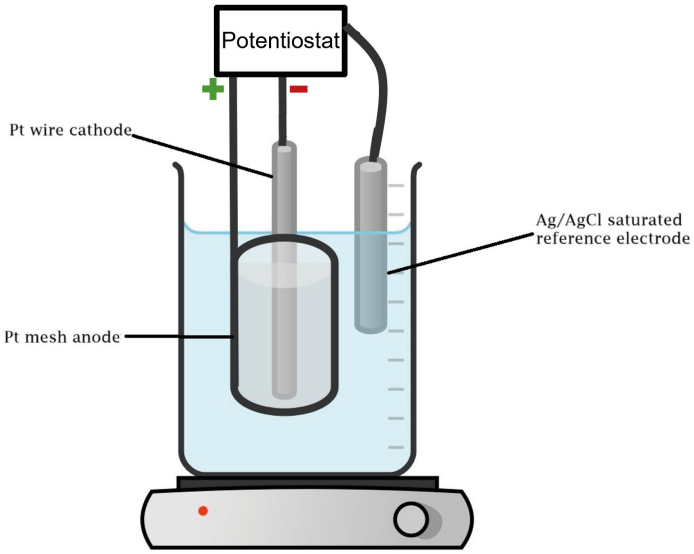


*Figure C.1: Visualisation of the setup used for electrochemical oxidation of $Fe^{2+}$ to $Fe^{3+}$.*

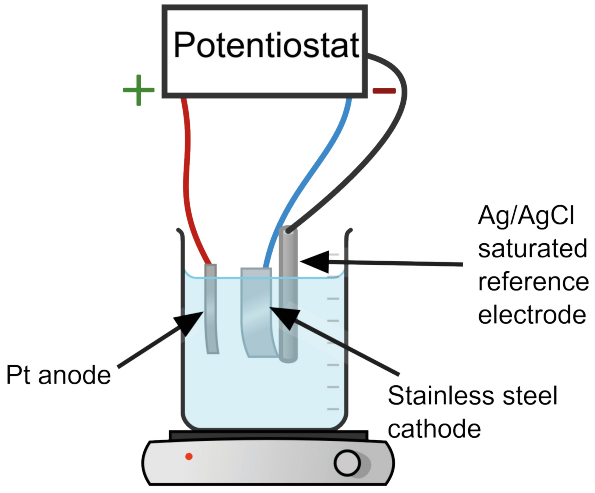


*Figure C.2: Visualisation of the setup used electro-deposition of Cu*

## XRD-analysis Preciptitates

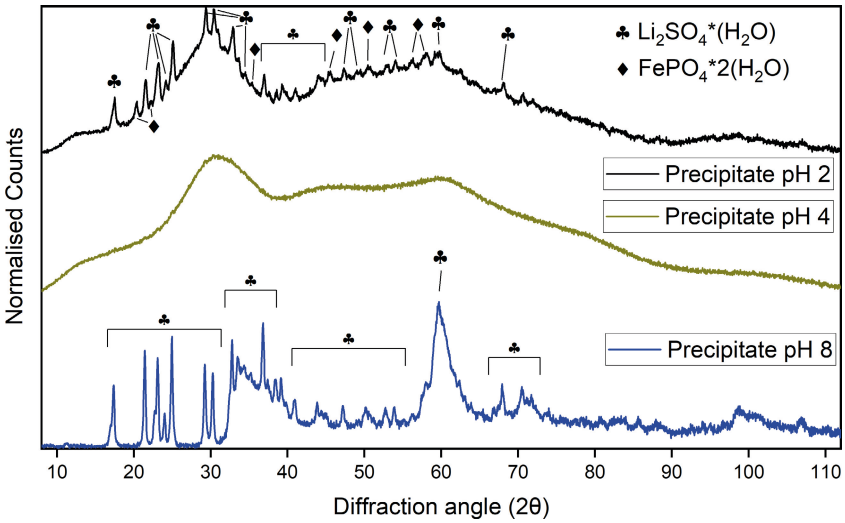


*Figure C.3: XRD-diffractograms of the precipitates formed after leaching of LFP BM and NMC BMs.*

## Visualization Nernst Equation for Fe-oxidation

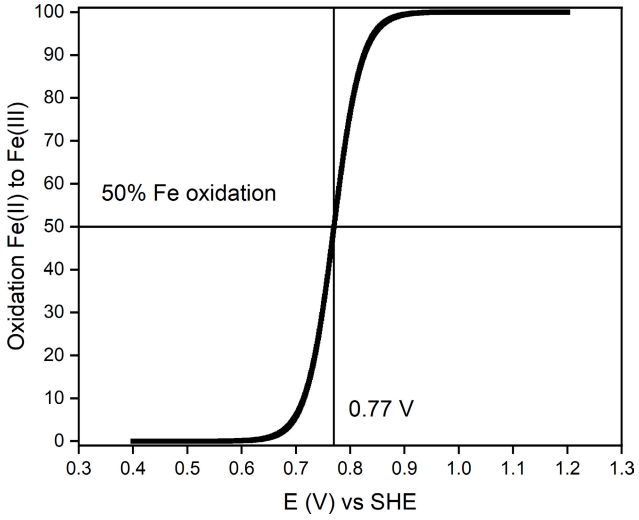


*Figure C.4: Dependence of Fe oxidation on the cell potential according to the Nernst Equation. Note that when $[Fe^{3+}] = [Fe^{2+}]$, $E=E^0$.*

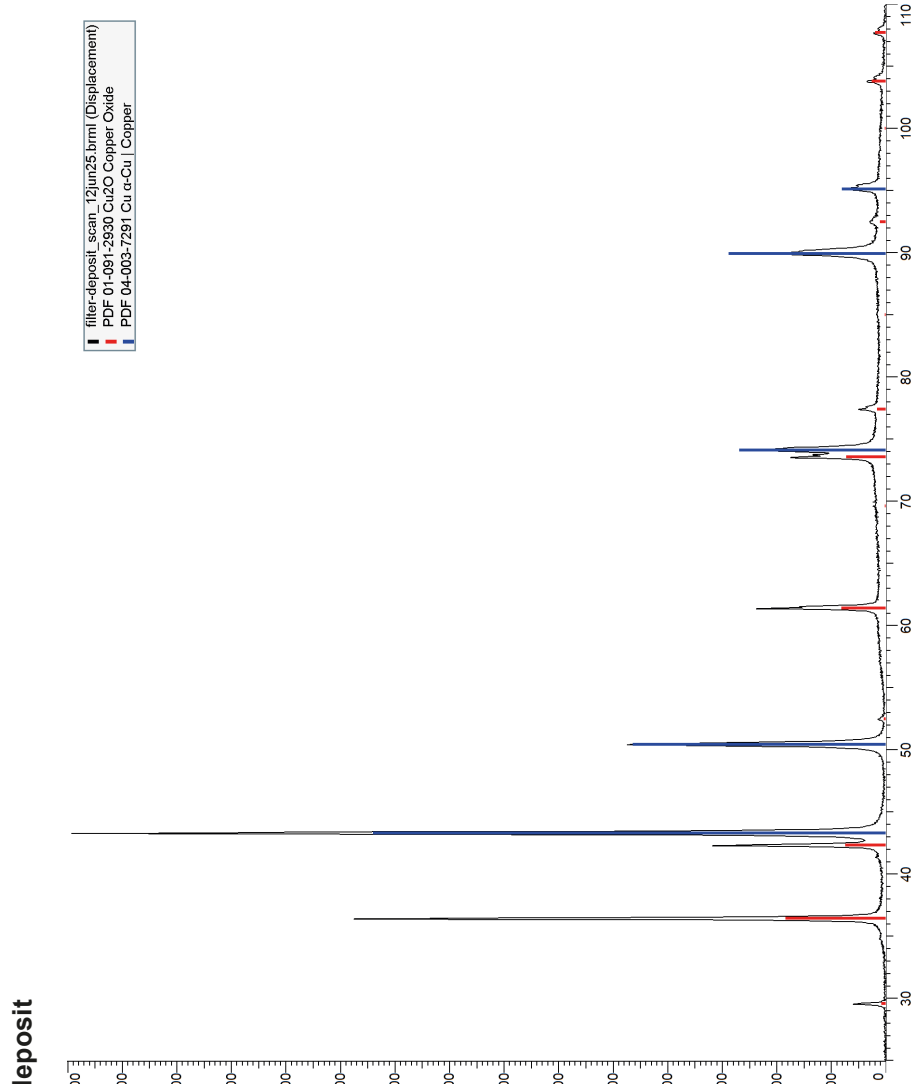


*Figure C.5: XRD-diffractogram of the cathode deposit during Fe electro-oxidation*

## Results Chronopotentiometry During Electrochemical Purification

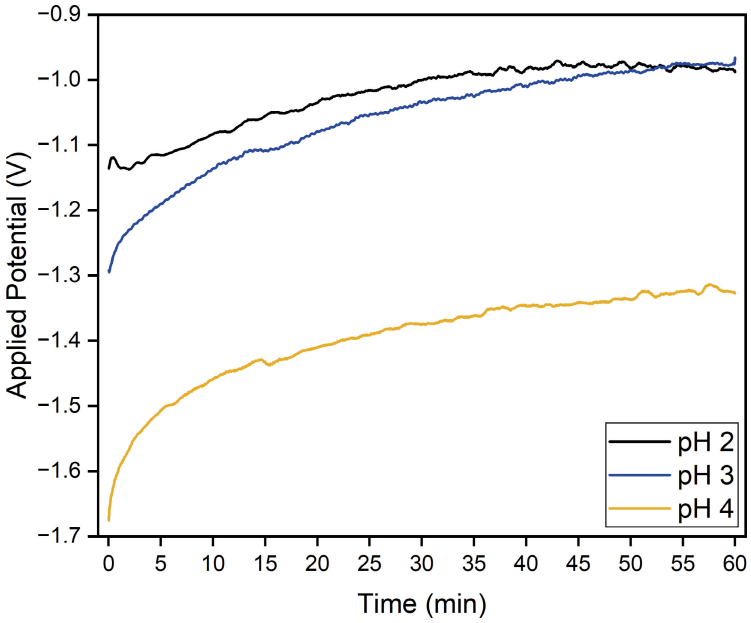


*Figure C.6: course of the applied potential during the Cu-deposition process.*

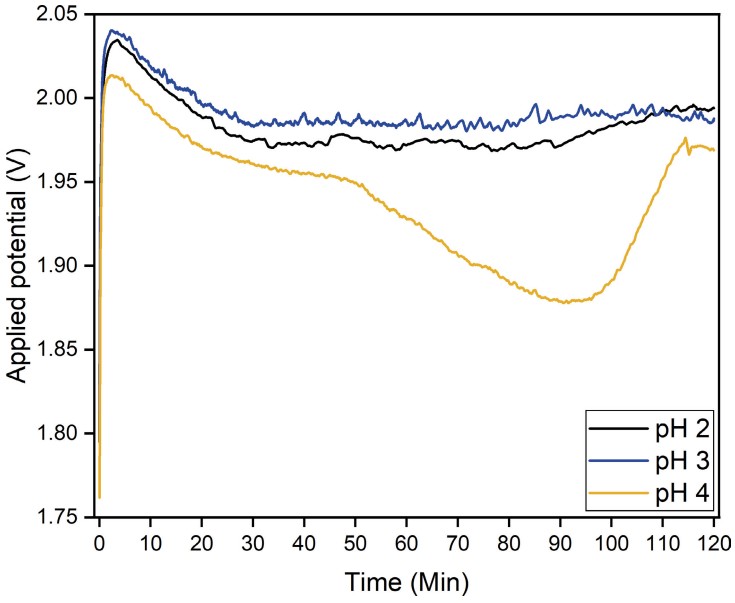


*Figure C.7: course of the applied potential during the Fe-oxidation process.*

# Appendix D

## SUPPLEMENTARY INFORMATION CHAPTER 6

### Results Precipitate Characterization Including Anions

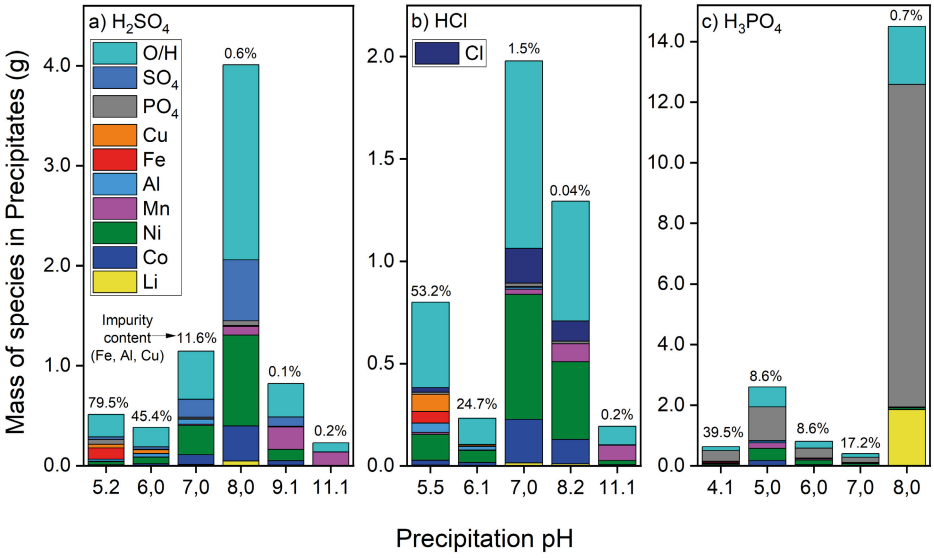


*Figure D.1: Compositions of the precipitates formed after pH adjustment with prior electrochemical purification in $H_2SO_4$ (a), HCl (b) or $H_3PO_4$ (c) as lixiviant, including anions. Oxygen and hydrogen are calculated through subtraction of measured elements from total mass. Impurity content according to Eq. 6.8 is indicated above the respective bar.*

## Visual explanation of calculations in process overviews

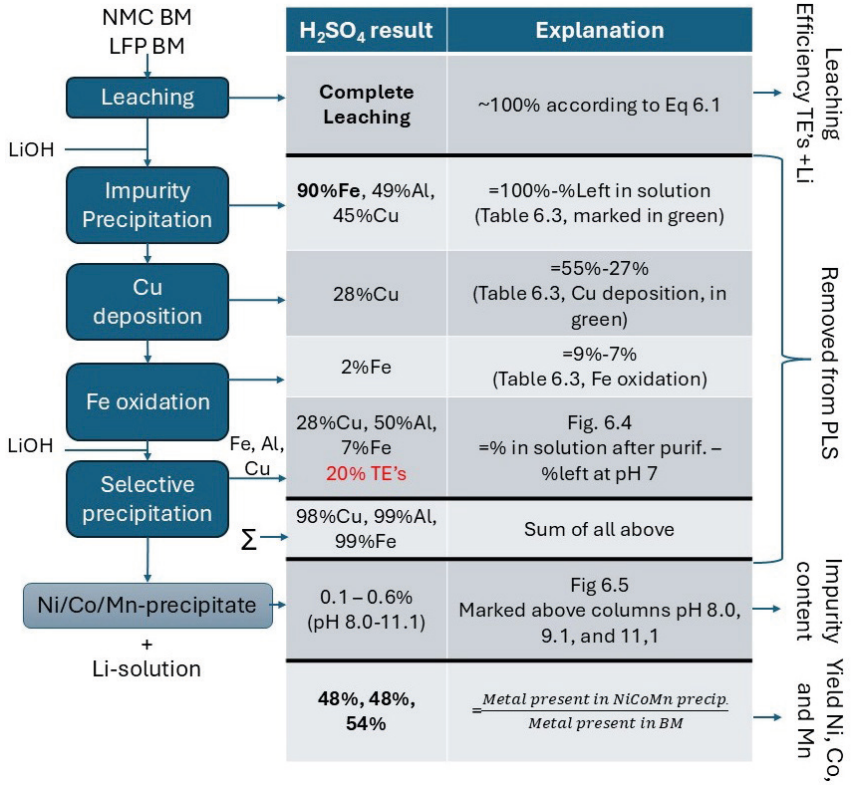


*Figure D.2: Overview of the calculations of leaching-, removal- and yield-percentages performed in the process overview of the $H_2SO_4$-based system. Calculations for the HCl- and $H_3PO_4$-systems are analog.*

# *Curriculum Vitae*

**Johannes Josephus Michaël Maria van de Ven**

## Education

| | |
|---|---|
| 2015 – 2019 | Bachelor of Science in Chemistry<br>Katholieke Universiteit Leuven<br>Leuven, Belgium |
| 2018 – 2021 | Master of Science in Chemistry, Cum Laude<br>Katholieke Universiteit Leuven<br>Leuven, Belgium |
| 2021 – present | Promovendus in Materials Science and Engineering, Chemistry<br>Delft University of Technology<br>Delft, The Netherlands<br>Thesis: Hydrometallurgical and Electrochemical Recycling of Mixed Li-ion Battery Waste<br>Promotor: Dr. Y. Yang<br>Copromotor: Dr. Ir. S.T. Abrahami |

# List of Publications

**Related to this dissertation:**

1. **van de Ven, J. J. M. M.**, Teeuwisse, P. J., Yang, Y., Abrahami, S. T. Influence of Lixiviant type on Recycling of Industrial LFP- and NMC-type Li-ion Battery Waste, *In preparation for journal submission*. (Chapter 6 of this dissertation)
2. **van de Ven, J. J. M. M.**, Anghel, M. A., Teeuwisse, P. J., Yang, Y., Abrahami, S. T. Leaching and Electrochemical Purification of Mixed Industrial LFP- and NMC type Lithium-ion Battery Waste. *Submitted for journal publication.* (Chapter 5 of this dissertation)
3. **van de Ven, J. J. M. M.**, Teeuwisse, P. J., Hendrikx, R. W. A., Yang, Y. & Abrahami, S. T. Simultaneous Recycling of Spent $LiFePO_4$ and $LiNi_xMn_yCo_zO_2$ Li-Ion Batteries Under Mild Leaching Conditions. *Journal of Sustainable Metallurgy* 1–12 (2025). (Chapter 4 of this dissertation)
4. **van de Ven, J. J. M. M.**, Yang, Y. & Abrahami, S. T. A closer look at lithium-ion batteries in E-waste and the potential for a universal hydrometallurgical recycling process. *Scientific Reports 2024 14:1* 14, 1–12 (2024). (Chapter 3 of this dissertation)

**Earlier work not related to this dissertation:**

5. Pucci Couto, C., **van de Ven, J. J. M. M.**, Yang, Y. & Abrahami, S. T. On the pre-treatment for recycling spent NdFeB permanent magnets: from disassembling, characterisation to de-coating. *Sustainable Materials and Technologies*, 41, 9 (2024).
6. Li, X., **van de Ven, J. J. M. M.**, Li, Z., Binnemans, K. Separation of Rare Earths and Transition Metals Using Ionic-Liquid-Based Aqueous Biphasic Systems, *Industrial & Engineering Chemistry Research*, 61, 17, 5 (2022).

# Dankwoord

Beste lezer,
Het is nu begin april. Ik ben reeds begonnen met mijn functie als postdoctoraal onderzoeker in dezelfde onderzoeksgroep als waar ik promoveer(de) en de zware, lange dagen waarin ik mijn proefschrift schreef liggen al even achter mij. Hierdoor hebben alle woorden, zinnen, nummers, afbeeldingen, citaties en experimenten kunnen bezinken, en kan ik met zorgvuldigheid iedereen bedanken die dat toekomt. Een promotie is tenslotte niet iets wat je alleen kunt!

Ten eerste wil ik mijn begeleidend team, Shoshan Abrahami en Yongxiang Yang, enorm bedanken voor de kans die ze me in 2021 hebben gegeven om te promoveren aan de TUDelft, hun begeleiding gedurende de afgelopen 4 jaar en hun veelvuldige wetenschappelijke inbreng. Dankzei jullie heb ik me zelfstandig kunnen ontwikkelen tot onderzoeker en kon ik mijn interesses navolgen, wat leidde tot kwaliteitsvolle hoofdstukken die in dit proefschrift terug te vinden zijn, alsook het tevergeefs proberen kristalliseren van ijzerfosfaat waar we het liever niet over hebben. Ik ben daarom blij dat we nog geen afscheid hoeven te nemen. Ik kijk al uit naar onze samenwerking van de komende 3 jaar!

Vervolgens wil ik iedereen bedanken die ook inhoudelijk heeft bijgedragen aan het onderzoek van de afgelopen jaren, in willekeurige volgorde. Sander van Aspen, technicus van het hydrolab gedurende mijn eerste twee jaar, bedank ik voor zijn steun, zowel praktisch in het lab als voor zijn raad tijdens mijn zwaardere, tweede promotiejaar. Michel van den Brink, technicus van het chemisch lab van P&E, bedank ik voor zijn hulp bij de vele ICP karakterisaties van de afgelopen jaren, degenen die hij voor me heeft uitgevoerd alsook de training en hulp bij het zelf uitvoeren van metingen. “Wie het kleine niet eert, is het grote niet weerd”. Daarom wil ik ook Hans Brouwer bedanken voor de hittebehandeling uitgevoerd in Hoofdstuk 5, waardoor het gevormde ijzerfosfaatproduct karakteriseerbaar was met XRD-analyse. Ruud Hendrikx bedank ik graag voor zijn talloze bijdrages aan het proefschrift in de vorm van XRF- en XRD analyses, en in het bijzonder voor zijn bijdrage als coauteur van het reeds gepubliceerde Hoofdstuk 4. Patrick Teeuwisse wil ik in het bijzonder bedanken voor al zijn bijdragen aan het gehele proefschrift, gaande van het uitvoeren van ontsluitingsexperimenten, tot het maken van onderdelen van elektrochemische opstellingen en het uitvoeren van ICP-analyses. Harm Duncker, masterstudent tijdens mijn tweede promotiejaar, wil ik bedanken voor zijn invloedrijke ideeën omtrent het samen recyclen van LFP en NMC, zijn onvermoeibare inzet tijdens het ontmantelen van batterijen en zijn bijdrage aan het voorbereidend werk voor Hoofdstuk 4 van dit proefschrift. Maria-Alexandra Anghel,

masterstudent tijdens mijn vierde promotiejaar, bedank ik voor haar waardevolle bijdrage aan Hoofdstuk 5 van dit proefschrift. Haar gedrevenheid en kennis van elektrochemie hebben ervoor gezorgd dat haar resultaten deel uitmaken van het vijfde hoofdstuk, waardoor ze ook coauteur zal zijn. Mulțumesc!

Het is vanzelfsprekend dat in een proefschrift van alles staat waarvoor er mensen bedankt kunnen worden. Echter had ik dit niet kunnen bereiken zonder de schat aan gesprekken, interacties, mentale steun en praktische hulp die ik heb gehad en gekregen. In het bijzonder wil ik daarvoor Phillipp Leerhoff en Camila Pucci Couto in het zonnetje zetten, vielen Dank, muito obrigado! Camila, 3 jaar lang met jou een kantoor delen, onze vele gesprekken over wetenschap en onze persoonlijke levens, onze gezamenlijke interesse in de Belgische biercultuur en de vele dagen in het hydrolab zijn van onschatbare waarde geweest gedurende mijn promotie! Philipp, we hebben dik 4 jaar lang lief en leed gedeeld tijdens onze promoties, die beide op 1 oktober 2021 startten. Ik denk dat het hebben van een vriend die precies begrijpt hoe het is om een poster te maken waar je absoluut geen zin in hebt, beleefd te moeten zijn tegen een reviewer die geen benul heeft van je onderzoek of een paragraaf in je proefschrift te moeten herschrijven waar je wekenlang aan hebt gewerkt ervoor zorgt dat een promotie een stuk draaglijker is! Julinha de Moraes Siedschlag, muito obrigado voor alle hulp tijdens mijn derde en vierde promotiejaar. Jouw komst zorgde voor een opleving van het “pyro”-deel van onze onderzoeksgroep, maar al jouw hulp in het hydrolab en onze goede vriendschap hebben ook mij persoonlijk enorm geholpen. Tevens bedank ik natuurlijk ook Elsa Best en Fabian Kadisch, merci beaucoup, vielen Dank! Elsa bedank ik voor de vele leuke gesprekken tijdens lunch, in het lab, of tijdens een group-meeting wanneer het weer eens over staalproductie ging en voor de vele uitjes, feesten en partijen die ze door de jaren heen heeft georganiseerd. Fabian, onze gezamenlijke liefde voor Oostenrijk, elektronische muziek en flauwe grappen heeft al voor veel mooie momenten gezorgd, waarvoor dank! Ik ben vereerd dat jullie, Elsa en Fabian, ermee hebben ingestemd paranymphs te zijn op mijn promotie.

Daarnaast bedank ik ook graag de technici en andere personeelsleden die een handje toestaken wanneer dat nodig was, door hulp met bestellingen, het verlenen van toegang tot hun lab en hun apparatuur of door hulp met experimentele methoden wanneer ik vast zat, Agnieszka Kooijman, Durga Mainali, Remko Seijffers, Hans Hofman, Kees Kwakernaak, Alice Dautezac en Georgy Filonenko. Maar ook de PhD-en postdoc collega’s van de afgelopen jaren, in willekeurige volgorde, Amir, Can, Daniel, Eszter, Gautham, Jasper, John, José, Khatereh, Luis, Tim, Jaji, Mohammed, Alfonso, Arjun, Gaojie, Nirmal, Pablo, Devi, Hannah, Ehsan, Arash, Jia-Ning, Zhaorui, Iftikhar, Konstantina, Milou, Pritish, Robert, Chryssa, Joost, Jungwan, Keer, Roberta, Timo, Soroush vavavooey, Yeli en natuurlijk

Vitória, bedank ik voor de vele leuke gesprekken tijdens pauzes of gewoon in de wandelgangen.

Ten slotte gaat mijn dank ook uit naar de familie en vrienden met wie het contact veel verder reikt dan alleen gedurende mijn promotie. Het blijvende contact met vriendengroepen van de lagere school in Moergestel, mijn middelbare school in Hoogstraten, mijn studie in Leuven en O.J.V. de Koornbeurs is iets wat ik koester en ik ben enorm dankbaar voor alle fijne herinneringen van de laatste jaren. Verder dank ik natuurlijk mijn familie, en in het bijzonder mijn zus Janneke, mijn moeder Sacha, mijn vader Niels en mijn vriendin Cynthia, zonder wiens steun ik mijn PhD ook niet had kunnen afronden. Nogmaals dank aan jullie allemaal! Ik kijk uit naar alle fijne momenten die nog gaan komen in de toekomst.

*er is niet meer bij weinig*
*noch is er minder*
*nog is onzeker wat er was*
*wat wordt wordt willoos*
*eerst als het is is het ernst*
*het herinnert zich heilloos*
*en blijft ijlings*

*alles van waarde is weerloos*
*wordt van aanraakbaarheid rijk*

*en aan alles gelijk*
*als het hart van de tijd*
*als het hart van de tijd*

Lucebert – *De zeer oude zingt* - 1974